

Study of the Impacts of Implements of Husbandry on Bridges

Volume III: Appendices

August 2017



Sponsored by

Iowa Highway Research Board (IHRB Project TR-613)

Iowa Department of Transportation (InTrans Projects 9-364 and 11-399)

Federal Highway Administration Transportation Pooled Fund TPF-5(232)



IOWA STATE UNIVERSITY
Institute for Transportation

About the Bridge Engineering Center

The mission of the Bridge Engineering Center (BEC) is to conduct research on bridge technologies to help bridge designers/owners design, build, and maintain long-lasting bridges.

About the Institute for Transportation

The mission of the Institute for Transportation (InTrans) at Iowa State University is to develop and implement innovative methods, materials, and technologies for improving transportation efficiency, safety, reliability, and sustainability while improving the learning environment of students, faculty, and staff in transportation-related fields.

Disclaimer Notice

The contents of this report reflect the views of the authors, who are responsible for the facts and the accuracy of the information presented herein. The opinions, findings and conclusions expressed in this publication are those of the authors and not necessarily those of the sponsors.

The sponsors assume no liability for the contents or use of the information contained in this document. This report does not constitute a standard, specification, or regulation.

The sponsors do not endorse products or manufacturers. Trademarks or manufacturers' names appear in this report only because they are considered essential to the objective of the document.

Iowa State University Non-Discrimination Statement

Iowa State University does not discriminate on the basis of race, color, age, ethnicity, religion, national origin, pregnancy, sexual orientation, gender identity, genetic information, sex, marital status, disability, or status as a U.S. veteran. Inquiries regarding non-discrimination policies may be directed to Office of Equal Opportunity, 3410 Beardshear Hall, 515 Morrill Road, Ames, Iowa 50011, Tel. 515-294-7612, Hotline: 515-294-1222, email eooffice@iastate.edu.

Iowa Department of Transportation Statements

Federal and state laws prohibit employment and/or public accommodation discrimination on the basis of age, color, creed, disability, gender identity, national origin, pregnancy, race, religion, sex, sexual orientation or veteran's status. If you believe you have been discriminated against, please contact the Iowa Civil Rights Commission at 800-457-4416 or Iowa Department of Transportation's affirmative action officer. If you need accommodations because of a disability to access the Iowa Department of Transportation's services, contact the agency's affirmative action officer at 800-262-0003.

The preparation of this report was financed in part through funds provided by the Iowa Department of Transportation through its "Second Revised Agreement for the Management of Research Conducted by Iowa State University for the Iowa Department of Transportation" and its amendments.

The opinions, findings, and conclusions expressed in this publication are those of the authors and not necessarily those of the Iowa Department of Transportation or the U.S. Department of Transportation Federal Highway Administration.

Technical Report Documentation Page

1. Report No. IHRB Project TR-613 and TPF-5(232)		2. Government Accession No.		3. Recipient's Catalog No.	
4. Title and Subtitle Study of the Impacts of Implements of Husbandry on Bridges Volume III: Appendices				5. Report Date August 2017	
				6. Performing Organization Code	
7. Author(s) Katelyn Freeseaman (orcid.org/0000-0003-0546-3760), Brent Phares (orcid.org/0000-0001-5894-4774), Lowell Greimann (orcid.org/0000-0003- 2488-6865), and Chandra Teja Kilaru (orcid.org/0000-0002-1399-7132)				8. Performing Organization Report No. InTrans Projects 9-364 and 11-399	
9. Performing Organization Name and Address Bridge Engineering Center Iowa State University 2711 South Loop Drive, Suite 4700 Ames, IA 50010-8664				10. Work Unit No. (TRAIS)	
				11. Contract or Grant No.	
12. Sponsoring Organization Name and Address Iowa Highway Research Board Iowa Department of Transportation 800 Lincoln Way Ames, IA 50010				13. Type of Report and Period Covered Volume III: Appendices	
14. Sponsoring Agency Code IHRB Project TR-613 and TPF-5(232)					
15. Supplementary Notes Visit www.intrans.iastate.edu for color pdfs of this and other research reports.					
16. Abstract <p>The objectives of this study were to develop guidance for engineers on how implements of husbandry loads are resisted by traditional bridges, with a specific focus on bridges commonly found on the secondary road system; provide recommendations for accurately analyzing bridges for these loading effects; and make suggestions for the rating and posting of these bridges.</p> <p>To achieve the objectives, the distribution of live load and dynamic impact effects for different types of farm vehicles on three general bridge types—steel-concrete, steel-timber, and timber-timber—were investigated through load testing and analytical modeling. The types of vehicles studied included, but were not limited to, grain wagons/grain carts, manure tank wagons, agriculture fertilizer applicators, and tractors.</p> <p>Once the effects of these vehicles had been determined, a parametric study was carried out to develop live load distribution factor (LLDF) equations that account for the effect of husbandry vehicle loads. Similarly, recommendations for dynamic effects were also developed. The live load distribution factors and dynamic load allowances are covered in the first volume of the report.</p> <p>Finally, suggestions on the analysis, rating, and posting of bridges for husbandry implements were developed. Those suggestions are covered in the second volume of the report.</p> <p>This third volume of the report contains six appendices that include the 19 mini-reports for field tested and analytically modeled steel-concrete, steel-timber, and timber-timber bridges, the farm implement and bridge inventories for the project, and survey responses.</p>					
17. Key Words bridge inventory—bridge testing mini-reports—farm implement inventory— live load testing—steel-concrete bridge tests—steel-timber bridge tests— survey responses—timber-timber bridge tests—live load testing				18. Distribution Statement No restrictions.	
19. Security Classification (of this report) Unclassified.		20. Security Classification (of this page) Unclassified.		21. No. of Pages 252	22. Price NA

STUDY OF THE IMPACTS OF IMPLEMENTS OF HUSBANDRY ON BRIDGES

**Volume III: Appendices
August 2017**

Principal Investigator

Brent Phares, Director
Bridge Engineering Center, Iowa State University

Co-Principal Investigator

Terry Wipf, Professor and Chair
Civil, Construction, and Environmental Engineering, Iowa State University

Authors

Katelyn Freeseaman, Brent Phares, Lowell Greimann, and Chandra Kilaru

Sponsored by

Iowa Highway Research Board
(IHRB Project TR-613),
Iowa Department of Transportation, and
Federal Highway Administration
Transportation Pooled Fund (TPF-5(232))

Preparation of this report was financed in part
through funds provided by the Iowa Department of Transportation
through its Research Management Agreement
with the Institute for Transportation
(InTrans Projects 9-364 and 11-399)

A report from

**Bridge Engineering Center and
Institute for Transportation**

Iowa State University

2711 South Loop Drive, Suite 4700

Ames, IA 50010-8664

Phone: 515-294-8103 / Fax: 515-294-0467

www.intrans.iastate.edu

TABLE OF CONTENTS

ACKNOWLEDGMENTS	xiii
THREE-VOLUME EXECUTIVE SUMMARY	xv
INTRODUCTION	1
Problem Statement	1
Research Objective and Scope	2
Research Methodology	2
Three-Volume Report Organization	2
Volume III: Appendices Content and Organization	2
APPENDIX A. FIELD TESTED STEEL-CONCRETE BRIDGES	3
A.1 Steel-Concrete Bridge 1	3
A.1.1 Background	3
A.1.2 Bridge Description	3
A.1.3 Field Testing	6
A.1.4 Analytical Modeling	10
A.1.5 Results	13
A.2 Steel-Concrete Bridge 2	14
A.2.1 Background	14
A.2.2 Bridge Description	15
A.2.3 Field Testing	18
A.2.4 Analytical Modeling	22
A.2.5 Results	25
A.3 Steel-Concrete Bridge 3	26
A.3.1 Background	26
A.3.2 Bridge Description	27
A.3.3 Field Testing	30
A.3.4 Analytical Modeling	34
A.3.5 Results	37
A.4 Steel-Concrete Bridge 4	38
A.4.1 Background	38
A.4.2 Bridge Description	39
A.4.3 Field Testing	42
A.4.4 Analytical Modeling	46
A.4.5 Results	48
A.5 Steel-Concrete Bridge 5	49
A.5.1 Background	49
A.5.2 Bridge Description	50
A.5.3 Field Testing	52
A.5.4 Analytical Modeling	56
A.5.5 Results	59
APPENDIX B. FIELD TESTED STEEL-TIMBER BRIDGES	61
B.1 Steel-Timber Bridge 1	61

B.1.1 Background	61
B.1.2 Bridge Description	61
B.1.3 Field Testing.....	64
B.1.4 Analytical Modeling.....	68
B.1.5 Results	70
B.2 Steel-Timber Bridge 2.....	71
B.2.1 Background	71
B.2.2 Bridge Description	72
B.2.3 Field Testing.....	74
B.2.4 Analytical Modeling.....	78
B.2.5 Results	81
B.3 Steel-Timber Bridge 3.....	82
B.3.1 Background	83
B.3.2 Bridge Description	83
B.3.3 Field Testing.....	84
B.3.4 Analytical Modeling.....	88
B.3.5 Results	91
B.4 Steel-Timber Bridge 4.....	92
B.4.1 Background	93
B.4.2 Bridge Description	93
B.4.3 Field Testing.....	94
B.4.4 Analytical Modeling.....	99
B.4.5 Results	102
B.5 Steel-Timber Bridge 5.....	103
B.5.1 Background	103
B.5.2 Bridge Description	104
B.5.3 Field Testing.....	106
B.5.4 Analytical Modeling.....	110
B.5.5 Results	113
B.6 Steel-Timber Bridge 6.....	114
B.6.1 Background	114
B.6.2 Bridge Description	115
B.6.3 Field Testing.....	117
B.6.4 Analytical Modeling.....	121
B.6.5 Results	124
B.7 Steel-Timber Bridge 7.....	125
B.7.1 Background	126
B.7.2 Bridge Description	126
B.7.3 Field Testing.....	128
B.7.4 Analytical Modeling.....	132
B.7.5 Results	135
B.8 Steel-Timber Bridge 8.....	136
B.8.1 Background	136
B.8.2 Bridge Description	137
B.8.3 Field Testing.....	139
B.8.4 Analytical Modeling.....	143

B.8.5 Results	145
B.9 Steel-Timber Bridge 9	146
B.9.1 Background	146
B.9.2 Bridge Description	147
B.9.3 Field Testing.....	149
B.9.4 Analytical Modeling.....	153
B.9.5 Results	156
B.10 Steel-Timber Bridge 10.....	157
B.10.1 Background	157
B.10.2 Bridge Description	158
B.10.3 Field Testing.....	160
B.10.4 Analytical Modeling.....	164
B.10.5 Results	167
B.11 Steel-Timber Bridge 11	168
B.11.1 Background	168
B.11.2 Bridge Description	169
B.11.3 Field Testing.....	170
B.11.4 Analytical Modeling.....	174
B.11.5 Results	176
APPENDIX C. FIELD TESTED TIMBER-TIMBER BRIDGES	179
C.1 Timber-Timber Bridge 1	179
C.1.1 Background	179
C.1.2 Bridge Description	179
C.1.3 Field Testing.....	181
C.1.4 Analytical Modeling.....	185
C.1.5 Results	188
C.2 Timber-Timber Bridge 2	189
C.2.1 Background	189
C.2.2 Bridge Description	190
C.2.3 Field Testing.....	191
C.2.4 Analytical Modeling.....	196
C.2.5 Results	199
C.3 Timber-Timber Bridge 3	200
C.3.1 Background	201
C.3.2 Bridge Description	201
C.3.3 Field Testing.....	202
C.3.4 Analytical Modeling.....	206
C.3.5 Results	209
APPENDIX D. FARM IMPLEMENT INVENTORY	211
APPENDIX E. BRIDGE INVENTORY	215
APPENDIX F. SURVEY RESPONSES	229
Survey	229
Responses.....	230

LIST OF FIGURES

Figure A-1. Location overview of Steel-Concrete Bridge 1	3
Figure A-2. Steel-Concrete Bridge 1: Elevation view (left) and end view (right)	4
Figure A-3. Steel-Concrete Bridge 1: Cross-section A-A (top) and plan (bottom).....	5
Figure A-4. Farm vehicles used for field testing	8
Figure A-5. Strain plot of a girder for all test vehicles for Steel-Concrete Bridge 1	9
Figure A-6. Comparison between static and dynamic strain for Steel-Concrete Bridge 1	10
Figure A-7. Finite element model of Steel-Concrete Bridge 1	12
Figure A-8. LLDFs for Steel-Concrete Bridge 1	14
Figure A-9. Location overview of Steel-Concrete Bridge 2.....	15
Figure A-10. Steel-Concrete Bridge 2: Elevation view (left) and end view (right)	15
Figure A-11. Steel-Concrete Bridge 2: Cross-section A-A (top) and plan (bottom).....	17
Figure A-12. Farm vehicles used for field testing	20
Figure A-13. Strain plot of a girder for all test vehicles for Steel-Concrete Bridge 2.....	21
Figure A-14. Comparison between static and dynamic strain for Steel-Concrete Bridge 2.....	22
Figure A-15. Finite element model of Steel-Concrete Bridge 2.....	24
Figure A-16. LLDFs for Steel-Concrete Bridge 2.....	26
Figure A-17. Location overview of Steel-Concrete Bridge 3.....	27
Figure A-18. Steel-Concrete Bridge 3: Elevation view (left) and end view (right)	27
Figure A-19. Steel-Concrete Bridge 3: Cross-section A-A (top) and plan (bottom).....	29
Figure A-20. Farm vehicles used for field testing	32
Figure A-21. Strain plot of a girder for all test vehicles for Steel-Concrete Bridge 3.....	33
Figure A-22. Comparison between static and dynamic strain for Steel-Concrete Bridge 3.....	34
Figure A-23. Finite element model of Steel-Concrete Bridge 3.....	36
Figure A-24. LLDFs for Steel-Concrete Bridge 3.....	38
Figure A-25. Location overview of Steel-Concrete Bridge 4.....	39
Figure A-26. Steel-Concrete Bridge 4: Elevation view (left) and end view (right)	39
Figure A-27. Steel-Concrete Bridge 4: Cross-section A-A (top) and plan (bottom).....	41
Figure A-28. Farm vehicles used for field testing	44
Figure A-29. Strain plot of a girder for all test vehicles for Steel-Concrete Bridge 4.....	45
Figure A-30. Finite element model of Steel-Concrete Bridge 4.....	47
Figure A-31. LLDFs for Steel-Concrete Bridge 4.....	49
Figure A-32. Location overview of Steel-Concrete Bridge 5.....	50
Figure A-33. Steel-Concrete Bridge 5: Elevation view (left) and end view (right)	50
Figure A-34. Steel-Concrete Bridge 5: Cross-section A-A (top) and plan (bottom).....	51
Figure A-35. Farm vehicles used for field testing	54
Figure A-36. Strain plot of a girder for all test vehicles for Steel-Concrete Bridge 5.....	55
Figure A-37. Comparison between static and dynamic strain for Steel-Concrete Bridge 5.....	56
Figure A-38. Finite element model of Steel-Concrete Bridge 5.....	58
Figure A-39. LLDFs for Steel-Concrete Bridge 5.....	60
Figure B-1. Location overview of Steel-Timber Bridge 1.....	61
Figure B-2. Steel-Timber Bridge 1: West elevation view (left) and north end view (right)	62
Figure B-3. Steel-Timber Bridge 1: Cross-section A-A (top) and plan (bottom).....	63
Figure B-4. Farm vehicles used for field testing.....	66
Figure B-5. Strain plot of a girder for all test vehicles for Steel-Timber Bridge 1.....	67

Figure B-6. Comparison between static and dynamic strain for Steel-Timber Bridge 1.....	68
Figure B-7. Finite element model of Steel-Timber Bridge 1.....	69
Figure B-8. LLDFs for Steel-Timber Bridge 1.....	71
Figure B-9. Location overview of Steel-Timber Bridge 2.....	72
Figure B-10. Steel-Timber Bridge 2: South elevation view (left) and west end view (right).....	73
Figure B-11. Steel-Timber Bridge 2: Cross-section A-A (top) and plan (bottom).....	73
Figure B-12. Farm vehicles used for field testing.....	76
Figure B-13. Strain plot of a girder for all test vehicles for Steel-Timber Bridge 2.....	77
Figure B-14. Comparison between static and dynamic strain for Steel-Timber Bridge 2.....	78
Figure B-15. Finite element model of Steel-Timber Bridge 2.....	80
Figure B-16. LLDFs for Steel-Timber Bridge 2.....	82
Figure B-17. Location overview of Steel-Timber Bridge 3.....	83
Figure B-18. Steel-Timber Bridge 3: Elevation view (left) and east end view (right).....	84
Figure B-19. Steel-Timber Bridge 3: Cross-section A-A (top) and plan (bottom).....	84
Figure B-20. Farm vehicles used for field testing.....	86
Figure B-21. Strain plot of a girder for all test vehicles for Steel-Timber Bridge 3.....	87
Figure B-22. Comparison between static and dynamic strain for Steel-Timber Bridge 3.....	88
Figure B-23. Finite element model of Steel-Timber Bridge 3.....	90
Figure B-24. LLDFs for Steel-Timber Bridge 3.....	92
Figure B-25. Location overview of Steel-Timber Bridge 4.....	93
Figure B-26. Bridge 4: Elevation view (left) and east end view (right).....	94
Figure B-27. Steel-Timber Bridge 4: Cross-section A-A (top) and plan (bottom).....	94
Figure B-28. Farm vehicles used for field testing.....	97
Figure B-29. Strain plot of a girder for all test vehicles for Steel-Timber Bridge 4.....	98
Figure B-30. Comparison between static and dynamic strain for Steel-Timber Bridge 4.....	99
Figure B-31. Finite element model of Steel-Timber Bridge 4.....	101
Figure B-32. LLDFs for Steel-Timber Bridge 4.....	103
Figure B-33. Location overview of Steel-Timber Bridge 5.....	104
Figure B-34. Bridge 5: West elevation view (left) and north end view (right).....	105
Figure B-35. Steel-Timber Bridge 5: Cross-section A-A (top) and plan (bottom).....	106
Figure B-36. Farm vehicles used for field testing.....	108
Figure B-37. Strain plot of a girder for all test vehicles for Steel-Timber Bridge 5.....	109
Figure B-38. Comparison between static and dynamic strain for Steel-Timber Bridge 5.....	110
Figure B-39. Finite element model of Steel-Timber Bridge 5.....	112
Figure B-40. LLDFs for Steel-Timber Bridge 5.....	114
Figure B-41. Location overview of Steel-Timber Bridge 6.....	115
Figure B-42. Steel-Timber Bridge 6: North elevation view (left) and east end view (right).....	116
Figure B-43. Steel-Timber Bridge 6: Cross-section A-A (top) and plan (bottom).....	116
Figure B-44. Farm vehicles used for field testing.....	119
Figure B-45. Strain plot of a girder for all test vehicles for Steel-Timber Bridge 6.....	120
Figure B-46. Comparison between static and dynamic strain for Steel-Timber Bridge 6.....	121
Figure B-47. Finite element model of Steel-Timber Bridge 6.....	123
Figure B-48. LLDFs for Steel-Timber Bridge 6.....	125
Figure B-49. Location overview of Steel-Timber Bridge 7.....	126

Figure B-50. Steel-Timber Bridge 7: West elevation view (left) and north end view (right)	127
Figure B-51. Steel-Timber Bridge 7: Cross-section A-A (top) and plan (bottom).....	128
Figure B-52. Farm vehicles used for field testing.....	130
Figure B-53. Strain plot of a girder for all test vehicles for Steel-Timber Bridge 7.....	131
Figure B-54. Comparison between static and dynamic strain for Steel-Timber Bridge 7.....	132
Figure B-55. Finite element model of Steel-Timber Bridge 7.....	134
Figure B-56. LLDFs for Steel-Timber Bridge 7.....	136
Figure B-57. Location overview of Steel-Timber Bridge 8.....	137
Figure B-58. Steel-Timber Bridge 8: South elevation view (left) and west end view (right)	138
Figure B-59. Steel-Timber Bridge 8: Cross-section A-A (top) and plan (bottom).....	139
Figure B-60. Farm vehicles used for field testing.....	141
Figure B-61. Strain plot of a girder for all test vehicles for Steel-Timber Bridge 8.....	142
Figure B-62. Finite element model of Steel-Timber Bridge 8.....	144
Figure B-63. LLDFs for Steel-Timber Bridge 8.....	146
Figure B-64. Location overview of Steel-Timber Bridge 9.....	147
Figure B-65. Steel-Timber Bridge 9: North elevation view (left) and east end view (right)	148
Figure B-66. Steel-Timber Bridge 9: Cross-section A-A (top) and plan (bottom).....	149
Figure B-67. Farm vehicles used for field testing.....	151
Figure B-68. Strain plot of a girder for all test vehicles for Steel-Timber Bridge 9.....	152
Figure B-69. Comparison between static and dynamic strain for Steel-Timber Bridge 9.....	153
Figure B-70. Finite element model of Steel-Timber Bridge 9.....	155
Figure B-71. LLDFs for Steel-Timber Bridge 9.....	157
Figure B-72. Location overview of Steel-Timber Bridge 10.....	158
Figure B-73. Steel-Timber Bridge 10: North elevation view (left) and east end view (right)	159
Figure B-74. Steel-Timber Bridge 10: Cross-section A-A (top) and plan (bottom).....	160
Figure B-75. Farm vehicles used for field testing.....	162
Figure B-76. Strain plot of a girder for all test vehicles for Steel-Timber Bridge 10.....	163
Figure B-77. Comparison between static and dynamic strain for Steel-Timber Bridge 10.....	164
Figure B-78. Finite element model of Steel-Timber Bridge 10.....	166
Figure B-79. LLDFs for Steel-Timber Bridge 10.....	168
Figure B-80. Location overview of Steel-Timber Bridge 11.....	169
Figure B-81. Steel-Timber Bridge 11: South elevation view (left) and east end view (right)	170
Figure B-82. Steel-Timber Bridge 11: Cross-section A-A (top) and plan (bottom).....	170
Figure B-83. Farm vehicles used for field testing.....	172
Figure B-84. Strain plot of a girder for all test vehicles for Steel-Timber Bridge 11.....	173
Figure B-85. Finite element model of Steel-Timber Bridge 11.....	175
Figure B-86. LLDFs for Steel-Timber Bridge 11.....	177
Figure C-1. Location overview of Timber-Timber Bridge 1.....	179
Figure C-2. Timber-Timber Bridge 1: West elevation view (left) and north end view (right)	180
Figure C-3. Timber-Timber Bridge 1: Cross-section A-A (top) and plan (bottom).....	181
Figure C-4. Farm vehicles used for field testing.....	183

Figure C-5. Strain plot of a girder for all test vehicles for Timber-Timber Bridge 1	184
Figure C-6. Comparison between static and dynamic strain for Timber-Timber Bridge 1	185
Figure C-7. Finite element model of Timber-Timber Bridge 1	187
Figure C-8. LLDFs for Timber-Timber Bridge 1	189
Figure C-9. Location overview of Timber-Timber Bridge 2	190
Figure C-10. Timber-Timber Bridge 2: West elevation view (left) and south end view (right)	191
Figure C-11. Timber-Timber Bridge 2: Cross-section A-A (top) and plan (bottom).....	191
Figure C-12. Farm vehicles used for field testing.....	194
Figure C-13. Strain plot of a girder for all test vehicles for Timber-Timber Bridge 2	195
Figure C-14. Comparison between static and dynamic strain for Timber-Timber Bridge 2	196
Figure C-15. Finite element model of Timber-Timber Bridge 2	198
Figure C-16. LLDFs for Timber-Timber Bridge 2	200
Figure C-17. Location overview of Timber-Timber Bridge 3	201
Figure C-18. Timber-Timber Bridge 3: Elevation view (left) and east end view (right)	202
Figure C-19. Timber-Timber Bridge 3: Cross-section A-A (top) and plan (bottom).....	202
Figure C-20. Farm vehicles used for field testing.....	204
Figure C-21. Strain plot of a girder for all test vehicles for Timber-Timber Bridge 3	205
Figure C-22. Comparison between static and dynamic strain for Timber-Timber Bridge 3	206
Figure C-23. Finite element model of Timber-Timber Bridge 3	208
Figure C-24. LLDFs for Timber-Timber Bridge 3	210
Figure F-1. Three-axle vehicle.....	229

LIST OF TABLES

Table A-1. Axle weight and total length of each testing vehicle.....	7
Table A-2. Model calibration for Steel-Concrete Bridge 1	13
Table A-3. Axle weight and total length of each testing vehicle.....	19
Table A-4. Model calibration for Steel-Concrete Bridge 2	25
Table A-5. Axle weight and total length of each testing vehicle.....	31
Table A-6. Model calibration for Steel-Concrete Bridge 3	37
Table A-7. Axle weight and total length of each testing vehicle.....	43
Table A-8. Model calibration for Steel-Concrete Bridge 4	48
Table A-9. Axle weight and total length of each testing vehicle.....	53
Table A-10. Model calibration for Steel-Concrete Bridge 5	59
Table B-1. Axle weight and total length of each testing vehicle	65
Table B-2. Model calibration for Steel-Timber Bridge 1	70
Table B-3. Axle weight and total length of each testing vehicle	75
Table B-4. Model calibration for Steel-Timber Bridge 2	81
Table B-5. Axle weight and total length of each testing vehicle	85
Table B-6. Model calibration for Steel-Timber Bridge 3	91
Table B-7. Axle weight and total length of each testing vehicle	96
Table B-8. Model calibration for Steel-Timber Bridge 4	102
Table B-9. Axle weight and total length of each testing vehicle	107

Table B-10. Model calibration for Steel-Timber Bridge 5	113
Table B-11. Axle weight and total length of each testing vehicle	118
Table B-12. Model calibration for Steel-Timber Bridge 6	124
Table B-13. Axle weight and total length of each testing vehicle	129
Table B-14. Model calibration for Steel-Timber Bridge 7	135
Table B-15. Axle weight and total length of each testing vehicle	140
Table B-16. Model calibration for Steel-Timber Bridge 8	145
Table B-17. Axle weight and total length of each testing vehicle	150
Table B-18. Model calibration for Steel-Timber Bridge 9	156
Table B-19. Axle weight and total length of each testing vehicle	161
Table B-20. Model calibration for Steel-Timber Bridge 10	167
Table B-21. Axle weight and total length of each testing vehicle	171
Table B-22. Model calibration for Steel-Timber Bridge 11	176
Table C-1. Axle weight and total length of each testing vehicle	182
Table C-2. Model calibration for Timber-Timber Bridge 1	188
Table C-3. Axle weight and total length of each testing vehicle	193
Table C-4. Model calibration for Timber-Timber Bridge 2	199
Table C-5. Axle weight and total length of each testing vehicle	203
Table C-6. Model calibration for Timber-Timber Bridge 3	209
Table D-1. Farm vehicle inventory	211
Table E-1a. One-way traffic lane steel-concrete bridges	215
Table E-1b. Multiple traffic lane steel-concrete bridges	216
Table E-1c. Skewed steel-concrete bridges	217
Table E-2a. One-way traffic lane steel-timber bridges	218
Table E-2b. Multiple traffic lane steel-timber bridges	219
Table E-2c. Skewed steel-timber bridges	220
Table E-3a. One-way traffic lane timber-timber bridges	220
Table E-3b. Multiple traffic lane timber-timber bridges	222
Table E-3c. Skewed timber-timber bridges	222
Table E-4. 174 Bridges used in Volume II	223
Table F-1. Definition of implements of husbandry	230
Table F-2. Gross weight limits and single-axle weight limits	233

ACKNOWLEDGMENTS

The research team would like to acknowledge the Iowa Highway Research Board, the Iowa Department of Transportation (DOT), and the Federal Highway Administration for sponsoring this research with support from the following Transportation Pooled Fund TPF-5(232) partners:

- Illinois
- Iowa (lead state)
- Kansas
- Minnesota
- Nebraska
- Oklahoma
- Wisconsin
- Wisconsin

The authors would like to express their gratitude to the Iowa DOT and the other pooled fund state partners for their financial support and technical assistance and also thank the USDA Forest Products Laboratory for their support of this project. In addition, the authors would like to acknowledge the support of the Iowa DOT Office of Bridges and Structures staff members, who continually provide great insight, guidance, and motivation for practical and implementable research.

THREE-VOLUME EXECUTIVE SUMMARY

The deterioration of bridges is a prevalent issue in the US. A portion of that deterioration comes from the frequent subsection of bridges to oversized loads. Of those oversized loads, implements of husbandry are of particular interest. Although states differ in their definition, an implement of husbandry can generally be thought of as a vehicle used to carry out agricultural activities. These vehicles often carry heavy loads, and little is known on how husbandry implements affect today's bridges.

The behavior of bridges with these vehicles, particularly regarding live load distribution and impact, is not explicitly enveloped within the design, rating, and posting vehicles presented in current American Association of State Highway and Transportation Officials (AASHTO) specifications. Because of the large axle loads and varying axle spacings, the current AASHTO vehicles, such as the HL-93 design truck and the HS20 rating truck, may not accurately represent husbandry implements.

The objectives of this research, presented in a three-volume report series, were to develop guidance for engineers on how implements of husbandry loads are resisted by traditional bridges, with a specific focus on bridges commonly found on the secondary road system; provide recommendations for accurately analyzing bridges for these loading effects; and make suggestions for the rating and posting of these bridges

Volume I focuses on the impacts of husbandry implements on actual bridges by way of field testing as well as analytical finite element models. With these data, the objective was to develop equations and limits for dynamic load allowances and live load distribution factors that apply directly to husbandry vehicles.

Included in the testing were bridges with steel girders with both concrete and timber decks as well as bridges with timber girders and timber decks. Field testing was conducted on 19 of the bridges in this collection. Brief reports for each of the 19 bridges are in Volume III: Appendices.

The data collected from field tests were used to determine a reasonable bound for impact factors for husbandry implements as well as to get a base understanding of how live load moments created by husbandry vehicles are distributed among girders. In addition to the field tests, finite element models were created for the 19 bridges and calibrated with the field test results. Using these models as guidelines, finite element modes were created for 151 bridges included in the inventory (also included in Volume III: Appendices). The finite element models were subjected to the loads of 121 typical husbandry vehicles inventoried (also included in Volume III: Appendices) and modeled using finite element analysis.

Results show that the impact factors currently presented in the AASHTO specifications are too low for husbandry vehicles. Similarly, provisions provided by AASHTO for live load distribution are, in some cases, drastically different from live load distribution factors determined from loading the 151 bridges with the 121 husbandry vehicles. Volume I provides

recommendations on upper limits for dynamic load allowances as well as several equations for determining live load distribution specifically for husbandry implements.

The purpose of the work covered in Volume II was to determine whether current AASHTO rating and posting vehicles can be used to accurately represent husbandry implements. Using software generated by the Bridge Engineering Center at Iowa State University's Institute for Transportation, AASHTO vehicles and the same 121 husbandry vehicles inventoried and used in the Volume I work were theoretically driven across 174 bridges (151 of which were also included in the parametric study in Volume I).

With the moments produced by both the AASHTO and husbandry vehicles on these bridges, comparisons were made between moment envelopes for both vehicle types as well as for theoretical operating ratings for both vehicle types. Results showed that the vehicles provided in AASHTO specifications do not accurately represent the effects caused by husbandry vehicles. In addition, on shorter span bridges, husbandry vehicles tend to produce lower operating ratings than the AASHTO vehicles. On longer span bridges, husbandry vehicles seem to lead to higher operating ratings than AASHTO vehicles.

Volume II presents the development of an overarching husbandry vehicle, recommendations on signage and posting for husbandry vehicles, as well as bridge rating examples, for both short and long span bridges, using updated distribution and impact factors as presented in Volume I.

Finally, Volume III is a collection of appendices referenced in Volumes I and II. Appendices A, B, and C are a series of mini reports for the 19 field tested bridges from Volume I. Appendix D includes detailed information of the 121 farm vehicles used for the study. Appendix E is a detailed inventory of the 151 bridges from Volume I and 174 bridges used in Volume II. Appendix F includes the survey sent to the state departments of transportation and responses to questions about their rules and regulations for husbandry implements on bridges.

INTRODUCTION

In the US, bridges are typically designed and load rated based on the specifications provided by the American Association of State Highway and Transportation Officials (AASHTO). These specifications were developed to ensure the safety of bridges for traditional highway vehicles. As a part of both the design and rating process, live loads in the form of a typical highway truck are distributed across the various structural elements to determine the shear and moments in those elements. Although the process to determine these shear and moments can be quite intensive, the process has been simplified to a degree through the use of the live load distribution factors (LLDFs) and the dynamic load allowance (IM) specified by the AASHTO standards and LRFD specifications (AASHTO 1996, AASHTO 2010).

LLDFs can be broadly defined as the ratio of the maximum live-load effect in a component to the maximum live-load effect in a system when using beam-line model techniques (Barker and Puckett 2013). LLDFs were developed to examine the bridge's capability to resist traditional highway-type vehicles (e.g., trucks, which tend to have relatively consistent widths and other characteristics) (AASHTO 1996, AASHTO 2010). AASHTO defines the dynamic load allowance, IM, as an increase in the applied static force effects to account for the dynamic interaction between the bridge and moving loads.

While the AASHTO specifications are generally thought to be conservative when used to predict the response of bridges to highway-type vehicles, concerns have been raised about their applicability to non-highway vehicles such as husbandry implements, which often have large axle loads and varying axle spacings.

Problem Statement

As of 2013, there were 607,380 bridges in the US (ASCE 2013), with the majority of these bridges found on secondary roadways and generally thought of as "rural" bridges. Statistics show that 13 percent of the rural bridges are structurally deficient and 10 percent are functionally obsolete (Orr 2012). Combining these statistics indicates that there are a large number of bridges in rural settings that do not meet current design standards, although this does not necessarily mean they are unsafe.

At the same time, changing technology in farming has led to heavier farm vehicles in a variety of configurations. While these vehicles are developed for use on a farm, they commonly travel on the roadway system as well. These vehicles tend to have different wheel spacing, gauge widths, wheel footprints, and dynamic coupling characteristics than traditional highway vehicles, which means they are likely resisted differently than the vehicles addressed by AASHTO specifications (Wood and Wipf 1999, Phares et al. 2005, Seo et al. 2013).

Currently, an engineer who wants to assess a bridge's ability to resist implements of husbandry must make many assumptions and use best judgement. Therefore, there is a need to provide engineers with the tools to accurately assess how highway bridges resist these atypical vehicles.

Research Objective and Scope

The objectives of this study were to develop guidance for engineers on how implements of husbandry loads are resisted by traditional bridges, with a specific focus on bridges commonly found on the secondary road system; provide recommendations for accurately analyzing bridges for these loading effects; and make suggestions for the rating and posting of these bridges.

Research Methodology

To achieve the objectives, the distribution of live load and dynamic impact effects for different types of farm vehicles on three general bridge types—steel-concrete, steel-timber, and timber-timber—were investigated by load testing and analytical modeling. The types of vehicles studied included, but were not limited to, grain wagons/grain carts, manure tank wagons, agriculture fertilizer applicators, and tractors.

Once the effects of these vehicles had been determined, a parametric study was carried out to develop live load distribution factor (LLDF) equations that account for the effect of husbandry vehicle loads. Similarly, recommendations for dynamic effects were also developed. Finally, suggestions on the analysis, rating, and posting of bridges for husbandry implements were developed.

Three-Volume Report Organization

This final report is presented in three volumes and summarizes the results of this project as follows.

Volume I: Live Load Distribution Factors and Dynamic Load Allowances

Volume II: Rating and Posting Recommendations

Volume III: Appendices

Volume III: Appendices Content and Organization

The appendices in Volume III are referenced in Volumes I and II. Volume III includes the following for this project:

- Appendix A. Field Tested Steel-Concrete Bridges
- Appendix B. Field Tested Steel-Timber Bridges
- Appendix C. Field Tested Timber-Timber Bridges
- Appendix D. Farm Implement Inventory
- Appendix E. Bridge Inventory
- Appendix F. Survey Responses

APPENDIX A. FIELD TESTED STEEL-CONCRETE BRIDGES

A.1 Steel-Concrete Bridge 1

This mini test and evaluation report documents the results of field testing and subsequent analysis of a steel girder bridge with a concrete deck (Steel-Concrete Bridge 1) under loading from multiple implements of husbandry. For completeness, this mini-report includes a description of the bridge, a description of the live load testing procedures followed, sample data, a description of analytical modeling, plots of analytical results, and a discussion of the overall behavior of the steel girder bridge under loading from implements of husbandry.

A.1.1 Background

The steel-concrete bridge described here is known in the National Bridge Inventory (NBI) database as Bridge 77560 and will be henceforth be referred to as Steel-Concrete Bridge 1. The bridge is located about 5 miles south of Beaver, on 250th Street over the East Beaver Creek, in Boone County, Iowa. Figure A-1 shows the general location of the bridge.



Map: ©Google 2014

Figure A-1. Location overview of Steel-Concrete Bridge 1

A.1.2 Bridge Description

Steel-Concrete Bridge 1 is open to a single lane of traffic and has one span with overall dimensions of 29.9 ft long by 18 ft wide with zero degrees of skew. The deck is comprised of continuous concrete decking with a thickness of 7.5 in. An elevation view and an end view of the bridge are shown in Figure A-2.



Figure A-2. Steel-Concrete Bridge 1: Elevation view (left) and end view (right)

The bridge consists of seven steel interior girders and two concrete exterior girders with spacing between adjacent girders of 2.3 ft for interior girders and 3.0 ft for exterior girders. The I cross-section girders are approximately 14.0 in. by 5.25 in. The rectangular concrete girders are approximately 18 in. by 9 in. Figure A-3 shows a typical cross-section and plan view of the bridge.

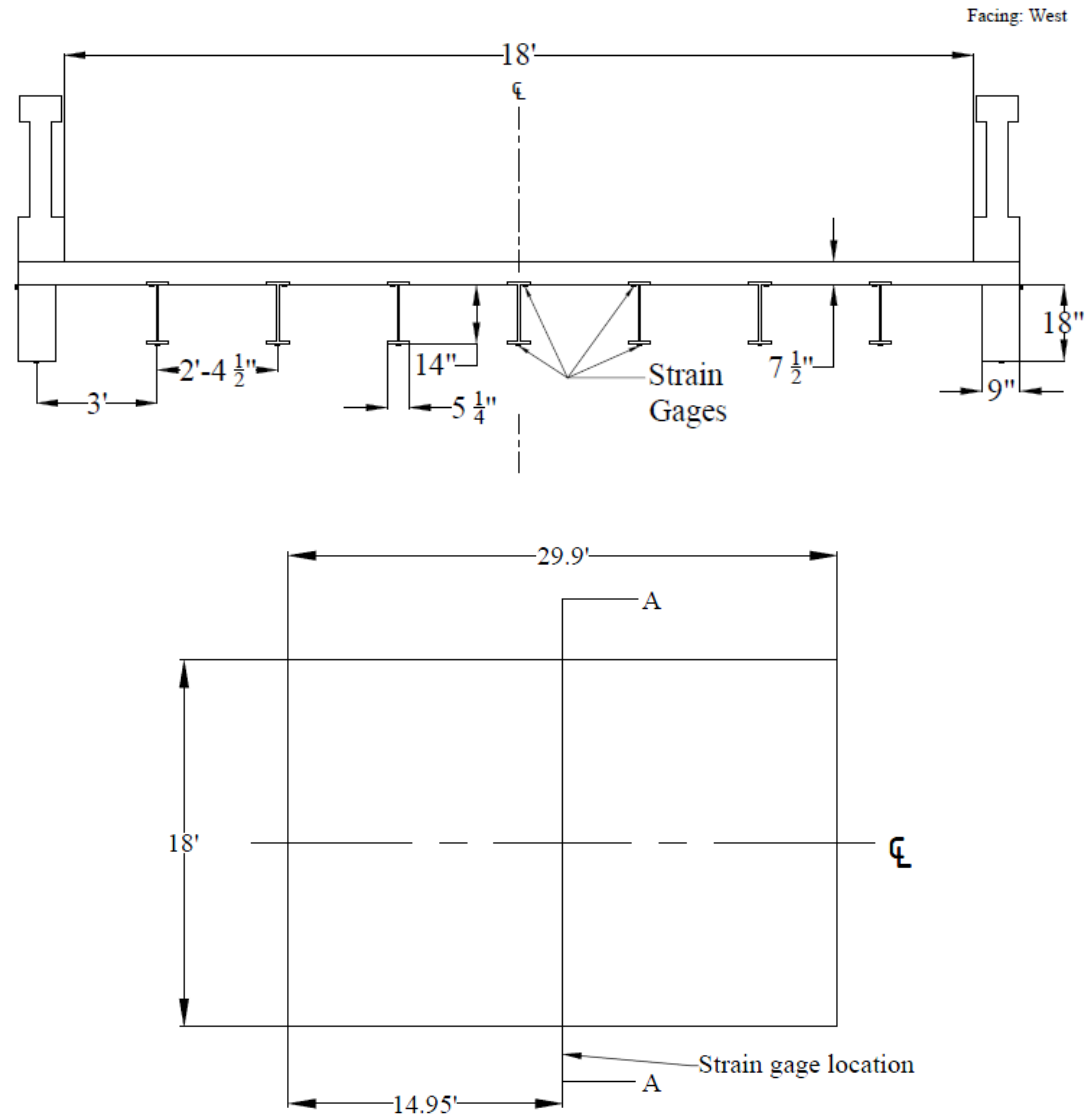


Figure A-3. Steel-Concrete Bridge 1: Cross-section A-A (top) and plan (bottom)

A.1.3 Field Testing

Field testing of this bridge was conducted for two reasons. First, field testing was conducted to determine experimental live load distribution factors (LLDFs) and dynamic impact factors for the individual bridge girders. Second, the field data were also used to calibrate analytical models, which were then used to conduct a detailed parametric study related to a wide variety of implements of husbandry. A description of field tests, the procedures followed, and sample field results are detailed in the following sections.

Field Inspections

According to the most recent field inspection report, the concrete deck of Steel-Concrete Bridge 1 is in fair condition with some spalling. The steel girders are in fair condition and show some signs of corrosion. These inspection-based observations were corroborated by the Iowa State University field testing team.

Instrumentation Plan

Given that the primary goal of the testing plan was to measure the live load response of the primary load-carrying members, a network of multiple strain gages was used to measure the strain under the weight of the vehicles. The strain gages were attached to the bottom and top of the girders at mid-span as shown in Figure A-3. The strain sensors used to conduct this testing were installed with a 3 in. gage length, and data were collected at a rate of 100 Hz during static testing and at 100 Hz during dynamic testing.

Test Load Paths

The vehicles utilized during field testing of this bridge consisted of four common farm vehicles and one typical highway truck. The vehicles included a terragator, a grain cart, a honey wagon with one tank, a honey wagon with two tanks, and a typical five-axle semi-truck. The individual axle loads, total weights, and lengths of the five vehicles used for field testing are summarized in Table A-1. As shown in Figure A-4, the configurations of the farm vehicles were notably different from that of the conventional highway truck.

Table A-1. Axle weight and total length of each testing vehicle

Farm Vehicles	Weight (lbs)					Total	Total Length (ft-in.)
	Front Axle	Rear Axle	Grain Wagon	Honey Wagon	Trailer		
Tractor Honey Wagon (one tank)	11,800	15,900	-	48,800	-	76,500	40'-8"
Tractor Honey Wagon (two tanks)	10,580	22,800	-	14,300 (front) 18,300 (rear)	-	68,900	63'-7"
Terragator	11,060	32,400	-	-	-	43,460	25'-7"
Tractor Grain Wagon	18,840	18,660	15,660	-	-	53,160	35'-2"
Semi-Truck	10,760	33,856	-	-	33,084	77,700	52'-2"



Honey Wagon



Honey Wagon - two tanks



Terragator



Tractor Grain Wagon



Semi Truck

Figure A-4. Farm vehicles used for field testing

During testing, the vehicles were driven across the bridge from north to south. In general, the centerlines of the bridge and vehicle were approximately aligned. Initial static load testing was completed with the vehicles traveling at approximately 3 mph such that the pseudo-static bridge response could be captured. Later, dynamic load testing was completed with the vehicles traveling at approximately 15 mph (maximum safe speed at the site).

Sample Field Results

Representative plots from static load testing, showing the strain experienced by one of the girders under all test vehicles, is shown in Figure A-5. It was observed that the girders at the center of the bridge experienced the maximum strain magnitudes as the test vehicles crossed the bridge.

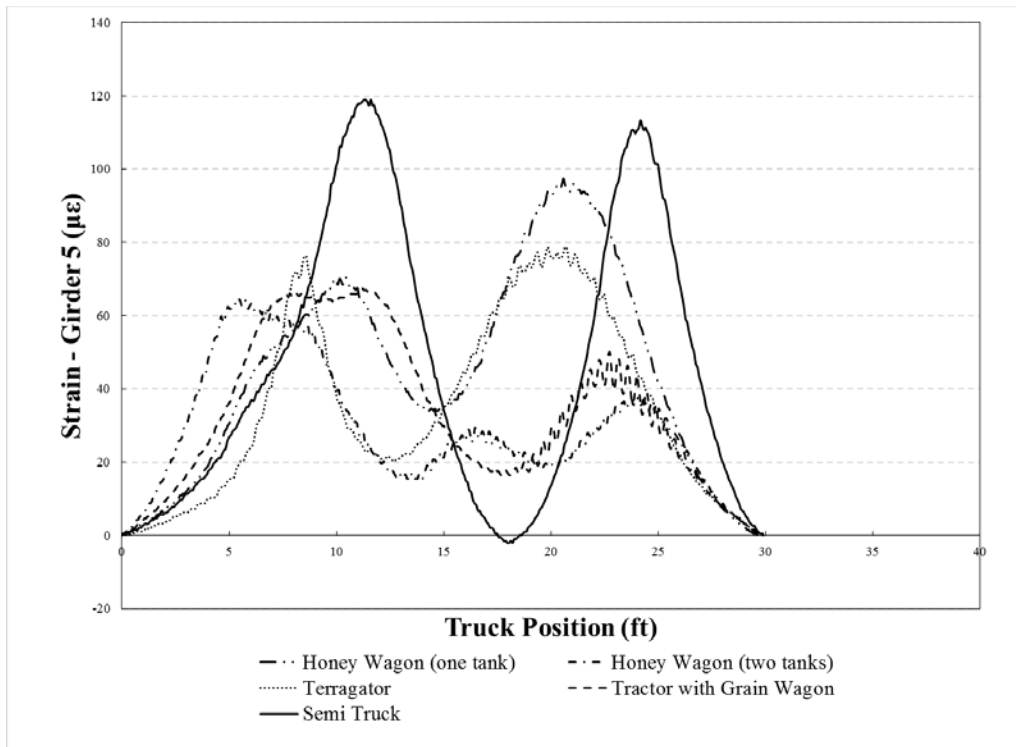


Figure A-5. Strain plot of a girder for all test vehicles for Steel-Concrete Bridge 1

The semi-truck normally results in higher strains compared to other farm vehicles, and this tendency can be seen in Figure A-5. These recorded strains were employed to calculate the field LLDFs for each girder based upon the following equation.

$$LLDF^f = \frac{\varepsilon^m \max i,t}{\sum_{i=1}^n \varepsilon^m \max i,t} \quad (1)$$

Where $LLDF^f$ is the field live load distribution factor and ϵ^m are the measured maximum strains for individual girders over time, respectively.

A representative plot showing the comparison between static and dynamic strain for one of the girders under a test vehicle is shown in Figure A-6.

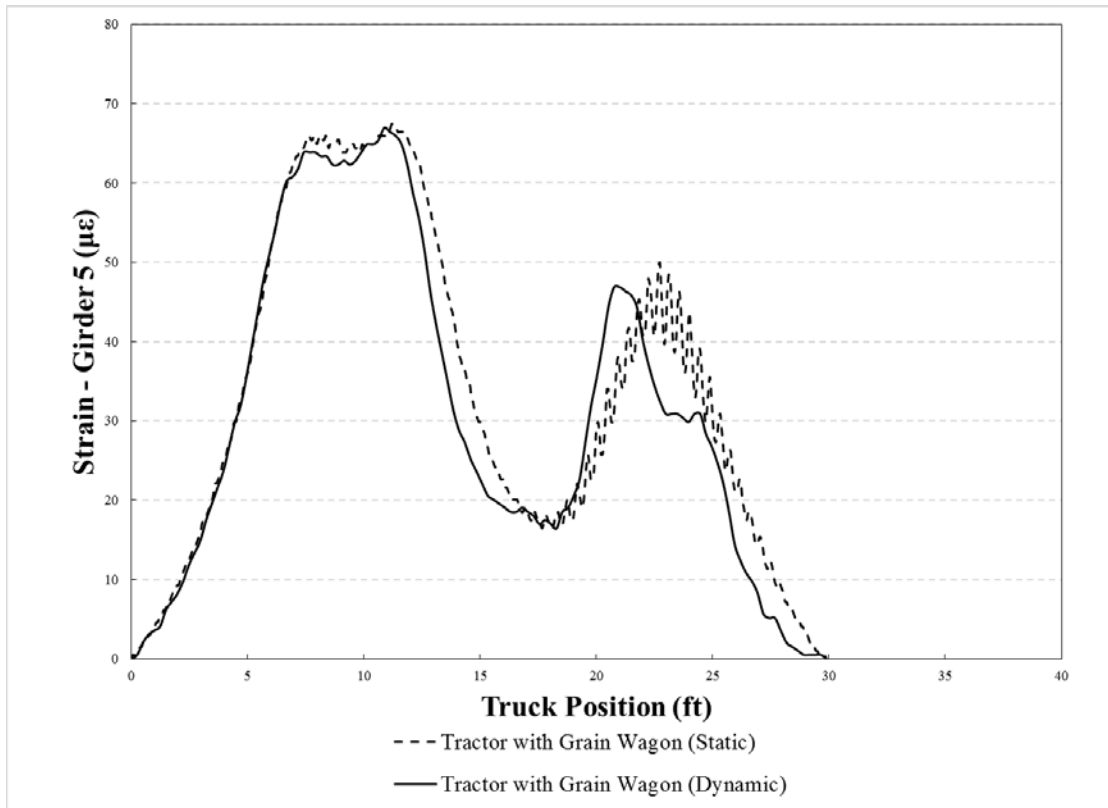


Figure A-6. Comparison between static and dynamic strain for Steel-Concrete Bridge 1

It was generally observed that the girders experience more strain under dynamic loads than under static loading. The strain values from dynamic load tests were utilized to calculate the dynamic amplification factors (DAFs) for each girder.

A.1.4 Analytical Modeling

In lieu of field testing with a large number of vehicles, finite element analysis (FEA) simulations were used to estimate LLDFs for other vehicle configurations. As a result, analytical LLDFs were determined based upon FEA simulations of over 121 different farm vehicles on Steel-Concrete Bridge 1. The FEA model was developed as described subsequently, and specific bridge information is presented in the following sections.

Model Generation

The bridge was initially modeled with the geometric and material properties taken directly from available bridge plans and/or field inspections using the BDI (Bridge Diagnostics, Inc.) finite element software WinGEN. A modulus of elasticity of 3200 ksi and 29000 ksi was used for all concrete and steel components in the model, respectively. The FEA model consisted of beam elements for the girders, shell elements for the deck, and rotational springs that simulated rotational restraint at the abutments and piers. Figure A-7 shows a representative model of the bridge.

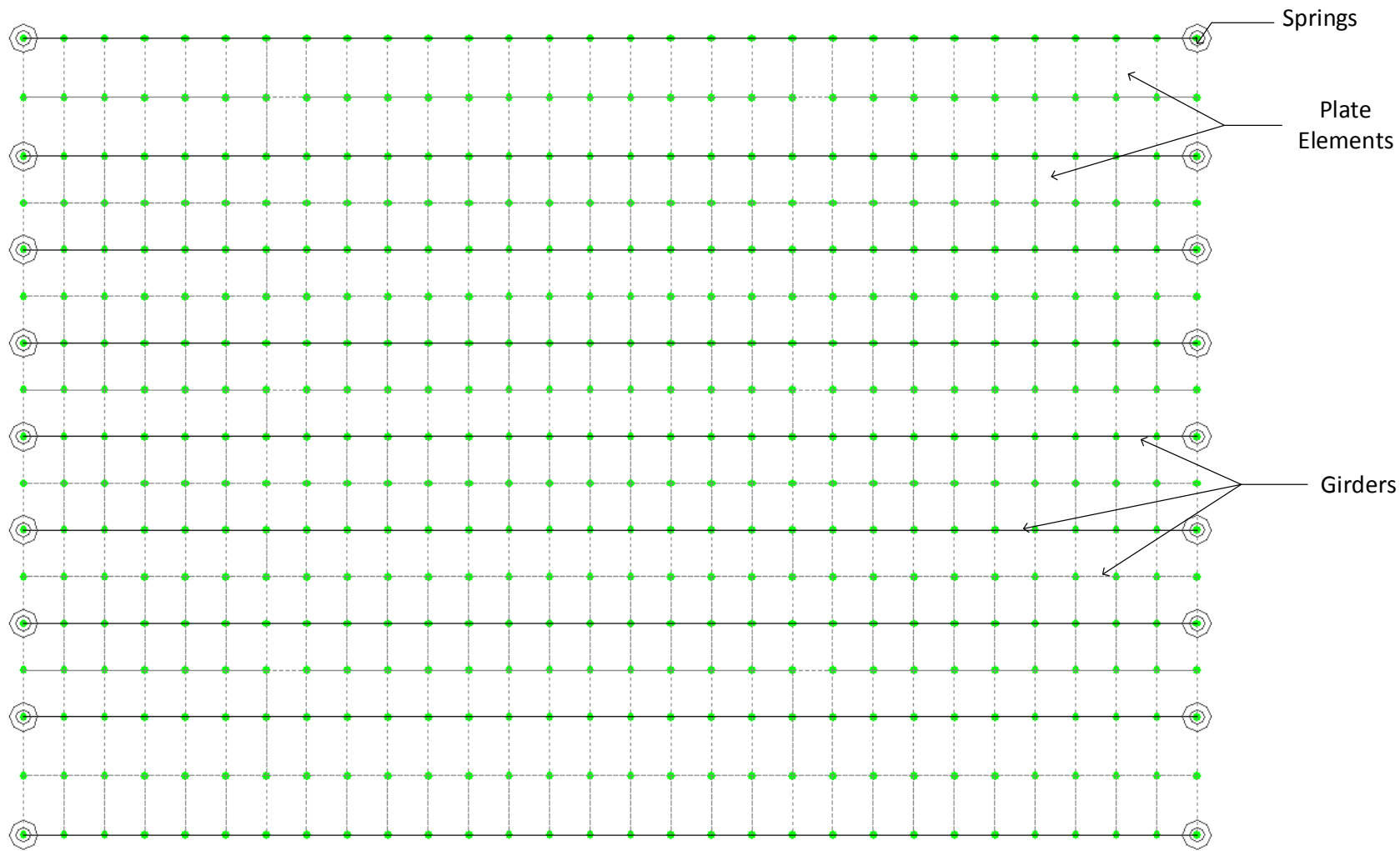


Figure A-7. Finite element model of Steel-Concrete Bridge 1

Model Calibration

To improve the model accuracy, a calibration process that identified the bridge properties that resulted in the lowest error was completed. Based upon similarities in the response and observed field condition, a single cross-section was considered for all the girders. Table A-2 summarizes the original and calibrated values for the various bridge components along with percent error and correlation coefficient values.

Table A-2. Model calibration for Steel-Concrete Bridge 1

Calibration Parameters	Bridge Components	Plan Value	Calibrated Value
Moment of Inertia, I (in ⁴)	Exterior Girder	17,760	14,160
	Intermediate Girder	1,296	1,128
	Interior Girder	1,320	1,128
Young's Modulus (ksi)	Deck	3,191	2,176
Rotational Stiffness, kr (Kips-in/rad)	Exterior Abutment	0	9.73 x 10 ⁵
	Interior Abutment	0	0.487
Statistical Results	Percent Error		3.9%
	Correlation Coefficients		0.98

Once model calibration was completed, the analytical model was loaded with 121 farm vehicles that covered a wide range of axle spacings, weights, and gage widths. The analytical strain response was then used to compute analytical LLDFs for each simulation vehicle using Equation (1).

To interpret the results, the LLDFs of the girders were grouped together as either interior or exterior girder LLDFs. Statistical control limits for the interior and exterior girder LLDFs were determined from cumulative distribution function (CDF) curves defined to be at the 95% confidence thresholds.

A.1.5 Results

The envelopes of LLDFs for Bridge 1 are presented in Figure A-8 for both the field and analytical LLDFs for each girder. In addition to the envelopes, the AASHTO LLDFs and statistical control limits for each group of interior and exterior girders are also shown.

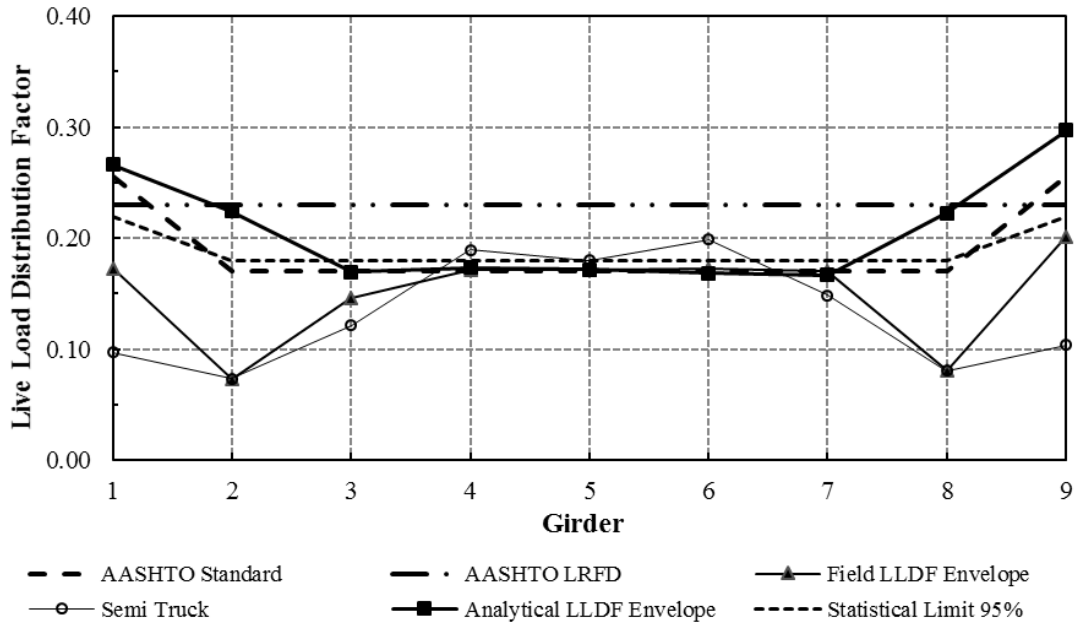


Figure A-8. LLDFs for Steel-Concrete Bridge 1

It appears that the analytical LLDF envelopes for the interior girders are smaller than those from the AASHTO LRFD specifications. The peak value of the analytical exterior girder LLDFs was observed in G9, which has an LLDF of 0.30, while that of the interior girders was found in G2, which has an LLDF of 0.22. The statistical limits for the interior girder group also show smaller values than the AASHTO LRFD specifications. The field LLDF envelope for this bridge has similar values to that of the semi-truck for most of the girders, indicating that farm vehicles result in similar values of LLDFs compared to those from the conventional highway vehicle.

A.2 Steel-Concrete Bridge 2

This mini test and evaluation report documents the results of field testing and subsequent analysis of a steel girder bridge with a concrete deck (Steel-Concrete Bridge 2) under multiple implements of husbandry. For completeness, this mini-report includes a description of the bridge, a description of the live load testing procedures followed, sample data, a description of analytical modeling, plots of analytical results, and a discussion of the overall behavior of the steel girder bridge under implements of husbandry.

A.2.1 Background

The steel-concrete bridge described here is known in the National Bridge Inventory (NBI) database as Bridge 76891 and will be henceforth be referred to as Steel-Concrete Bridge 2. The bridge is located about 4 miles northeast of Madrid, on 290th Avenue over Big Creek, in Boone County, Iowa. Figure A-9 shows the general location of the bridge.



Map: ©Google 2014

Figure A-9. Location overview of Steel-Concrete Bridge 2

A.2.2 Bridge Description

Steel-Concrete Bridge 2 is open to two-lane traffic and has one span with overall dimensions of 39.7 ft long by 26.9 ft wide with zero degrees of skew. The deck is comprised of continuous concrete decking with a thickness of 7.5 in. An elevation view and an end view of the bridge are shown in Figure A-10.



Figure A-10. Steel-Concrete Bridge 2: Elevation view (left) and end view (right)

The bridge consists of 10 steel interior girders and 2 concrete exterior girders with spacing between adjacent girders of 2.3 ft for interior girders and 3.3 ft for exterior girders. The I cross-section steel girders are approximately 20 in. by 6 in. and the concrete I girders are

approximately 32 in. by 10 in. Figure A-11 shows a typical cross-section and plan view of the bridge.

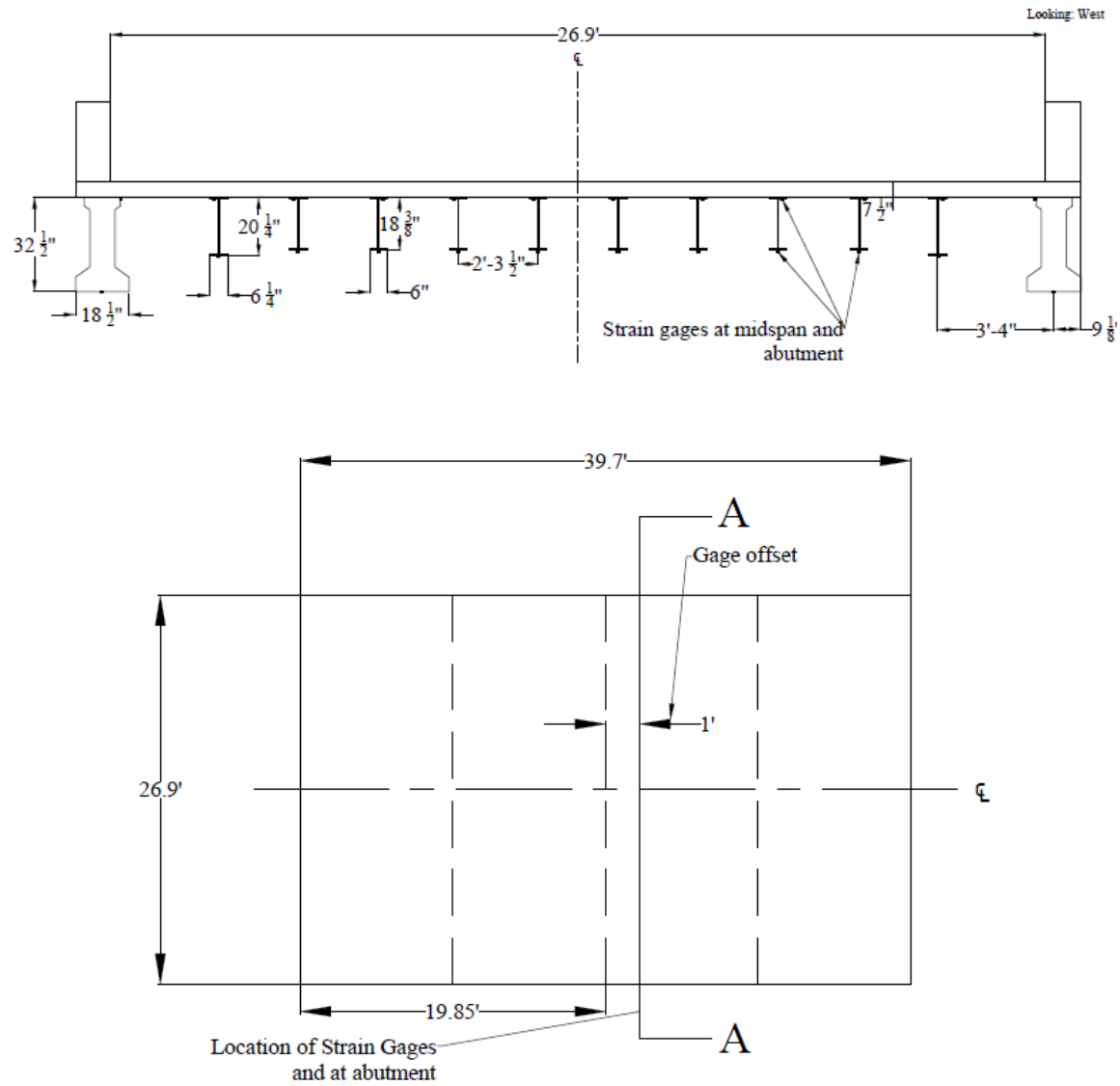


Figure A-11. Steel-Concrete Bridge 2: Cross-section A-A (top) and plan (bottom)

A.2.3 Field Testing

Field testing of this bridge was conducted for two reasons. First, field testing was conducted to determine experimental live load distribution factors (LLDFs) and dynamic impact factors for the individual bridge girders. Second, these field data were also used to calibrate analytical models, which were then used to conduct a detailed parametric study related to a wide variety of implements of husbandry. A description of field tests, the procedures followed, and sample field results are detailed in the following sections.

Field Inspections

According to the most recent field inspection report, the concrete deck of Steel-Concrete Bridge 2 is in satisfactory condition. The steel girders are in good condition. These inspection-based observations were corroborated by the Iowa State University field testing team.

Instrumentation Plan

Given that the primary goal of the testing plan was to measure the live load response of the primary load-carrying members, a network of multiple strain gages was used to measure the strain under the weight of the vehicles. The strain gages were attached to the bottom and the top of the girders one foot off mid-span and at the abutment as shown in Figure A-11. The strain sensors used to conduct this testing were installed with a 3 in. gage length, and data were collected at a rate of 100 Hz during static testing and at 100 Hz during dynamic testing.

Test Load Paths

The vehicles utilized during field testing of this bridge consisted of four common farm vehicles and one typical highway truck. The vehicles included a terragator, a grain cart, a honey wagon with one tank, a honey wagon with two tanks, and a typical five-axle semi-truck. The individual axle loads, total weights, and lengths of the five vehicles used for field testing are summarized in Table A-3. As shown in Figure A-12, the configurations of the farm vehicles were notably different from that of the conventional highway truck.

Table A-3. Axle weight and total length of each testing vehicle

Farm Vehicles	Weight (lbs)					Total	Total Length (ft-in.)
	Front Axle	Rear Axle	Grain Wagon	Honey Wagon	Trailer		
Tractor Honey Wagon (one tank)	11,800	15,900	-	48,800	-	76,500	40'-8"
Tractor Honey Wagon (two tanks)	10,580	22,800	-	14,300 (front) 18,300 (rear)	-	68,900	63'-7"
Terragator	11,060	32,400	-	-	-	43,460	25'-7"
Tractor Grain Wagon	18,840	18,660	15,660	-	-	53,160	35'-2"
Semi-Truck	10,760	33,856	-	-	33,084	77,700	52'-2"



Honey Wagon



Honey Wagon- two tanks



Terragator



Tractor Grain Wagon



Semi Truck

Figure A-12. Farm vehicles used for field testing

During testing the vehicles were driven across the bridge from north to south. In general the centerlines of the bridge and vehicle were approximately aligned. Initial static load testing was completed with the vehicles traveling at approximately 3 mph such that the pseudo-static bridge response could be captured. Later, dynamic load testing was completed with the vehicles traveling at approximately 15 mph (maximum safe speed at the site).

Sample Field Results

Representative plots from static load testing showing the strain experienced by one of the girders under all test vehicles is shown in Figure A-13. It was observed that the girders at the center of the bridge experienced the maximum strain magnitudes as the test vehicles crossed the bridge.

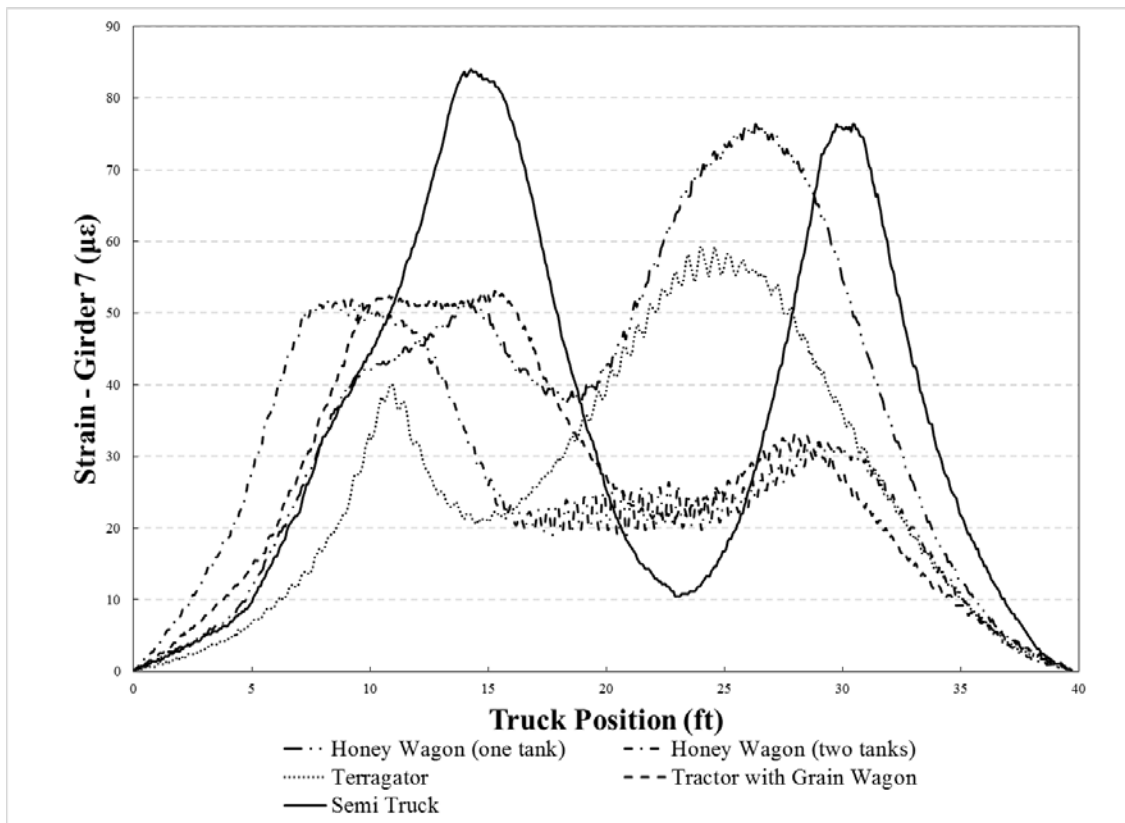


Figure A-13. Strain plot of a girder for all test vehicles for Steel-Concrete Bridge 2

The semi-truck normally results in higher strains compared to other farm vehicles, and this tendency can be seen in Figure A-13. These recorded strains were employed to calculate the field LLDFs for each girder based upon the following equation.

$$LLDF^f = \frac{\varepsilon^m \max_{i,t}}{\sum_{i=1}^n \varepsilon^m \max_{i,t}} \quad (1)$$

Where $LLDF^f$ is the field live load distribution factor and ϵ^m are the measured maximum strains for individual girders over time, respectively.

A representative plot showing the comparison between static and dynamic strain for one of the girders under a test vehicle is shown in Figure A-14. It was generally observed that the girders experience more strain under dynamic loads than under static loading. The strain values from dynamic load tests were utilized to calculate the dynamic amplification factors (DAFs) for each girder.

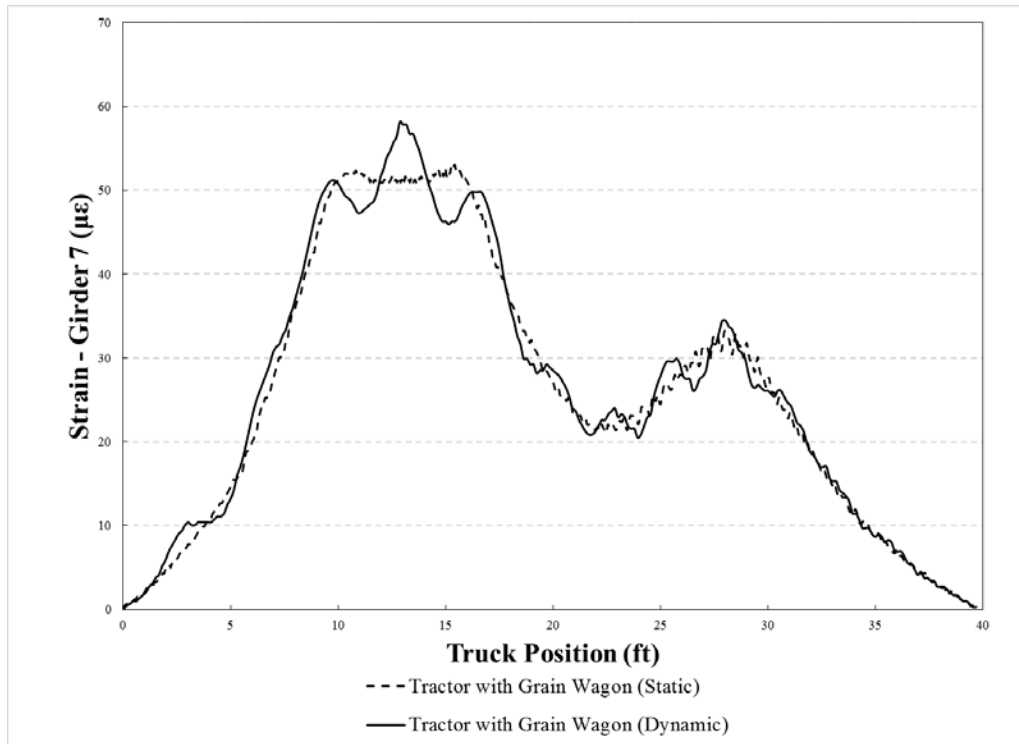


Figure A-14. Comparison between static and dynamic strain for Steel-Concrete Bridge 2

A.2.4 Analytical Modeling

In lieu of field testing with a large number of vehicles, finite element analysis (FEA) simulations were used to estimate LLDFs for other vehicle configurations. As a result, analytical LLDFs were determined based upon FEA simulations of over 121 different farm vehicles on Steel-Concrete Bridge 2. The FEA model was developed as described subsequently, and specific bridge information is presented in the following sections.

Model Generation

The bridge was initially modeled with the geometric and material properties taken directly from available bridge plans and/or field inspections using the BDI (Bridge Diagnostics, Inc.) finite element software WinGEN. A modulus of elasticity of 3200 ksi and 29000 ksi was used for all

concrete and steel components in the model, respectively. The FEA model consisted of beam elements for the girders, shell elements for the deck, and rotational springs that simulated rotational restraint at the abutments and piers. Figure A-15 shows a representative model of the bridge.

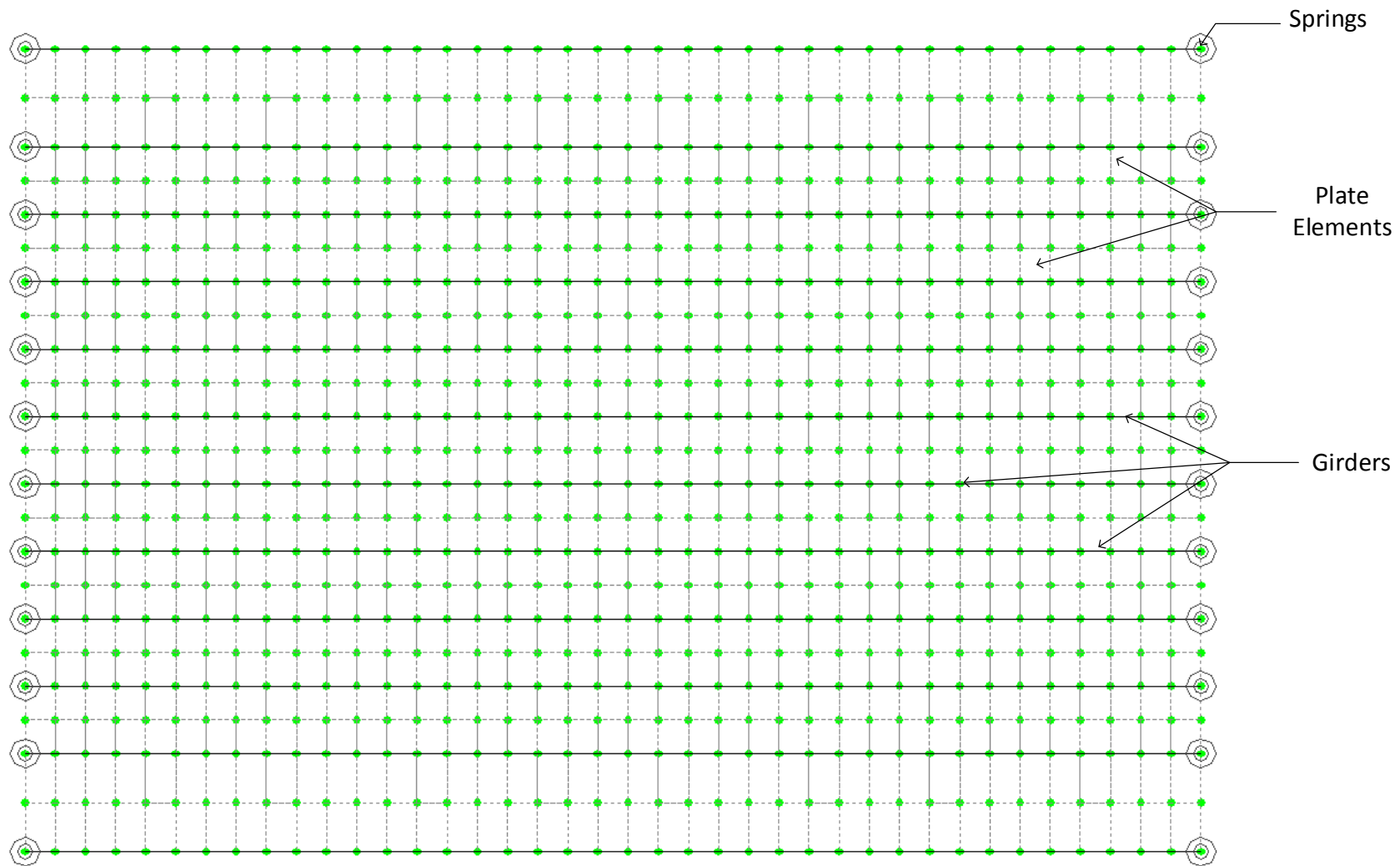


Figure A-15. Finite element model of Steel-Concrete Bridge 2

Model Calibration

To improve the model accuracy, a calibration process that identified the bridge properties that resulted in the lowest error was completed. Based upon similarities in the response and observed field condition, a single cross-section was considered for all the girders. Table A-4 summarizes the original and calibrated values for the various bridge components along with percent error and correlation coefficient values.

Table A-4. Model calibration for Steel-Concrete Bridge 2

Calibration Parameters	Bridge Components	Plan Value	Calibrated Value
Moment of Inertia, I (in ⁴)	Exterior Girder	160,800	194,400
	Intermediate Girder	2,232	1,752
	Interior Girder	3,600	4,080
Young's Modulus (ksi)	Deck	3,191	3,916
Rotational Stiffness, kr (Kips-in/rad)	Exterior Abutment	0	97,354
	Interior Abutment	0	37,172
Statistical Results	Percent Error		2.8%
	Correlation Coefficients		0.99

Once model calibration was completed, the analytical model was loaded with 121 farm vehicles covering a wide range of axle spacings, weights, and gage widths. The analytical strain response was then used to compute analytical LLDFs for each simulation vehicle using Equation (1).

To interpret the results, the LLDFs of the girders were grouped together as either interior or exterior girder LLDFs. Statistical control limits for the interior and exterior girder LLDFs were determined from cumulative distribution function (CDF) curves defined to be at the 95% confidence thresholds.

A.2.5 Results

The envelopes of LLDFs for Steel-Concrete Bridge 2 are presented in Figure A-16 for both the field and analytical LLDFs for each girder. In addition to the envelopes, the AASHTO LLDFs and statistical control limits for each group of interior and exterior girders are also shown.

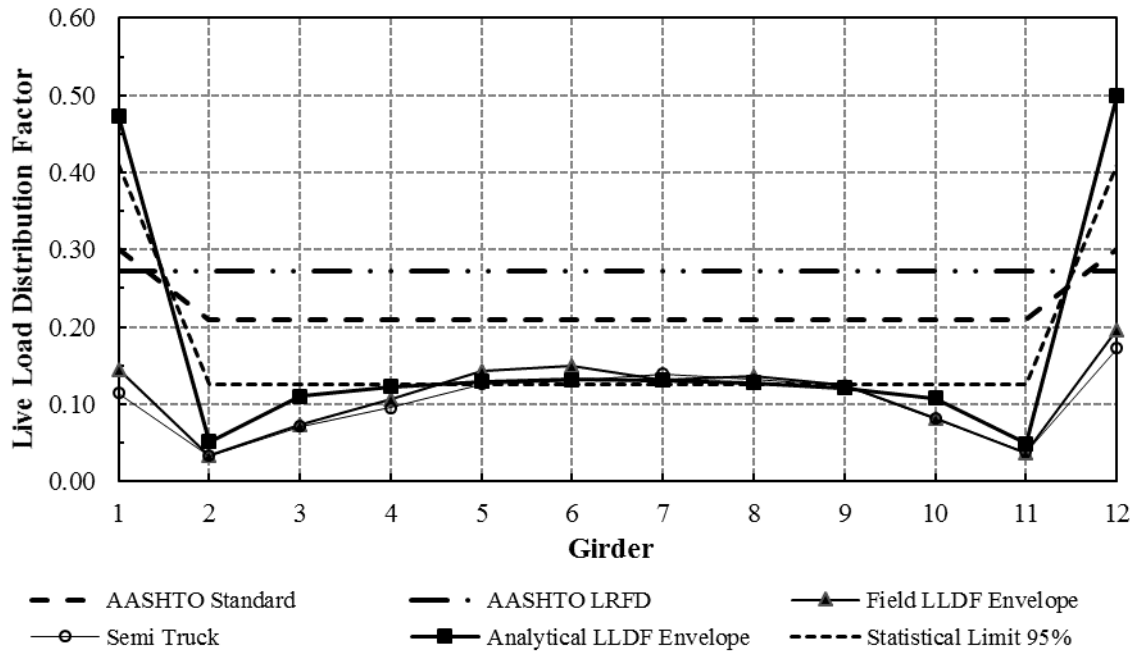


Figure A-16. LLDFs for Steel-Concrete Bridge 2

It appears that the analytical LLDF envelope for the interior girders are much smaller than those from the AASHTO standard and LRFD specifications. The peak value of the analytical exterior girder LLDFs was observed in G12, which has an LLDF of 0.50, while that of the interior girders was found in G6, which has an LLDF of 0.13. The statistical limits for the interior girder group also show smaller values than the AASHTO specifications. The field LLDF envelope has similar values to that of the semi-truck for most of the girders, indicating for this bridge that farm vehicles result in similar values of LLDFs compared to those from the conventional highway vehicle.

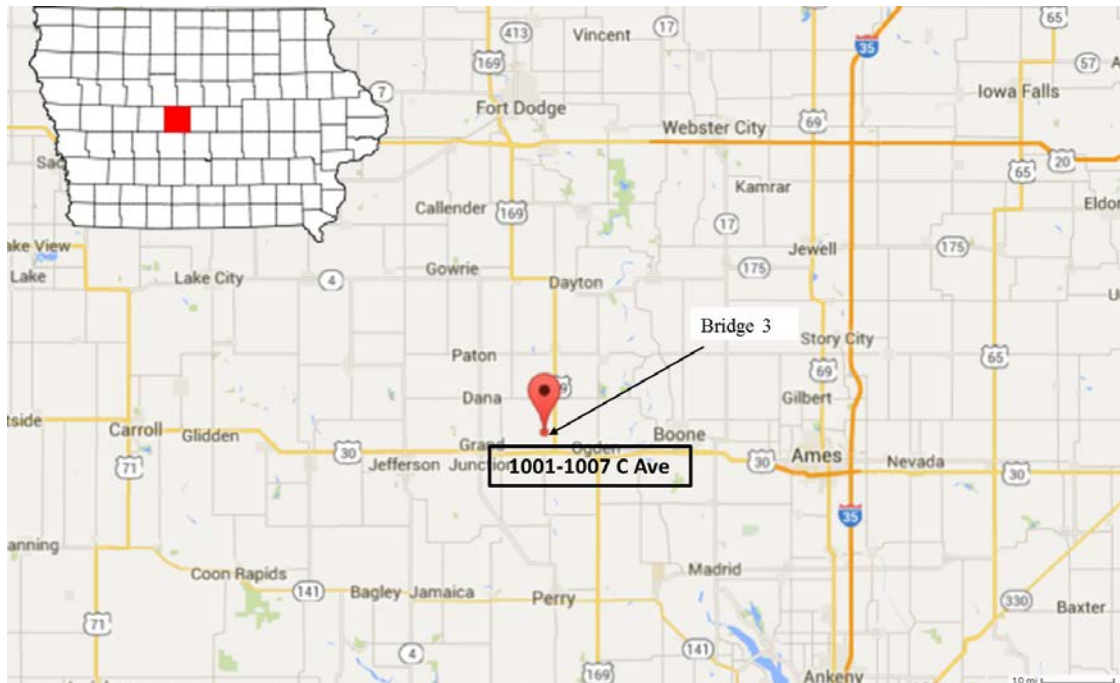
A.3 Steel-Concrete Bridge 3

This mini test and evaluation report documents the results of field testing and subsequent analysis of a steel girder bridge with a concrete deck (Steel-Concrete Bridge 3) under multiple implements of husbandry. For completeness, this mini-report includes a description of the bridge, a description of the live load testing procedures followed, sample data, a description of analytical modeling, plots of analytical results, and a discussion of the overall behavior of the steel girder bridge under implements of husbandry.

A.3.1 Background

The steel-concrete bridge described here is known in the National Bridge Inventory (NBI) database as Bridge 78060 and will be henceforth be referred to as Steel-Concrete Bridge 3. The

bridge is located about 2 miles north of Beaver, on C Avenue, in Boone County, Iowa. Figure A-17 shows the general location of the bridge.



Map: ©Google 2014

Figure A-17. Location overview of Steel-Concrete Bridge 3

A.3.2 Bridge Description

Steel-Concrete Bridge 3 is open to a single lane of traffic and has one span with overall dimensions of 36.1 ft long by 18 ft wide with zero degrees of skew. The deck is comprised of continuous concrete decking with a thickness of 7.5 in. An elevation view and an end view of the bridge are shown in Figure A-18.



Figure A-18. Steel-Concrete Bridge 3: Elevation view (left) and end view (right)

The bridge consists of seven interior steel girders and two exterior concrete girders with a spacing between adjacent girders of 2.3 ft. The I cross-section steel girders are approximately 18.0 in. by 6.0 in. The concrete girders are approximately 17.0 in. by 12.5 in. Figure A-19 shows a typical cross-section and plan view of the bridge.

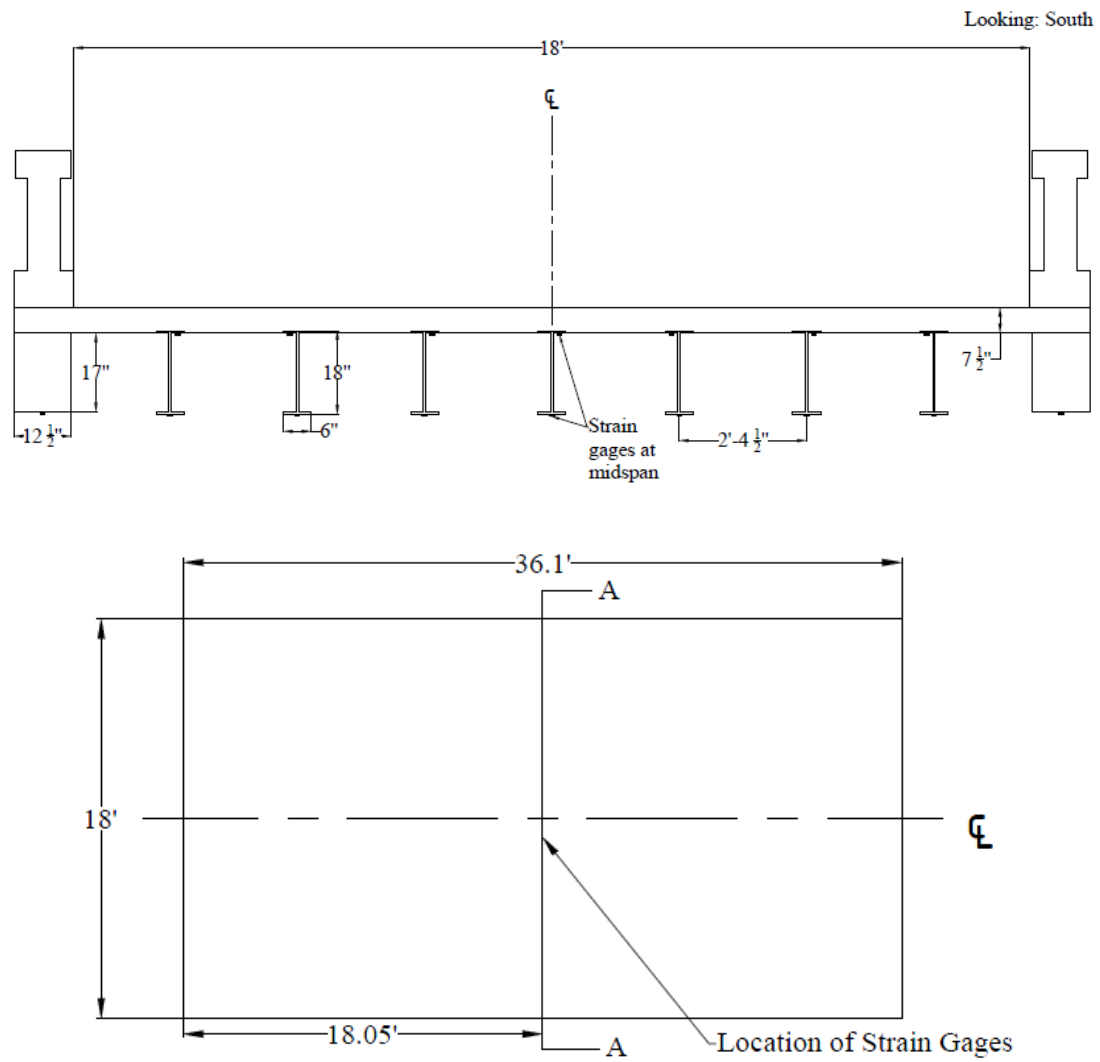


Figure A-19. Steel-Concrete Bridge 3: Cross-section A-A (top) and plan (bottom)

A.3.3 Field Testing

Field testing of this bridge was conducted for two reasons. First, field testing was conducted to determine experimental live load distribution factors (LLDFs) and dynamic impact factors for the individual bridge girders. Second these field data were also used to calibrate analytical models, which were then used to conduct a detailed parametric study related to a wide variety of implements of husbandry. A description of field tests, the procedures followed, and sample field results are detailed in the following sections.

Field Inspections

According to the most recent field inspection report, the concrete deck of Steel-Concrete Bridge 3 is in poor condition with cracking and leaching. The steel girders are in poor condition. These inspection-based observations were corroborated by the Iowa State University field testing team.

Instrumentation Plan

Given that the primary goal of the testing plan was to measure the live load response of the primary load-carrying members, a network of multiple strain gages was used to measure the strain under the weight of the vehicles. The strain gages were attached to the bottom and top of the girders at mid-span as shown in Figure A-19. The strain sensors used to conduct this testing were installed with a 3 in. gage length, and data were collected at a rate of 100 Hz during static testing and at 100 Hz during dynamic testing.

Test Load Paths

The vehicles utilized during field testing of this bridge consisted of four common farm vehicles and one typical highway truck. The farm vehicles included a terragator, a grain cart, a honey wagon with one tank, a honey wagon with two tanks, and a typical five-axle semi-truck. The individual axle loads, total weights, and lengths of the five vehicles used for field testing are summarized in Table A-5. As shown in Figure A-20, the configurations of the farm vehicles were notably different from that of the conventional highway truck.

Table A-5. Axle weight and total length of each testing vehicle

Farm Vehicles	Weight (lbs)					Total	Total Length (ft-in.)
	Front Axle	Rear Axle	Grain Wagon	Honey Wagon	Trailer		
Tractor Honey Wagon (one tank)	11,800	15,900	-	48,800	-	76,500	40'-8"
Tractor Honey Wagon (two tanks)	10,580	22,800	-	14,300 (front) 18,300 (rear)	-	68,900	63'-7"
Terragator	11,060	32,400	-	-	-	43,460	25'-7"
Tractor Grain Wagon	18,840	18,660	15,660	-	-	53,160	35'-2"
Semi-Truck	10,760	33,856	-	-	33,084	77,700	52'-2"



Honey Wagon - one tank



Honey Wagon- two tanks



Terragator



Tractor Grain Wagon



Semi Truck

Figure A-20. Farm vehicles used for field testing

During testing the vehicles were driven across the bridge from north to south. In general the centerlines of the bridge and vehicle were approximately aligned. Initial static load testing was completed with the vehicles traveling at approximately 3 mph such that the pseudo-static bridge response could be captured. Later, dynamic load testing was completed with the vehicles traveling at approximately 15 mph (maximum safe speed at the site).

Sample Field Results

Representative plots from static load testing showing the strain experienced by one of the girders under all test vehicles is shown in Figure A-21. It was observed that the girders at the center of the bridge experienced the maximum strain magnitudes as the test vehicles crossed the bridge.

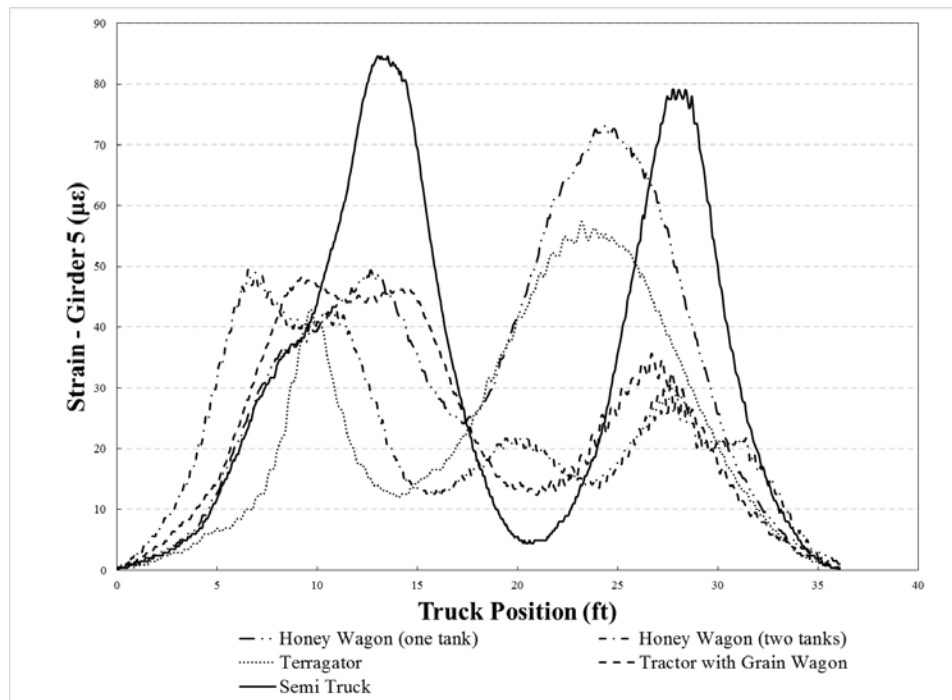


Figure A-21. Strain plot of a girder for all test vehicles for Steel-Concrete Bridge 3

The semi-truck normally results in higher strains compared to other farm vehicles, and this tendency can be seen in Figure A-21. These recorded strains were employed to calculate the field LLDFs for each girder based upon the following equation.

$$LLDF^f = \frac{\epsilon^m \max i,t}{\sum_{i=1}^n \epsilon^m \max i,t} \quad (1)$$

Where $LLDF^f$ is the field live load distribution factor and ϵ^m are the measured maximum strains for individual girders over time, respectively.

A representative plot showing the comparison between static and dynamic strain for one of the girders under a test vehicle is shown in Figure A-22. It was generally observed that the girders experience more strain under dynamic loads than under static loading. The strain values from dynamic load tests were utilized to calculate the dynamic amplification factors (DAFs) for each girder.

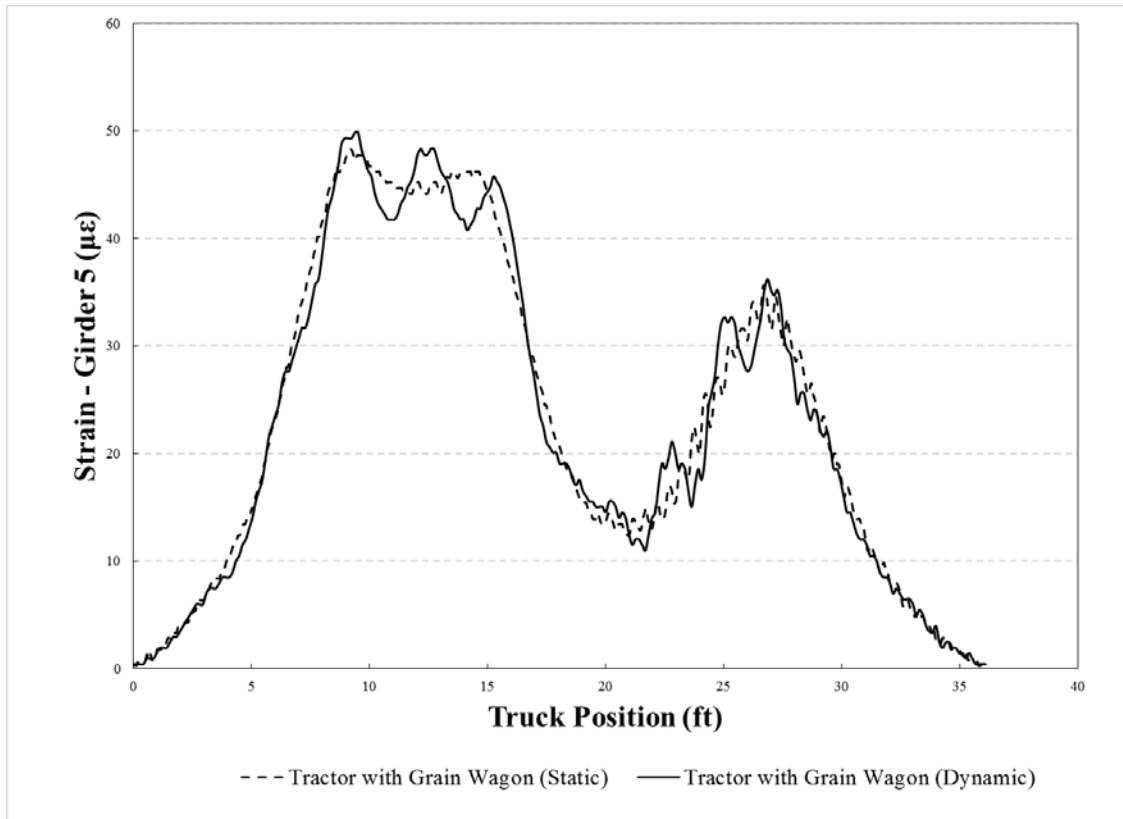


Figure A-22. Comparison between static and dynamic strain for Steel-Concrete Bridge 3

A.3.4 Analytical Modeling

In lieu of field testing with a large number of vehicles, finite element analysis (FEA) simulations were used to estimate LLDFs for other vehicle configurations. As a result, analytical LLDFs were determined based upon FEA simulations of over 121 different farm vehicles on Steel-Concrete Bridge 3. The FEA model was developed as described subsequently, and specific bridge information is presented in the following sections.

Model Generation

The bridge was initially modeled with the geometric and material properties taken directly from available bridge plans and/or field inspections using the BDI (Bridge Diagnostics, Inc.) finite element software WinGEN. A modulus of elasticity of 3200 ksi and 29000 ksi was used for all concrete and steel components in the model, respectively. The FEA model consisted of beam

elements for the girders, shell elements for the deck, and rotational springs that simulated rotational restraint at the abutments and piers. Figure A-23 shows a representative model of the bridge.

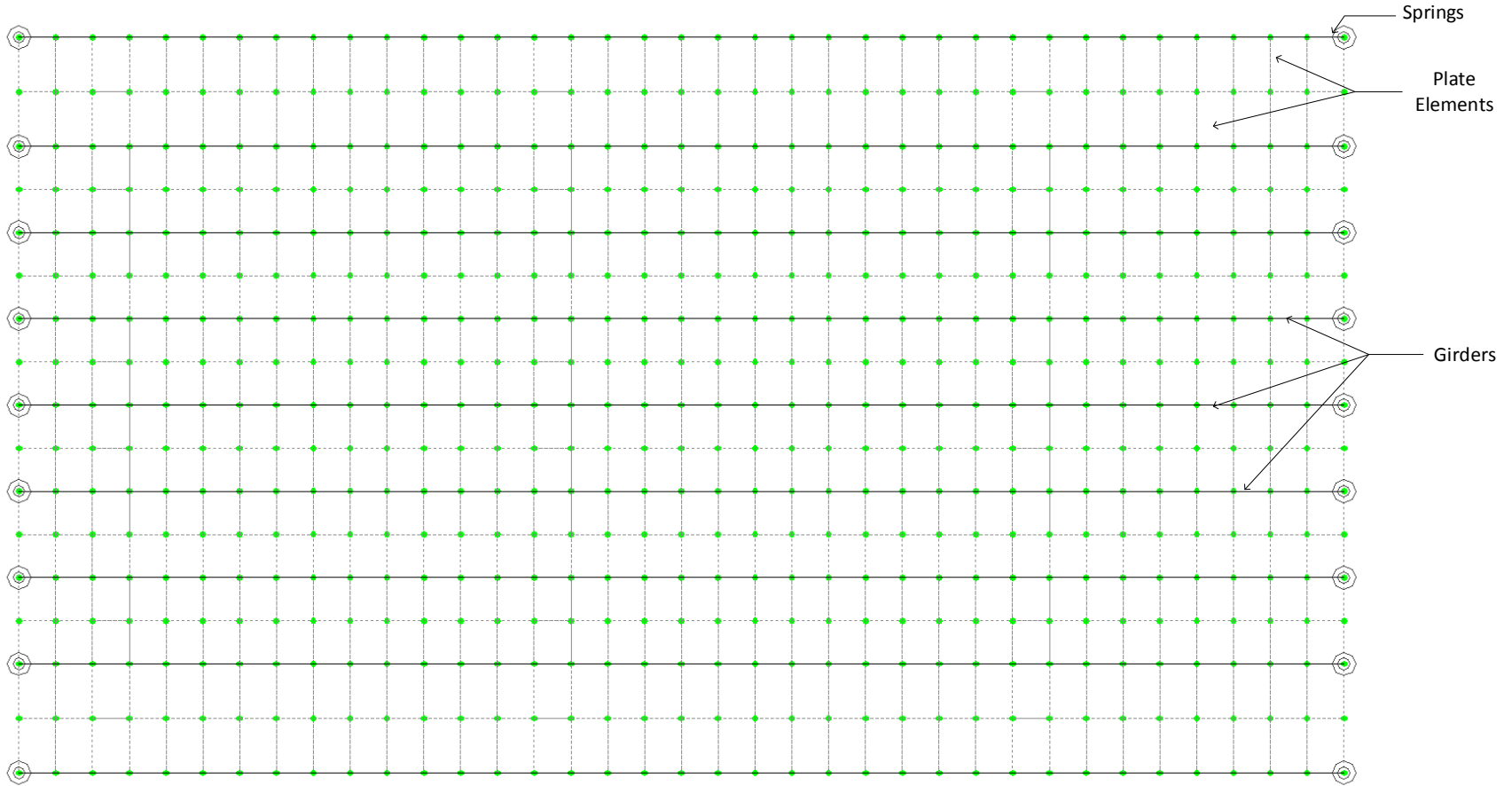


Figure A-23. Finite element model of Steel-Concrete Bridge 3

Model Calibration

To improve the model accuracy, a calibration process that identified the bridge properties that resulted in the lowest error was completed. Based upon similarities in the response and observed field condition, a single cross-section was considered for all the girders. Table A-6 summarizes the original and calibrated values for the various bridge components along with percent error and correlation coefficient values.

Table A-6. Model calibration for Steel-Concrete Bridge 3

Calibration Parameters	Bridge Components	Plan Value	Calibrated Value
Moment of Inertia, I (in ⁴)	Exterior Girder	33,600	40,800
	Intermediate Girder	1,704	2,112
	Interior Girder	1,704	1,560
Young's Modulus (ksi)	Deck	3,191	4,061
Rotational Stiffness, kr (Kips-in/rad)	Exterior Abutment	0	1.86 x 10 ⁶
	Interior Abutment	0	1.86 x 10 ⁶
Statistical Results	Percent Error		4.4%
	Correlation Coefficients		0.98

Once model calibration was completed, the analytical model was loaded with 121 farm vehicles covering a wide range of axle spacings, weights, and gage widths. The analytical strain response was then used to compute analytical LLDFs for each simulation vehicle using Equation (1).

To interpret the results, the LLDFs of the girders were grouped together as either interior or exterior girder LLDFs. Statistical control limits for the interior and exterior girder LLDFs were determined from cumulative distribution function (CDF) curves defined to be at the 95% confidence thresholds.

A.3.5 Results

The envelopes of LLDFs for Steel-Concrete Bridge 3 are presented in Figure A-24 for both the field and analytical LLDFs for each girder. In addition to the envelopes, the AASHTO LLDFs and statistical control limits for each group of interior and exterior girders are also shown.

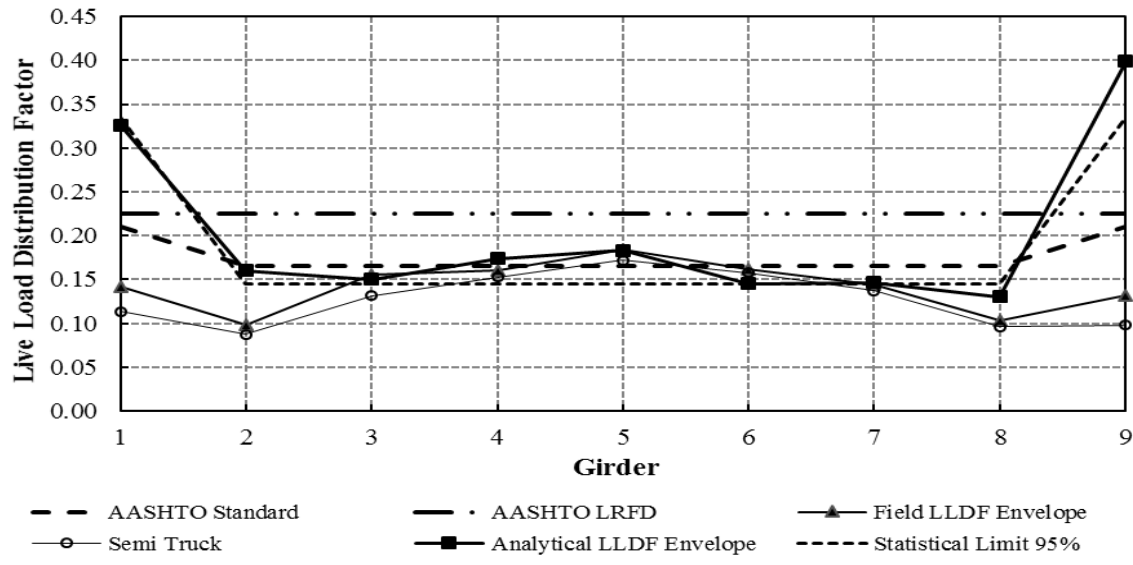


Figure A-24. LLDFs for Steel-Concrete Bridge 3

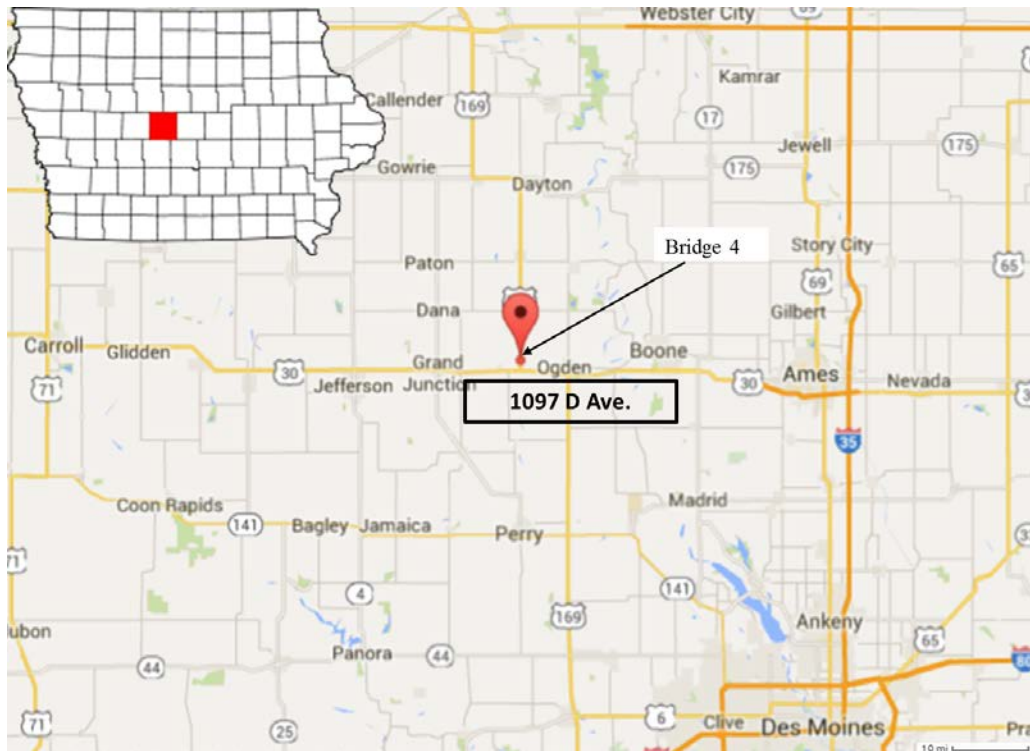
It appears that the analytical LLDF envelope for the interior girders are smaller than those from the AASHTO LRFD specifications. The peak value of the analytical exterior girder LLDFs was observed in G9, which has an LLDF of 0.40, while that of the interior girders was found in G5, which has an LLDF of 0.18. The statistical limits for interior girders also show smaller values than the AASHTO specifications. The field LLDF envelope has similar values to that of the semi-truck for most of the girders, indicating for this bridge that farm vehicles result in similar values of LLDFs compared to those from the conventional highway vehicle.

A.4 Steel-Concrete Bridge 4

This mini test and evaluation report documents the results of field testing and subsequent analysis of a steel girder bridge with a concrete deck (Steel-Concrete Bridge 4) under multiple implements of husbandry. For completeness, this mini-report includes a description of the bridge, a description of the live load testing procedures followed, sample data, a description of analytical modeling, plots of analytical results, and a discussion of the overall behavior of the steel girder bridge under implements of husbandry.

A.4.1 Background

The steel-concrete bridge described here is known in the National Bridge Inventory (NBI) database as Bridge 78100 and will be henceforth be referred to as Steel-Concrete Bridge 4. The bridge is located about 3 miles northeast of Beaver, on D Avenue over Middle Beaver Creek, in Boone County, Iowa. Figure A-25 shows the general location of the bridge.



Map: ©Google 2014

Figure A-25. Location overview of Steel-Concrete Bridge 4

A.4.2 Bridge Description

Steel-Concrete Bridge 4 is open to one lane of traffic and has one span with overall dimensions of 37 ft long by 19.4 ft wide with zero degrees of skew. The deck is comprised of continuous concrete decking with a thickness of 7.5 in. An elevation view and an end view of the bridge are shown in Figure A-26.



Figure A-26. Steel-Concrete Bridge 4: Elevation view (left) and end view (right)

The bridge consists of five steel girders with spacing between adjacent girders of 4.9 ft. The I cross-section girders are approximately 23.5 in. by 7 in. Figure A-27 shows a typical cross-section and plan view of the bridge.

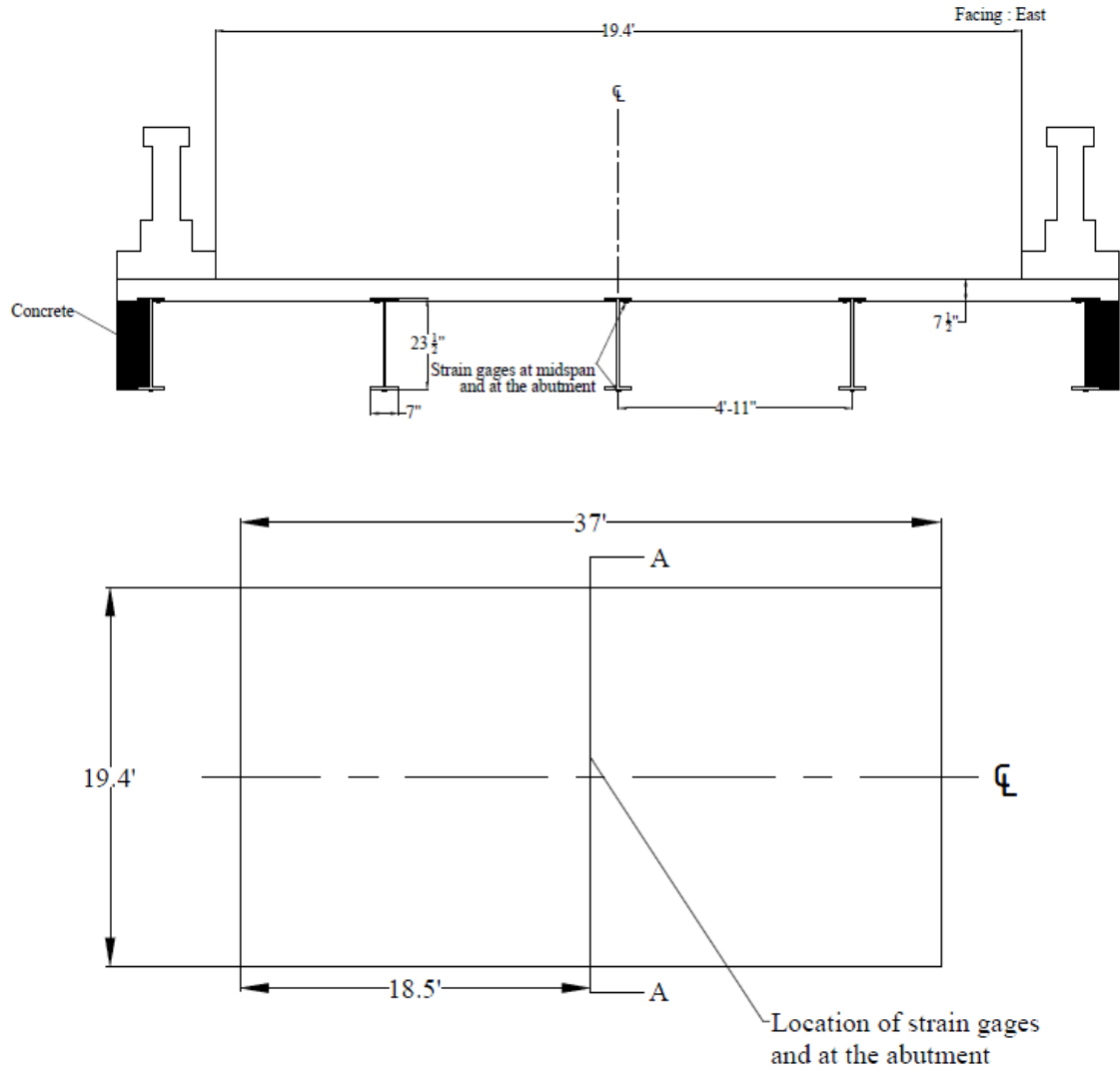


Figure A-27. Steel-Concrete Bridge 4: Cross-section A-A (top) and plan (bottom)

A.4.3 Field Testing

Field testing of this bridge was conducted for two reasons. First, field testing was conducted to determine experimental live load distribution factors (LLDFs) and dynamic impact factors for the individual bridge girders. Second, these field data were also used to calibrate analytical models, which were then used to conduct a detailed parametric study related to a wide variety of implements of husbandry. A description of field tests, the procedures followed, and sample field results are detailed in the following sections.

Field Inspections

According to the most recent field inspection report, the concrete deck of Steel-Concrete Bridge 4 is in poor condition with scaling, delamination, cracking, and spalling. The steel girders are in fair condition and show some signs of rust. These inspection-based observations were corroborated by the Iowa State University field testing team.

Instrumentation Plan

Given that the primary goal of the testing plan was to measure the live load response of the primary load-carrying members, a network of multiple strain gages was used to measure the strain under the weight of the vehicles. The strain gages were attached to the bottom and top of the girders at mid-span and at the abutment as shown in Figure A-27. The strain sensors used to conduct this testing were installed with a 3 in. gage length, and data were collected at a rate of 100 Hz during static testing and at 100 Hz during dynamic testing.

Test Load Paths

The vehicles utilized during field testing of this bridge consisted of four common farm vehicles and one typical highway truck. The vehicles included a terragator, a grain cart, a honey wagon with one tank, a honey wagon with two tanks, and a typical five-axle semi-truck. The individual axle loads, total weights, and lengths of the five vehicles used for field testing are summarized in Table A-7. As shown in Figure A-28, the configurations of the farm vehicles were notably different from that of the conventional highway truck.

Table A-7. Axle weight and total length of each testing vehicle

Farm Vehicles	Weight (lbs)					Total	Total Length (ft-in.)
	Front Axle	Rear Axle	Grain Wagon	Honey Wagon	Trailer		
Tractor Honey Wagon (one tank)	11,800	15,900	-	48,800	-	76,500	40'-8"
Tractor Honey Wagon (two tanks)	10,580	22,800	-	14,300 (front) 18,300 (rear)	-	68,900	63'-7"
Terragator	11,060	32,400	-	-	-	43,460	25'-7"
Tractor Grain Wagon	18,840	18,660	15,660	-	-	53,160	35'-2"
Semi-Truck	10,760	33,856	-	-	33,084	77,700	52'-2"



Honey Wagon



Honey Wagon- two tanks



Terragator



Tractor Grain Wagon



Semi Truck

Figure A-28. Farm vehicles used for field testing

During testing the vehicles were driven across the bridge from north to south. In general the centerlines of the bridge and vehicle were approximately aligned. Initial static load testing was completed with the vehicles traveling at approximately 3 mph such that the pseudo-static bridge response could be captured. Later, dynamic load testing was completed with the vehicles traveling at approximately 15 mph (maximum safe speed at the site).

Sample Field Results

Representative plots from static load testing showing the strain experienced by one of the girders under all test vehicles is shown in Figure A-29. It was observed that the girders at the center of the bridge experienced the maximum strain magnitudes as the test vehicles crossed the bridge.

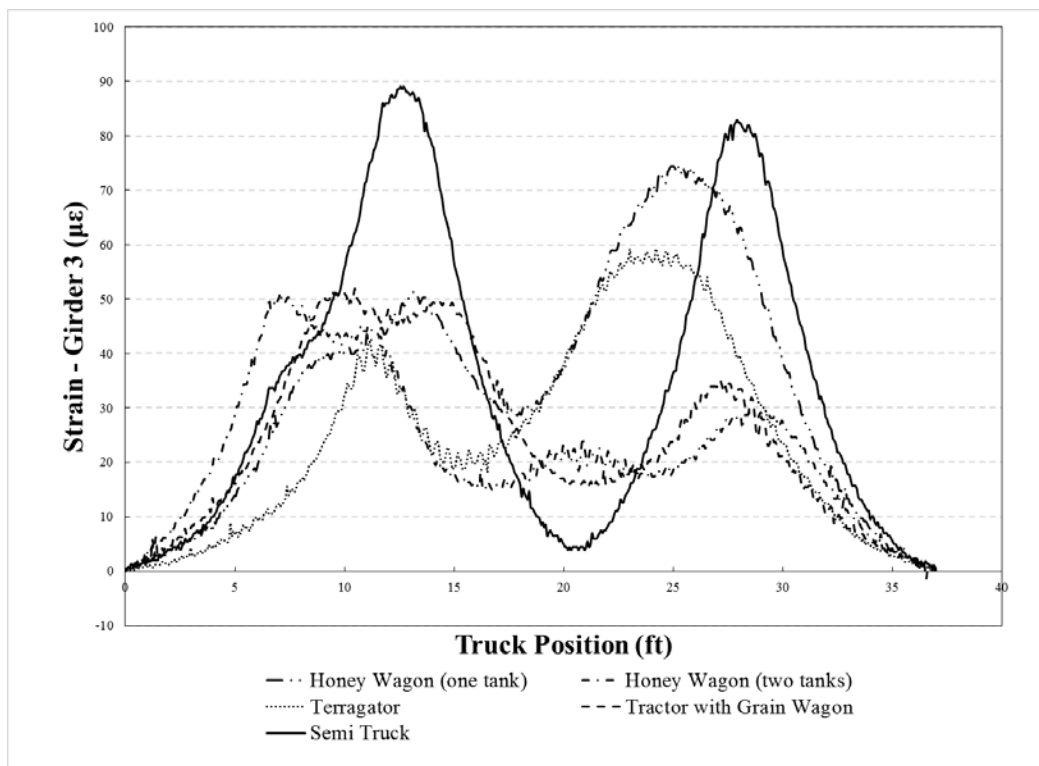


Figure A-29. Strain plot of a girder for all test vehicles for Steel-Concrete Bridge 4

The semi-truck normally results in higher strains compared to other farm vehicles, and this tendency can be seen in Figure A-29. These recorded strains were employed to calculate the field LLDFs for each girder based upon the following equation.

$$LLDF^f = \frac{\varepsilon^m \max i,t}{\sum_{i=1}^n \varepsilon^m \max i,t} \quad (1)$$

Where $LLDF^f$ is the field live load distribution factor and ϵ^m are the measured maximum strains for individual girders over time, respectively.

A.4.4 Analytical Modeling

In lieu of field testing with a large number of vehicles, finite element analysis (FEA) simulations were used to estimate LLDFs for other vehicle configurations. As a result, analytical LLDFs were determined based upon FEA simulations of over 121 different farm vehicles on Steel-Concrete Bridge 4. The FEA model was developed as described subsequently, and specific bridge information is presented in the following sections.

Model Generation

The bridge was initially modeled with the geometric and material properties taken directly from available bridge plans and/or field inspections using the BDI (Bridge Diagnostics, Inc.) finite element software WinGEN. A modulus of elasticity of 3200 ksi and 29000 ksi was used for all concrete and steel components in the model, respectively. The FEA model consisted of beam elements for the girders, shell elements for the deck, and rotational springs that simulated rotational restraint at the abutments and piers. Figure A-30 shows a representative model of the bridge.

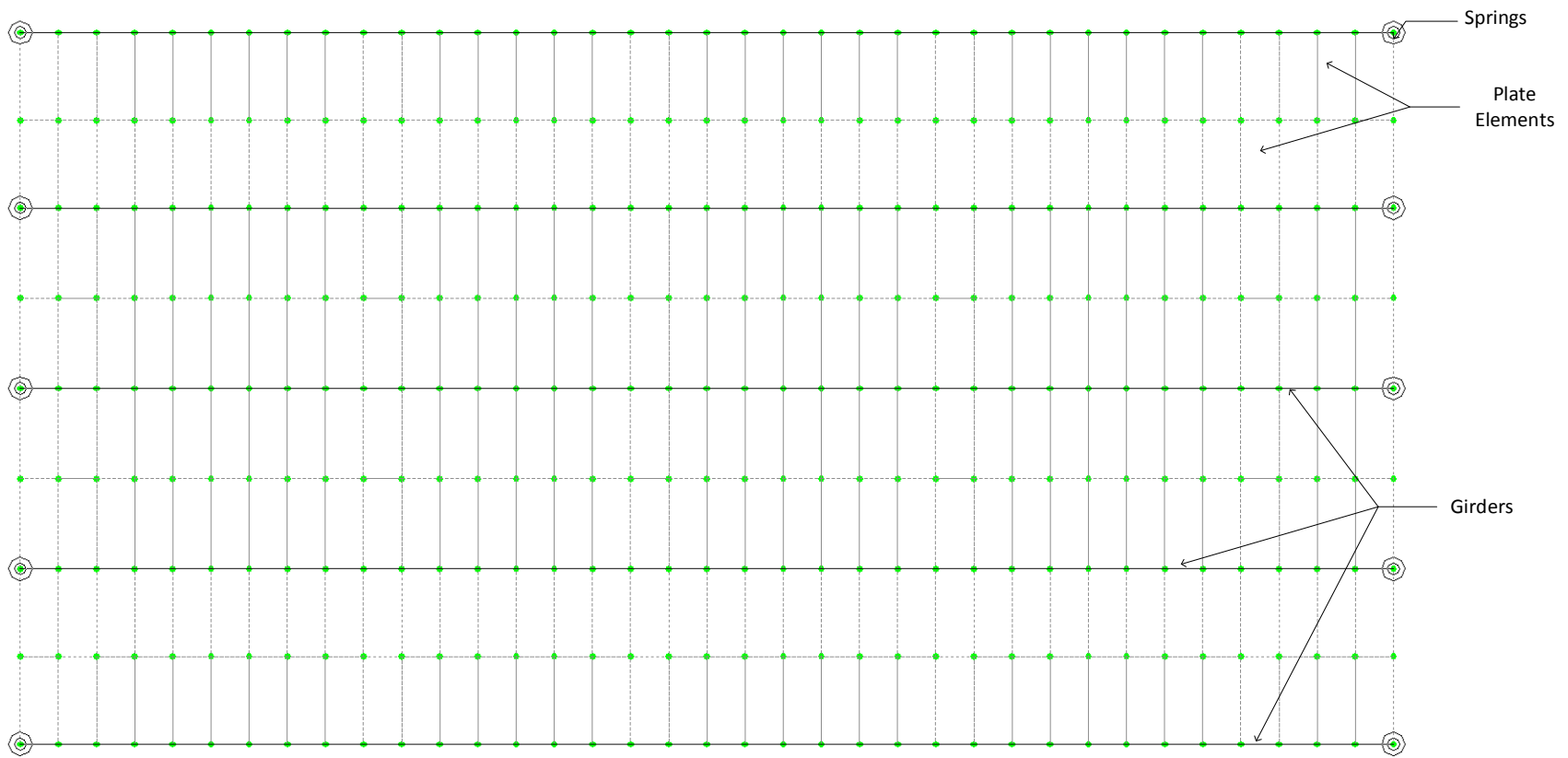


Figure A-30. Finite element model of Steel-Concrete Bridge 4

Model Calibration

To improve the model accuracy, a calibration process that identified the bridge properties that resulted in the lowest error was completed. Based upon similarities in the response and observed field condition, a single cross-section was considered for all the girders. Table A-8 summarizes the original and calibrated values for the various bridge components along with percent error and correlation coefficient values.

Table A-8. Model calibration for Steel-Concrete Bridge 4

Calibration Parameters	Bridge Components	Plan Value	Calibrated Value
Moment of Inertia, I (in ⁴)	Exterior Girder	18,720	23,280
	Intermediate Girder	4,800	6,000
	Interior Girder	4,800	6,000
Young's Modulus (ksi)	Deck	3,191	2,466
Rotational Stiffness, kr (Kips-in/rad)	Exterior Abutment	0	2.39 x 10 ⁶
	Interior Abutment	0	2.39 x 10 ⁶
Statistical Results	Percent Error		2.3%
	Correlation Coefficients		0.99

Once model calibration was completed, the analytical model was loaded with 121 farm vehicles covering a wide range of axle spacings, weights, and gage widths. The analytical strain response was then used to compute analytical LLDFs for each simulation vehicle using Equation (1).

To interpret the results, the LLDFs of the girders were grouped together as either interior or exterior girder LLDFs. Statistical control limits for the interior and exterior girder LLDFs were determined from cumulative distribution function (CDF) curves defined to be at the 95% confidence thresholds.

A.4.5 Results

The envelopes of LLDFs for Steel-Concrete Bridge 4 are presented in Figure A-31 for both the field and analytical LLDFs for each girder. In addition to the envelopes, the AASHTO LLDFs and statistical control limits for each group of interior and exterior girders are also shown.

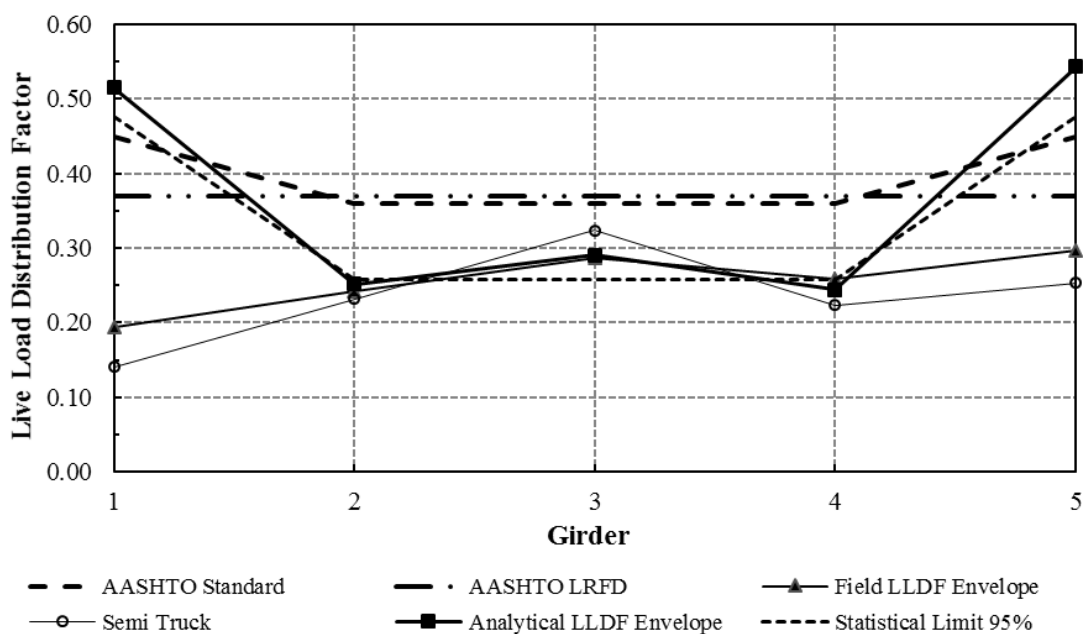


Figure A-31. LLDFs for Steel-Concrete Bridge 4

It appears that the analytical LLDF envelope for the interior girders are smaller than those from the AASHTO standard and LRFD specifications. The peak value of the analytical exterior girder LLDFs was observed in G5, which has an LLDF of 0.54, while that of the interior girders was found in G4, which has an LLDF of 0.24. The statistical limits for interior girders also show smaller values than the AASHTO specifications. The field LLDF envelope has similar values to that of the semi-truck for most of the girders, indicating for this bridge that farm vehicles result in similar values of LLDFs compared to those from the conventional highway vehicle.

A.5 Steel-Concrete Bridge 5

This mini test and evaluation report documents the results of field testing and subsequent analysis of a steel girder bridge with a concrete deck (Steel-Concrete Bridge 5) under multiple implements of husbandry. For completeness, this mini-report includes a description of the bridge, a description of the live load testing procedures followed, sample data, a description of analytical modeling, plots of analytical results, and a discussion of the overall behavior of the steel girder bridge under implements of husbandry.

A.5.1 Background

The steel-concrete bridge described here is known in the National Bridge Inventory (NBI) database as Bridge 162060 and will be henceforth be referred to as Steel-Concrete Bridge 5. The bridge is located about 3 miles east of Grand Junction, on County Road P-46 over West Beaver Creek, in Greene County, Iowa. Figure A-32 shows the general location of the bridge.



Map: ©Google 2014

Figure A-32. Location overview of Steel-Concrete Bridge 5

A.5.2 Bridge Description

Steel-Concrete Bridge 5 is open to two-lane traffic and has one span with overall dimensions of 42 ft long by 24.3 ft wide with zero degrees of skew. The deck is comprised of continuous concrete decking with a thickness of 7.5 in. An elevation view and an end view of the bridge are shown in Figure A-33.



Figure A-33. Steel-Concrete Bridge 5: Elevation view (left) and end view (right)

The bridge consists of nine steel girders with spacing between adjacent girders of 3.3 ft for the interior girders and 3.0 ft for the exterior girders. The I cross-section girders are approximately 24 in. by 7 in. Figure A-34 shows a typical cross-section and plan view of the bridge.

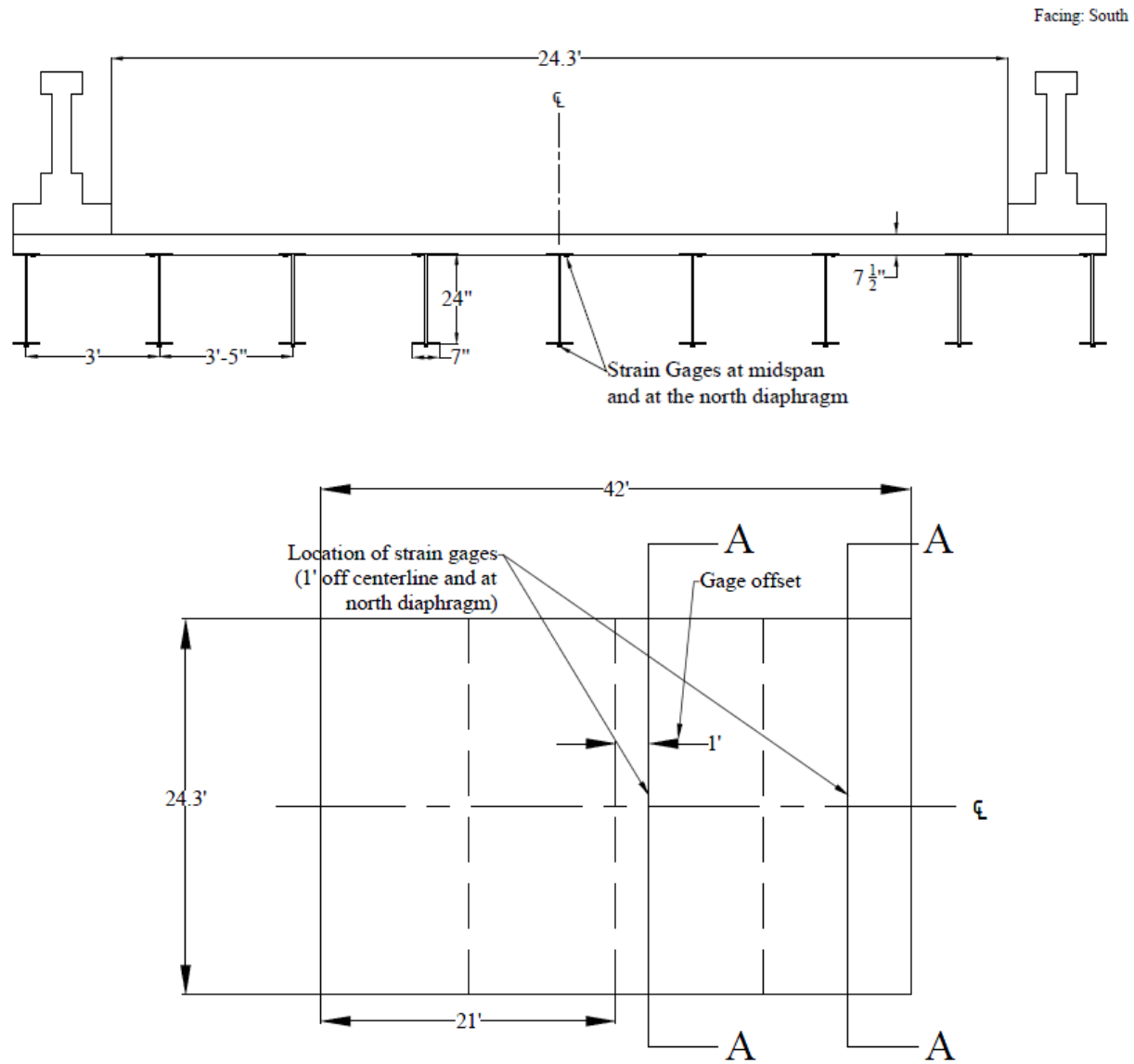


Figure A-34. Steel-Concrete Bridge 5: Cross-section A-A (top) and plan (bottom)

A.5.3 Field Testing

Field testing of this bridge was conducted for two reasons. First, field testing was conducted to determine experimental live load distribution factors (LLDFs) and dynamic impact factors for the individual bridge girders. Second, these field data were also used to calibrate analytical models, which were then used to conduct a detailed parametric study related to a wide variety of implements of husbandry. A description of field tests, the procedures followed, and sample field results are detailed in the following sections.

Field Inspections

According to the most recent field inspection report, the concrete deck of Steel-Concrete Bridge 5 is in fair condition with numerous pits and popouts, and the fascia is spalled and crumbling. The steel girders are in satisfactory condition. These inspection-based observations were corroborated by the Iowa State University field testing team.

Instrumentation Plan

Given that the primary goal of the testing plan was to measure the live load response of the primary load-carrying members, a network of multiple strain gages was used to measure the strain under the weight of the vehicles. The strain gages were attached to the bottom and top of the girders at mid-span and at the north diaphragm as shown in Figure A-35. The strain sensors used to conduct this testing were installed with a 3 in. gage length, and data were collected at a rate of 100 Hz during static testing and at 100 Hz during dynamic testing.

Test Load Paths

The vehicles utilized during field testing of this bridge consisted of four common farm vehicles and one typical highway truck. The vehicles included a terragator, a grain cart, a honey wagon with one tank, a honey wagon with two tanks, and a typical five-axle semi-truck. The individual axle loads, total weights, and lengths of the five vehicles used for field testing are summarized in Table A-9. As shown in Figure A-35, the configurations of the farm vehicles were notably different from that of the conventional highway truck.

Table A-9. Axle weight and total length of each testing vehicle

Farm Vehicles	Weight (lbs)					Total	Total Length (ft-in.)
	Front Axle	Rear Axle	Grain Wagon	Honey Wagon	Trailer		
Tractor Honey Wagon (one tank)	11,800	15,900	-	48,800	-	76,500	40'-8"
Tractor Honey Wagon (two tanks)	10,580	22,800	-	14,300 (front) 18,300 (rear)	-	68,900	63'-7"
Terragator	11,060	32,400	-	-	-	43,460	25'-7"
Tractor Grain Wagon	18,840	18,660	15,660	-	-	53,160	35'-2"
Semi-Truck	10,760	33,856	-	-	33,084	77,700	52'-2"



Honey Wagon



Honey Wagon- two tanks



Terragator



Tractor Grain Wagon



Semi Truck

Figure A-35. Farm vehicles used for field testing

During testing, the vehicles were driven across the bridge from north to south. In general the centerlines of the bridge and vehicle were approximately aligned. Initial static load testing was completed with the vehicles traveling at approximately 3 mph such that the pseudo-static bridge response could be captured. Later, dynamic load testing was completed with the vehicles traveling at approximately 15 mph (maximum safe speed at the site).

Sample Field Results

Representative plots from static load testing showing the strain experienced by one of the girders under all test vehicles is shown in Figure A-36. It was observed that the girders at the center of the bridge experienced the maximum strain magnitudes as the test vehicles crossed the bridge.

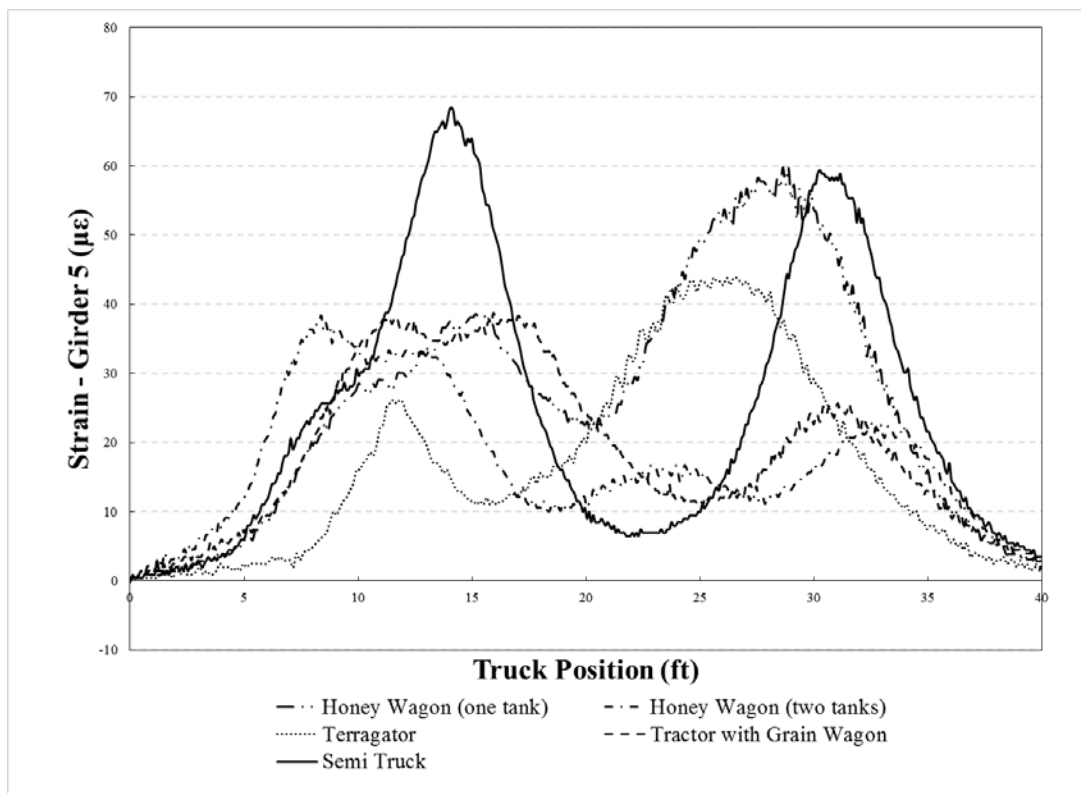


Figure A-36. Strain plot of a girder for all test vehicles for Steel-Concrete Bridge 5

The semi-truck normally results in higher strains compared to other farm vehicles, and this tendency can be seen in Figure A-36. These recorded strains were employed to calculate the field LLDFs for each girder based upon the following equation.

$$LLDF^f = \frac{\varepsilon^m \max i,t}{\sum_{i=1}^n \varepsilon^m \max i,t} \quad (1)$$

Where $LLDF^f$ is the field live load distribution factor and ϵ^m are the measured maximum strains for individual girders over time, respectively.

A representative plot showing the comparison between static and dynamic strain for one of the girders under a test vehicle is shown in Figure A-37. It was generally observed that the girders experience more strain under dynamic loads than under static loading. The strain values from dynamic load tests were utilized to calculate the dynamic amplification factors (DAFs) for each girder.

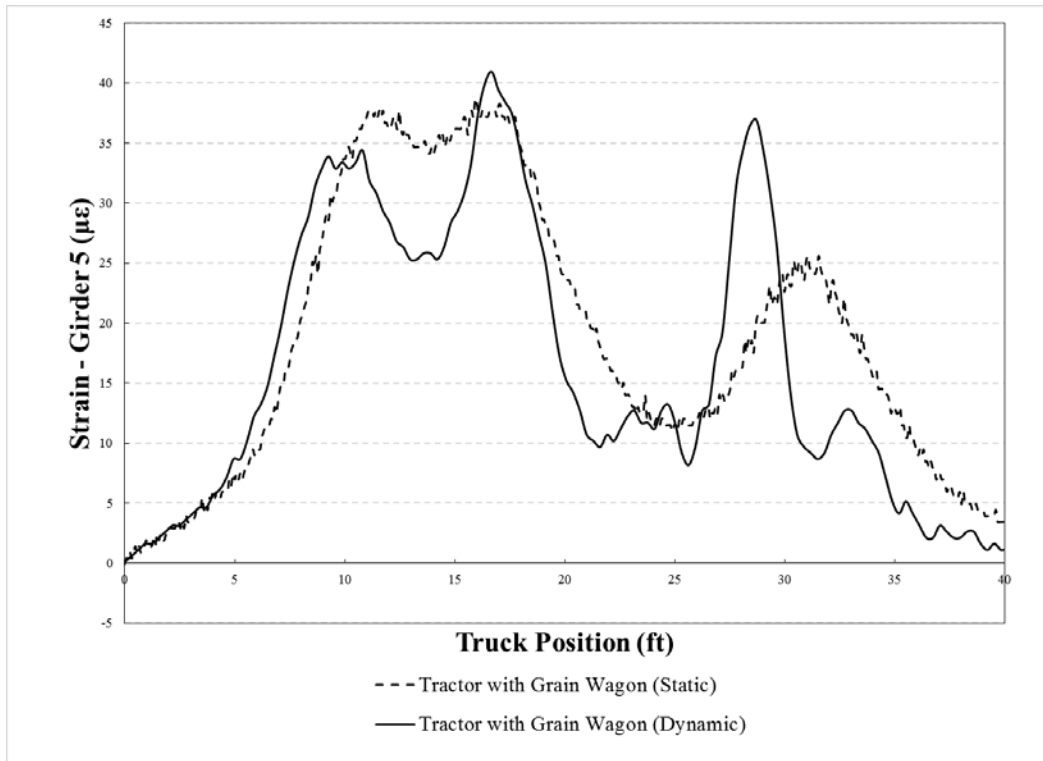


Figure A-37. Comparison between static and dynamic strain for Steel-Concrete Bridge 5

A.5.4 Analytical Modeling

In lieu of field testing with a large number of vehicles, finite element analysis (FEA) simulations were used to estimate LLDFs for other vehicle configurations. As a result, analytical LLDFs were determined based upon FEA simulations of over 121 different farm vehicles on Steel-Concrete Bridge 5. The FEA model was developed as described subsequently, and specific bridge information is presented in the following sections.

Model Generation

The bridge was initially modeled with the geometric and material properties taken directly from available bridge plans and/or field inspections using the BDI (Bridge Diagnostics, Inc.) finite

element software WinGEN. A modulus of elasticity of 3200 ksi and 29000 ksi was used for all concrete and steel components in the model, respectively. The FEA model consisted of beam elements for the girders, shell elements for the deck, and rotational springs that simulated rotational restraint at the abutments and piers. Figure A-38 shows a representative model of the bridge.

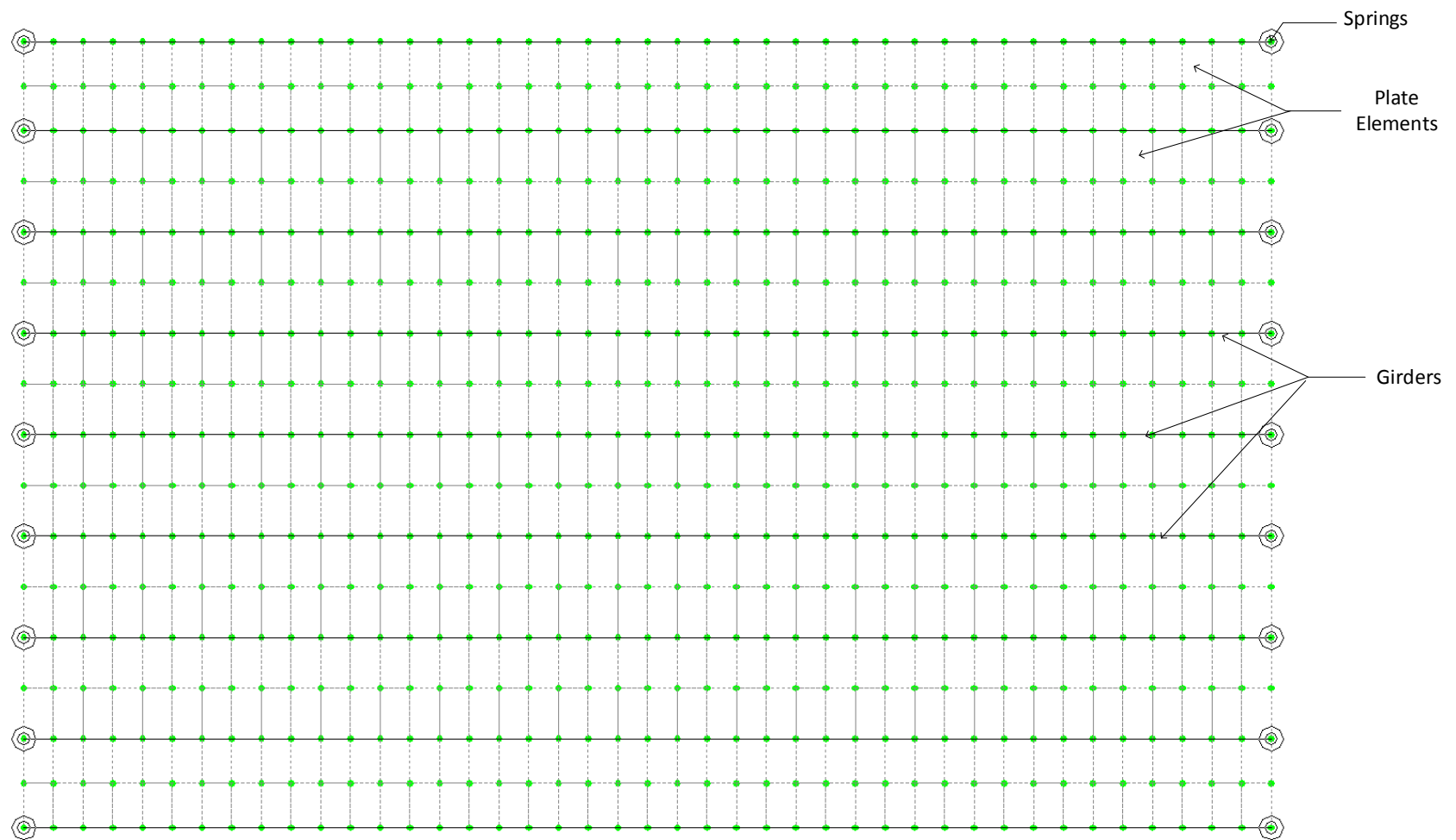


Figure A-38. Finite element model of Steel-Concrete Bridge 5

Model Calibration

To improve the model accuracy, a calibration process that identified the bridge properties that resulted in the lowest error was completed. Based upon similarities in the response and observed field condition, a single cross-section was considered for all the girders. Table A-10 summarizes the original and calibrated values for the various bridge components along with percent error and correlation coefficient values.

Table A-10. Model calibration for Steel-Concrete Bridge 5

Calibration Parameters	Bridge Components	Plan Value	Calibrated Value
Moment of Inertia, I (in ⁴)	Exterior Girder	5,280	6,480
	Intermediate Girder	4,560	5,760
	Interior Girder	4,560	5,760
Young's Modulus (ksi)	Deck	3,191	4,061
Rotational Stiffness, kr (Kips-in/rad)	Exterior Abutment	0	2,478
	Interior Abutment	0	2,478
Statistical Results	Percent Error		7.9%
	Correlation Coefficients		0.97

Once model calibration was completed, the analytical model was loaded with 121 farm vehicles covering a wide range of axle spacings, weights, and gage widths. The analytical strain response was then used to compute analytical LLDFs for each simulation vehicle using Equation (1).

To interpret the results, the LLDFs of the girders were grouped together as either interior or exterior girder LLDFs. Statistical control limits for the interior and exterior girder LLDFs were determined from cumulative distribution function (CDF) curves defined to be at the 95% confidence thresholds.

A.5.5 Results

The envelopes of LLDFs for Steel-Concrete Bridge 5 are presented in Figure A-39 for both the field and analytical LLDFs for each girder. In addition to the envelopes, the AASHTO LLDFs and statistical control limits for each group of interior and exterior girders are also shown.

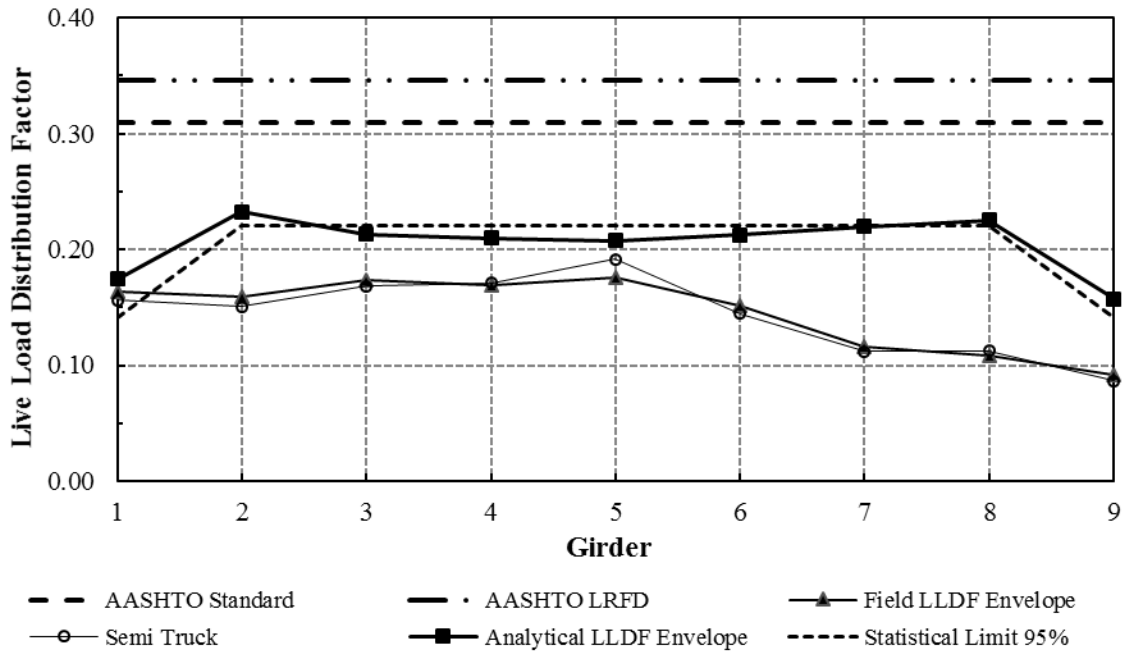


Figure A-39. LLDFs for Steel-Concrete Bridge 5

It appears that the analytical LLDF envelope for all the girders is much smaller than those from the AASHTO standard and LRFD specifications. The peak value of the analytical exterior girder LLDFs was observed in G1, which has an LLDF of 0.17, while that of the interior girders was found in G2, which has an LLDF of 0.23. The statistical limits for either the interior or exterior girder group also show smaller values than the AASHTO specifications. The field LLDF envelope has similar values to that of the semi-truck for most of the girders, indicating for this bridge that farm vehicles result in similar values of LLDFs compared to those from the conventional highway vehicle.

APPENDIX B. FIELD TESTED STEEL-TIMBER BRIDGES

B.1 Steel-Timber Bridge 1

This mini test and evaluation report documents the results of field testing and subsequent analysis of a steel girder bridge with a timber deck (Steel-Timber Bridge 1) under multiple implements of husbandry. For completeness, this mini-report includes a description of the bridge, a description of the live load testing procedures followed, sample data, a description of analytical modeling, plots of analytical results, and a discussion of the overall behavior of the steel girder bridge under implements of husbandry.

B.1.1 Background

The steel-timber bridge described here is known in the National Bridge Inventory (NBI) database as Bridge 126231 and will be henceforth be referred to as Steel-Timber Bridge 1. The bridge is located about 12 miles west of Manning, on 360th Street, in Crawford County, Iowa. Figure B-1 shows the general location of the bridge.



Map: ©Google 2014

Figure B-1. Location overview of Steel-Timber Bridge 1

B.1.2 Bridge Description

Steel-Timber Bridge 1 is open to two-lane traffic and has one span with overall dimensions of 31 ft long by 24.7 ft wide with zero degrees of skew. The deck is comprised of continuous timber decking with a thickness of 4 in. An elevation view and an end view of the bridge are shown in Figure B-2.



Figure B-2. Steel-Timber Bridge 1: West elevation view (left) and north end view (right)

The bridge consists of 10 timber girders with spacing between adjacent girders of 2.6 ft. The I cross-section girders are approximately 15.0 in. by 5.5 in. Figure B-3 shows a typical cross-section and plan view of the bridge.

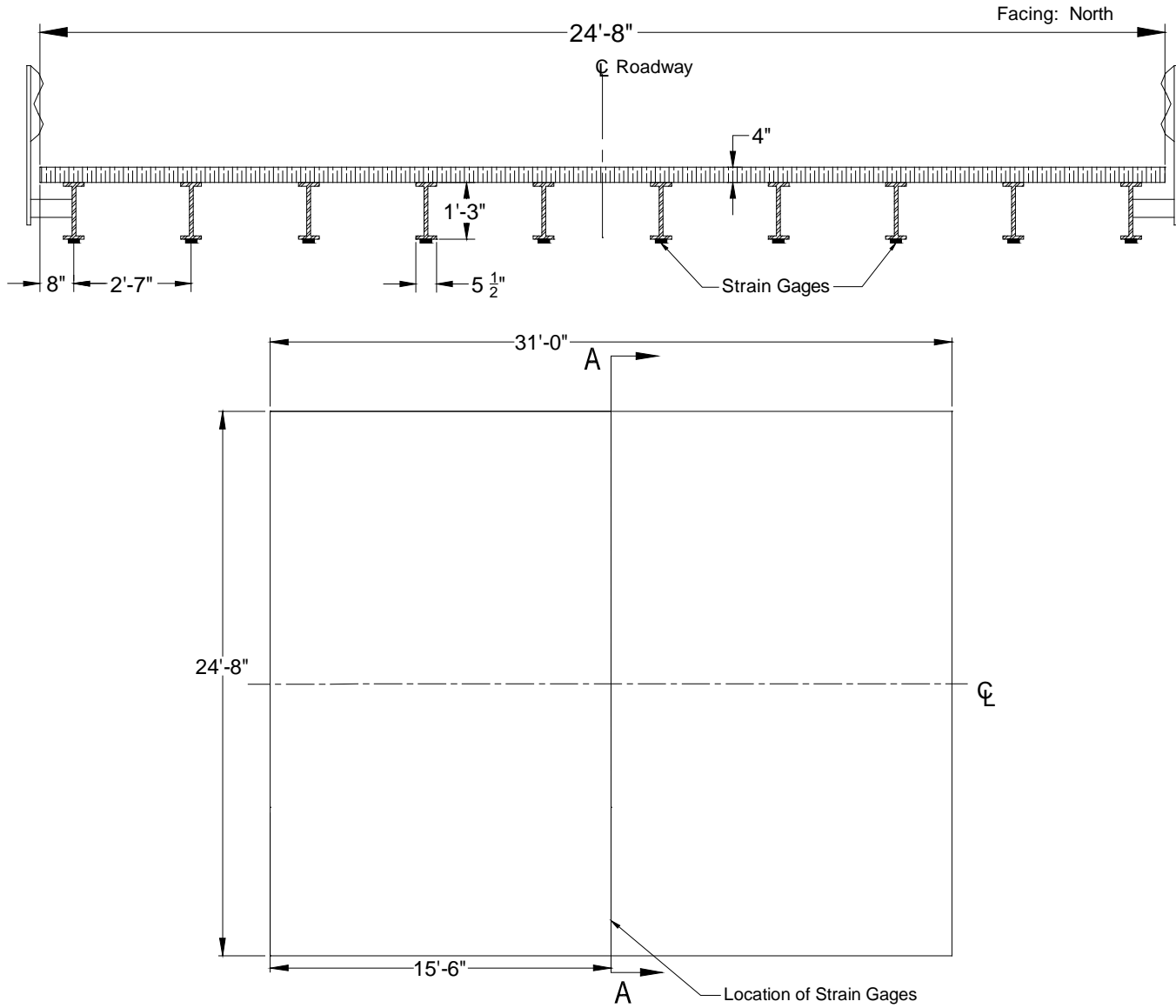


Figure B-3. Steel-Timber Bridge 1: Cross-section A-A (top) and plan (bottom)

B.1.3 Field Testing

Field testing of this bridge was conducted for two reasons. First, field testing was conducted to determine experimental live load distribution factors (LLDFs) and dynamic impact factors for the individual bridge girders. Second, these field data were also used to calibrate analytical models, which were then used to conduct a detailed parametric study related to a wide variety of implements of husbandry. A description of field tests, the procedures followed, and sample field results are detailed in the following sections.

Field Inspections

According to of the most recent field inspection report, the timber deck of Steel-Timber Bridge 1 is in very good condition. The steel girders are in good condition and show some signs of rust. These inspection-based observations were corroborated by the Iowa State University field testing team.

Instrumentation Plan

Given that the primary goal of the testing plan was to measure the live load response of the primary load-carrying members, a network of multiple strain gages was used to measure the strain under the weight of the vehicles. The strain gages were attached to the bottom of the girders at mid-span as shown in Figure B-3. The strain sensors used to conduct this testing were installed with a 3 in. gage length, and data were collected at a rate of 100 Hz during static testing and at 100 Hz during dynamic testing.

Test Load Paths

The vehicles utilized during field testing of this bridge consisted of four common farm vehicles and one typical highway truck. The vehicles included a terragator, a grain cart, a honey wagon with one tank, a honey wagon with two tanks, and a typical five-axle semi-truck. The individual axle loads, total weights, and lengths of the five vehicles used for field testing are summarized in Table B-1. As shown in Figure B-4, the configurations of the farm vehicles were notably different from that of the conventional highway truck.

Table B-1. Axle weight and total length of each testing vehicle

Farm Vehicles	Weight (lbs)					Total	Total Length (ft-in.)
	Front Axle	Rear Axle	Grain Wagon	Honey Wagon	Trailer		
Tractor Honey Wagon (empty)	10,960	15,740	-	26,720	-	53,420	40'-4"
Tractor Honey Wagon (half full with water)	10,580	22,800	-	40,620	-	74,000	40'-4"
Terragator	23,380	17,840	-	-	-	41,220	19'-0"
Tractor Grain Wagon	24,480	19,700	11,980	-	-	56,160	31'-0"
Semi-Truck	10,760	33,856	-	-	33,084	77,700	52'-1"



Honey Wagon



Honey Wagon- two tanks



Terragator



Tractor Grain Wagon



Semi Truck

Figure B-4. Farm vehicles used for field testing

During testing, the vehicles were driven across the bridge from north to south. In general the centerlines of the bridge and vehicle were approximately aligned. Initial static load testing was completed with the vehicles traveling at approximately 3 mph such that the pseudo-static bridge response could be captured. Later, dynamic load testing was completed with the vehicles traveling at approximately 15 mph (maximum safe speed at the site).

Sample Field Results

Representative plots from static load testing showing the strain experienced by one of the girders under all test vehicles is shown in Figure B-5. It was observed that the girders at the center of the bridge experienced the maximum strain magnitudes as the test vehicles crossed the bridge.

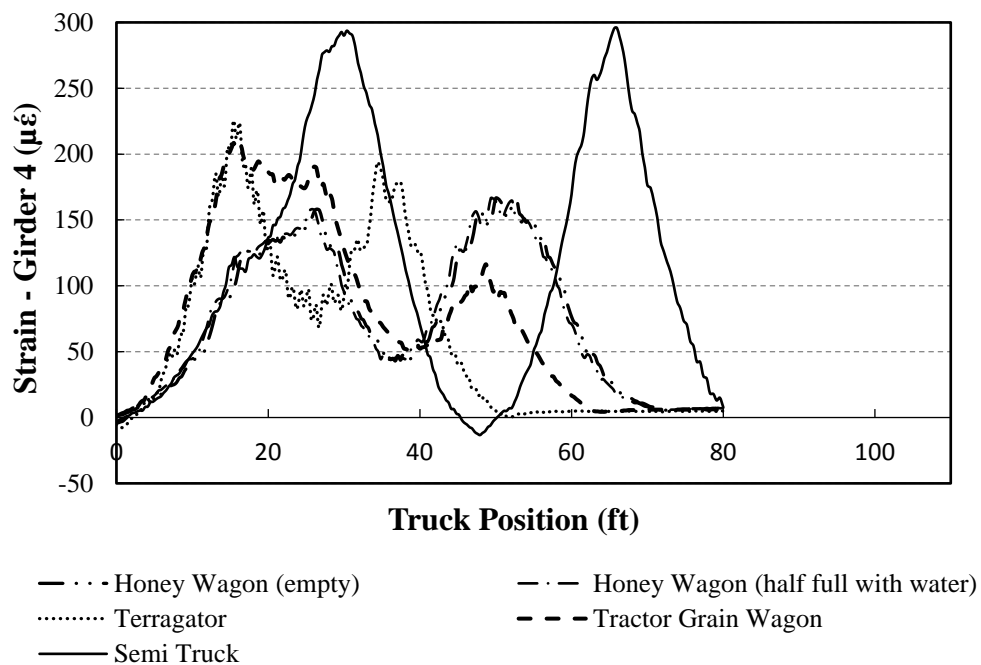


Figure B-5. Strain plot of a girder for all test vehicles for Steel-Timber Bridge 1

The semi-truck normally results in higher strains compared to other farm vehicles, and this tendency can be seen in Figure B-5. These recorded strains were employed to calculate the field LLDFs for each girder based upon the following equation.

$$LLDF^f = \frac{\epsilon^m \max i, t}{\sum_{i=1}^n \epsilon^m \max i, t} \quad (1)$$

Where $LLDF^f$ is the field live load distribution factor and ϵ^m are the measured maximum strains for individual girders over time, respectively.

A representative plot showing the comparison between static and dynamic strain for one of the girders under a test vehicle is shown in Figure B-6. It was generally observed that the girders experience more strain under dynamic loads than under static loading. The strain values from dynamic load tests were utilized to calculate the dynamic amplification factors (DAFs) for each girder.

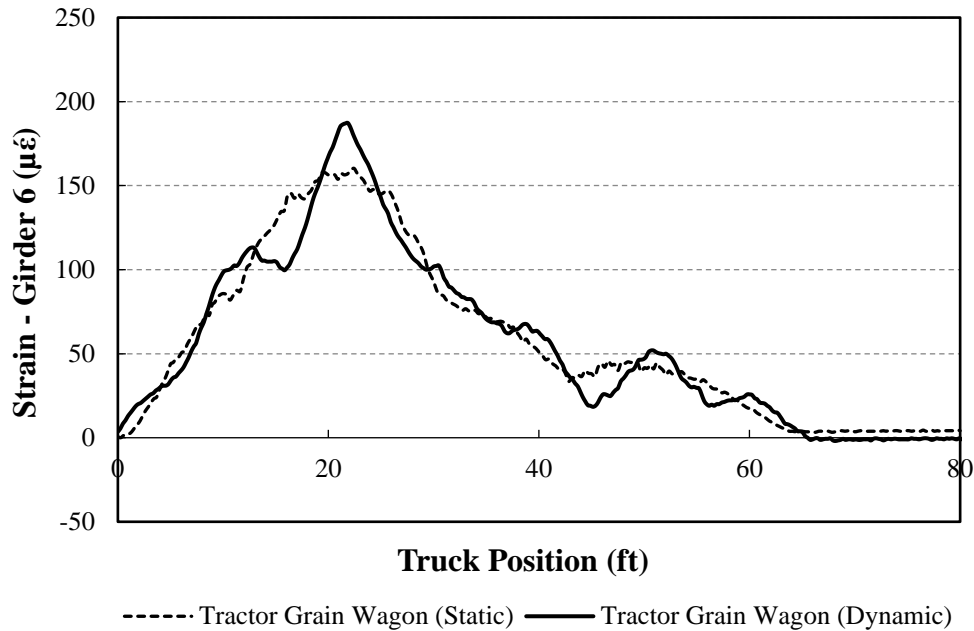


Figure B-6. Comparison between static and dynamic strain for Steel-Timber Bridge 1

B.1.4 Analytical Modeling

In lieu of field testing with a large number of vehicles, finite element analysis (FEA) simulations were used to estimate LLDFs for other vehicle configurations. As a result, analytical LLDFs were determined based upon FEA simulations of over 121 different farm vehicles on Steel-Timber Bridge 1. The FEA model was developed as described subsequently, and specific bridge information is presented in the following sections.

Model Generation

The bridge was initially modeled with the geometric and material properties taken directly from available bridge plans and/or field inspections using the BDI (Bridge Diagnostics, Inc.) finite element software WinGEN. A modulus of elasticity of 1600 ksi and 29000 ksi was used for all timber and steel components in the model, respectively. The FEA model consisted of beam elements for the girders, shell elements for the deck, and rotational springs that simulated rotational restraint at the abutments and piers. Figure B-7 shows a representative model of the bridge.

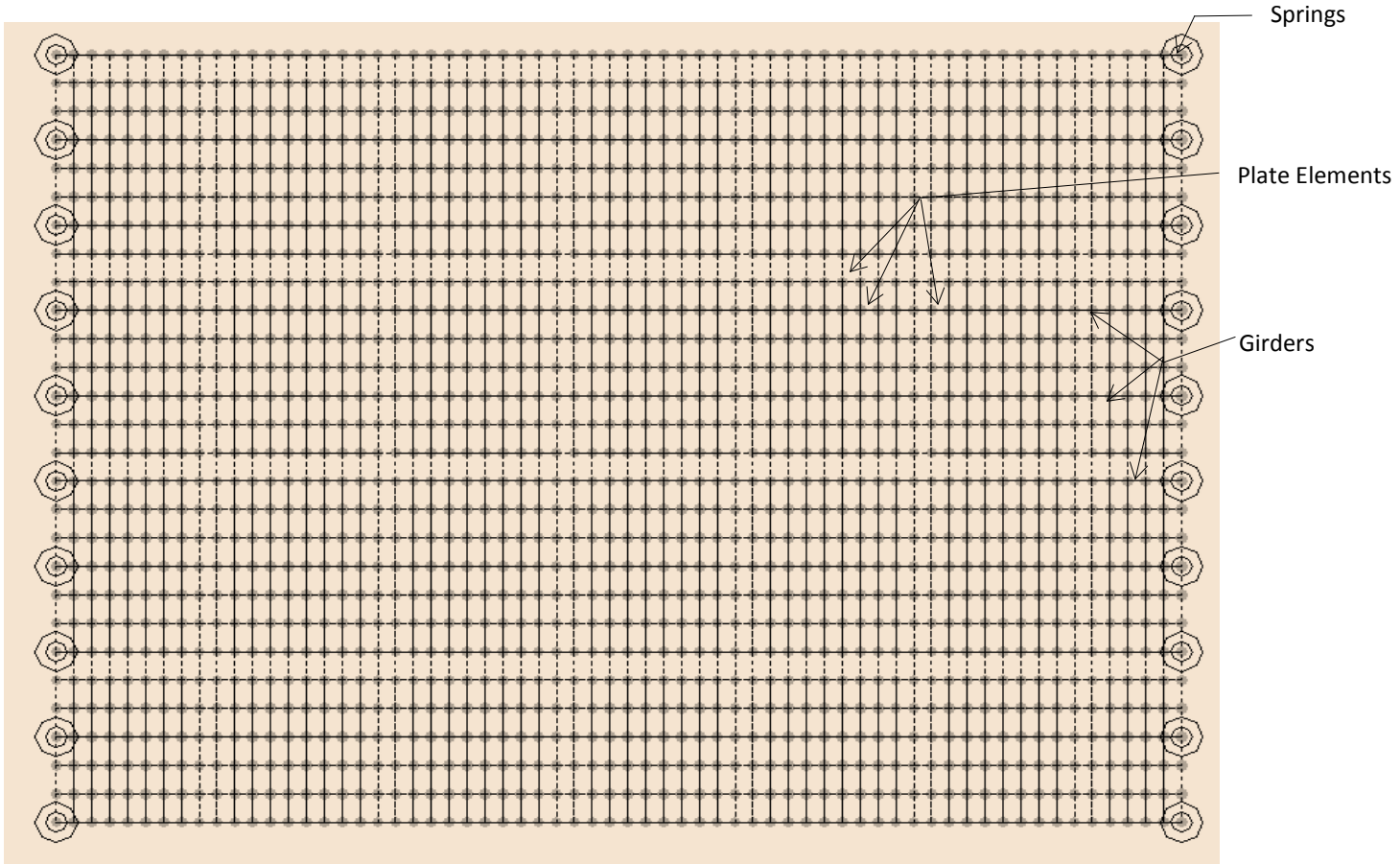


Figure B-7. Finite element model of Steel-Timber Bridge 1

Model Calibration

To improve the model accuracy, a calibration process that identified the bridge properties that resulted in the lowest error was completed. Based upon similarities in the response and observed field condition, a single cross-section was considered for all the girders. Table B-2 summarizes the original and calibrated values for the various bridge components along with percent error and correlation coefficient values.

Table B-2. Model calibration for Steel-Timber Bridge 1

Calibration Parameters	Bridge Components	Plan Value	Calibrated Value
Moment of Inertia, I (in ⁴)	All Girders	377	375
Modulus of Elasticity, E (Ksi)	Deck	1600	1551
Rotational Stiffness, kr (Kips-in/rad)	Support Connections (springs)	0	82540
Statistical Results	Percent Error		9.6%
	Correlation Coefficients		0.94

Once model calibration was completed, the analytical model was loaded with 121 farm vehicles covering a wide range of axle spacings, weights, and gage widths. The analytical strain response was then used to compute analytical LLDFs for each simulation vehicle using Equation (1).

To interpret the results, the LLDFs of the girders were grouped together as either interior or exterior girder LLDFs. Statistical control limits for the interior and exterior girder LLDFs were determined from cumulative distribution function (CDF) curves defined to be at the 95% confidence thresholds.

B.1.5 Results

The envelopes of LLDFs for Steel-Timber Bridge 1 are presented in Figure B-8 for both the field and analytical LLDFs for each girder. In addition to the envelopes, the AASHTO LLDFs and statistical control limits for each group of interior and exterior girders are also shown.

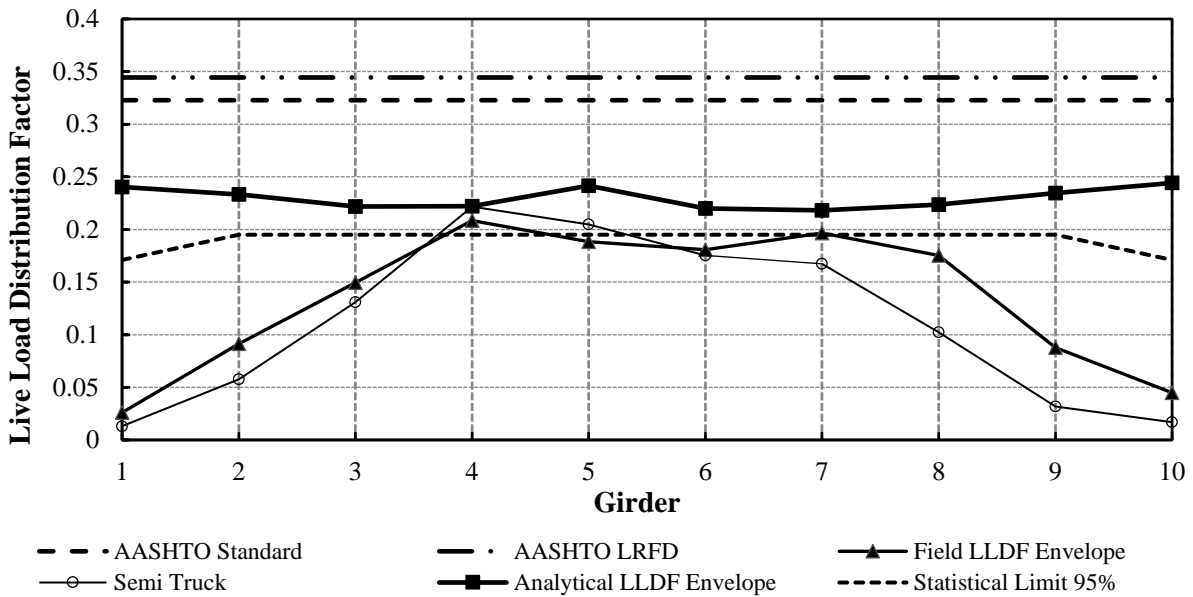


Figure B-8. LLDFs for Steel-Timber Bridge 1

It appears that the analytical LLDF envelope for all the girders is much smaller than those from the AASHTO standard and LRFD specifications. The peak value of the analytical exterior girder LLDFs was observed in G10, which has an LLDF of 0.24, while that of the interior girders was found in G5, which has an LLDF of 0.24. The statistical limits for either the interior or exterior girder group also show smaller values than the AASHTO specifications. The field LLDF envelope represents the highest LLDF observed in each girder due to field testing using farm vehicles, whereas the semi-truck envelope represents the extreme LLDFs for field testing using a five-axle semi-truck. The field LLDF envelope has larger values than that for the semi-truck for most of the girders, indicating for this bridge that farm vehicles result in higher values of LLDFs compared to those from the conventional highway vehicle.

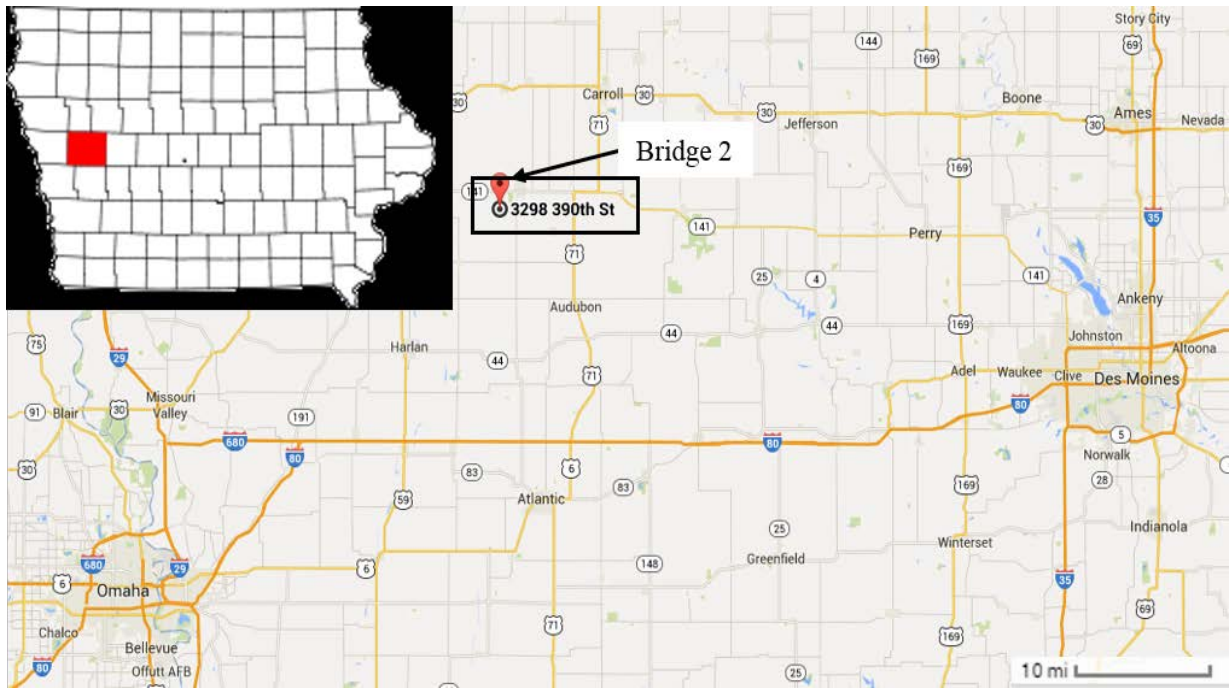
B.2 Steel-Timber Bridge 2

This mini test and evaluation report documents the results of field testing and subsequent analysis of a steel girder bridge with a timber deck (Steel-Timber Bridge 2) under multiple implements of husbandry. For completeness, this mini-report includes a description of the bridge, a description of the live load testing procedures followed, sample data, a description of analytical modeling, plots of analytical results, and a discussion of the overall behavior of the steel girder bridge under implements of husbandry.

B.2.1 Background

The steel-timber bridge described here is known in the National Bridge Inventory (NBI) database as Bridge 126252 and will be henceforth be referred to as Steel-Timber Bridge 2. The bridge is

located about 12 miles west of Manning, on 390th Street, in Crawford County, Iowa. Figure B-9 shows the general location of the bridge.



Map: ©Google 2014

Figure B-9. Location overview of Steel-Timber Bridge 2

B.2.2 Bridge Description

Steel-Timber Bridge 2 is open to two-lane traffic and has one span with overall dimensions of 33.5 ft long by 24.5 ft wide with 30 degrees of skew. The deck is comprised of continuous timber decking with a thickness of 3 in. An elevation view and an end view of the bridge are shown in Figure B-10. The bridge consists of nine steel girders with spacing between adjacent girders of 2.8 ft. The I cross-section girders are approximately 20.0 in. by 7.0 in. Figure B-11 shows a typical cross-section and plan view of the bridge.



Figure B-10. Steel-Timber Bridge 2: South elevation view (left) and west end view (right)

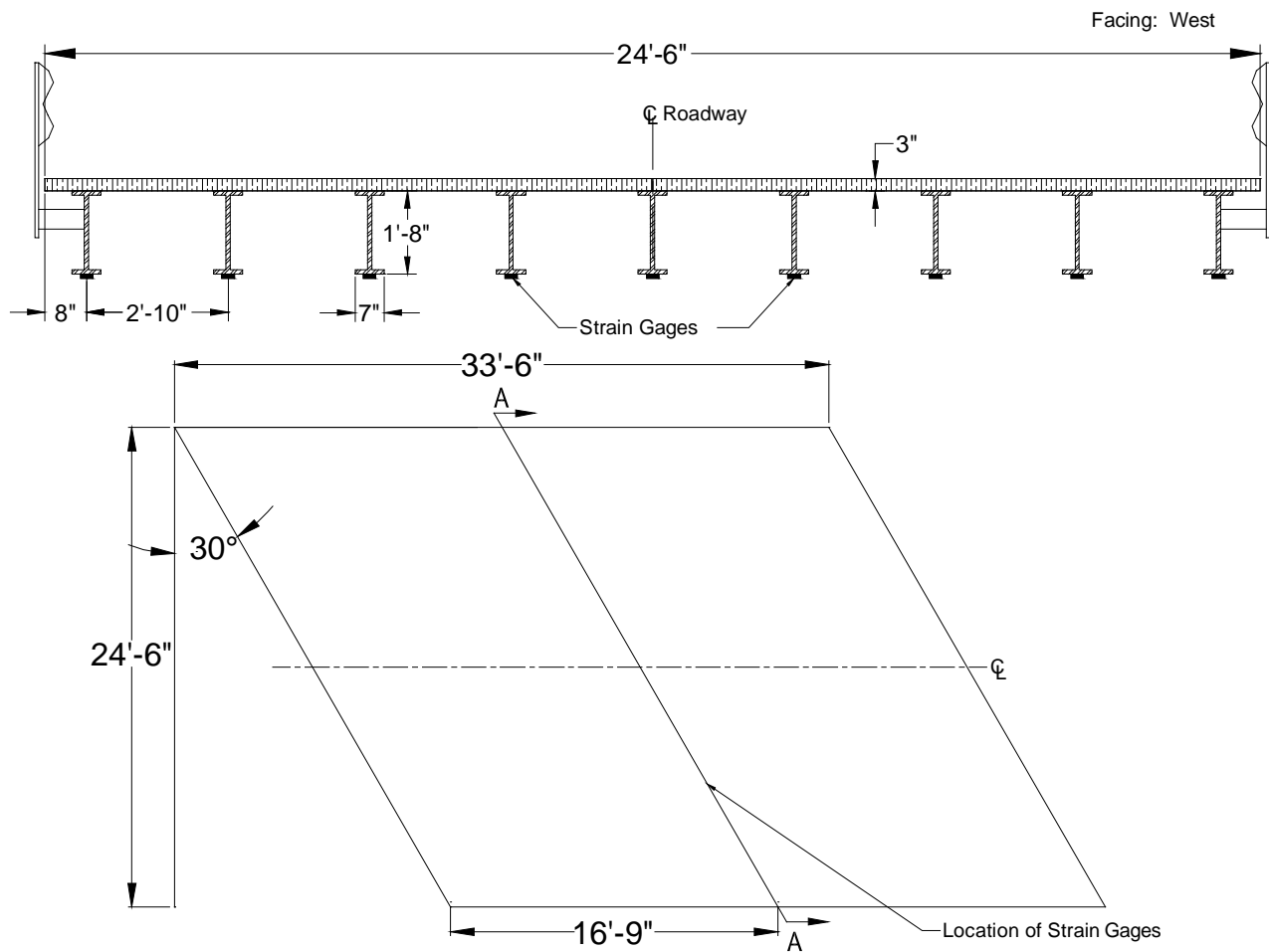


Figure B-11. Steel-Timber Bridge 2: Cross-section A-A (top) and plan (bottom)

B.2.3 Field Testing

Field testing of this bridge was conducted for two reasons. First, field testing was conducted to determine experimental live load distribution factors (LLDFs) and dynamic impact factors for the individual bridge girders. Second, these field data were also used to calibrate analytical models, which were then used to conduct a detailed parametric study related to a wide variety of implements of husbandry. A description of field tests, the procedures followed, and sample field results are detailed in the following sections.

Field Inspections

According to the most recent field inspection report, the Steel-Timber Bridge 2 timber deck is in very good condition with no problems noted. The steel girders are also in good condition. These inspection-based observations were corroborated by the Iowa State University field testing team.

Instrumentation Plan

Given that the primary goal of the testing plan was to measure the live load response of the primary load-carrying members, a network of multiple strain gages was used to measure the strain under the weight of the vehicles. The strain gages were attached to the bottom of the girders at mid-span as shown in Figure B-11. The strain sensors used to conduct this testing were installed with a 3 in. gage length, and data were collected at a rate of 20 Hz during static testing and at 20 Hz during dynamic testing.

Test Load Paths

The vehicles utilized during field testing of this bridge consisted of four common farm vehicles and one typical highway truck. The vehicles included a terragator, a grain cart, a honey wagon with one tank, a honey wagon with two tanks, and a typical five-axle semi-truck. The individual axle loads, total weights, and lengths of the five vehicles used for field testing are summarized in Table B-3. As shown in Figure B-12, the configurations of the farm vehicles were notably different from that of the conventional highway truck.

Table B-3. Axle weight and total length of each testing vehicle

Farm Vehicles	Weight (lbs)					Total	Total Length (ft-in.)
	Front Axle	Rear Axle	Grain Wagon	Honey Wagon	Trailer		
Tractor Honey Wagon (empty)	10,960	15,740	-	26,720	-	53,420	40'-4"
Tractor Honey Wagon (half full with water)	10,580	22,800	-	40,620	-	74,000	40'-4"
Terragator	23,380	17,840	-	-	-	41,220	19'-0"
Tractor Grain Wagon	24,480	19,700	11,980	-	-	56,160	31'-0"
Semi-Truck	10,760	33,856	-	-	33,084	77,700	52'-1"



Honey Wagon



Honey Wagon- two tanks



Terragator



Tractor Grain Wagon



Semi Truck

Figure B-12. Farm vehicles used for field testing

During testing, the vehicles were driven across the bridge from south to north. In general the centerlines of the bridge and vehicle were approximately aligned. Initial static load testing was completed with the vehicles traveling at approximately 3 mph such that the pseudo-static bridge response could be captured. Later, two sets of dynamic load testing was completed with the vehicles traveling at approximately 10 and 25 mph (maximum safe speed at the site) respectively.

Sample Field Results

Representative plots from static load testing showing the strain experienced by one of the girders under all test vehicles is shown in Figure B-13. It was observed that the girders at the center of the bridge experienced the maximum strain magnitudes as the test vehicles crossed the bridge.

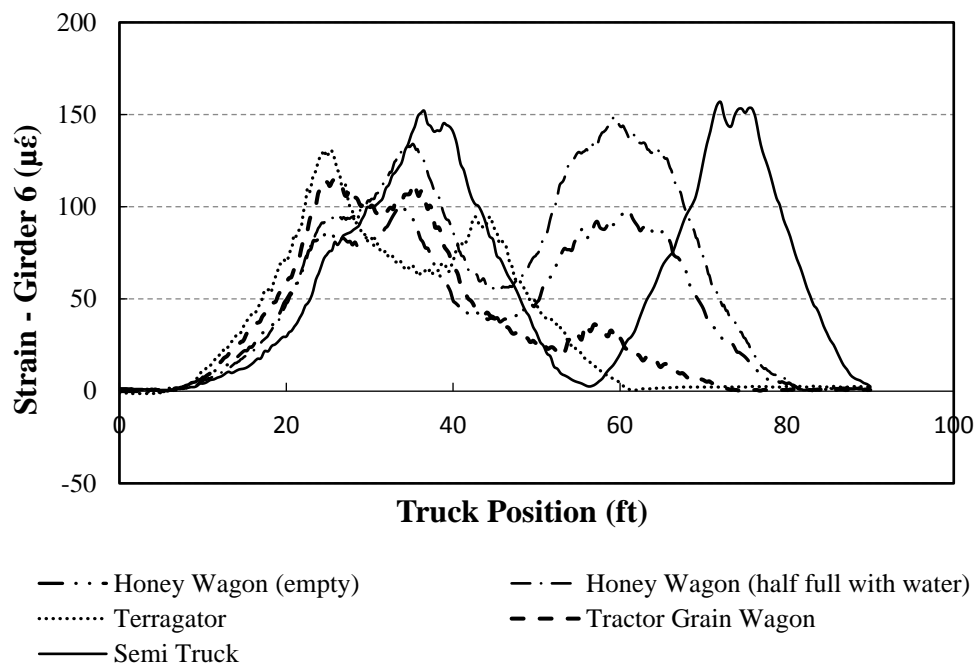


Figure B-13. Strain plot of a girder for all test vehicles for Steel-Timber Bridge 2

The semi-truck normally results in higher strains compared to other farm vehicles, and this tendency can be seen in Figure B-13. These recorded strains were employed to calculate the field LLDFs for each girder based upon the following equation.

$$LLDF^f = \frac{\epsilon^m \max i, t}{\sum_{i=1}^n \epsilon^m \max i, t} \quad (1)$$

Where $LLDF^f$ is the field live load distribution factor and ϵ^m are the measured maximum strains for individual girders over time, respectively.

A representative plot showing the comparison between static and dynamic strain for one of the girders under a test vehicle is shown in Figure B-14. It was generally observed that the girders experience more strain under dynamic loads than under static loading. The strain values from dynamic load tests were utilized to calculate the dynamic amplification factors (DAFs) for each girder.

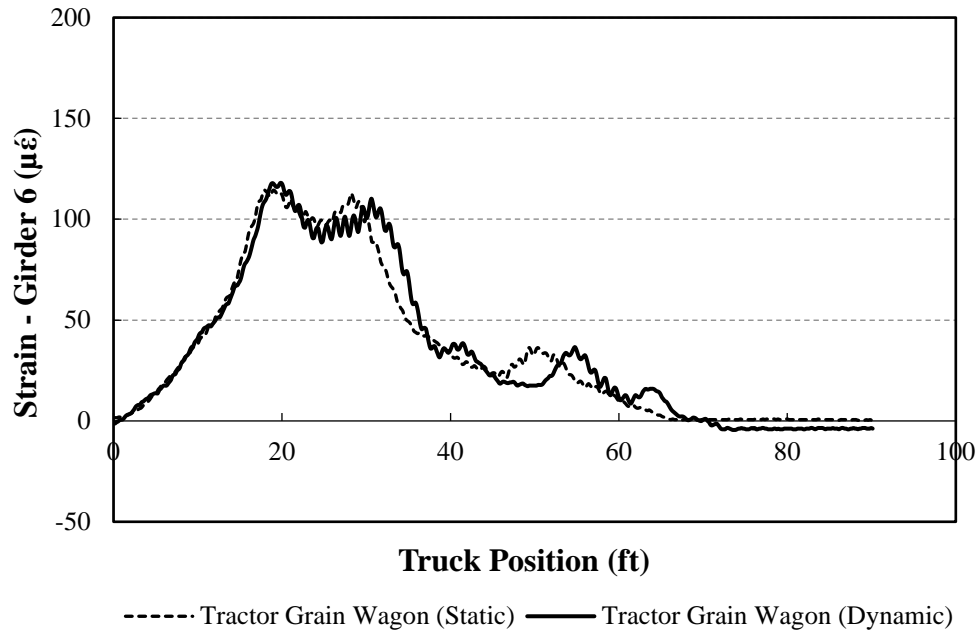


Figure B-14. Comparison between static and dynamic strain for Steel-Timber Bridge 2

B.2.4 Analytical Modeling

In lieu of field testing with a large number of vehicles, finite element analysis (FEA) simulations were used to estimate LLDFs for other vehicle configurations. As a result, analytical LLDFs were determined based upon FEA simulations of over 121 different farm vehicles on Bridge 2. The FEA model was developed as described subsequently, and specific bridge information is presented in the following sections.

Model Generation

The bridge was initially modeled with the geometric and material properties taken directly from available bridge plans and/or field inspections using the BDI (Bridge Diagnostics, Inc.) finite element software WinGEN. A modulus of elasticity of 1600 ksi and 29000 ksi was used for all timber and steel components in the model respectively. The FEA model consisted of beam elements for the girders, shell elements for the deck, and rotational springs that simulated rotational restraint at the abutments and piers. Figure B-15 shows a representative model of the bridge.

Model Calibration

To improve the model accuracy, a calibration process that identified the bridge properties that resulted in the lowest error was completed. Based upon similarities in the response and observed field condition, a single cross-section was considered for all the girders. Table B-4 summarizes the original and calibrated values for the various bridge components along with percent error and correlation coefficient values.

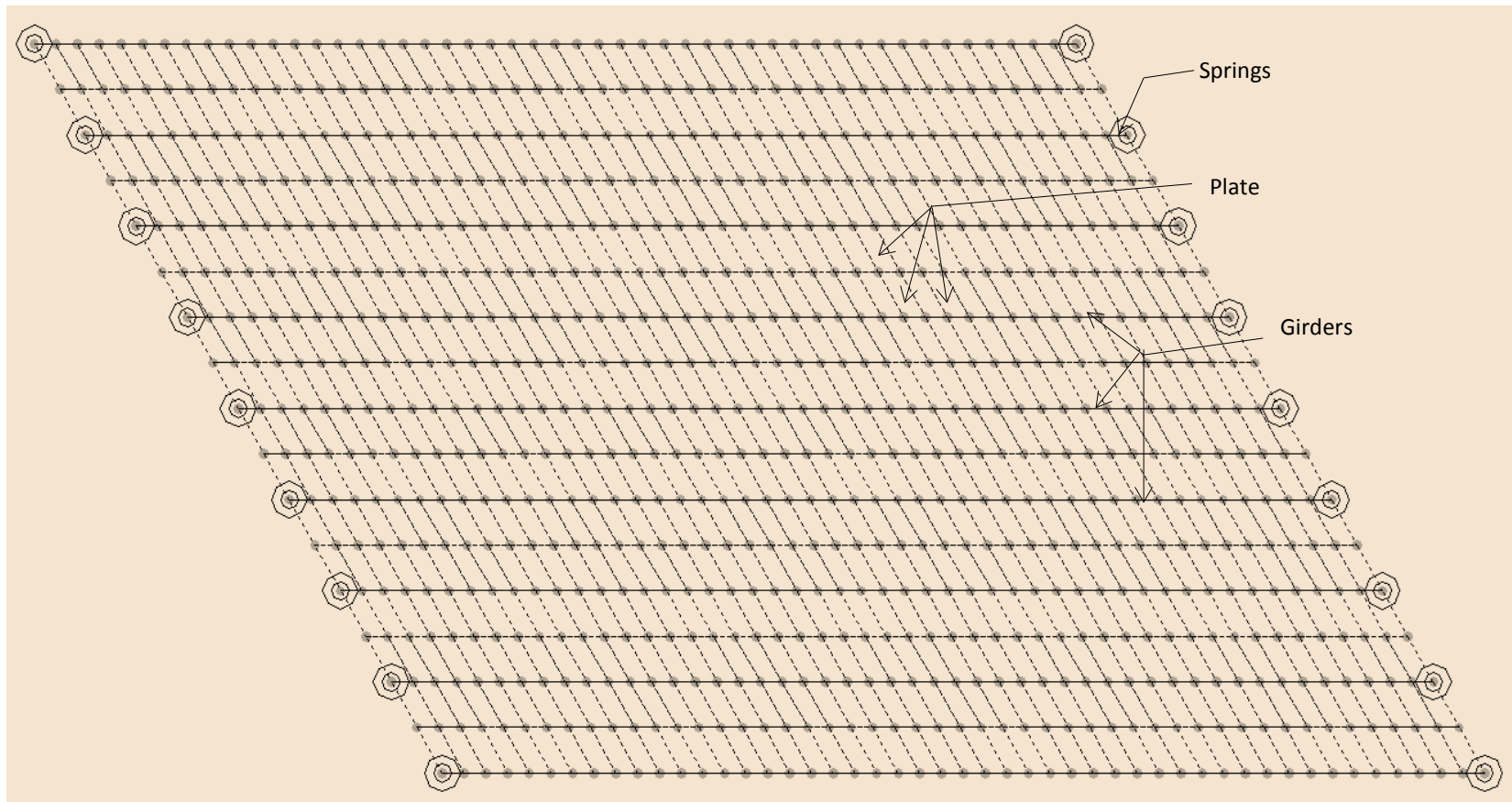


Figure B-15. Finite element model of Steel-Timber Bridge 2

Table B-4. Model calibration for Steel-Timber Bridge 2

Calibration Parameters	Bridge Components	Plan Value	Calibrated Value
Moment of Inertia, I (in ⁴)	All Girders	1250	1165
Modulus of Elasticity, E (Ksi)	Deck	1600	1943
Rotational Stiffness, kr (Kips-in/rad)	Support Connections (springs)	0	22980
Statistical Results	Percent Error		16.1%
	Correlation Coefficients		0.89

Once model calibration was completed, the analytical model was loaded with 121 farm vehicles covering a wide range of axle spacings, weights, and gage widths. The analytical strain response was then used to compute analytical LLDFs for each simulation vehicle using Equation (1).

To interpret the results efficiently, the LLDFs of the girders were grouped together as either interior or exterior girder LLDFs. Statistical limits for the interior and exterior girder LLDFs were determined from cumulative distribution function (CDF) curves defined to be at the 95% confidence thresholds.

B.2.5 Results

The envelopes of LLDFs for Steel-Timber Bridge 2 are presented in Figure B-16 for both the field and analytical LLDFs for each girder. In addition to the envelopes, the AASHTO LLDFs and statistical control limits for each group of interior and exterior girders are also shown.

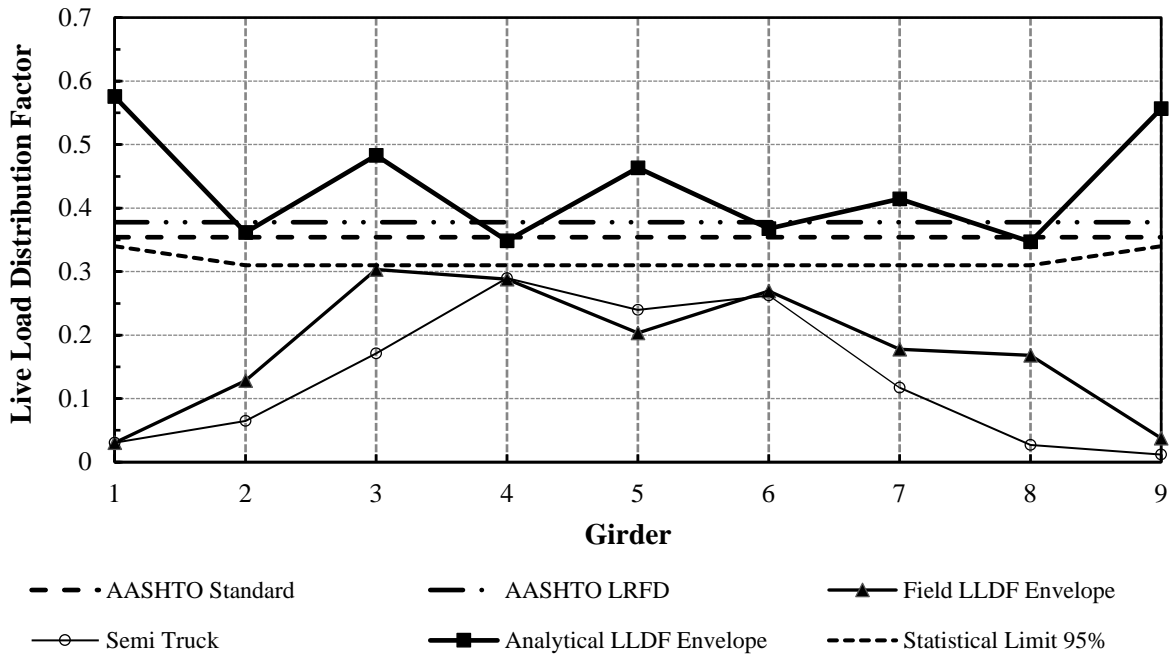


Figure B-16. LLDFs for Steel-Timber Bridge 2

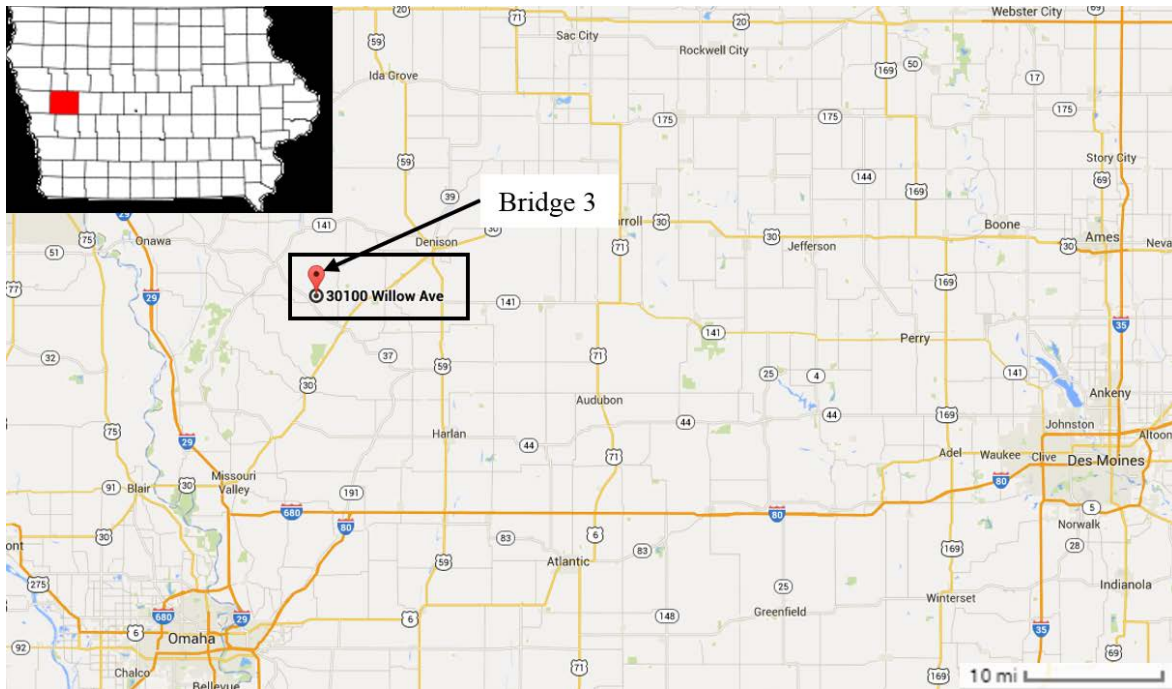
It appears that the analytical LLDF envelope for most of the girders is larger than those based on the AASHTO values. For girders G2, G4, G6, and G8, the analytical values are very close to AASHTO Standard and AASHTO LRFD specifications. The variability of LLDFs can be attributed to the skewness of the bridge. When a farm vehicle with an axle width of 10 ft is made to run across the bridge, which is 24.5 ft wide and has a 30-degree skew angle, there is a chance that one wheel is on the bridge and other is completely off the bridge, which causes unexpected moments on the girders and results in different LLDFs. The peak value of the analytical exterior girder LLDFs was observed in G1, which has an LLDF of 0.57, while that of the interior girders was found in G3, which has an LLDF of 0.48. The field LLDF envelope represents the highest LLDF observed in each girder due to field testing using farm vehicles, whereas the semi-truck envelope represents the extreme LLDFs for field testing using a five-axle semi-truck. The field LLDF envelope has larger values than that for the semi-truck for most of the girders, indicating for this bridge that farm vehicles result in higher values of LLDFs compared to the values from the conventional highway vehicle. The statistical limits for either the interior or exterior girder group show smaller values than the AASHTO specifications.

B.3 Steel-Timber Bridge 3

This mini test and evaluation report documents the results of field testing and subsequent analysis of a steel girder bridge with a timber deck (Steel-Timber Bridge 3) under multiple implements of husbandry. For completeness, this mini-report includes a description of the bridge, a description of the live load testing procedures followed, sample data, a description of analytical modeling, plots of analytical results, and a discussion of the overall behavior of the steel girder bridge under implements of husbandry.

B.3.1 Background

The steel-timber bridge described here is known in the National Bridge Inventory (NBI) database as Bridge 127121 and will be henceforth be referred to as Steel-Timber Bridge 3. The bridge is located about 25 miles east of Loess Hills State Forest, on O'Banion Road, in Dunlap near Crawford County, Iowa. Figure B-17 shows the general location of the bridge.



Map: ©Google 2014

Figure B-17. Location overview of Steel-Timber Bridge 3

B.3.2 Bridge Description

Steel-Timber Bridge 3 is open to two-lane traffic and has three spans with overall dimensions of 102 ft long by 24 ft wide with zero degrees of skew. The deck is comprised of continuous timber decking with a thickness of 4 in. An elevation view and an end view of the bridge are shown in Figure B-18. The bridge consists of seven steel girders with spacing between adjacent girders of 3.5 ft. The I cross-section girders are approximately 24.0 in. by 9.0 in. Figure B-19 shows a typical cross-section and plan view of the bridge.



Figure B-18. Steel-Timber Bridge 3: Elevation view (left) and east end view (right)

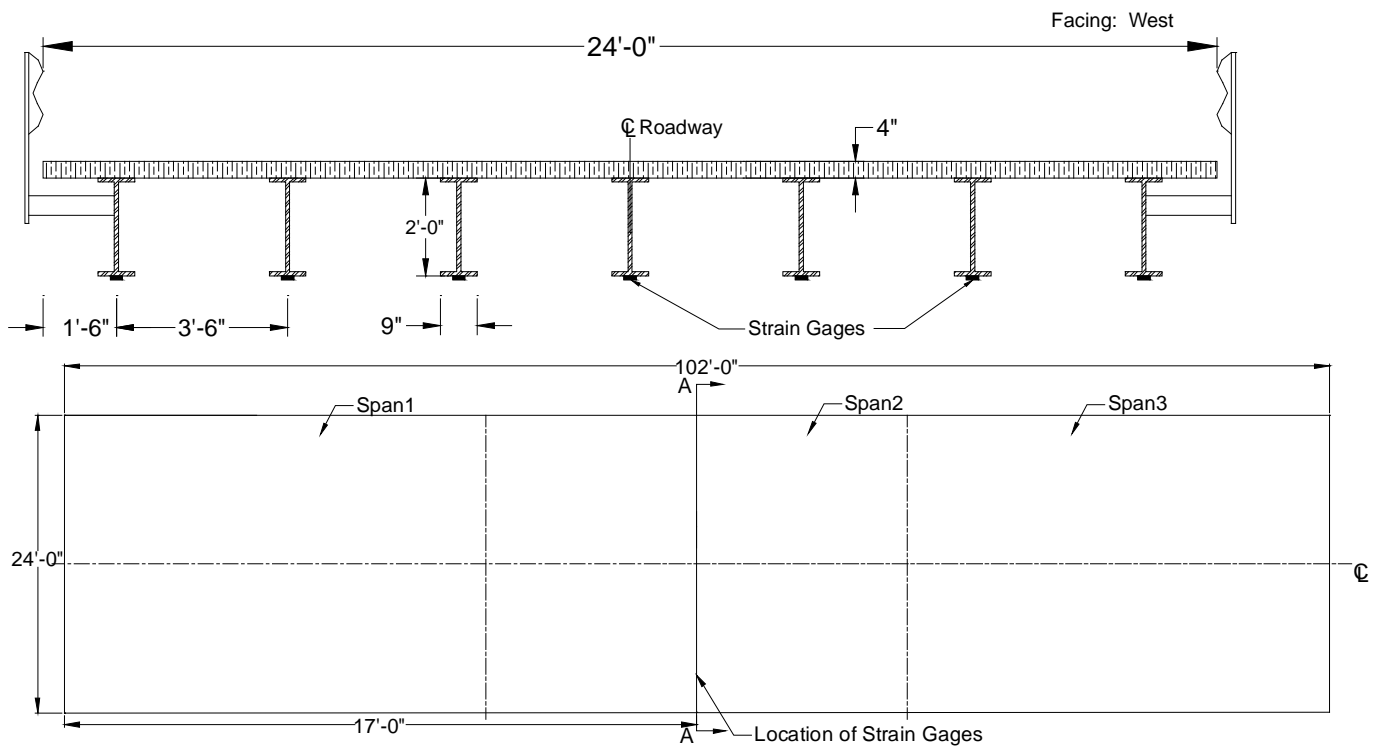


Figure B-19. Steel-Timber Bridge 3: Cross-section A-A (top) and plan (bottom)

B.3.3 Field Testing

Field testing of this bridge was conducted for two reasons. First, field testing was conducted to determine experimental live load distribution factors (LLDFs) and dynamic impact factors for the individual bridge girders. Second, these field data were also used to calibrate analytical models, which were then used to conduct a detailed parametric study related to a wide variety of implements of husbandry. A description of field tests, the procedures followed, and sample field results are detailed in the following sections.

Field Inspections

According to the most recent field inspection report, the Steel-Timber Bridge 3 timber deck is in good condition with some minor problems. The steel girders are also in good condition and show some signs of rust on them. These inspection-based observations were corroborated by the Iowa State University field testing team.

Instrumentation Plan

Given that the primary goal of the testing plan was to measure the live load response of the primary load-carrying members, a network of multiple strain gages was used to measure the strain under the weight of the vehicles. The strain gages were attached to the bottom of the girders at mid-span of Span 2 as shown in Figure B-19. The strain sensors used to conduct this testing were installed with a 3 in. gage length, and data were collected at a rate of 20 Hz during static testing and at 20 Hz during dynamic testing.

Test Load Paths

The vehicles utilized during field testing of this bridge consisted of four common farm vehicles and one typical highway truck. The vehicles included a terragator, a grain cart, a honey wagon with one tank, a honey wagon with two tanks, and a typical five-axle semi-truck. The individual axle loads, total weights, and lengths of the five vehicles used for field testing are summarized in Table B-5. As shown in Figure B-20, the configurations of the farm vehicles were notably different from that of the conventional highway truck.

Table B-5. Axle weight and total length of each testing vehicle

Farm Vehicles	Weight (lbs)					Total	Total Length (ft-in.)
	Front Axle	Rear Axle	Grain Wagon	Honey Wagon	Trailer		
Tractor Honey Wagon (empty)	10,960	15,740	-	26,720	-	53,420	40'-4"
Tractor Honey Wagon (half full with water)	10,580	22,800	-	40,620	-	74,000	40'-4"
Terragator	23,380	17,840	-	-	-	41,220	19'-0"
Tractor Grain Wagon	24,480	19,700	11,980	-	-	56,160	31'-0"
Semi-Truck	10,760	33,856	-	-	33,084	77,700	52'-1"



Honey Wagon



Honey Wagon- two tanks



Terragator



Tractor Grain Wagon



Semi Truck

Figure B-20. Farm vehicles used for field testing

During testing, the vehicles were driven across the bridge from west to east. In general the centerlines of the bridge and vehicle were approximately aligned. Initial static load testing was completed with the vehicles traveling at approximately 3 mph such that the pseudo-static bridge response could be captured. The dynamic load testing was completed with the vehicles traveling at approximately 15 mph (maximum safe speed at the site).

Sample Field Results

Representative plots from static load testing showing the strain experienced by one of the girders under all test vehicles is shown in Figure B-21. It was observed that the girders at the center of the bridge experienced the maximum strain magnitudes as the test vehicles crossed the bridge.

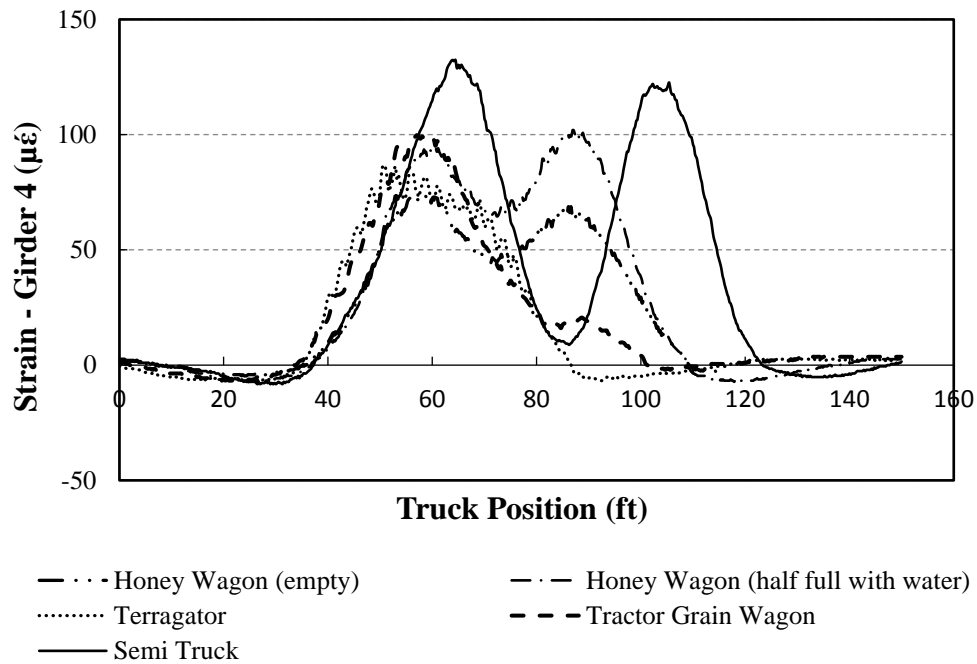


Figure B-21. Strain plot of a girder for all test vehicles for Steel-Timber Bridge 3

The semi-truck normally results in higher strains compared to other farm vehicles, and this tendency can be seen in Figure B-21. These recorded strains were employed to calculate the field LLDFs for each girder based upon the following equation.

$$LLDF^f = \frac{\epsilon^m \max i, t}{\sum_{i=1}^n \epsilon^m \max i, t} \quad (1)$$

Where $LLDF^f$ is the field live load distribution factor and ϵ^m are the measured maximum strains for individual girders over time, respectively.

A representative plot showing the comparison between static and dynamic strain for one of the girders under a test vehicle is shown in Figure B-22. It was generally observed that the girders experience more strain under dynamic loads than under static loading. The strain values from dynamic load tests were utilized to calculate the dynamic amplification factors (DAFs) for each girder.

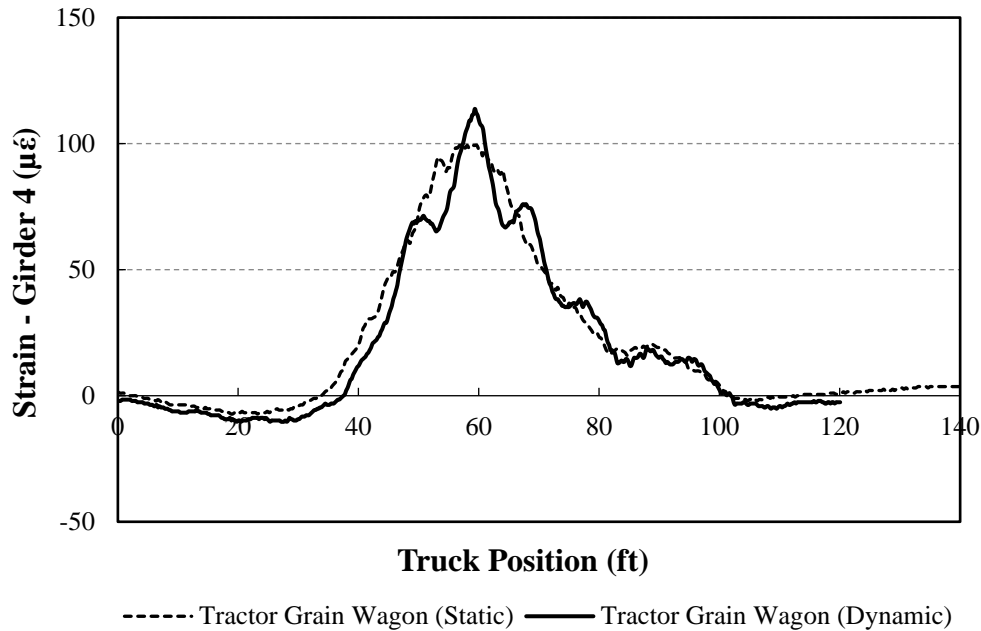


Figure B-22. Comparison between static and dynamic strain for Steel-Timber Bridge 3

B.3.4 Analytical Modeling

In lieu of field testing with a large number of vehicles, finite element analysis (FEA) simulations were used to estimate LLDFs for other vehicle configurations. As a result, analytical LLDFs were determined based upon FEA simulations of over 121 different farm vehicles on Steel-Timber Bridge 3. The FEA model was developed as described subsequently, and specific bridge information is presented in the following sections.

Model Generation

The bridge was initially modeled with the geometric and material properties taken directly from available bridge plans and/or field inspections using the BDI (Bridge Diagnostics, Inc.) finite element software WinGEN. A modulus of elasticity of 1600 ksi and 29000 ksi was used for all timber and steel components in the model respectively. The FEA model consisted of beam elements for the girders, shell elements for the deck, and rotational springs that simulated rotational restraint at the abutments and piers. Figure B-23 shows a representative model of the bridge.

Model Calibration

To improve the model accuracy, a calibration process that identified the bridge properties that resulted in the lowest error was completed. Based upon similarities in the response and observed field condition, a single cross-section was considered for all the girders. Table B-6 summarizes the original and calibrated values for the various bridge components along with percent error and correlation coefficient values. The moderately high percent error is most likely due to the highly variable material properties associated with timber components.

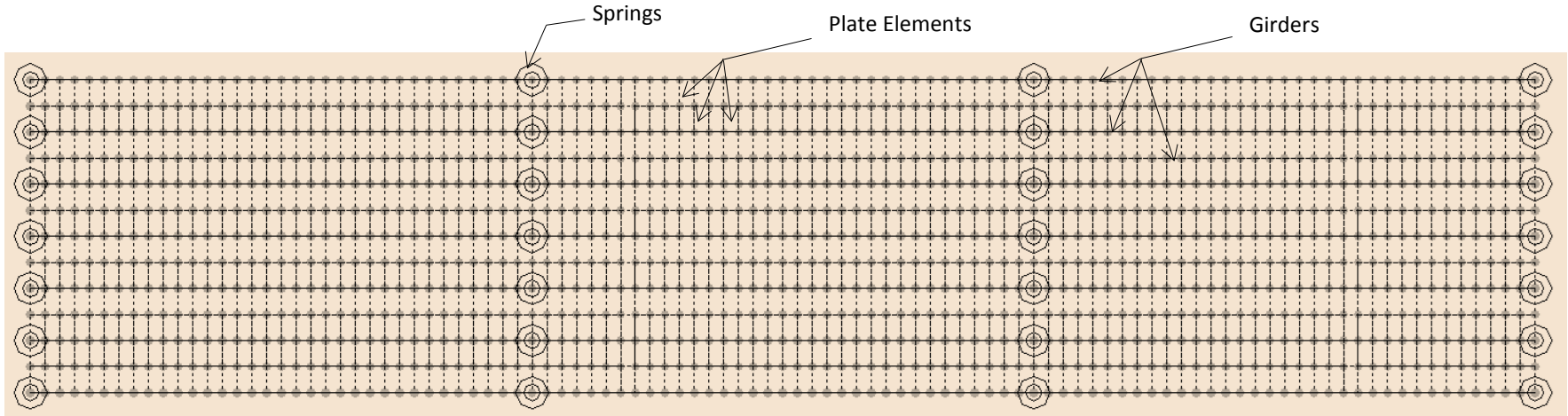


Figure B-23. Finite element model of Steel-Timber Bridge 3

Table B-6. Model calibration for Steel-Timber Bridge 3

Calibration Parameters	Bridge Components	Plan Value	Calibrated Value
Moment of Inertia, I (in ⁴)	All Girders	2080	1620
Modulus of Elasticity, E (Ksi)	Deck	1600	1200
Rotational Stiffness, kr (Kips-in/rad)	Support Connections (springs)	0	618666
Statistical Results	Percent Error		10.41%
	Correlation Coefficients		0.90

Once model calibration was completed, the analytical model was loaded with 121 farm vehicles covering a wide range of axle spacings, weights, and gage widths. The analytical strain response was then used to compute analytical LLDFs for each simulation vehicle using Equation (1).

To interpret the results efficiently, the LLDFs of the girders were grouped together as either interior or exterior girder LLDFs. Statistical limits for the interior and exterior girder LLDFs were determined from cumulative distribution function (CDF) curves defined to be at the 95% confidence thresholds.

B.3.5 Results

The envelopes of LLDFs for Steel-Timber Bridge 3 are presented in Figure B-24 for both the field and analytical LLDFs for each girder. In addition to the envelopes, the AASHTO LLDFs and statistical control limits for each group of interior and exterior girders are also shown.

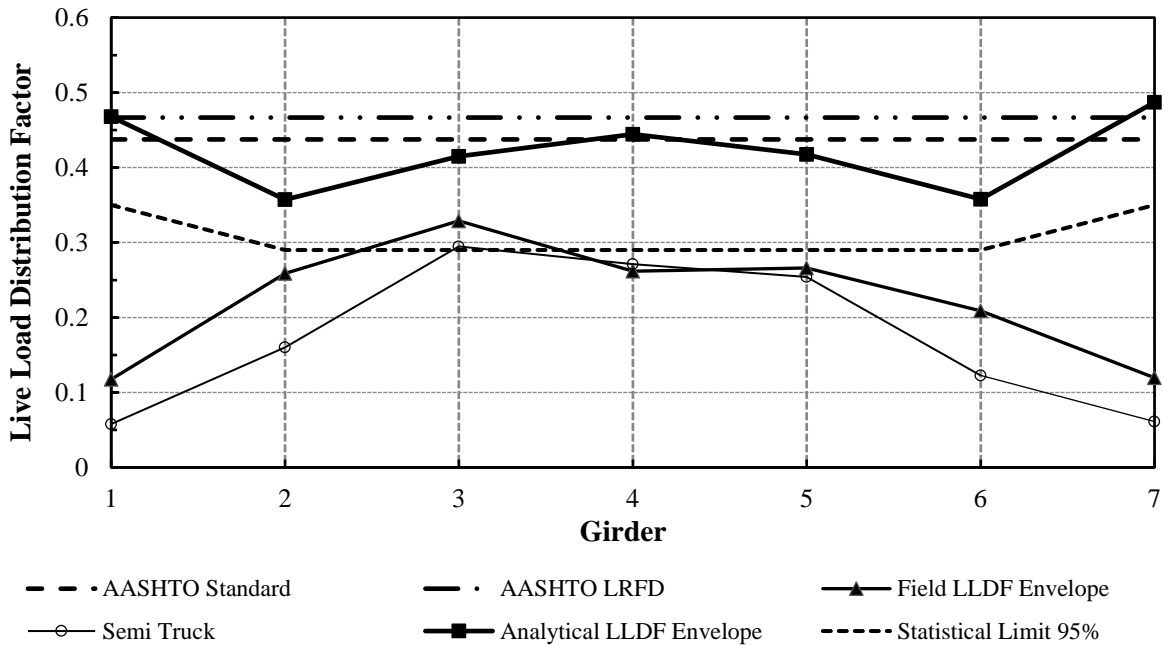


Figure B-24. LLDFs for Steel-Timber Bridge 3

It appears that the analytical LLDF envelope for all the interior girders are smaller than those from the AASHTO standard and LRFD specifications. In the case of exterior girders, the analytical LLDFs merely exceed the AASHTO values. The peak value of the analytical exterior girder LLDFs was observed in G7, which has an LLDF of 0.49, while that of the interior girders was found in G4, which has an LLDF of 0.44. The field LLDF envelope represents the highest LLDF observed in each girder due to field testing using farm vehicles, whereas the semi-truck envelope represents the extreme LLDFs for field testing using a five-axle semi-truck. The field LLDF envelope has larger values than that for the semi-truck for most of the girders. The statistical limits for either the interior or exterior girder group show smaller values than the AASHTO specifications.

B.4 Steel-Timber Bridge 4

This mini test and evaluation report documents the results of field testing and subsequent analysis of a steel girder bridge with a timber deck (Steel-Timber Bridge 4) under multiple implements of husbandry. For completeness, this mini-report includes a description of the bridge, a description of the live load testing procedures followed, sample data, a description of analytical modeling, plots of analytical results, and a discussion of the overall behavior of the steel girder bridge under implements of husbandry.

B.4.1 Background

The steel-timber bridge described here is known in the National Bridge Inventory (NBI) database as Bridge 128051 and will be henceforth be referred to as Steel-Timber Bridge 4. The bridge is located at intersection of O Avenue and 220th Street, in Arion, Crawford County, Iowa. Figure B-25 shows the general location of the bridge.

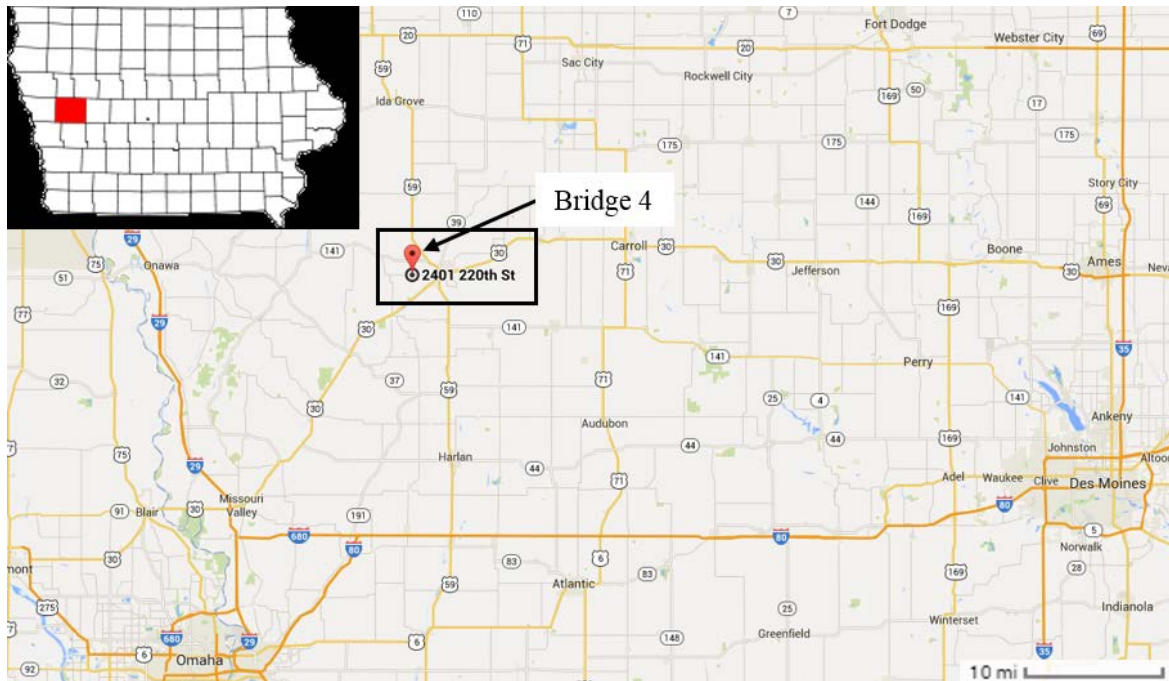


Figure B-25. Location overview of Steel-Timber Bridge 4

B.4.2 Bridge Description

Steel-Timber Bridge 4 is open to two-lane traffic and has two spans with overall dimensions of 75.7 ft long by 23.7 ft wide with zero degrees of skew. The deck is comprised of continuous timber decking with a thickness of 4 in. An elevation view and an end view of the bridge are shown in Figure B-26. The bridge consists of eight steel girders with spacing between adjacent girders of 3.2 ft. The I cross-section girders are approximately 24.0 in. by 9.0 in. Figure B-27 shows a typical cross-section and plan view of the bridge.



Figure B-26. Bridge 4: Elevation view (left) and east end view (right)

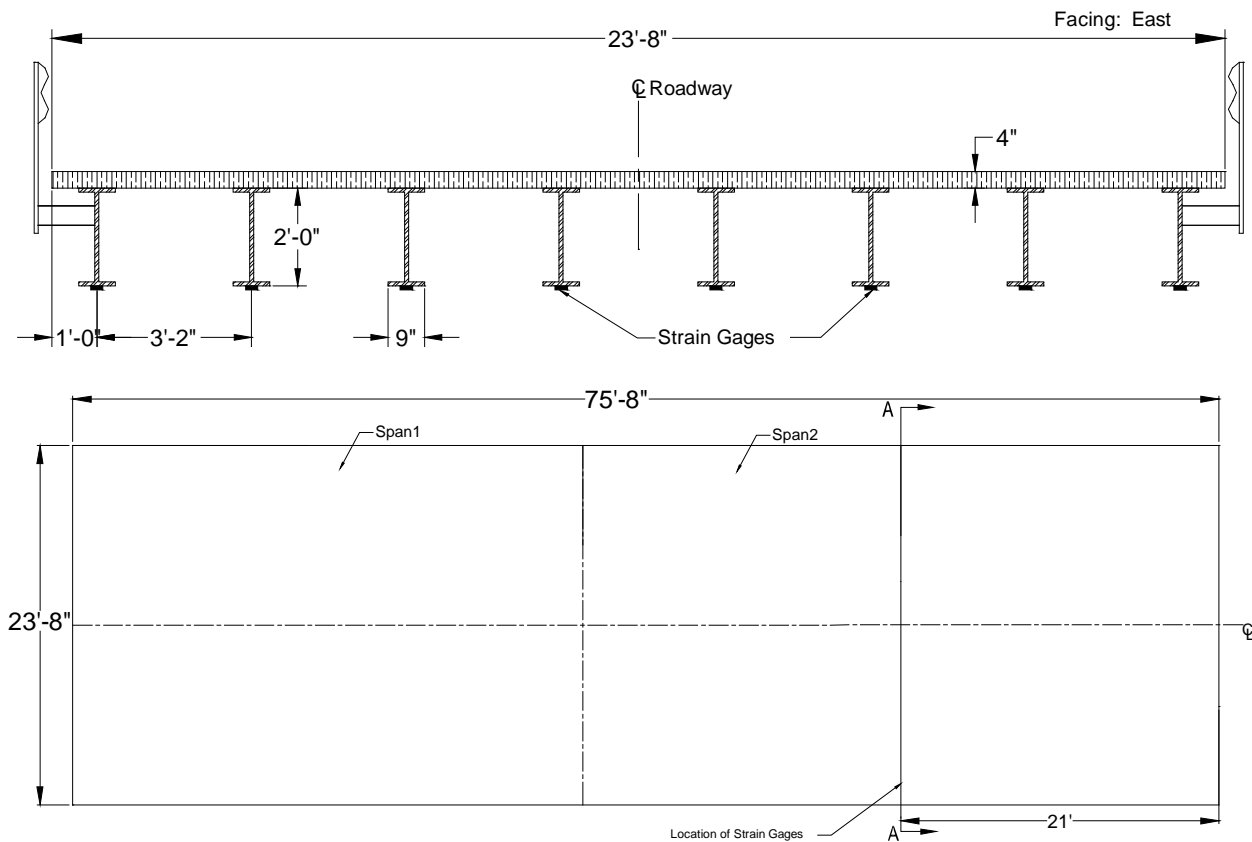


Figure B-27. Steel-Timber Bridge 4: Cross-section A-A (top) and plan (bottom)

B.4.3 Field Testing

Field testing of this bridge was conducted for two reasons. First, field testing was conducted to determine experimental live load distribution factors (LLDFs) and dynamic impact factors for the individual bridge girders. Second, these field data were also used to calibrate analytical

models, which were then used to conduct a detailed parametric study related to a wide variety of implements of husbandry. A description of field tests, the procedures followed, and sample field results are detailed in the following sections.

Field Inspections

According to the most recent field inspection report, the Steel-Timber Bridge 4 timber deck is in good condition with some minor problems. The steel girders are also in good condition. These inspection-based observations were corroborated by the Iowa State University field testing team.

Instrumentation Plan

Given that the primary goal of the testing plan was to measure the live load response of the primary load-carrying members, a network of multiple strain gages was used to measure the strain under the weight of the vehicles. The strain gages were attached to the bottom of the girders at mid-span of Span 2 as shown in Figure B-27. The strain sensors used to conduct this testing were installed with a 3 in. gage length, and data were collected at a rate of 20 Hz during static testing and at 20 Hz during dynamic testing.

Test Load Paths

The vehicles utilized during field testing of this bridge consisted of four common farm vehicles and one typical highway truck. The vehicles included a terragator, a grain cart, a honey wagon with one tank, a honey wagon with two tanks, and a typical five-axle semi-truck. The individual axle loads, total weights, and lengths of the five vehicles used for field testing are summarized in Table B-7. As shown in Figure B-28, the configurations of the farm vehicles were notably different from that of the conventional highway truck.

Table B-7. Axle weight and total length of each testing vehicle

Farm Vehicles	Weight (lbs)					Total	Total Length (ft-in.)
	Front Axle	Rear Axle	Grain Wagon	Honey Wagon	Trailer		
Tractor Honey Wagon (empty)	10,960	15,740	-	26,720	-	53,420	40'-4"
Tractor Honey Wagon (half full with water)	10,580	22,800	-	40,620	-	74,000	40'-4"
Terragator	23,380	17,840	-	-	-	41,220	19'-0"
Tractor Grain Wagon	24,480	19,700	11,980	-	-	56,160	31'-0"
Semi-Truck	10,760	33,856	-	-	33,084	77,700	52'-1"



Honey Wagon



Honey Wagon- two tanks



Terragator



Tractor Grain Wagon



Semi Truck

Figure B-28. Farm vehicles used for field testing

During testing, the vehicles were driven across the bridge from east to west. In general the centerlines of the bridge and vehicle were approximately aligned. Initial static load testing was completed with the vehicles traveling at approximately 3 mph such that the pseudo-static bridge response could be captured. The dynamic load testing was completed with the vehicles traveling at approximately 15 mph (maximum safe speed at the site).

Sample Field Results

Representative plots from static load testing showing the strain experienced by one of the girders under all test vehicles is shown in Figure B-29. It was observed that the girders at the center of the bridge experienced the maximum strain magnitudes as the test vehicles crossed the bridge.

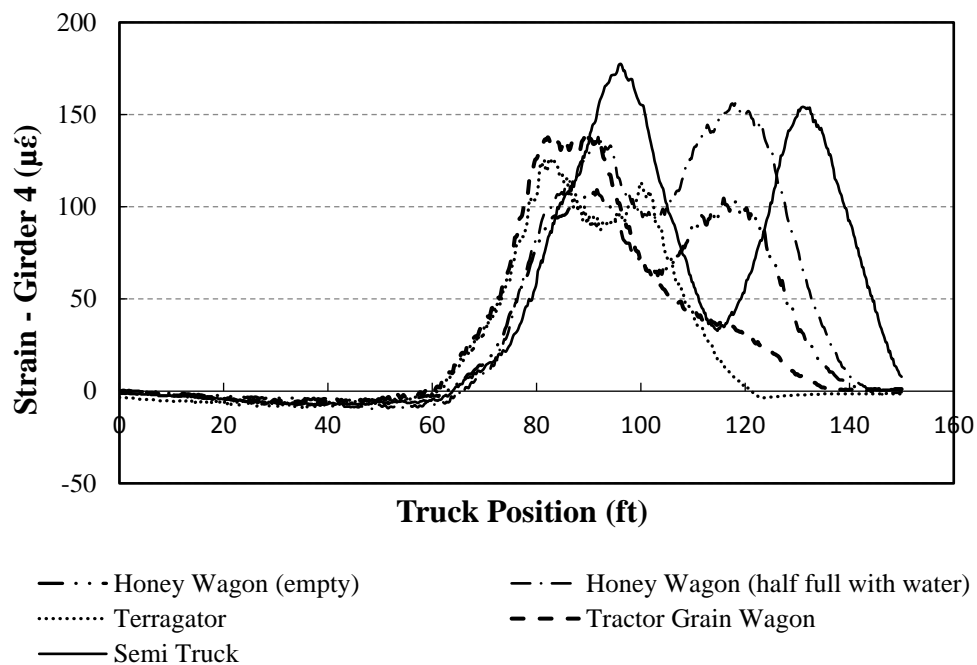


Figure B-29. Strain plot of a girder for all test vehicles for Steel-Timber Bridge 4

The semi-truck normally results in higher strains compared to other farm vehicles, and this tendency can be seen in Figure B-29. These recorded strains were employed to calculate the field LLDFs for each girder based upon the following equation.

$$LLDF^f = \frac{\epsilon^m \max i, t}{\sum_{i=1}^n \epsilon^m \max i, t} \quad (1)$$

Where $LLDF^f$ is the field live load distribution factor and ϵ^m are the measured maximum strains for individual girders over time, respectively.

A representative plot showing the comparison between static and dynamic strain for one of the girders under a test vehicle is shown in Figure B-30. It was generally observed that the girders experience more strain under dynamic loads than under static loading. The strain values from dynamic load tests were utilized to calculate the dynamic amplification factors (DAFs) for each girder.

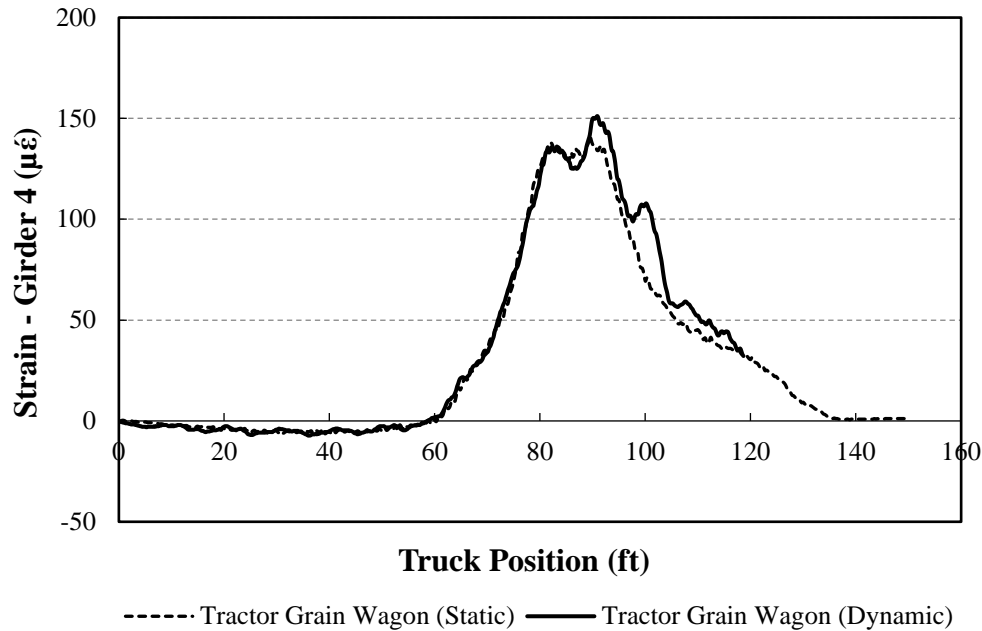


Figure B-30. Comparison between static and dynamic strain for Steel-Timber Bridge 4

B.4.4 Analytical Modeling

In lieu of field testing with a large number of vehicles, finite element analysis (FEA) simulations were used to estimate LLDFs for other vehicle configurations. As a result, analytical LLDFs were determined based upon FEA simulations of over 121 different farm vehicles on Steel-Timber Bridge 4. The FEA model was developed as described subsequently, and specific bridge information is presented in the following sections.

Model Generation

The bridge was initially modeled with the geometric and material properties taken directly from available bridge plans and/or field inspections using the BDI (Bridge Diagnostics, Inc.) finite element software WinGEN. A modulus of elasticity of 1600 ksi and 29000 ksi was used for all timber and steel components in the model respectively. The FEA model consisted of beam elements for the girders, shell elements for the deck, and rotational springs that simulated rotational restraint at the abutments and piers. Figure B-31 shows a representative model of the bridge.

Model Calibration

To improve the model accuracy, a calibration process that identified the bridge properties that resulted in the lowest error was completed. Based upon similarities in the response and observed field condition, a single cross-section was considered for all the girders. Table B-8 summarizes the original and calibrated values for the various bridge components along with percent error and correlation coefficient values. The moderately high percent error is most likely due to the highly variable material properties associated with timber components.

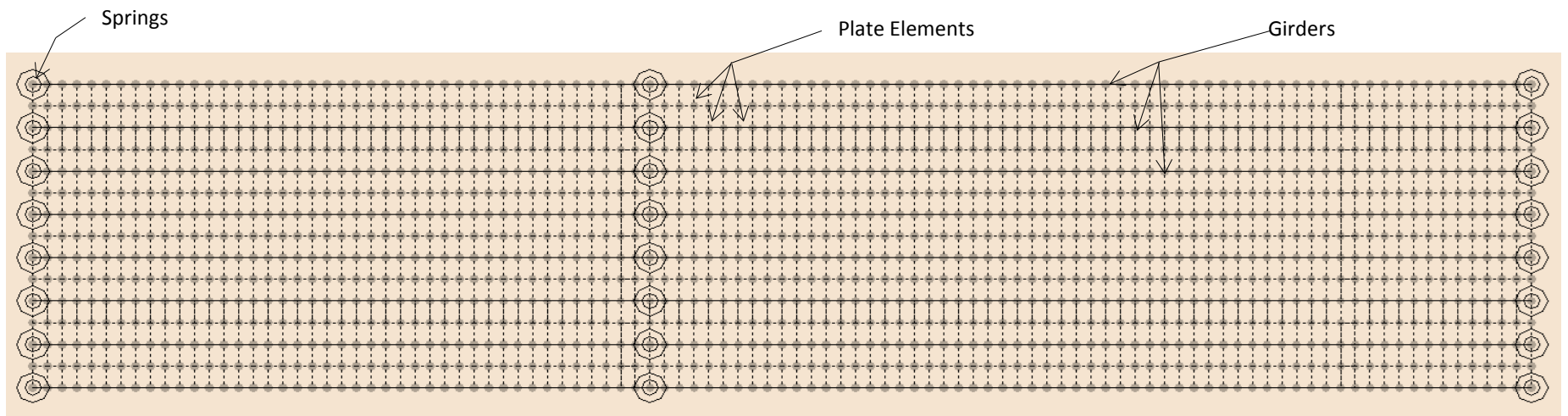


Figure B-31. Finite element model of Steel-Timber Bridge 4

Table B-8. Model calibration for Steel-Timber Bridge 4

Calibration Parameters	Bridge Components	Plan Value	Calibrated Value
Moment of Inertia, I (in ⁴)	All Girders	2360	2300
Modulus of Elasticity, E (Ksi)	Deck	1600	1494
Rotational Stiffness, kr (Kips-in/rad)	Support Connections (springs)	0	155772
Statistical Results	Percent Error		10.41%
	Correlation Coefficients		0.90

Once model calibration was completed, the analytical was model loaded with 121 farm vehicles covering a wide range of axle spacings, weights, and gage widths. The analytical strain response was then used to compute analytical LLDFs for each simulation vehicle using Equation (1).

To interpret the results efficiently, the LLDFs of the girders were grouped together as either interior or exterior girder LLDFs. Statistical limits for the interior and exterior girder LLDFs were determined from cumulative distribution function (CDF) curves defined to be at the 95% confidence thresholds.

B.4.5 Results

The envelopes of LLDFs for Steel-Timber Bridge 4 are presented in Figure B-32 for both the field and analytical LLDFs for each girder. In addition to the envelopes, the AASHTO LLDFs and statistical control limits for each group of interior and exterior girders are also shown.

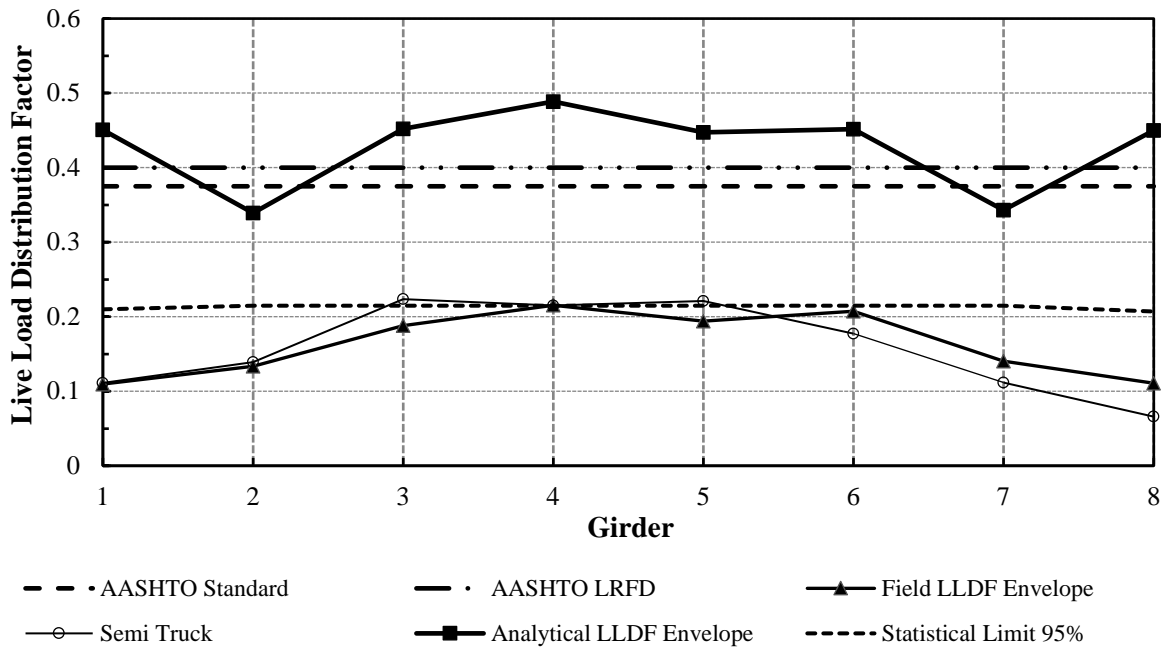


Figure B-32. LLDFs for Steel-Timber Bridge 4

It appears that the analytical LLDF envelope for most of the interior and exterior girders are larger than those from the AASHTO standard and LRFD specifications. The peak value of the analytical exterior girder LLDFs was observed in G1, which has an LLDF of 0.45, while that of the interior girders was found in G4, which has an LLDF of 0.49. The field LLDF envelope represents the highest LLDF observed in each girder due to field testing using farm vehicles, whereas the semi-truck envelope represents the extreme LLDFs for field testing using a five-axle semi-truck. The field LLDF envelope has larger values than that for the semi-truck for most of the girders. The statistical limits for either the interior or exterior girder group show smaller values than the AASHTO specifications.

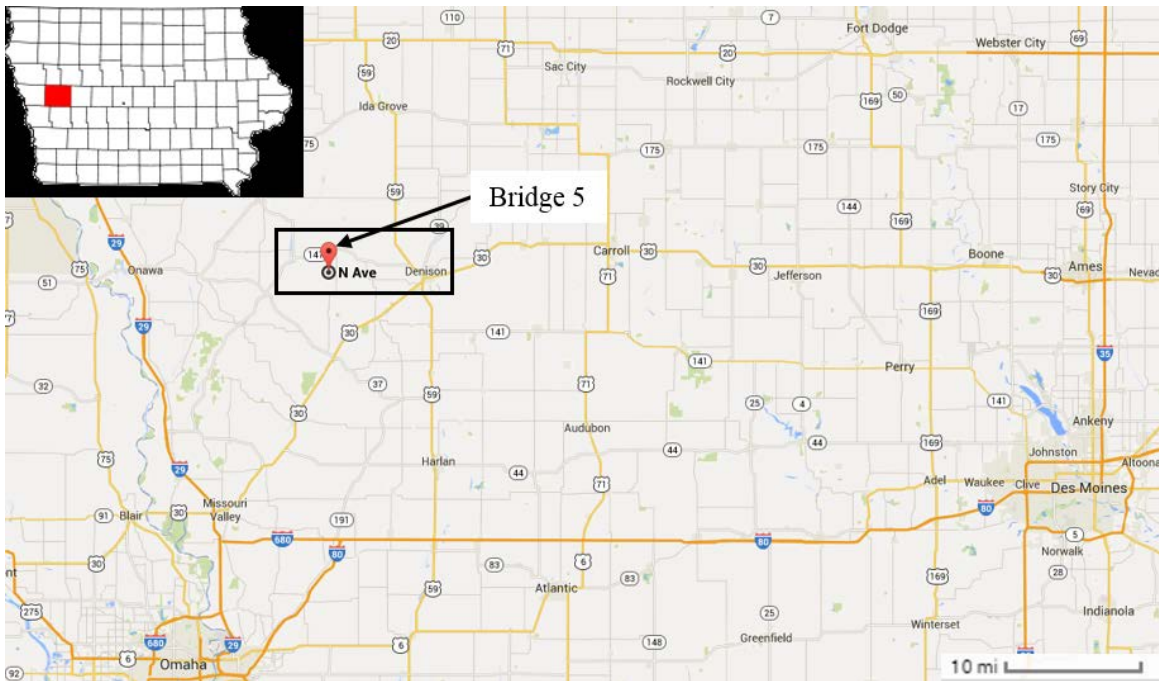
B.5 Steel-Timber Bridge 5

This mini test and evaluation report documents the results of field testing and subsequent analysis of a steel girder bridge with a timber deck (Steel-Timber Bridge 5) under multiple implements of husbandry. For completeness, this mini-report includes a description of the bridge, a description of the live load testing procedures followed, sample data, a description of analytical modeling, plots of analytical results, and a discussion of the overall behavior of the steel girder bridge under implements of husbandry.

B.5.1 Background

The steel-timber bridge described here is known in the National Bridge Inventory (NBI) database as Bridge 128211 and will be henceforth be referred to as Steel-Timber Bridge 5. The bridge is

located at intersection of N Avenue and 130th Street, in Arion, Crawford County, Iowa. Figure B-33 shows the general location of the bridge.



Map: ©Google 2014

Figure B-33. Location overview of Steel-Timber Bridge 5

B.5.2 Bridge Description

Bridge 5 is open to two-lane traffic and has one span with overall dimensions of 38.1 ft long by 22.0 ft wide with zero degrees of skew. The deck is comprised of continuous timber decking with a thickness of 4 in. An elevation view and an end view of the bridge are shown in Figure B-34. The bridge consists of nine steel girders with spacing between adjacent girders of 2.7 ft. The I cross-section girders are approximately 16.1 in. by 8.8 in. Figure B-35 shows a typical cross-section and plan view of the bridge.



Figure B-34. Bridge 5: West elevation view (left) and north end view (right)

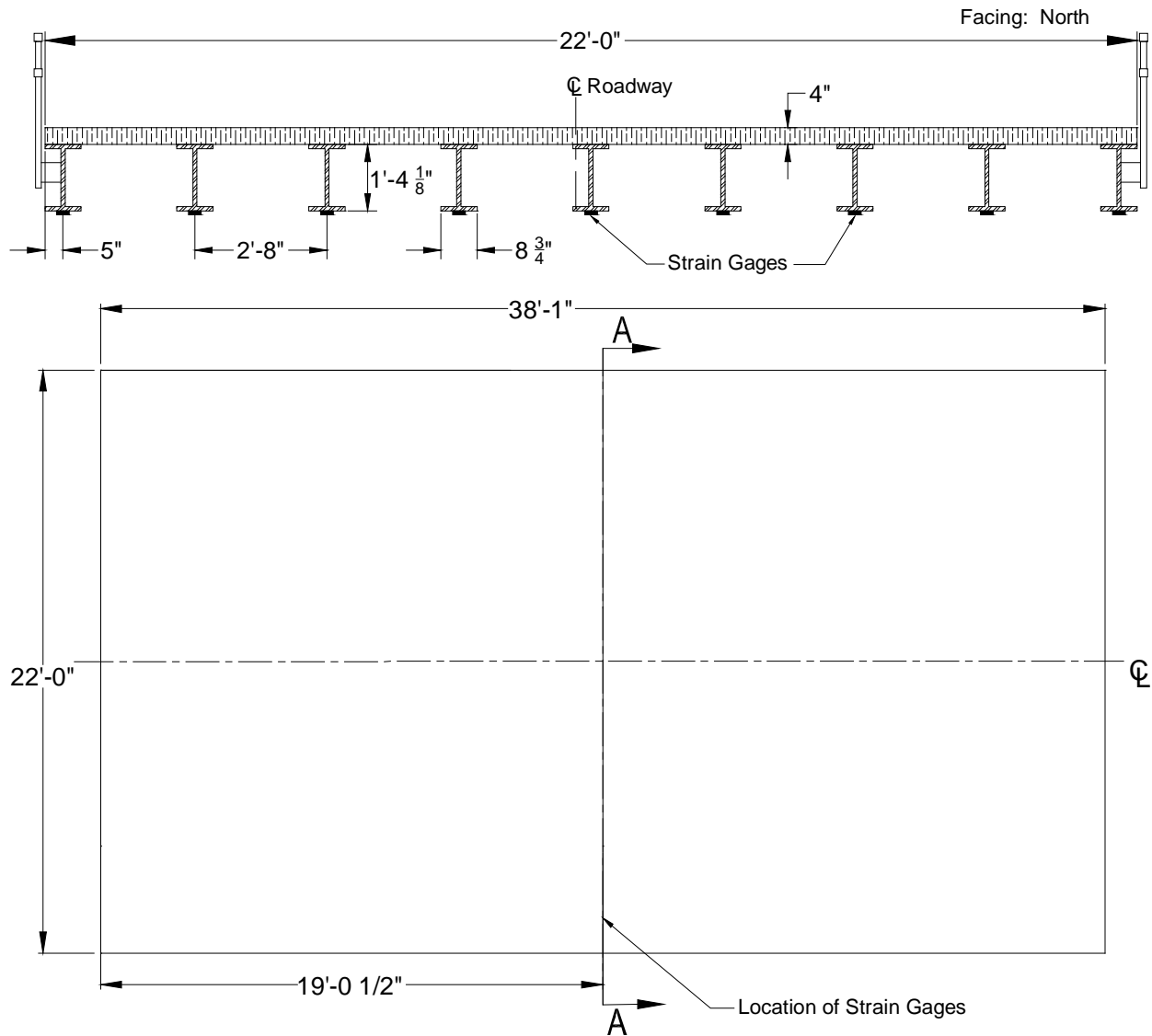


Figure B-35. Steel-Timber Bridge 5: Cross-section A-A (top) and plan (bottom)

B.5.3 Field Testing

Field testing of this bridge was conducted for two reasons. First, field testing was conducted to determine experimental live load distribution factors (LLDFs) and dynamic impact factors for the individual bridge girders. Second, these field data were also used to calibrate analytical models, which were then used to conduct a detailed parametric study related to a wide variety of implements of husbandry. A description of field tests, the procedures followed, and sample field results are detailed in the following sections.

Field Inspections

According to the most recent field inspection report, the Steel-Timber Bridge 5 timber deck is in good condition with some minor problems. The steel girders are also in good condition. These inspection-based observations were corroborated by the Iowa State University field testing team.

Instrumentation Plan

Given that the primary goal of the testing plan was to measure the live load response of the primary load-carrying members, a network of multiple strain gages was used to measure the strain under the weight of the vehicles. The strain gages were attached to the bottom of the girders at mid-span as shown in Figure B-35. The strain sensors used to conduct this testing were installed with a 3 in. gage length, and data were collected at a rate of 20 Hz during static testing and at 20 Hz during dynamic testing.

Test Load Paths

The vehicles utilized during field testing of this bridge consisted of four common farm vehicles and one typical highway truck. The farm vehicles included a terragator, a grain cart, a honey wagon with one tank, a honey wagon with two tanks, and a typical five-axle semi-truck. The individual axle loads, total weights, and lengths of the five vehicles used for field testing are summarized in Table 1. As shown in Figure B-36, the configurations of the farm vehicles were notably different from that of the conventional highway truck.

Table B-9. Axle weight and total length of each testing vehicle

Farm Vehicles	Weight (lbs)					Total	Total Length (ft-in.)
	Front Axle	Rear Axle	Grain Wagon	Honey Wagon	Trailer		
Tractor Honey Wagon (empty)	10,960	15,740	-	26,720	-	53,420	40'-4"
Tractor Honey Wagon (half full with water)	10,580	22,800	-	40,620	-	74,000	40'-4"
Terragator	23,380	17,840	-	-	-	41,220	19'-0"
Tractor Grain Wagon	24,480	19,700	11,980	-	-	56,160	31'-0"
Semi-Truck	10,760	33,856	-	-	33,084	77,700	52'-1"



Honey Wagon



Honey Wagon- two tanks



Terragator



Tractor Grain Wagon



Semi Truck

Figure B-36. Farm vehicles used for field testing

During testing, the vehicles were driven across the bridge from east to west. In general the centerlines of the bridge and vehicle were approximately aligned. Initial static load testing was completed with the vehicles traveling at approximately 3 mph such that the pseudo-static bridge response could be captured. The dynamic load testing was completed with the vehicles traveling at approximately 15 mph (maximum safe speed at the site).

Sample Field Results

Representative plots from static load testing showing the strain experienced by one of the girders under all test vehicles is shown in Figure B-37. It was observed that the girders at the center of the bridge experienced the maximum strain magnitudes as the test vehicles crossed the bridge.

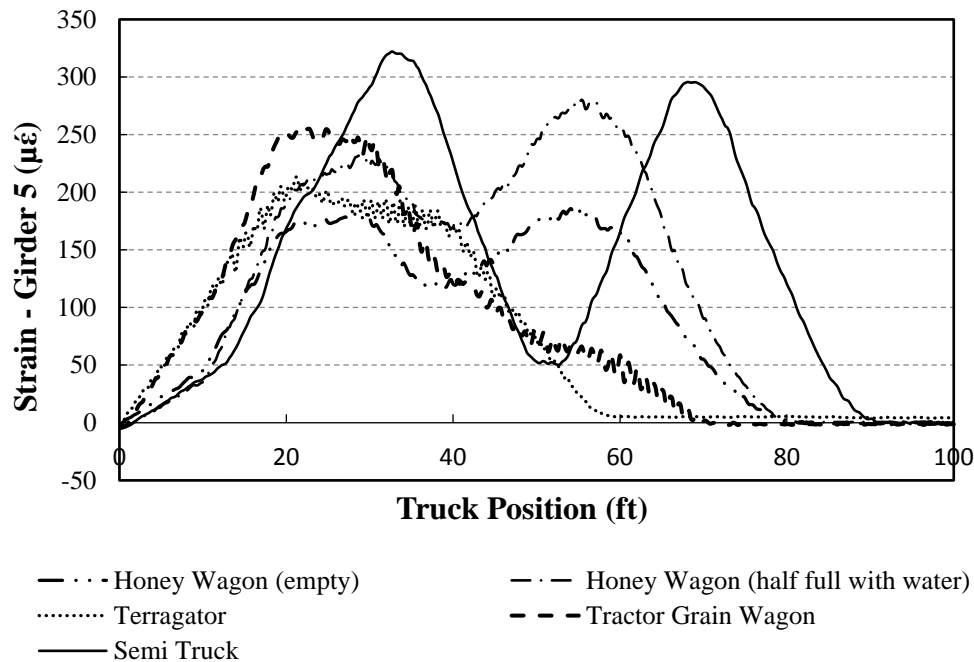


Figure B-37. Strain plot of a girder for all test vehicles for Steel-Timber Bridge 5

The semi-truck normally results in higher strains compared to other farm vehicles, and this tendency can be seen in Figure B-37. These recorded strains were employed to calculate the field LLDFs for each girder based upon the following equation.

$$LLDF^f = \frac{\epsilon^m \max i,t}{\sum_{i=1}^n \epsilon^m \max i,t} \quad (1)$$

Where $LLDF^f$ is the field live load distribution factor and ϵ^m are the measured maximum strains for individual girders over time, respectively.

A representative plot showing the comparison between static and dynamic strain for one of the girders under a test vehicle is shown in Figure B-38. It was generally observed that the girders experience more strain under dynamic loads than under static loading. The strain values from dynamic load tests were utilized to calculate the dynamic amplification factors (DAFs) for each girder.

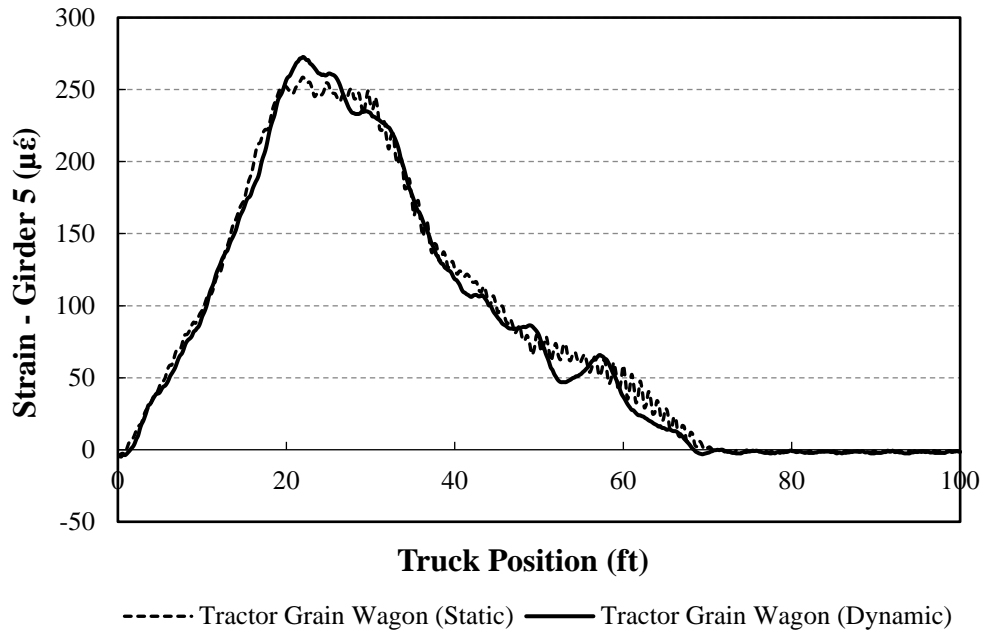


Figure B-38. Comparison between static and dynamic strain for Steel-Timber Bridge 5

B.5.4 Analytical Modeling

In lieu of field testing with a large number of vehicles, finite element analysis (FEA) simulations were used to estimate LLDFs for other vehicle configurations. As a result, analytical LLDFs were determined based upon FEA simulations of over 121 different farm vehicles on Steel-Timber Bridge 5. The FEA model was developed as described subsequently, and specific bridge information is presented in the following sections.

Model Generation

The bridge was initially modeled with the geometric and material properties taken directly from available bridge plans and/or field inspections using the BDI (Bridge Diagnostics, Inc.) finite element software WinGEN. A modulus of elasticity of 1600 ksi and 29000 ksi was used for all timber and steel components in the model respectively. The FEA model consisted of beam elements for the girders, shell elements for the deck, and rotational springs that simulated rotational restraint at the abutments and piers. Figure B-39 shows a representative model of the bridge.

Model Calibration

To improve the model accuracy, a calibration process that identified the bridge properties that resulted in the lowest error was completed. Based upon similarities in the response and observed field condition, a single cross-section was considered for all the girders. Table B-10 summarizes the original and calibrated values for the various bridge components along with percent error and correlation coefficient values. The moderately high percent error is most likely due to the highly variable material properties associated with timber components.

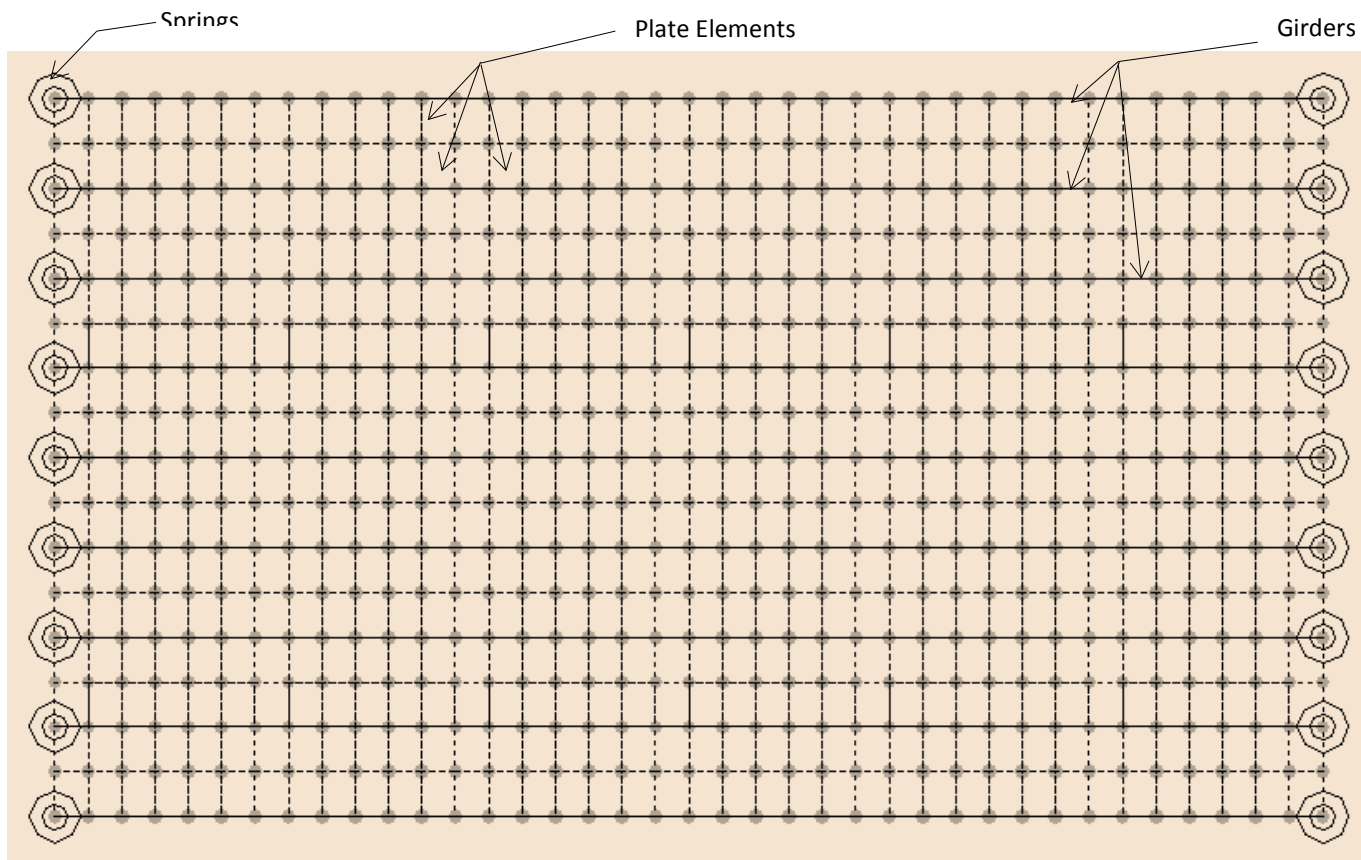


Figure B-39. Finite element model of Steel-Timber Bridge 5

Table B-10. Model calibration for Steel-Timber Bridge 5

Calibration Parameters	Bridge Components	Plan Value	Calibrated Value
Moment of Inertia, I (in ⁴)	All Girders	490	480
Modulus of Elasticity, E (Ksi)	Deck	1600	1200
Rotational Stiffness, kr (Kips-in/rad)	Support Connections (springs)	0	10001
Statistical Results	Percent Error		7.2%
	Correlation Coefficients		0.96

Once model calibration was completed, the analytical model was loaded with 121 farm vehicles covering a wide range of axle spacings, weights, and gage widths. The analytical strain response was then used to compute analytical LLDFs for each simulation vehicle using Equation (1).

To interpret the results efficiently, the LLDFs of the girders were grouped together as either interior or exterior girder LLDFs. Statistical limits for the interior and exterior girder LLDFs were determined from cumulative distribution function (CDF) curves defined to be at the 95% confidence thresholds.

B.5.5 Results

The envelopes of LLDFs for Steel-Timber Bridge 5 are presented in Figure B-40 for both the field and analytical LLDFs for each girder. In addition to the envelopes, the AASHTO LLDFs and statistical control limits for each group of interior and exterior girders are also shown.

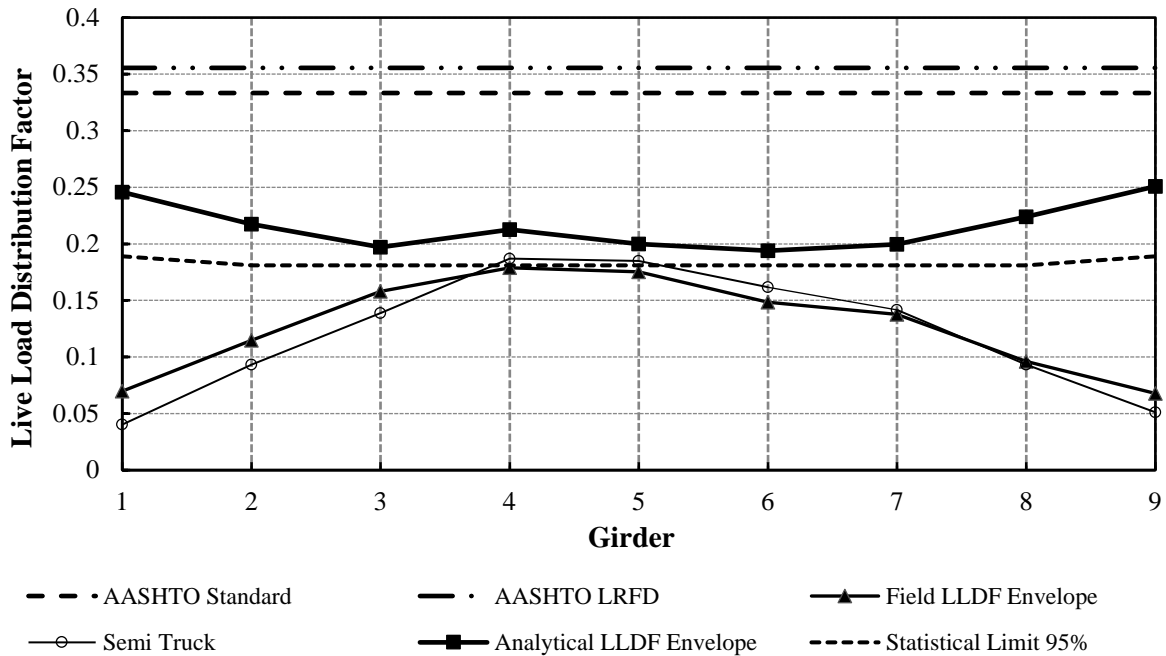


Figure B-40. LLDFs for Steel-Timber Bridge 5

It appears that the analytical LLDF envelope for all the interior and exterior girders are smaller than those from the AASHTO standard and LRFD specifications. The peak value of the analytical exterior girder LLDFs was observed in G9, which has an LLDF of 0.25, while that of the interior girders was found in G4, which has an LLDF of 0.22. The field LLDF envelope represents the highest LLDF observed in each girder due to field testing using farm vehicles, whereas the semi-truck envelope represents the extreme LLDFs for field testing using a five-axle semi-truck. The field LLDF envelope has larger values than that for the semi-truck for most of the girders. The statistical limits for either the interior or exterior girder group show smaller values than the AASHTO specifications.

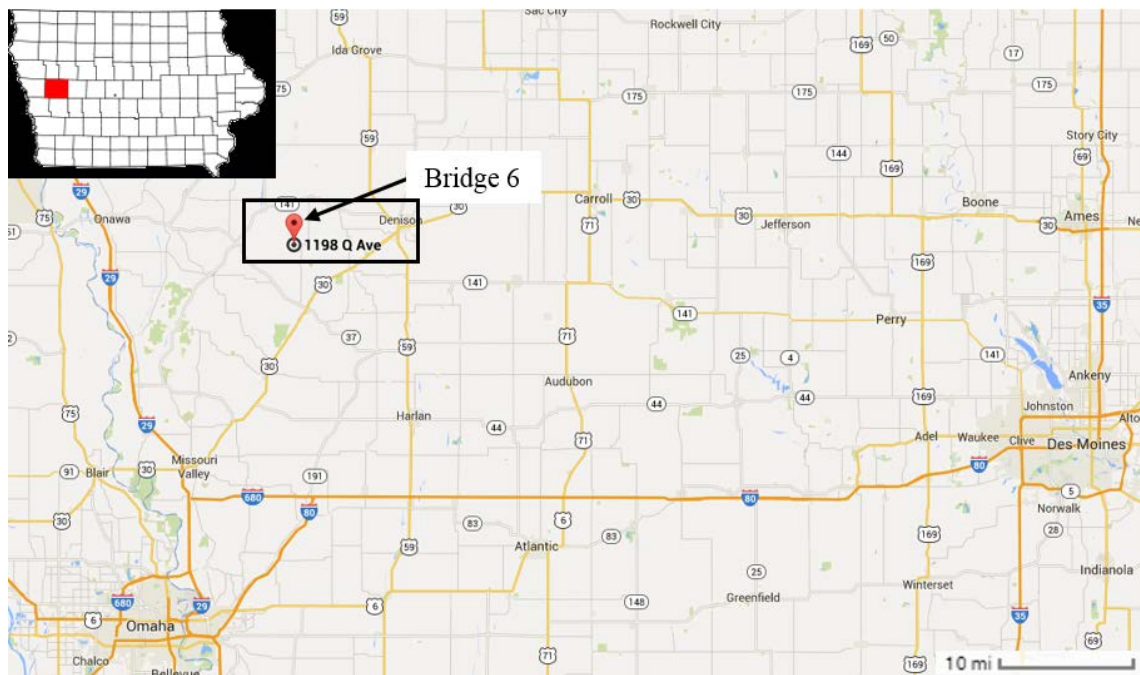
B.6 Steel-Timber Bridge 6

This mini test and evaluation report documents the results of field testing and subsequent analysis of a steel girder bridge with a timber deck (Steel-Timber Bridge 6) under multiple implements of husbandry. For completeness, this mini-report includes a description of the bridge, a description of the live load testing procedures followed, sample data, a description of analytical modeling, plots of analytical results, and a discussion of the overall behavior of the steel girder bridge under implements of husbandry.

B.6.1 Background

The steel-timber bridge described here is known in the National Bridge Inventory (NBI) database as Bridge 128370 and will be henceforth be referred to as Steel-Timber Bridge 6. The bridge is

located on Q Avenue in between 120th and 130th Street, in Arion, Crawford County, Iowa. Figure B-41 shows the general location of the bridge.



Map: ©Google 2014

Figure B-41. Location overview of Steel-Timber Bridge 6

B.6.2 Bridge Description

Steel-Timber Bridge 6 is open to two-lane traffic and has two spans with overall dimensions of 66.0 ft long by 21.0 ft wide with zero degrees of skew. The deck is comprised of continuous timber decking with a thickness of 4 in. An elevation view and an end view of the bridge are shown in Figure B-42. The bridge consists of seven steel girders with spacing between adjacent girders of 3.2 ft. The I cross-section girders are approximately 27.0 in. by 10.0 in. Figure B-43 shows a typical cross-section and plan view of the bridge.



Figure B-42. Steel-Timber Bridge 6: North elevation view (left) and east end view (right)

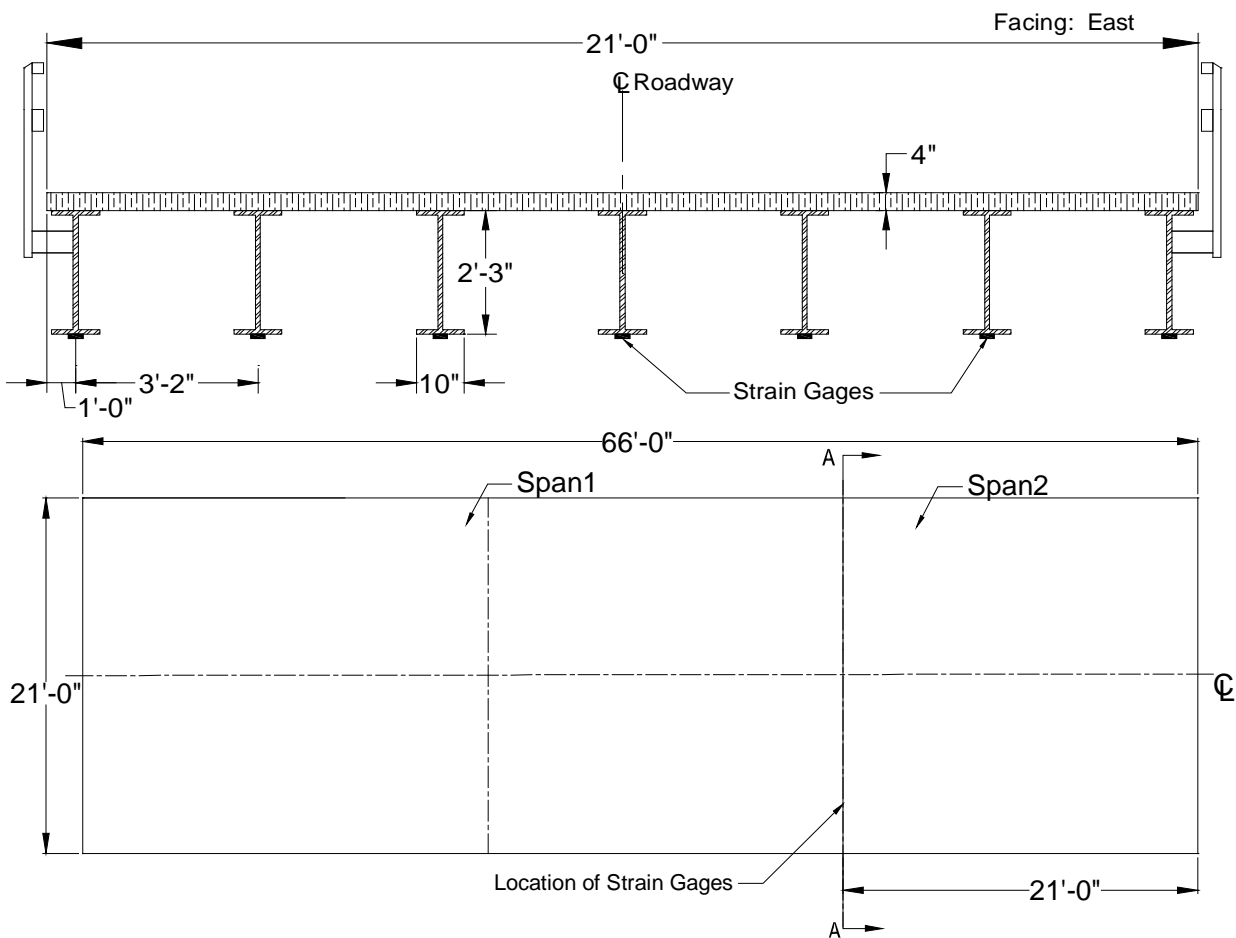


Figure B-43. Steel-Timber Bridge 6: Cross-section A-A (top) and plan (bottom)

B.6.3 Field Testing

Field testing of this bridge was conducted for two reasons. First, field testing was conducted to determine experimental live load distribution factors (LLDFs) and dynamic impact factors for the individual bridge girders. Second, these field data were also used to calibrate analytical models, which were then used to conduct a detailed parametric study related to a wide variety of implements of husbandry. A description of field tests, the procedures followed, and sample field results are detailed in the following sections.

Field Inspections

According to the most recent field inspection report, the Steel-Timber Bridge 6 timber deck is in good condition with some minor problems. The steel girders are also in good condition. These inspection-based observations were corroborated by the Iowa State University field testing team.

Instrumentation Plan

Given that the primary goal of the testing plan was to measure the live load response of the primary load-carrying members, a network of multiple strain gages was used to measure the strain under the weight of the vehicles. The strain gages were attached to the bottom of the girders at mid-span of Span 2 as shown in Figure B-43. The strain sensors used to conduct this testing were installed with a 3 in. gage length, and data were collected at a rate of 20 Hz during static testing and at 20 Hz during dynamic testing.

Test Load Paths

The vehicles utilized during field testing of this bridge consisted of four common farm vehicles and one typical highway truck. The vehicles included a terragator, a grain cart, a honey wagon with one tank, a honey wagon with two tanks, and a typical five-axle semi-truck. The individual axle loads, total weights, and lengths of the five vehicles used for field testing are summarized in Table B-11. As shown in Figure B-44, the configurations of the farm vehicles were notably different from that of the conventional highway truck.

Table B-11. Axle weight and total length of each testing vehicle

Farm Vehicles	Weight (lbs)					Total	Total Length (ft-in.)
	Front Axle	Rear Axle	Grain Wagon	Honey Wagon	Trailer		
Tractor Honey Wagon (empty)	10,960	15,740	-	26,720	-	53,420	40'-4"
Tractor Honey Wagon (half full with water)	10,580	22,800	-	40,620	-	74,000	40'-4"
Terragator	23,380	17,840	-	-	-	41,220	19'-0"
Tractor Grain Wagon	24,480	19,700	11,980	-	-	56,160	31'-0"
Semi-Truck	10,760	33,856	-	-	33,084	77,700	52'-1"



Honey Wagon



Honey Wagon- two tanks



Terragator



Tractor Grain Wagon



Semi Truck

Figure B-44. Farm vehicles used for field testing

During testing, the vehicles were driven across the bridge from east to west. In general the centerlines of the bridge and vehicle were approximately aligned. Initial static load testing was completed with the vehicles traveling at approximately 3 mph such that the pseudo-static bridge response could be captured. The dynamic load testing was completed with the vehicles traveling at approximately 15 mph (maximum safe speed at the site).

Sample Field Results

Representative plots from static load testing showing the strain experienced by one of the girders under all test vehicles is shown in Figure B-45. It was observed that the girders at the center of the bridge experienced the maximum strain magnitudes as the test vehicles crossed the bridge.

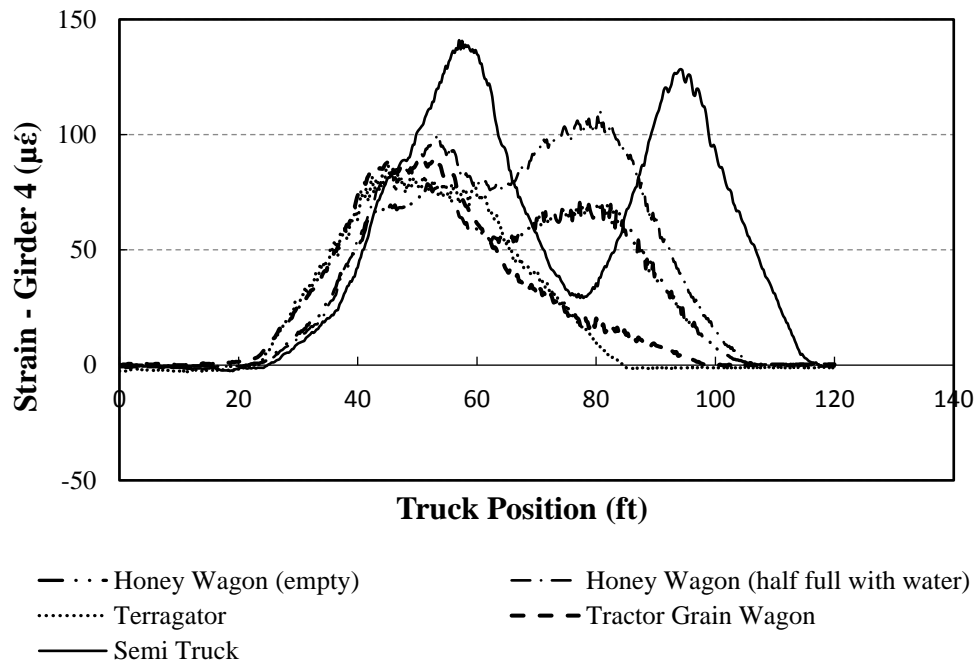


Figure B-45. Strain plot of a girder for all test vehicles for Steel-Timber Bridge 6

The semi-truck normally results in higher strains compared to other farm vehicles, and this tendency can be seen in Figure B-45. These recorded strains were employed to calculate the field LLDFs for each girder based upon the following equation.

$$LLDF^f = \frac{\varepsilon^m \max i,t}{\sum_{i=1}^n \varepsilon^m \max i,t} \quad (1)$$

Where $LLDF^f$ is the field live load distribution factor and ε^m are the measured maximum strains for individual girders over time, respectively.

A representative plot showing the comparison between static and dynamic strain for one of the girders under a test vehicle is shown in Figure B-46. It was generally observed that the girders experience more strain under dynamic loads than under static loading. The strain values from dynamic load tests were utilized to calculate the dynamic amplification factors (DAFs) for each girder.

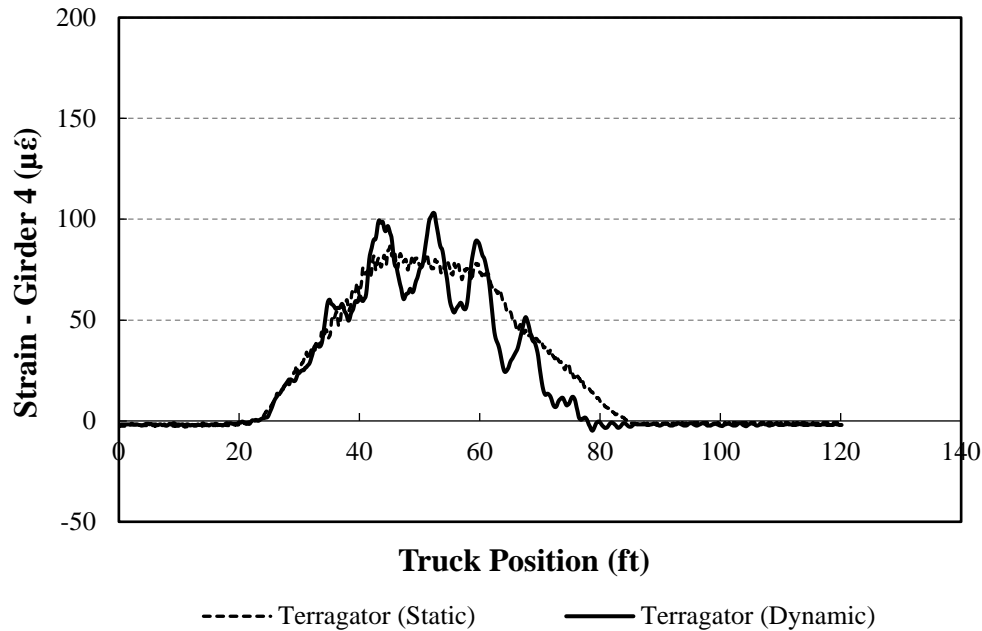


Figure B-46. Comparison between static and dynamic strain for Steel-Timber Bridge 6

B.6.4 Analytical Modeling

In lieu of field testing with a large number of vehicles, finite element analysis (FEA) simulations were used to estimate LLDFs for other vehicle configurations. As a result, analytical LLDFs were determined based upon FEA simulations of over 121 different farm vehicles on Steel-Timber Bridge 6. The FEA model was developed as described subsequently, and specific bridge information is presented in the following sections.

Model Generation

The bridge was initially modeled with the geometric and material properties taken directly from available bridge plans and/or field inspections using the BDI (Bridge Diagnostics, Inc.) finite element software WinGEN. A modulus of elasticity of 1600 ksi and 29000 ksi was used for all timber and steel components in the model respectively. The FEA model consisted of beam elements for the girders, shell elements for the deck, and rotational springs that simulated rotational restraint at the abutments and piers. Figure B-47 shows a representative model of the bridge.

Model Calibration

To improve the model accuracy, a calibration process that identified the bridge properties that resulted in the lowest error was completed. Based upon similarities in the response and observed field condition, a single cross-section was considered for all the girders. Table B-12 summarizes the original and calibrated values for the various bridge components along with percent error and correlation coefficient values. The moderately high percent error is most likely due to the highly variable material properties associated with timber components.

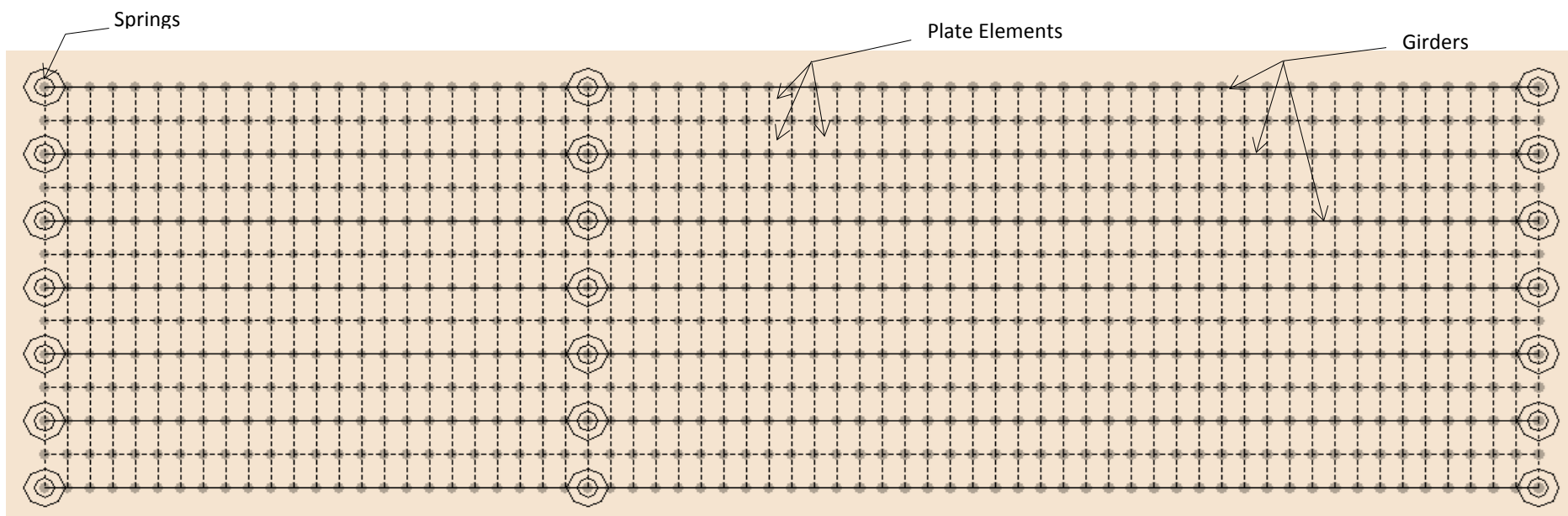


Figure B-47. Finite element model of Steel-Timber Bridge 6

Table B-12. Model calibration for Steel-Timber Bridge 6

Calibration Parameters	Bridge Components	Plan Value	Calibrated Value
Moment of Inertia, I (in ⁴)	All Girders	3245	2550
Modulus of Elasticity, E (Ksi)	Deck	1600	1500
Rotational Stiffness, kr (Kips-in/rad)	Support Connections (springs)	0	78595
Statistical Results	Percent Error		11.56%
	Correlation Coefficients		0.93

Once model calibration was completed, the analytical model was loaded with 121 farm vehicles covering a wide range of axle spacings, weights, and gage widths. The analytical strain response was then used to compute analytical LLDFs for each simulation vehicle using Equation (1).

To interpret the results efficiently, the LLDFs of the girders were grouped together as either interior or exterior girder LLDFs. Statistical limits for the interior and exterior girder LLDFs were determined from cumulative distribution function (CDF) curves defined to be at the 95% confidence thresholds.

B.6.5 Results

The envelopes of LLDFs for Steel-Timber Bridge 6 are presented in Figure B-48 for both the field and analytical LLDFs for each girder. In addition to the envelopes, the AASHTO LLDFs and statistical control limits for each group of interior and exterior girders are also shown.

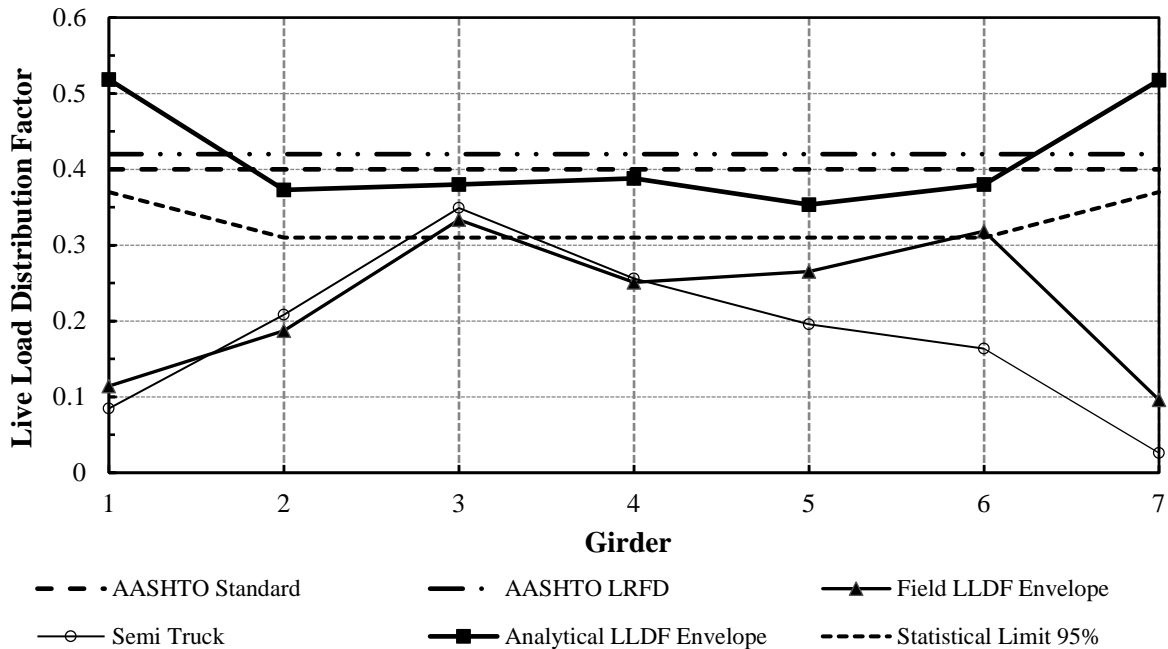


Figure B-48. LLDFs for Steel-Timber Bridge 6

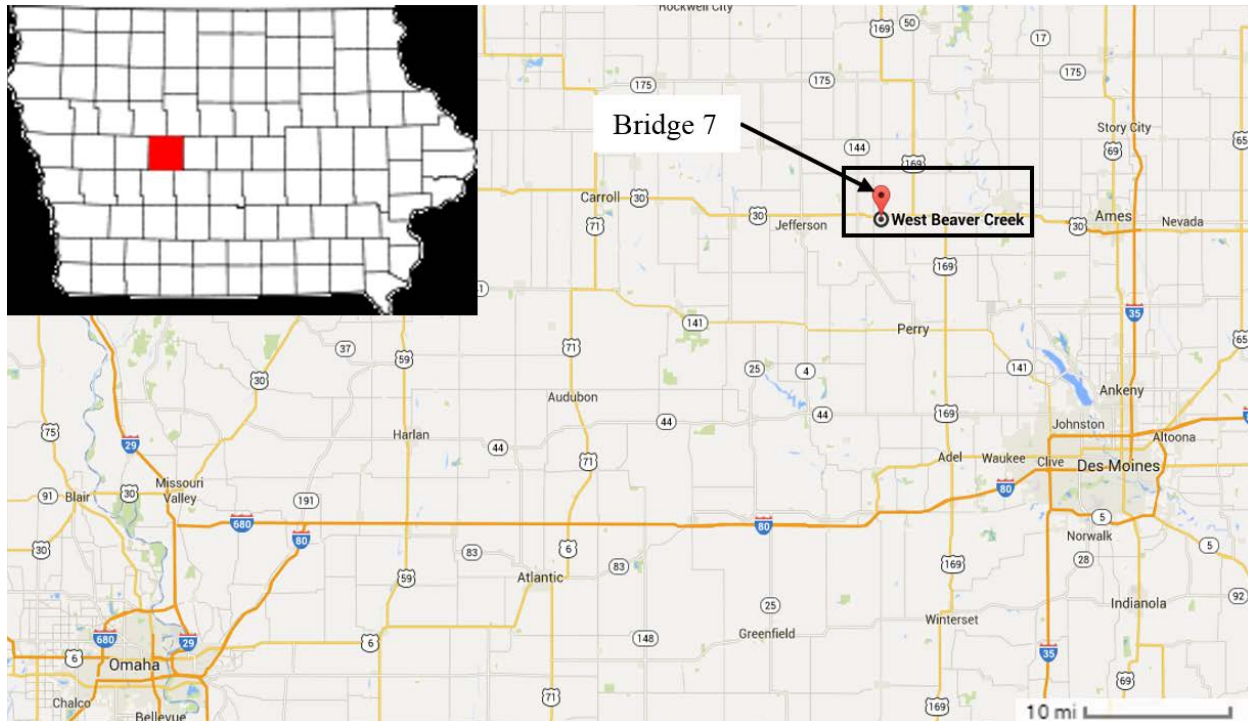
It appears that the analytical LLDF envelope for all the interior girders are smaller than those from the AASHTO standard and LRFD specifications. In the case of exterior girders, the analytical LLDFs are larger than AASHTO values. The peak value of the analytical exterior girder LLDFs was observed in G7, which has an LLDF of 0.52, while that of the interior girders was found in G4, which has an LLDF of 0.39. The field LLDF envelope represents the highest LLDF observed in each girder due to field testing using farm vehicles, whereas the semi-truck envelope represents the extreme LLDFs for field testing using a five-axle semi-truck. The field LLDF envelope has larger values than that for the semi-truck for most of the girders. The statistical limits for either the interior or exterior girder group show smaller values than the AASHTO specifications.

B.7 Steel-Timber Bridge 7

This mini test and evaluation report documents the results of field testing and subsequent analysis of a steel girder bridge with a timber deck (Steel-Timber Bridge 7) under multiple implements of husbandry. For completeness, this mini-report includes a description of the bridge, a description of the live load testing procedures followed, sample data, a description of analytical modeling, plots of analytical results, and a discussion of the overall behavior of the steel girder bridge under implements of husbandry.

B.7.1 Background

The steel-timber bridge described here is known in the National Bridge Inventory (NBI) database as Bridge 162051 and will be henceforth be referred to as Steel-Timber Bridge 7. The bridge is located on X Avenue about 7 miles east of Grand Junction, in Greene County, Iowa. Figure B-49 shows the general location of the bridge.



Map: ©Google 2014

Figure B-49. Location overview of Steel-Timber Bridge 7

B.7.2 Bridge Description

Steel-Timber Bridge 7 is open to two-lane traffic and has two spans with overall dimensions of 39.4 ft long by 23.6 ft wide with zero degrees of skew. The deck is comprised of continuous timber decking with a thickness of 4 in. An elevation view and an end view of the bridge are shown in Figure B-50. The bridge consists of 15 steel girders with approximate spacing between adjacent girders of 1.6 ft. The exterior girders are C-section and are approximately 15.0 in. by 3.4 in.; whereas, the interior girders are I cross-section and are approximately 15.0 in. by 5.5 in. Figure B-51 shows a typical cross-section and plan view of the bridge.



Figure B-50. Steel-Timber Bridge 7: West elevation view (left) and north end view (right)

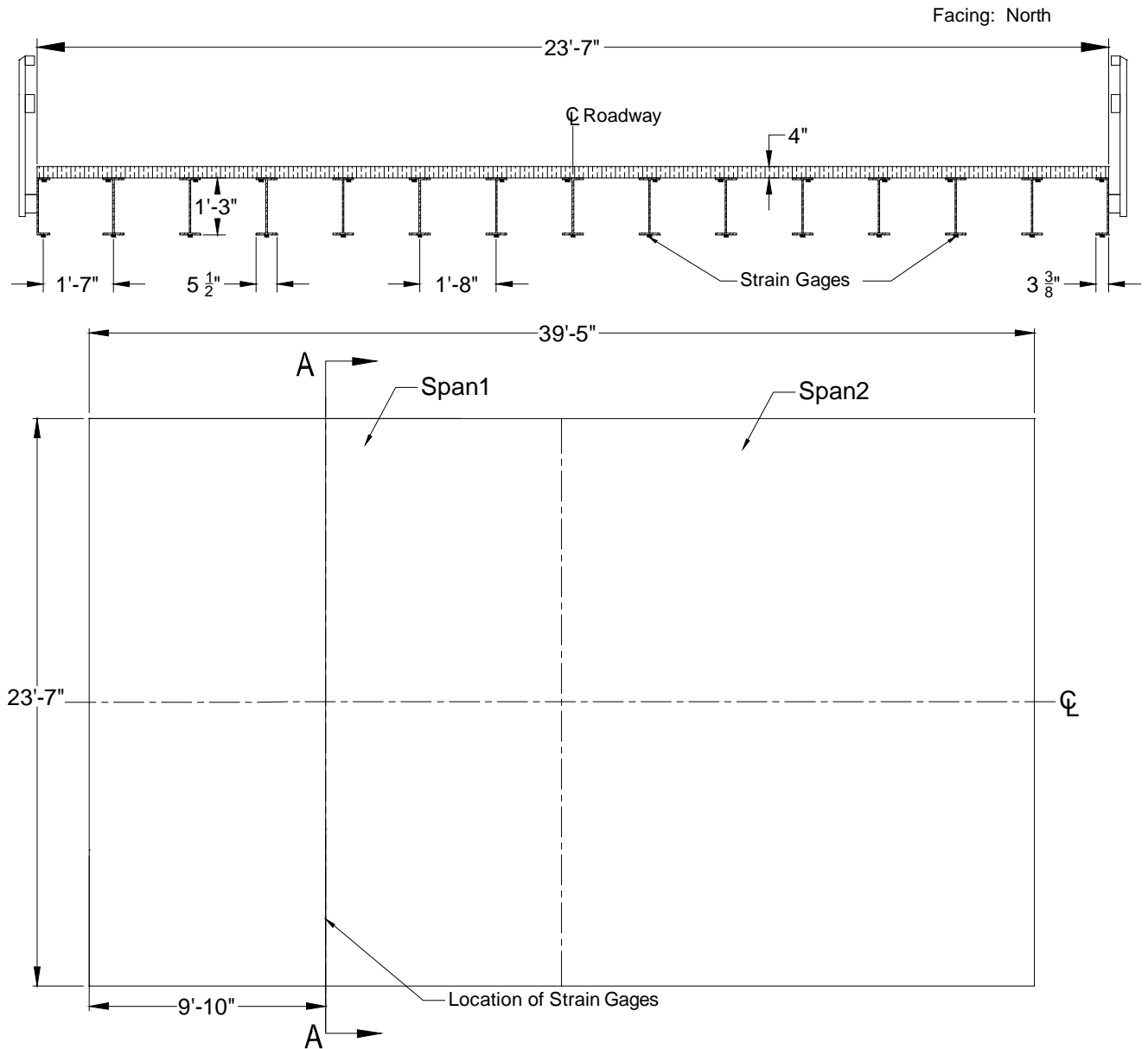


Figure B-51. Steel-Timber Bridge 7: Cross-section A-A (top) and plan (bottom)

B.7.3 Field Testing

Field testing of this bridge was conducted for two reasons. First, field testing was conducted to determine experimental live load distribution factors (LLDFs) and dynamic impact factors for the individual bridge girders. Second, these field data were also used to calibrate analytical models, which were then used to conduct a detailed parametric study related to a wide variety of implements of husbandry. A description of field tests, the procedures followed, and sample field results are detailed in the following sections.

Field Inspections

According to the most recent field inspection report, the Steel-Timber Bridge 7 timber deck is in good condition with some minor problems. The steel girders are in good condition. These inspection-based observations were corroborated by the Iowa State University field testing team.

Instrumentation Plan

Given that the primary goal of the testing plan was to measure the live load response of the primary load-carrying members, a network of multiple strain gages was used to measure the strain under the weight of the vehicles. The strain gages were attached to the bottom of the girders at mid-span as shown in Figure B-51. The strain sensors used to conduct this testing were installed with a 3 in. gage length, and data were collected at a rate of 20 Hz during static testing and at 20 Hz during dynamic testing.

Test Load Paths

The vehicles utilized during field testing of this bridge consisted of four common farm vehicles and one typical highway truck. The vehicles included a terragator, a tractor with grain wagon, a tractor with one liquid manure applicator tank, a tractor with two liquid manure applicator tanks, and a typical five-axle semi-truck. The individual axle loads, total weights, and lengths of the five vehicles used for field testing are summarized in Table B-13. As shown in Figure B-52, the configurations of the farm vehicles were notably different from that of the conventional highway truck.

Table B-13. Axle weight and total length of each testing vehicle

Farm Vehicles	Weight (lbs)					Total Length (ft-in.)	
	Front Axle	Rear Axle	Grain Wagon	Tanks	Trailer		
Tractor w/ 1 tank	11,800	15,900	-	48,800	-	76,500	40'-8"
Tractor w/ 2 tanks	11,800	15,900	-	32,600	-	68,900	63'-7"
Terragator	11,060	32,400	-	-	-	43,460	25'-7"
Tractor Grain Wagon	18,840	18,660	15,660	-	-	53,160	35'-2"
Semi-Truck	10,760	33,856	-	-	33,084	77,700	52'-1"



Tractor w/ 1 tank



Tractor w/ 2 tanks



Terragator



Tractor Grain Wagon



Semi Truck

Figure B-52. Farm vehicles used for field testing

During testing, the vehicles were driven across the bridge from south to north. In general the centerlines of the bridge and vehicle were approximately aligned. Initial static load testing was completed with the vehicles traveling at approximately 3 mph such that the pseudo-static bridge response could be captured. Later, dynamic load testing was completed with the vehicles traveling at approximately 20 mph (maximum safe speed at the site).

Sample Field Results

Representative plots from static load testing showing the strain experienced by one of the girders under all test vehicles is shown in Figure B-53. It was observed that the girders at the center of the bridge experienced the maximum strain magnitudes as the test vehicles crossed the bridge.

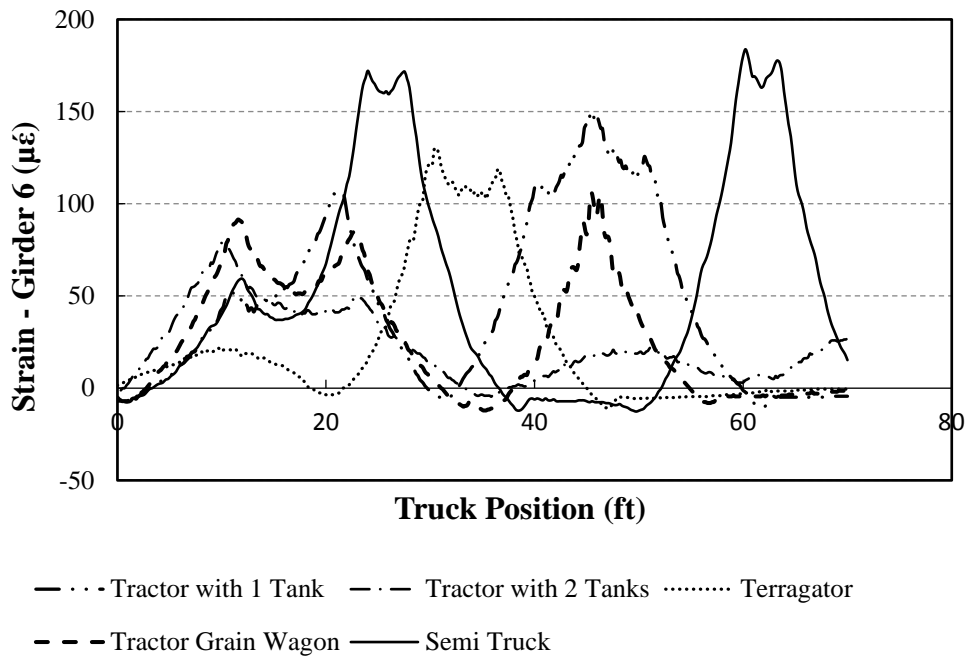


Figure B-53. Strain plot of a girder for all test vehicles for Steel-Timber Bridge 7

The semi-truck normally results in higher strains compared to other farm vehicles, and this tendency can be seen in Figure B-53. These recorded strains were employed to calculate the field LLDFs for each girder based upon the following equation.

$$LLDF^f = \frac{\epsilon^m \max i, t}{\sum_{i=1}^n \epsilon^m \max i, t} \quad (1)$$

Where $LLDF^f$ is the field live load distribution factor and ϵ^m are the measured maximum strains for individual girders over time, respectively.

A representative plot showing the comparison between static and dynamic strain for one of the girders under a test vehicle is shown in Figure B-54. It was generally observed that the girders experience more strain under dynamic loads than under static loading. The strain values from dynamic load tests were utilized to calculate the dynamic amplification factors (DAFs) for each girder.

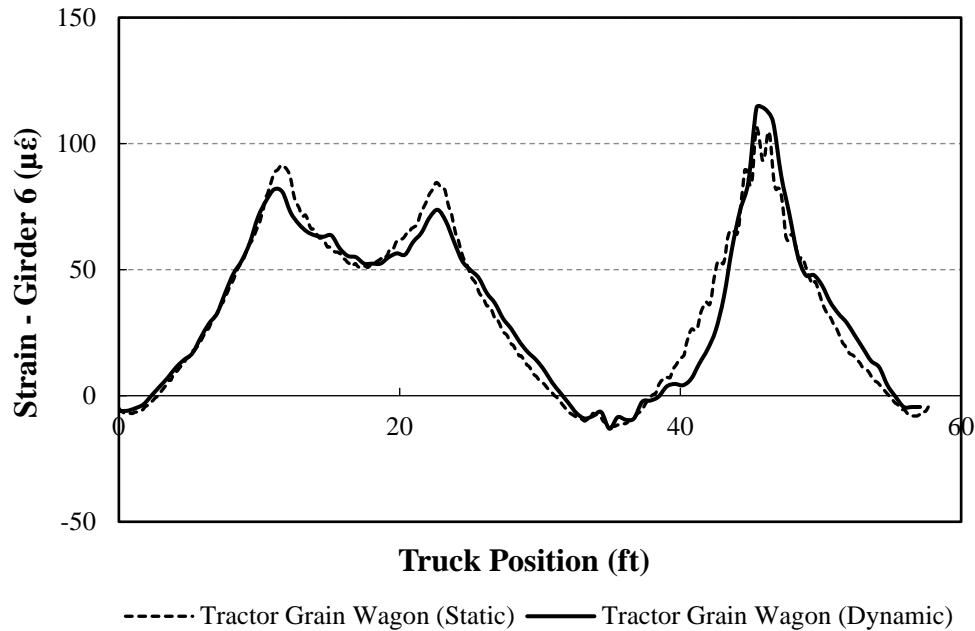


Figure B-54. Comparison between static and dynamic strain for Steel-Timber Bridge 7

B.7.4 Analytical Modeling

In lieu of field testing with a large number of vehicles, finite element analysis (FEA) simulations were used to estimate LLDFs for other vehicle configurations. As a result, analytical LLDFs were determined based upon FEA simulations of over 121 different farm vehicles on Steel-Timber Bridge 7. The FEA model was developed as described subsequently, and specific bridge information is presented in the following sections.

Model Generation

The bridge was initially modeled with the geometric and material properties taken directly from available bridge plans and/or field inspections using the BDI (Bridge Diagnostics, Inc.) finite element software WinGEN. A modulus of elasticity of 1600 ksi and 29000 ksi was used for all timber and steel components in the model respectively. The FEA model consisted of beam elements for the girders, shell elements for the deck, and rotational springs that simulated rotational restraint at the abutments and piers. Figure B-55 shows a representative model of the bridge.

Model Calibration

To improve the model accuracy, a calibration process that identified the bridge properties that resulted in the lowest error was completed. Based upon similarities in the response and observed field condition, a single cross-section was considered for all the girders. Table B-14 summarizes the original and calibrated values for the various bridge components along with percent error and correlation coefficient values.

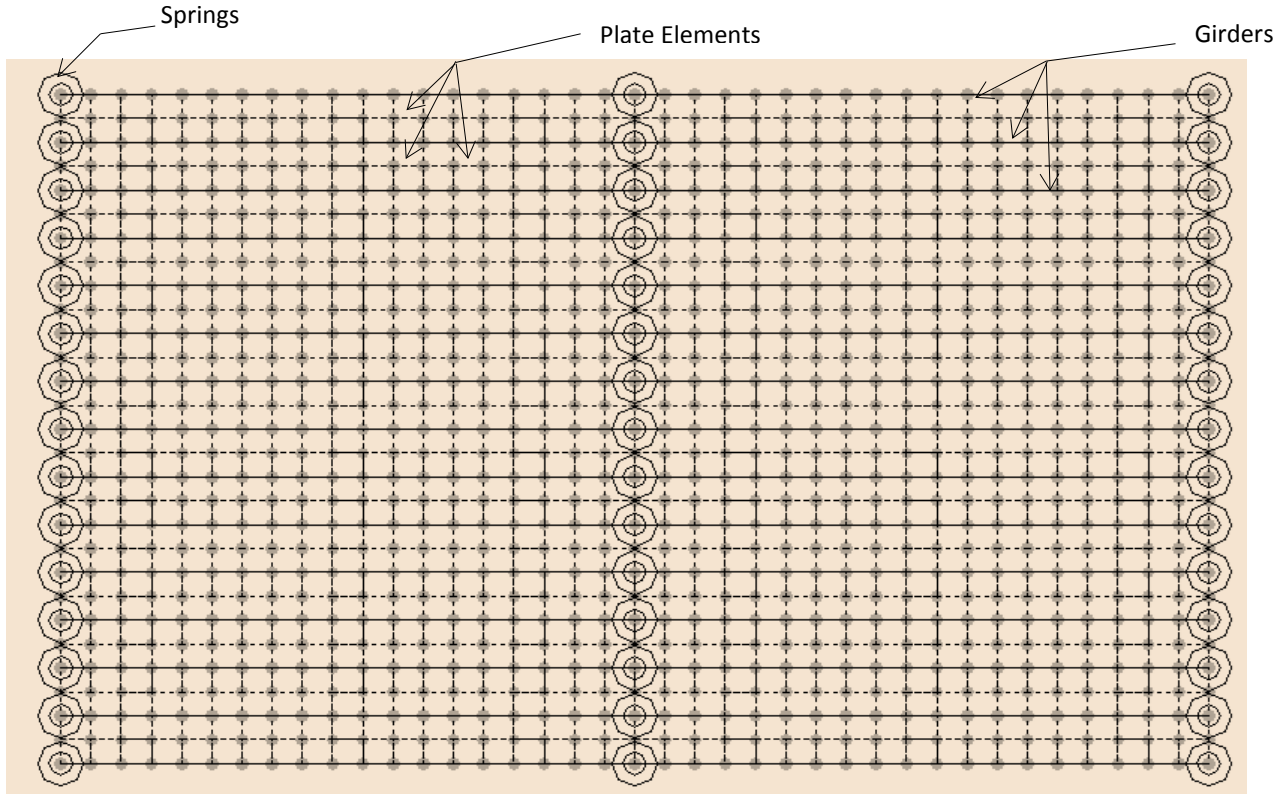


Figure B-55. Finite element model of Steel-Timber Bridge 7

Table B-14. Model calibration for Steel-Timber Bridge 7

Calibration Parameters	Bridge Components	Plan Value	Calibrated Value
Moment of Inertia, I (in ⁴)	Exterior Girders	257	250
	Interior Girders	341	341
Modulus of Elasticity, E (Ksi)	Deck	1600	1200
Rotational Stiffness, kr (Kips-in/rad)	Support Connections (springs)	0	21418
Statistical Results	Percent Error		10.5%
	Correlation Coefficients		0.92

Once model calibration was completed, the analytical model was loaded with 121 farm vehicles covering a wide range of axle spacings, weights, and gage widths. The analytical strain response was then used to compute analytical LLDFs for each simulation vehicle using Equation (1).

To interpret the results efficiently, the LLDFs of the girders were grouped together as either interior or exterior girder LLDFs. Statistical limits for the interior and exterior girder LLDFs were determined from cumulative distribution function (CDF) curves defined to be at the 95% confidence thresholds.

B.7.5 Results

The envelopes of LLDFs for Steel-Timber Bridge 7 are presented in Figure B-56 for both the field and analytical LLDFs for each girder. In addition to the envelopes, the AASHTO LLDFs and statistical control limits for each group of interior and exterior girders are also shown.

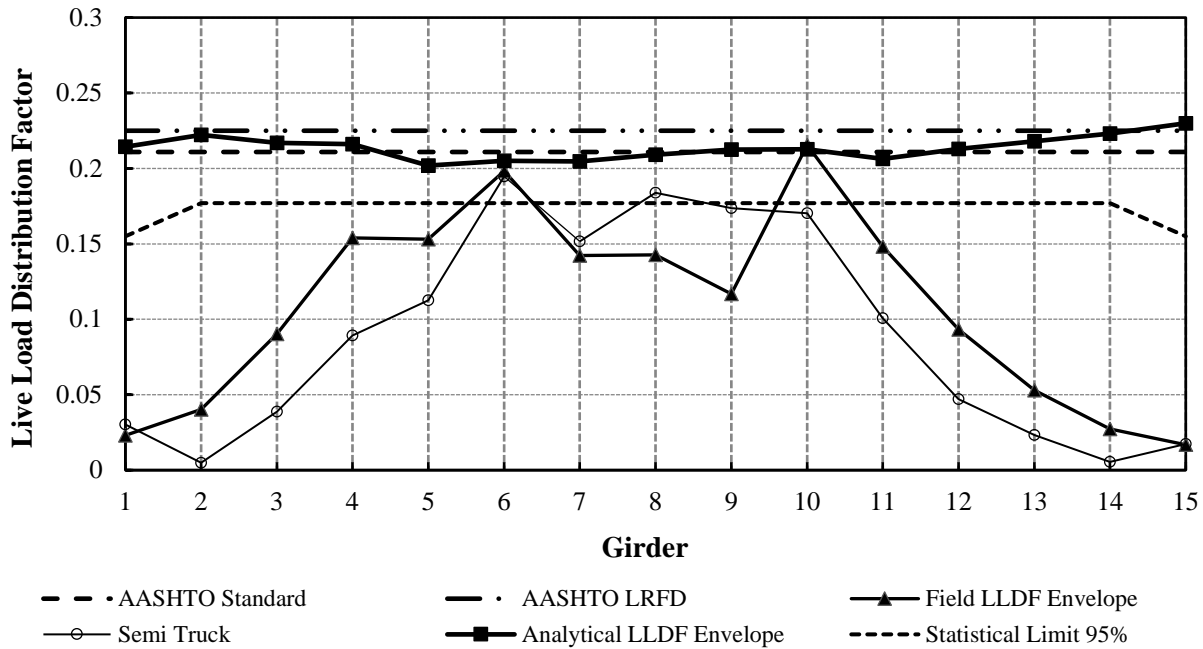


Figure B-56. LLDFs for Steel-Timber Bridge 7

It appears that the analytical LLDF envelope for all the girders is equivalent to those from the AASHTO standard and LRFD specifications. The peak value of the analytical exterior girder LLDFs was observed in G15, which has an LLDF of 0.23, while that of the interior girders was found in G2, G3, G4, G13, and G14, which have LLDFs of 0.22. The statistical limits for either the interior or exterior girder group show smaller values than the AASHTO specifications. The field LLDF envelope represents the highest LLDF observed in each girder due to field testing using farm vehicles, whereas the semi-truck envelope represents the extreme LLDFs for field testing using a five-axle semi-truck. The field LLDF envelope has larger values than that for the semi-truck for most of the girders.

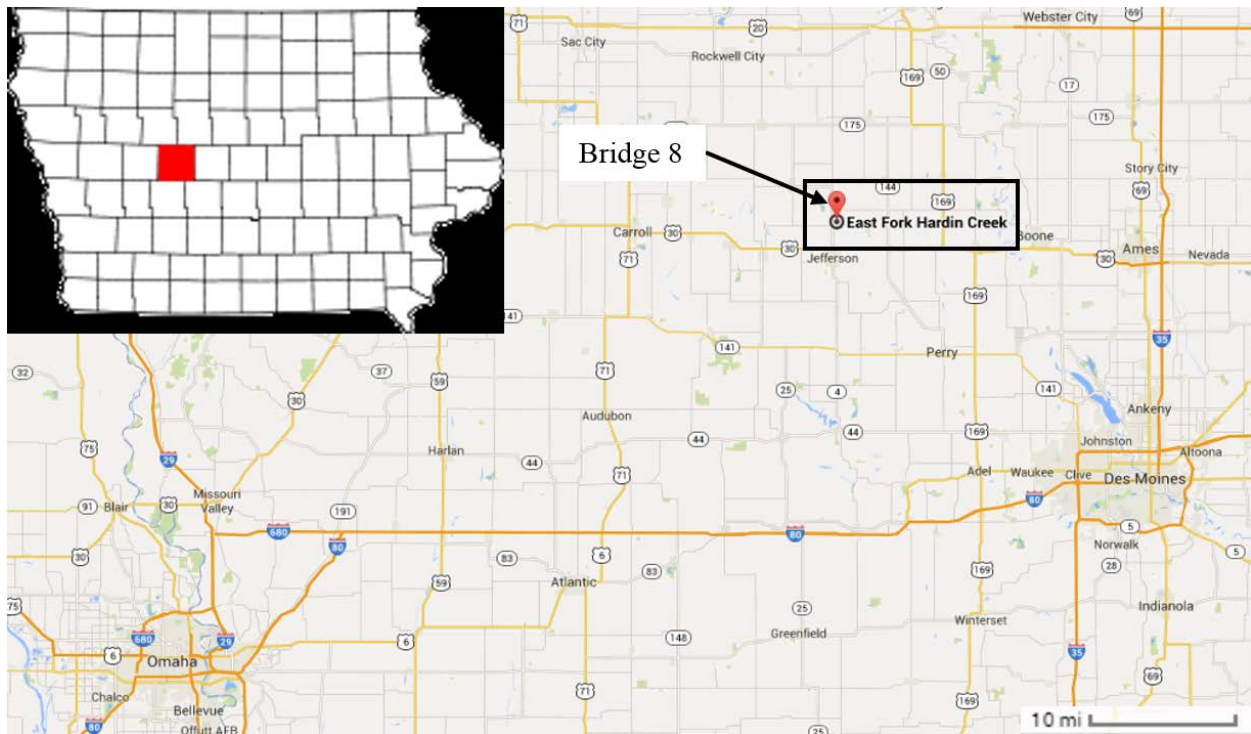
B.8 Steel-Timber Bridge 8

This mini test and evaluation report documents the results of field testing and subsequent analysis of a steel girder bridge with a timber deck (Steel-Timber Bridge 8) under multiple implements of husbandry. For completeness, this mini-report includes a description of the bridge, a description of the live load testing procedures followed, sample data, a description of analytical modeling, plots of analytical results, and a discussion of the overall behavior of the steel girder bridge under implements of husbandry.

B.8.1 Background

The steel-timber bridge described here is known in the National Bridge Inventory (NBI) database as Bridge 162511 and will be henceforth be referred to as Steel-Timber Bridge 8. The bridge is

located on 185th Street about 6 miles North of Jefferson, in Greene County, Iowa. Figure B-57 shows the general location of the bridge.



Map: ©Google 2014

Figure B-57. Location overview of Steel-Timber Bridge 8

B.8.2 Bridge Description

Steel-Timber Bridge 8 is open to two-lane traffic and has two spans with overall dimensions of 28.9 ft long by 20.4 ft wide with 7.3 degrees of skew. The deck is comprised of continuous timber decking with a thickness of 4 in. An elevation view and an end view of the bridge are shown in Figure B-58. The bridge consists of 13 steel girders with spacing between adjacent girders of 1.5 ft. The exterior girders are C-section and are approximately 15.0 in. by 3.5 in.; whereas, the interior girders are I cross-section and are approximately 15.0 in. by 5.5 in. Figure B-59 shows a typical cross-section and plan view of the bridge.



Figure B-58. Steel-Timber Bridge 8: South elevation view (left) and west end view (right)

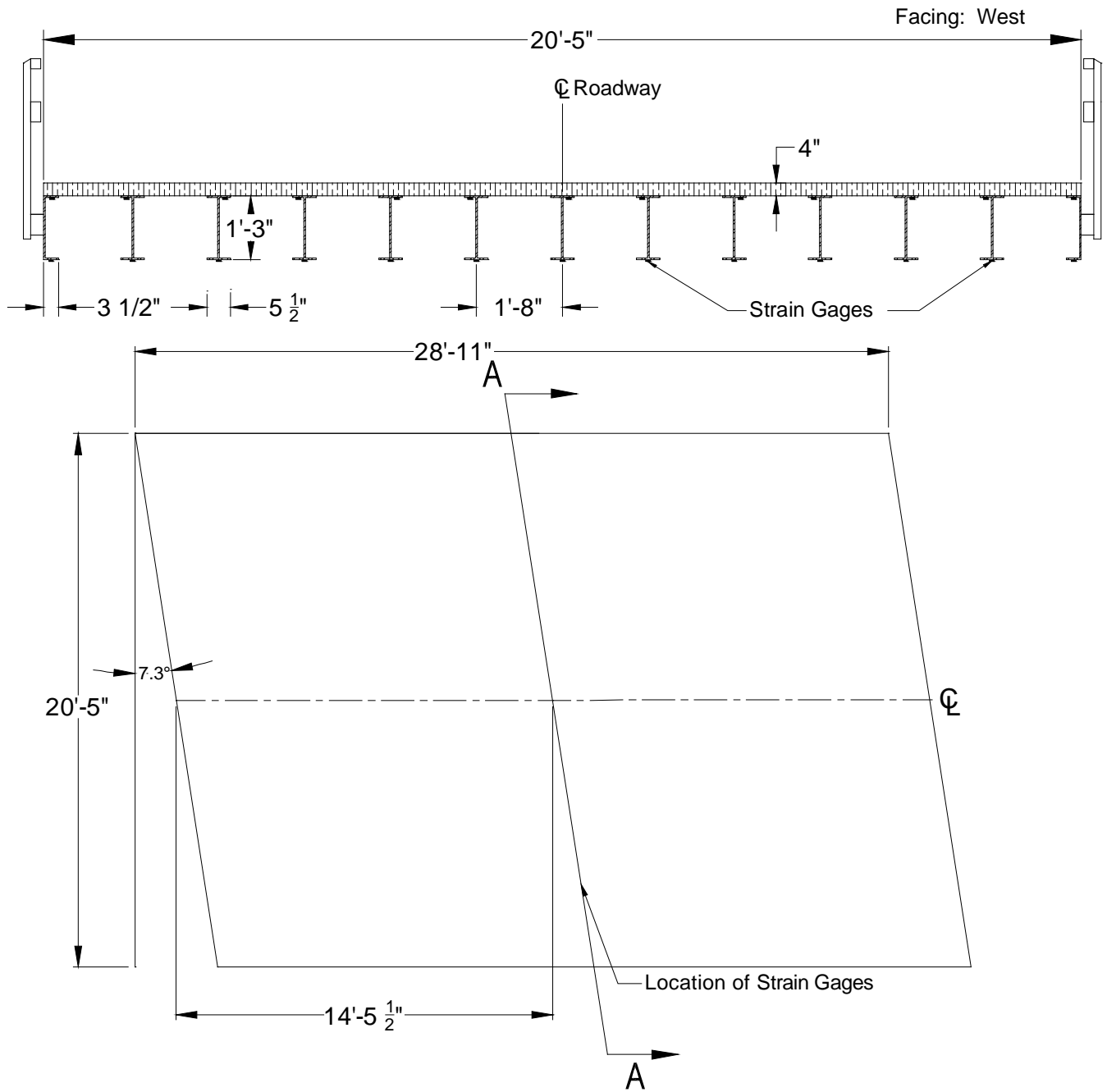


Figure B-59. Steel-Timber Bridge 8: Cross-section A-A (top) and plan (bottom)

B.8.3 Field Testing

Field testing of this bridge was conducted for two reasons. First, field testing was conducted to determine experimental live load distribution factors (LLDFs) for the individual bridge girders. Second, these field data were also used to calibrate analytical models, which were then used to conduct a detailed parametric study related to a wide variety of implements of husbandry. A

description of field tests, the procedures followed, and sample field results are detailed in the following sections.

Field Inspections

According to the most recent field inspection report, the Steel-Timber Bridge 8 timber deck is in good condition with some minor problems. The steel girders are in average condition and show signs of rust. These inspection-based observations were corroborated by the Iowa State University field testing team.

Instrumentation Plan

Given that the primary goal of the testing plan was to measure the live load response of the primary load-carrying members, a network of multiple strain gages was used to measure the strain under the weight of the vehicles. The strain gages were attached to the bottom of the girders at mid-span as shown in Figure B-59. The strain sensors used to conduct this testing were installed with a 3 in. gage length, and data were collected at a rate of 20 Hz during static testing.

Test Load Paths

The vehicles utilized during field testing of this bridge consisted of four common farm vehicles and one typical highway truck. The vehicles included a terragator, a tractor with grain wagon, a tractor with one liquid manure applicator tank, a tractor with two liquid manure applicator tanks, and a typical five-axle semi-truck. The individual axle loads, total weights, and lengths of the five vehicles used for field testing are summarized in Table B-15. As shown in Figure B-60, the configurations of the farm vehicles were notably different from that of the conventional highway truck.

Table B-15. Axle weight and total length of each testing vehicle

Farm Vehicles	Weight (lbs)					Total	Total Length (ft-in.)
	Front Axle	Rear Axle	Grain Wagon	Tanks	Trailer		
Tractor w/ 1 tank	11,800	15,900	-	48,800	-	76,500	40'-8"
Tractor w/ 2 tanks	11,800	15,900	-	32,600	-	68,900	63'-7"
Terragator	11,060	32,400	-	-	-	43,460	25'-7"
Tractor Grain Wagon	18,840	18,660	15,660	-	-	53,160	35'-2"
Semi-Truck	10,760	33,856	-	-	33,084	77,700	52'-1"



Tractor w/ 1 tank



Tractor w/ 2 tanks



Terragator



Tractor Grain Wagon



Semi Truck

Figure B-60. Farm vehicles used for field testing

During testing, the vehicles were driven across the bridge from east to west. In general the centerlines of the bridge and vehicle were approximately aligned. Static load testing was completed with the vehicles traveling at approximately 3 mph such that the pseudo-static bridge response could be captured.

Sample Field Results

Representative plots from static load testing showing the strain experienced by one of the girders under all test vehicles is shown in Figure B-61. It was observed that the girders at the center of the bridge experienced the maximum strain magnitudes as the test vehicles crossed the bridge.

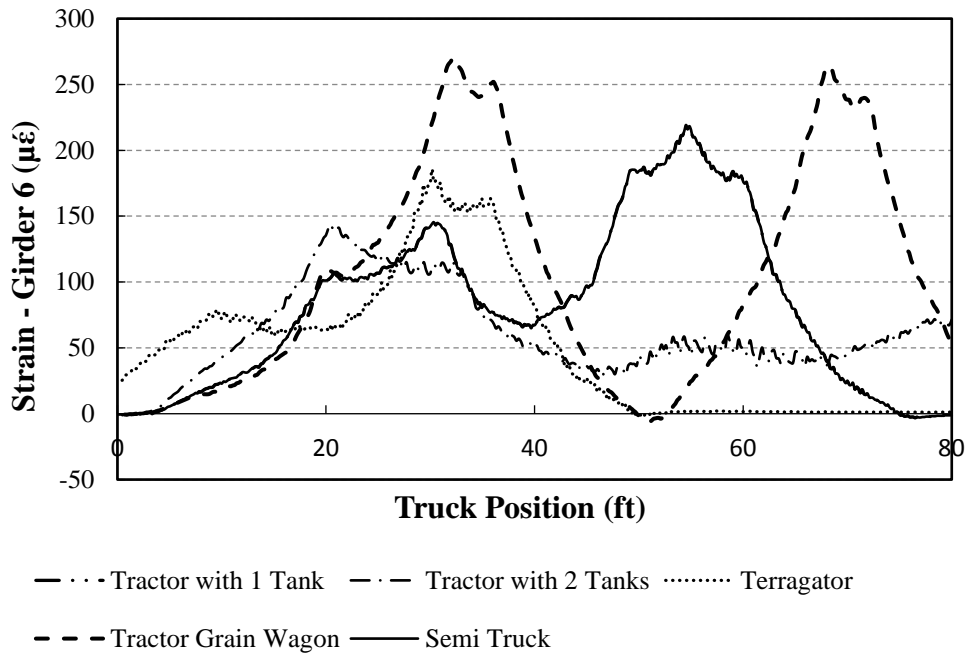


Figure B-61. Strain plot of a girder for all test vehicles for Steel-Timber Bridge 8

The semi-truck normally results in higher strains compared to other farm vehicles, and this tendency can be seen in Figure B-61. These recorded strains were employed to calculate the field LLDFs for each girder based upon the following equation.

$$LLDF^f = \frac{\epsilon^m \max i,t}{\sum_{i=1}^n \epsilon^m \max i,t} \quad (1)$$

Where $LLDF^f$ is the field live load distribution factor and ϵ^m are the measured maximum strains for individual girders over time, respectively.

B.8.4 Analytical Modeling

In lieu of field testing with a large number of vehicles, finite element analysis (FEA) simulations were used to estimate LLDFs for other vehicle configurations. As a result, analytical LLDFs were determined based upon FEA simulations of over 121 different farm vehicles on Bridge 8. The FEA model was developed as described subsequently, and specific bridge information is presented in the following sections.

Model Generation

The bridge was initially modeled with the geometric and material properties taken directly from available bridge plans and/or field inspections using the BDI (Bridge Diagnostics, Inc.) finite element software WinGEN. A modulus of elasticity of 1600 ksi and 29000 ksi was used for all timber and steel components in the model respectively. The FEA model consisted of beam elements for the girders, shell elements for the deck, and rotational springs that simulated rotational restraint at the abutments and piers. Figure B-62 shows a representative model of the bridge.

Model Calibration

To improve the model accuracy, a calibration process that identified the bridge properties that resulted in the lowest error was completed. Based upon similarities in the response and observed field condition, a single cross-section was considered for all the girders. Table B-16 summarizes the original and calibrated values for the various bridge components along with percent error and correlation coefficient values.

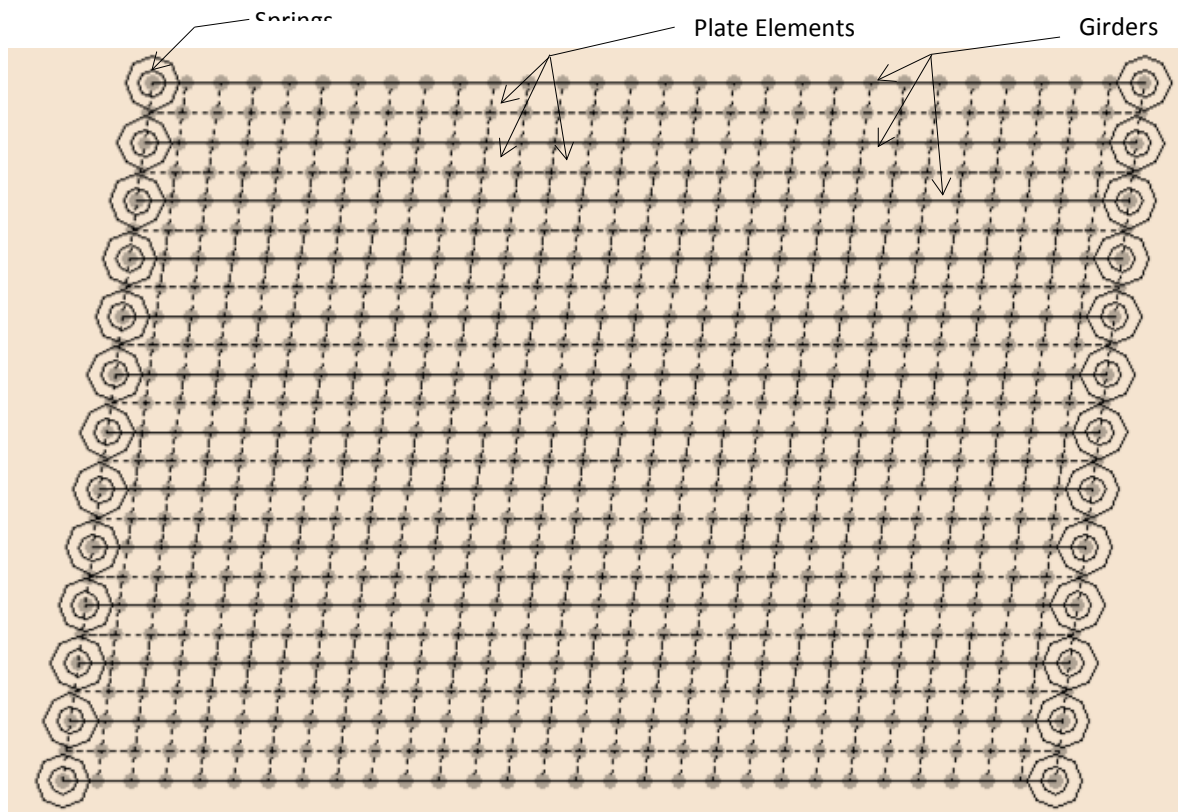


Figure B-62. Finite element model of Steel-Timber Bridge 8

Table B-16. Model calibration for Steel-Timber Bridge 8

Calibration Parameters	Bridge Components	Plan Value	Calibrated Value
Moment of Inertia, I (in ⁴)	Exterior Girders	262	262
	Interior Girders	341	341
Modulus of Elasticity, E (Ksi)	Deck	1600	1363
Rotational Stiffness, kr (Kips-in/rad)	Support Connections (springs)	0	34606
Statistical Results	Percent Error		12.9%
	Correlation Coefficients		0.89

Once model calibration was completed, the analytical model was loaded with 121 farm vehicles covering a wide range of axle spacings, weights, and gage widths. The analytical strain response was then used to compute analytical LLDFs for each simulation vehicle using Equation (1).

To interpret the results efficiently, the LLDFs of the girders were grouped together as either interior or exterior girder LLDFs. Statistical limits for the interior and exterior girder LLDFs were determined from cumulative distribution function (CDF) curves defined to be at the 95% confidence thresholds.

B.8.5 Results

The envelopes of LLDFs for Steel-Timber Bridge 8 are presented in Figure B-63 for both the field and analytical LLDFs for each girder. In addition to the envelopes, the AASHTO LLDFs and statistical control limits for each group of interior and exterior girders are also shown.

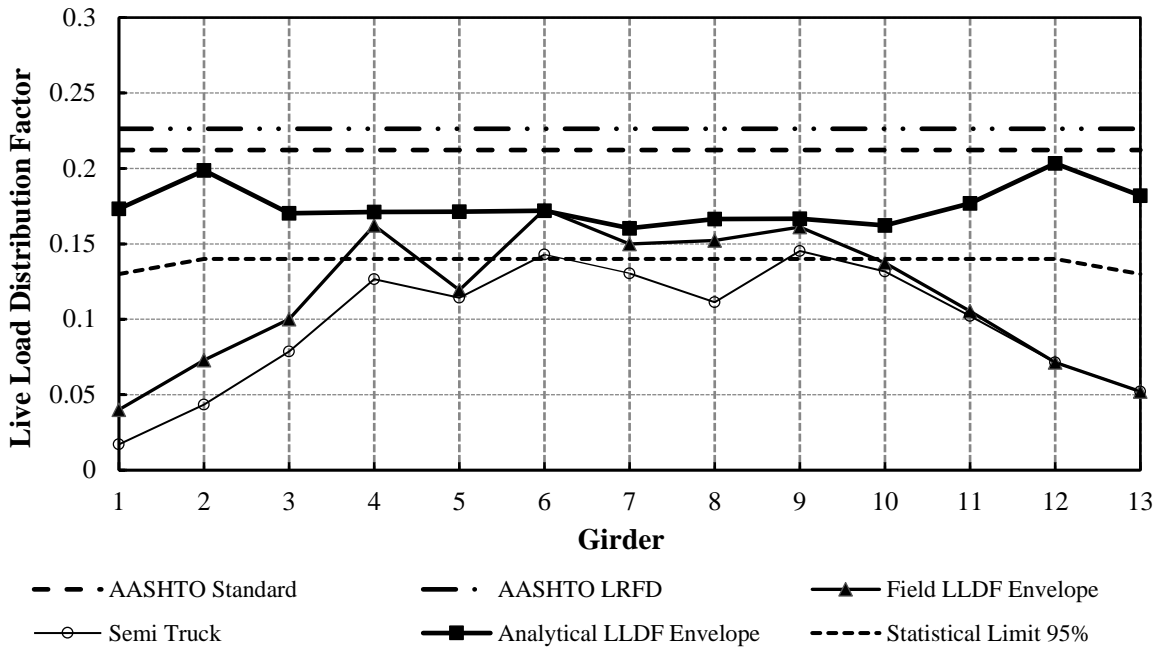


Figure B-63. LLDFs for Steel-Timber Bridge 8

It appears that the analytical LLDF envelope for all the girders is smaller than those from the AASHTO standard and LRFD specifications. The peak value of the analytical exterior girder LLDFs was observed in G13, which has an LLDF of 0.18, while that of the interior girders was found in G2 and G12, which have LLDFs of 0.20. The statistical limits for either the interior or exterior girder group also show smaller values than the AASHTO specifications. The field LLDF envelope represents the highest LLDF observed in each girder due to field testing using farm vehicles, whereas the semi-truck envelope represents the extreme LLDFs for field testing using a five-axle semi-truck. The field LLDF envelope has larger values than that for the semi-truck for most of the girders.

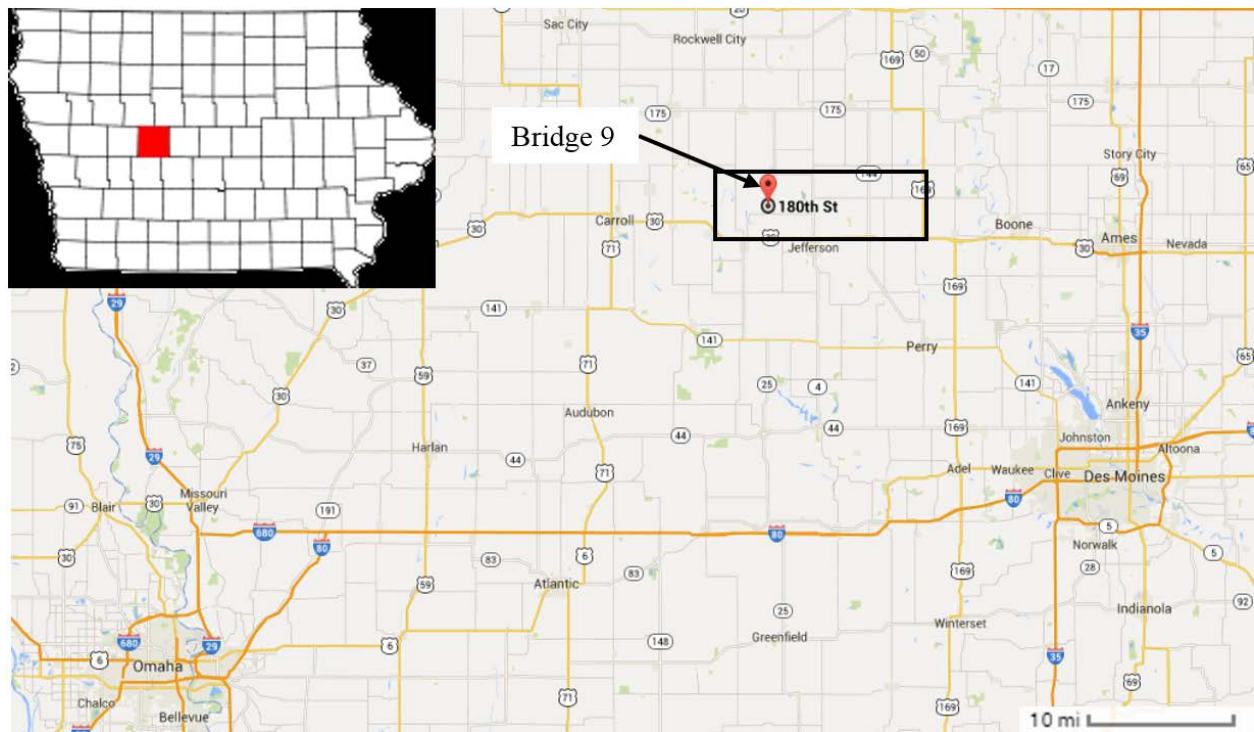
B.9 Steel-Timber Bridge 9

This mini test and evaluation report documents the results of field testing and subsequent analysis of a steel girder bridge with a timber deck (Steel-Timber Bridge 9) under multiple implements of husbandry. For completeness, this mini-report includes a description of the bridge, a description of the live load testing procedures followed, sample data, a description of analytical modeling, plots of analytical results, and a discussion of the overall behavior of the steel girder bridge under implements of husbandry.

B.9.1 Background

The steel-timber bridge described here is known in the National Bridge Inventory (NBI) database as Bridge 162691 and will be henceforth be referred to as Steel-Timber Bridge 9. The bridge is

located on 180th Street at the intersection of X Avenue, about 10 miles north of Jefferson, in Greene County, Iowa. Figure B-64 shows the general location of the bridge.



Map: ©Google 2014

Figure B-64. Location overview of Steel-Timber Bridge 9

B.9.2 Bridge Description

Steel-Timber Bridge 9 is open to two-lane traffic and has one span with overall dimensions of 29.5 ft long by 20.3 ft wide with zero degrees of skew. The deck is comprised of continuous timber decking with a thickness of 3 in. An elevation view and an end view of the bridge are shown in Figure B-65. The bridge consists of 13 steel girders with approximate spacing between adjacent girders of 1.7 ft. The exterior girders are C-section and are approximately 15.0 in. by 3.1 in.; whereas, the interior girders are I cross-section and are approximately 15.0 in. by 5.4 in. Figure B-66 shows a typical cross-section and plan view of the bridge.



Figure B-65. Steel-Timber Bridge 9: North elevation view (left) and east end view (right)

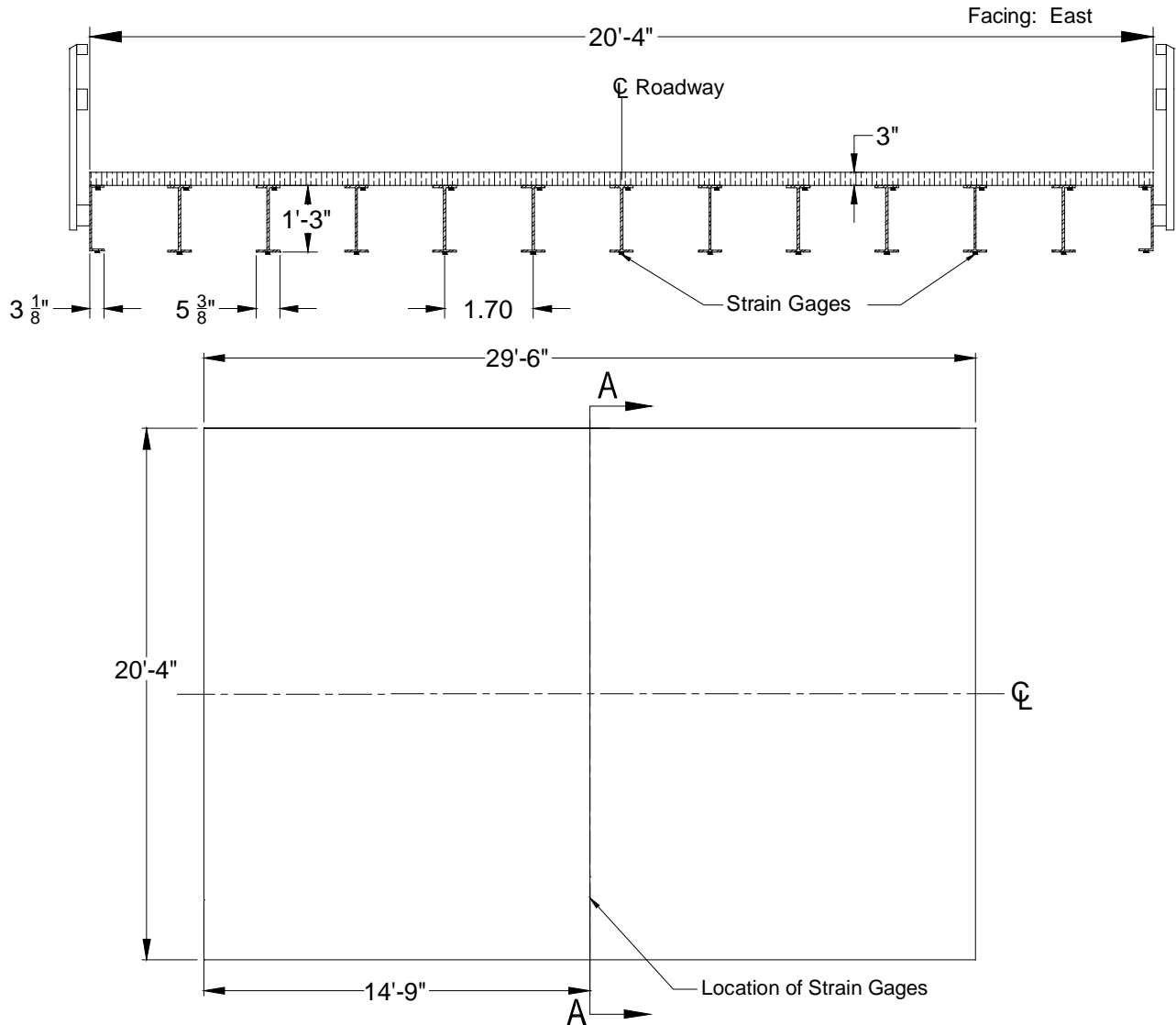


Figure B-66. Steel-Timber Bridge 9: Cross-section A-A (top) and plan (bottom)

B.9.3 Field Testing

Field testing of this bridge was conducted for two reasons. First, field testing was conducted to determine experimental live load distribution factors (LLDFs) and dynamic impact factors for the individual bridge girders. Second, these field data were also used to calibrate analytical models, which were then used to conduct a detailed parametric study related to a wide variety of implements of husbandry. A description of field tests, the procedures followed, and sample field results are detailed in the following sections.

Field Inspections

According to the most recent field inspection report, the Steel-Timber Bridge 9 timber deck is in satisfactory condition with minor deterioration. The steel girders are in good condition. These inspection-based observations were corroborated by the Iowa State University field testing team.

Instrumentation Plan

Given that the primary goal of the testing plan was to measure the live load response of the primary load-carrying members, a network of multiple strain gages was used to measure the strain under the weight of the vehicles. The strain gages were attached to the bottom of the girders at mid-span as shown in Figure B-66. The strain sensors used to conduct this testing were installed with a 3 in. gage length, and data were collected at a rate of 50 Hz during static testing and at 50 Hz during dynamic testing.

Test Load Paths

The vehicles utilized during field testing of this bridge consisted of four common farm vehicles and one typical highway truck. The vehicles included a terragator, a tractor with grain wagon, a tractor with one liquid manure applicator tank, a tractor with two liquid manure applicator tanks, and a typical five-axle semi-truck. The individual axle loads, total weights, and lengths of the five vehicles used for field testing are summarized in Table B-17. As shown in Figure B-67, the configurations of the farm vehicles were notably different from that of the conventional highway truck.

Table B-17. Axle weight and total length of each testing vehicle

Farm Vehicles	Weight (lbs)					Total Length (ft-in.)	
	Front Axle	Rear Axle	Grain Wagon	Tanks	Trailer		
Tractor w/ 1 tank	11,800	15,900	-	48,800	-	76,500	40'-8"
Tractor w/ 2 tanks	11,800	15,900	-	32,600	-	68,900	63'-7"
Terragator	11,060	32,400	-	-	-	43,460	25'-7"
Tractor Grain Wagon	18,840	18,660	15,660	-	-	53,160	35'-2"
Semi-Truck	10,760	33,856	-	-	33,084	77,700	52'-1"



Tractor w/ 1 tank



Tractor w/ 2 tanks



Terragator



Tractor Grain Wagon



Semi Truck

Figure B-67. Farm vehicles used for field testing

During testing, the vehicles were driven across the bridge from west to east. In general the centerlines of the bridge and vehicle were approximately aligned. Initial static load testing was completed with the vehicles traveling at approximately 3 mph such that the pseudo-static bridge response could be captured. Later, dynamic load testing was completed with the vehicles traveling at approximately 20 mph (maximum safe speed at the site).

Sample Field Results

Representative plots from static load testing showing the strain experienced by one of the girders under all test vehicles is shown in Figure B-68. It was observed that the girders at the center of the bridge experienced the maximum strain magnitudes as the test vehicles crossed the bridge.

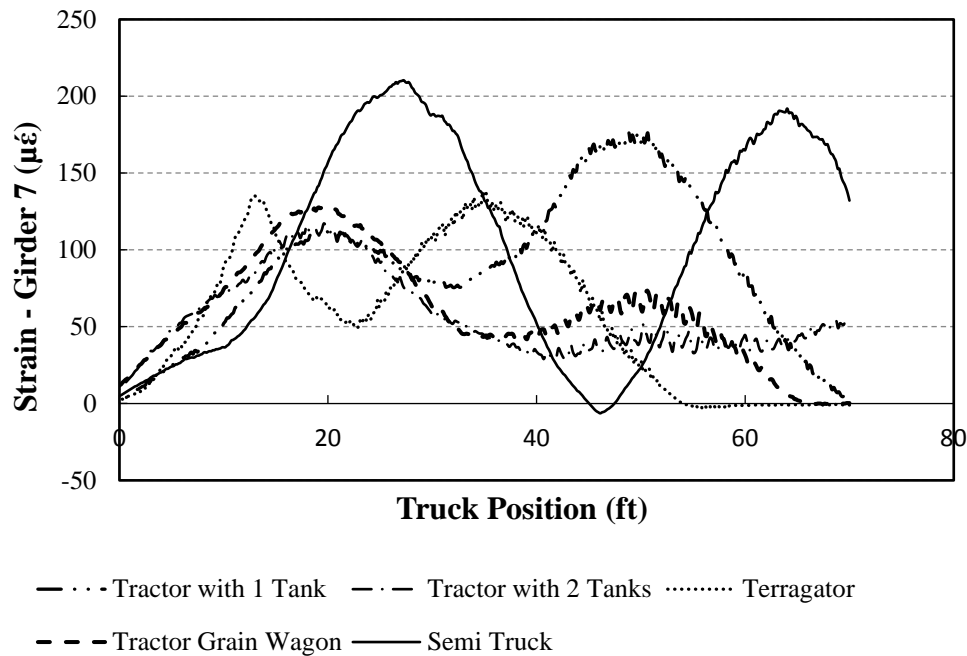


Figure B-68. Strain plot of a girder for all test vehicles for Steel-Timber Bridge 9

The semi-truck normally results in higher strains compared to other farm vehicles, and this tendency can be seen in Figure B-68. These recorded strains were employed to calculate the field LLDFs for each girder based upon the following equation.

$$LLDF^f = \frac{\epsilon^m \max i, t}{\sum_{i=1}^n \epsilon^m \max i, t} \quad (1)$$

Where $LLDF^f$ is the field live load distribution factor and ϵ^m are the measured maximum strains for individual girders over time, respectively.

A representative plot showing the comparison between static and dynamic strain for one of the girders under a test vehicle is shown in Figure B-69. It was generally observed that the girders experience more strain under dynamic loads than under static loading. The strain values from dynamic load tests were utilized to calculate the dynamic amplification factors (DAFs) for each girder.

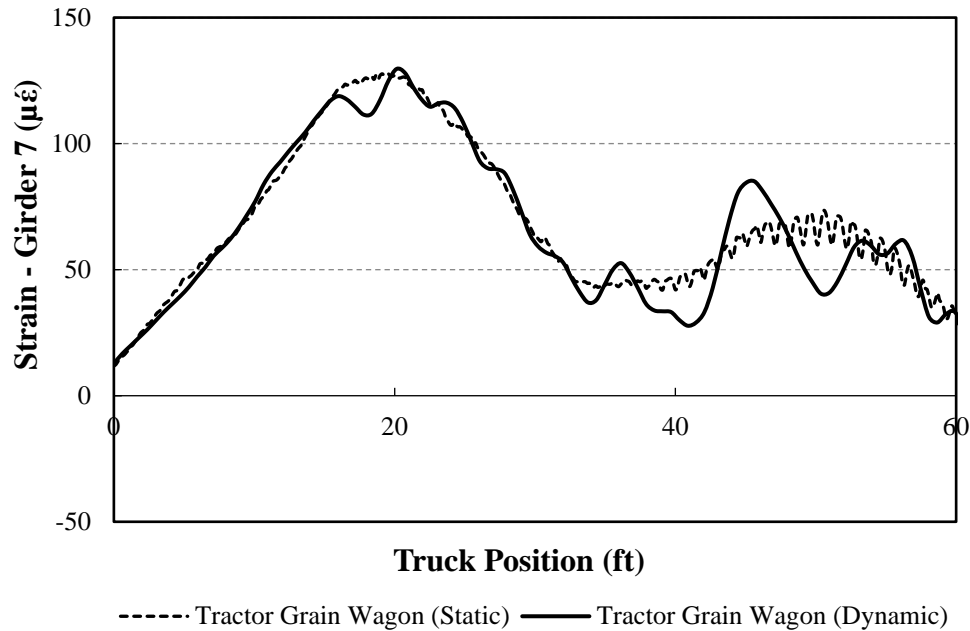


Figure B-69. Comparison between static and dynamic strain for Steel-Timber Bridge 9

B.9.4 Analytical Modeling

In lieu of field testing with a large number of vehicles, finite element analysis (FEA) simulations were used to estimate LLDFs for other vehicle configurations. As a result, analytical LLDFs were determined based upon FEA simulations of over 121 different farm vehicles on Steel-Timber Bridge 9. The FEA model was developed as described subsequently, and specific bridge information is presented in the following sections.

Model Generation

The bridge was initially modeled with the geometric and material properties taken directly from available bridge plans and/or field inspections using the BDI (Bridge Diagnostics, Inc.) finite element software WinGEN. A modulus of elasticity of 1600 ksi and 29000 ksi was used for all timber and steel components in the model respectively. The FEA model consisted of beam elements for the girders, shell elements for the deck, and rotational springs that simulated rotational restraint at the abutments and piers. Figure B-70 shows a representative model of the bridge.

Model Calibration

To improve the model accuracy, a calibration process that identified the bridge properties that resulted in the lowest error was completed. Based upon similarities in the response and observed field condition, a single cross-section was considered for all the girders. Table B-18 summarizes the original and calibrated values for the various bridge components along with percent error and correlation coefficient values.

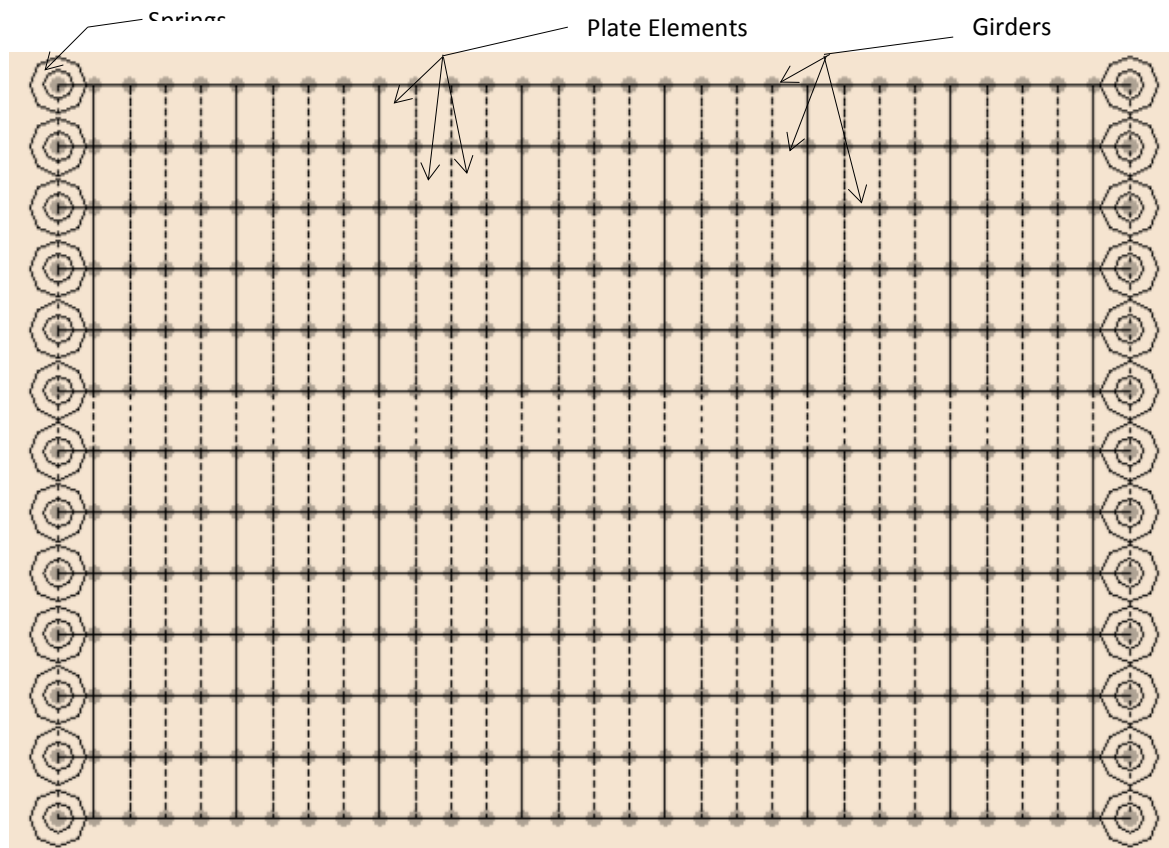


Figure B-70. Finite element model of Steel-Timber Bridge 9

Table B-18. Model calibration for Steel-Timber Bridge 9

Calibration Parameters	Bridge Components	Plan Value	Calibrated Value
Moment of Inertia, I (in ⁴)	Exterior Girders	216	262
	Interior Girders	368	458
Modulus of Elasticity, E (Ksi)	Deck	1600	1200
Rotational Stiffness, kr (Kips-in/rad)	Support Connections (springs)	0	978
Statistical Results	Percent Error		8.4%
	Correlation Coefficients		0.93

Once model calibration was completed, the analytical model was loaded with 121 farm vehicles covering a wide range of axle spacings, weights, and gage widths. The analytical strain response was then used to compute analytical LLDFs for each simulation vehicle using Equation (1).

To interpret the results efficiently, the LLDFs of the girders were grouped together as either interior or exterior girder LLDFs. Statistical limits for the interior and exterior girder LLDFs were determined from cumulative distribution function (CDF) curves defined to be at the 95% confidence thresholds.

B.9.5 Results

The envelopes of LLDFs for Steel-Timber Bridge 9 are presented in Figure B-71 for both the field and analytical LLDFs for each girder. In addition to the envelopes, the AASHTO LLDFs and statistical control limits for each group of interior and exterior girders are also shown.

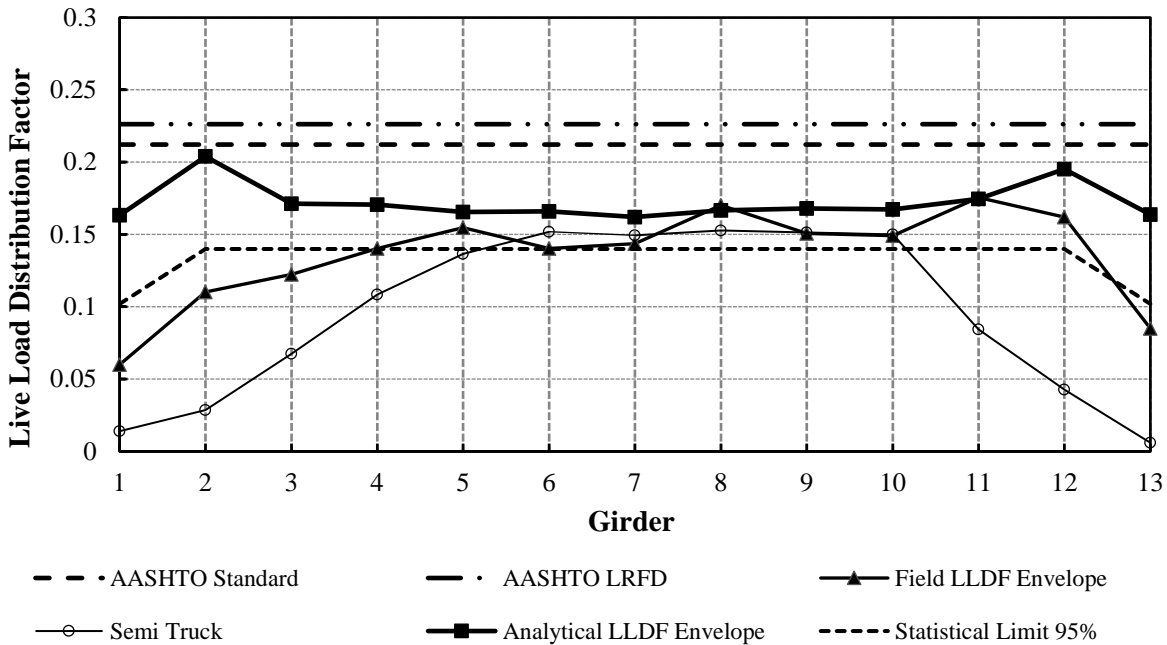


Figure B-71. LLDFs for Steel-Timber Bridge 9

It appears that the analytical LLDF envelope for all the girders is much smaller than those from the AASHTO standard and LRFD specifications. The peak value of the analytical exterior girder LLDFs was observed in G1 and G13, which have LLDFs of 0.16, while that of the interior girders was found in G2, which has an LLDF of 0.20. The statistical limits for either the interior or exterior girder group also show smaller values than the AASHTO specifications. The field LLDF envelope represents the highest LLDF observed in each girder due to field testing using farm vehicles, whereas the semi-truck envelope represents the extreme LLDFs for field testing using a five-axle semi-truck. The field LLDF envelope has larger values than that for the semi-truck for most of the girders.

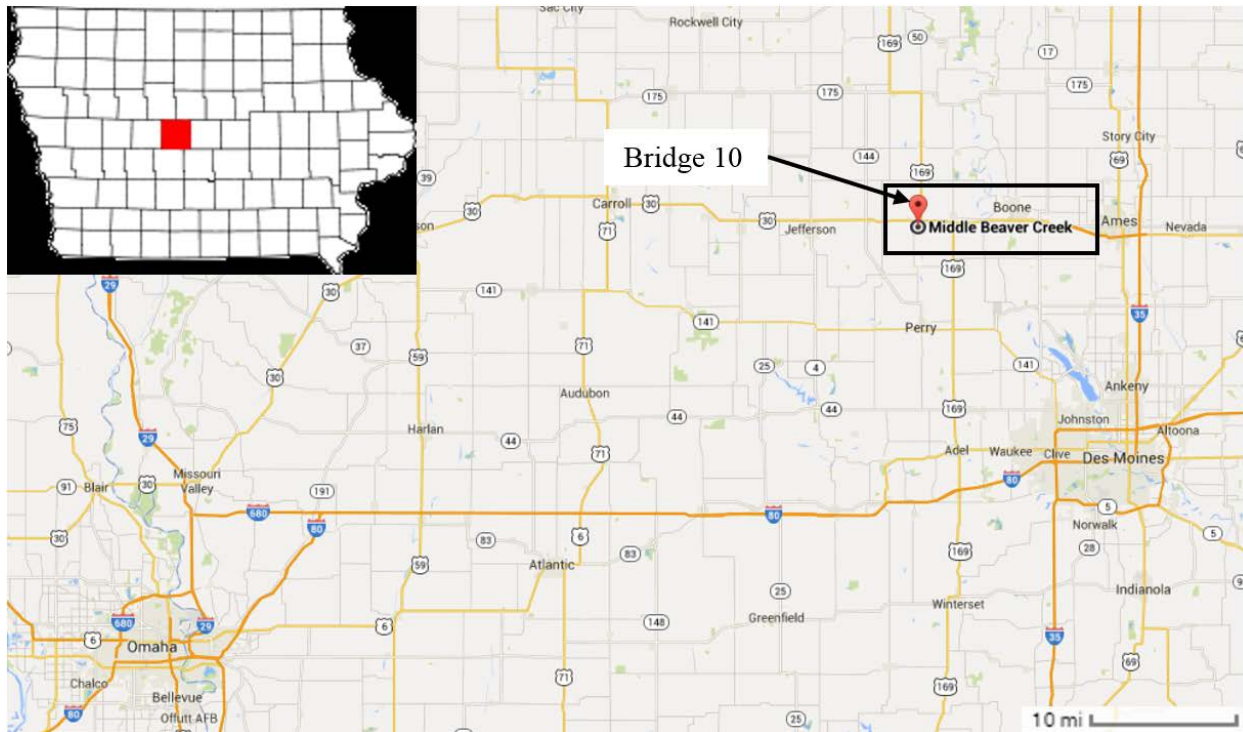
B.10 Steel-Timber Bridge 10

This mini test and evaluation report documents the results of field testing and subsequent analysis of a steel girder bridge with a timber deck (Steel-Timber Bridge 10) under multiple implements of husbandry. For completeness, this mini-report includes a description of the bridge, a description of the live load testing procedures followed, sample data, a description of analytical modeling, plots of analytical results, and a discussion of the overall behavior of the steel girder bridge under implements of husbandry.

B.10.1 Background

The steel-timber bridge described here is known in the National Bridge Inventory (NBI) database as Bridge 77470 and will be henceforth be referred to as Steel-Timber Bridge 10. The bridge is

located at intersection of 201st Street and D Avenue, about 5 miles west of Ogden, in Boone County, Iowa. Figure B-72 shows the general location of the bridge.



Map: ©Google 2014

Figure B-72. Location overview of Steel-Timber Bridge 10

B.10.2 Bridge Description

Steel-Timber Bridge 10 is open to one-lane traffic and has one span with overall dimensions of 29.9 ft long by 18.0 ft wide with zero degrees of skew. The deck is comprised of continuous timber decking with a thickness of 3 in. An elevation view and an end view of the bridge are shown in Figure B-73. The bridge consists of eight steel girders with approximate spacing between adjacent girders of 2.5 ft. The girders are I cross-section and are approximately 21.3 in. by 8.3 in. Figure B-74 shows a typical cross-section and plan view of the bridge.



Figure B-73. Steel-Timber Bridge 10: North elevation view (left) and east end view (right)

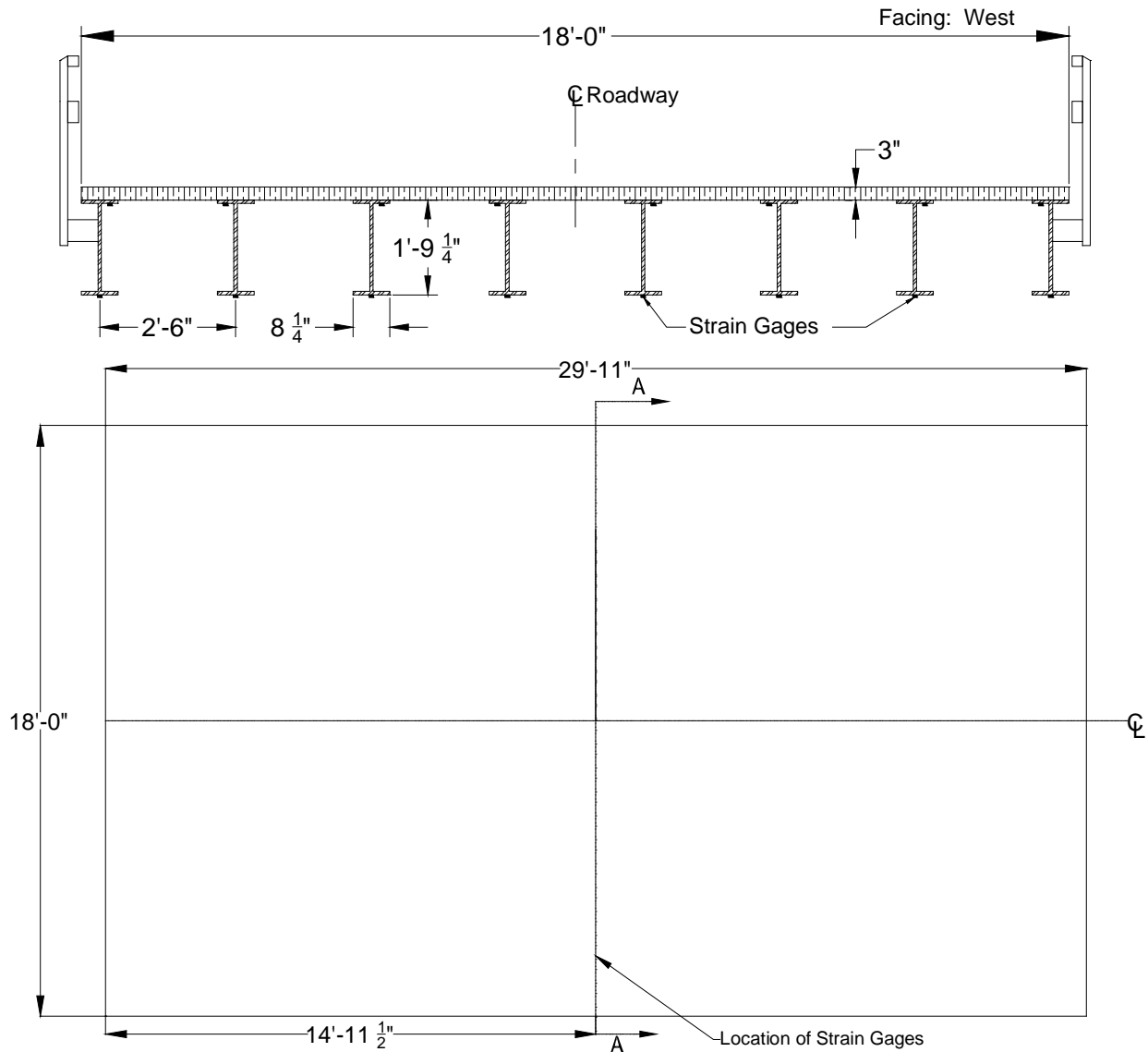


Figure B-74. Steel-Timber Bridge 10: Cross-section A-A (top) and plan (bottom)

B.10.3 Field Testing

Field testing of this bridge was conducted for two reasons. First, field testing was conducted to determine experimental live load distribution factors (LLDFs) and dynamic impact factors for the individual bridge girders. Second, these field data were also used to calibrate analytical models, which were then used to conduct a detailed parametric study related to a wide variety of implements of husbandry. A description of field tests, the procedures followed, and sample field results are detailed in the following sections.

Field Inspections

According to the most recent field inspection report, the Steel-Timber Bridge 10 timber deck is in fair condition with minor section loss. The steel girders are in satisfactory condition and show signs of rust. These inspection-based observations were corroborated by the Iowa State University field testing team.

Instrumentation Plan

Given that the primary goal of the testing plan was to measure the live load response of the primary load-carrying members, a network of multiple strain gages was used to measure the strain under the weight of the vehicles. The strain gages were attached to the bottom of the girders at mid-span as shown in Figure B-74. The strain sensors used to conduct this testing were installed with a 3 in. gage length, and data were collected at a rate of 20 Hz during static testing and at 20 Hz during dynamic testing.

Test Load Paths

The vehicles utilized during field testing of this bridge consisted of four common farm vehicles and one typical highway truck. The vehicles included a terragator, a tractor with grain wagon, a tractor with one liquid manure applicator tank, a tractor with two liquid manure applicator tanks, and a typical five-axle semi-truck. The individual axle loads, total weights, and lengths of the five vehicles used for field testing are summarized in Table B-19. As shown in Figure B-75, the configurations of the farm vehicles were notably different from that of the conventional highway truck.

Table B-19. Axle weight and total length of each testing vehicle

Farm Vehicles	Weight (lbs)					Total	Total Length (ft-in.)
	Front Axle	Rear Axle	Grain Wagon	Tanks	Trailer		
Tractor w/ 1 tank	11,800	15,900	-	48,800	-	76,500	40'-8"
Tractor w/ 2 tanks	11,800	15,900	-	32,600	-	68,900	63'-7"
Terragator	11,060	32,400	-	-	-	43,460	25'-7"
Tractor Grain Wagon	18,840	18,660	15,660	-	-	53,160	35'-2"
Semi-Truck	10,760	33,856	-	-	33,084	77,700	52'-1"



Tractor w/ 1 tank



Tractor w/ 2 tanks



Terragator



Tractor Grain Wagon



Semi Truck

Figure B-75. Farm vehicles used for field testing

During testing, the vehicles were driven across the bridge from west to east. In general the centerlines of the bridge and vehicle were approximately aligned. Initial static load testing was completed with the vehicles traveling at approximately 3 mph such that the pseudo-static bridge response could be captured. Later, dynamic load testing was completed with the vehicles traveling at approximately 20 mph (maximum safe speed at the site).

Sample Field Results

Representative plots from static load testing showing the strain experienced by one of the girders under all test vehicles is shown in Figure B-76. It was observed that the girders at the center of the bridge experienced the maximum strain magnitudes as the test vehicles crossed the bridge.

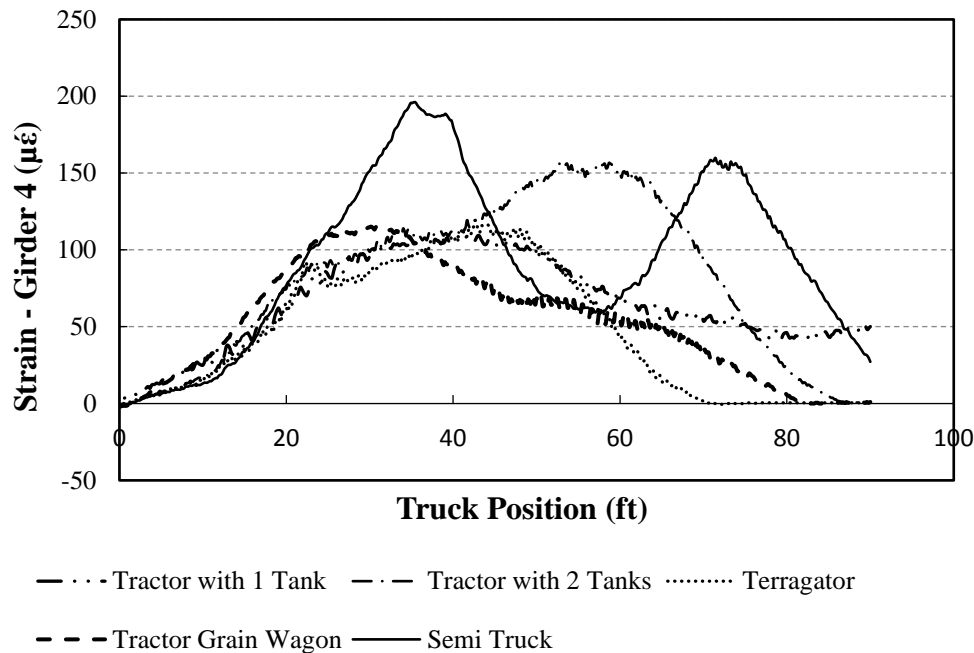


Figure B-76. Strain plot of a girder for all test vehicles for Steel-Timber Bridge 10

The semi-truck normally results in higher strains compared to other farm vehicles, and this tendency can be seen in Figure B-76. These recorded strains were employed to calculate the field LLDFs for each girder based upon the following equation.

$$LLDF^f = \frac{\epsilon^m \max i, t}{\sum_{i=1}^n \epsilon^m \max i, t} \quad (1)$$

Where $LLDF^f$ is the field live load distribution factor and ϵ^m are the measured maximum strains for individual girders over time, respectively.

A representative plot showing the comparison between static and dynamic strain for one of the girders under a test vehicle is shown in Figure B-77. It was generally observed that the girders experience more strain under dynamic loads than under static loading. The strain values from dynamic load tests were utilized to calculate the dynamic amplification factors (DAFs) for each girder.

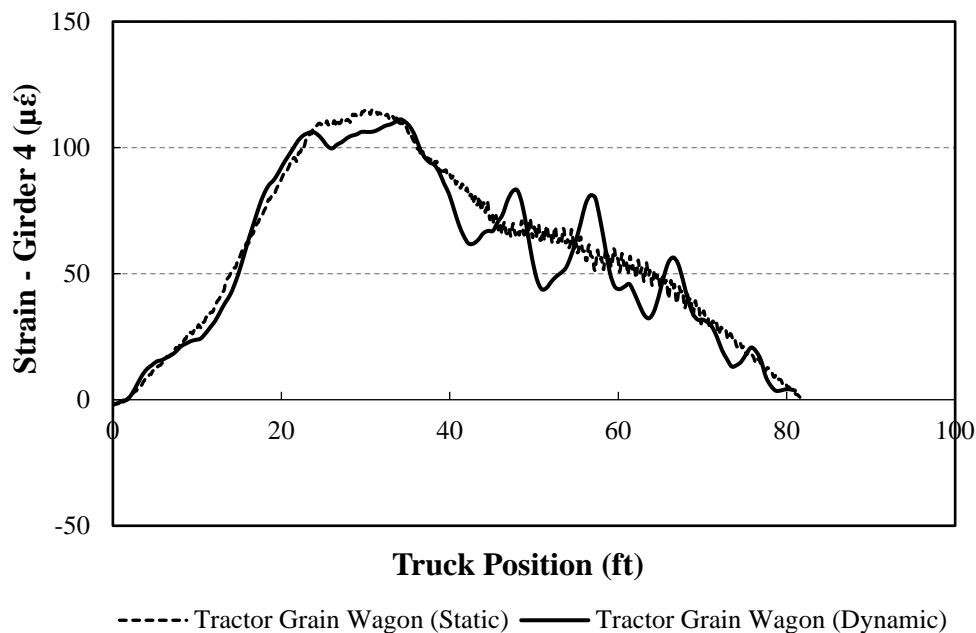


Figure B-77. Comparison between static and dynamic strain for Steel-Timber Bridge 10

B.10.4 Analytical Modeling

In lieu of field testing with a large number of vehicles, finite element analysis (FEA) simulations were used to estimate LLDFs for other vehicle configurations. As a result, analytical LLDFs were determined based upon FEA simulations of over 121 different farm vehicles on Steel-Timber Bridge 10. The FEA model was developed as described subsequently, and specific bridge information is presented in the following sections.

Model Generation

The bridge was initially modeled with the geometric and material properties taken directly from available bridge plans and/or field inspections using the BDI (Bridge Diagnostics, Inc.) finite element software WinGEN. A modulus of elasticity of 1600 ksi and 29000 ksi was used for all timber and steel components in the model respectively. The FEA model consisted of beam elements for the girders, shell elements for the deck, and rotational springs that simulated rotational restraint at the abutments and piers. Figure B-78 shows a representative model of the bridge.

Model Calibration

To improve the model accuracy, a calibration process that identified the bridge properties that resulted in the lowest error was completed. Based upon similarities in the response and observed field condition, a single cross-section was considered for all the girders. Table B-20 summarizes the original and calibrated values for the various bridge components along with percent error and correlation coefficient values.

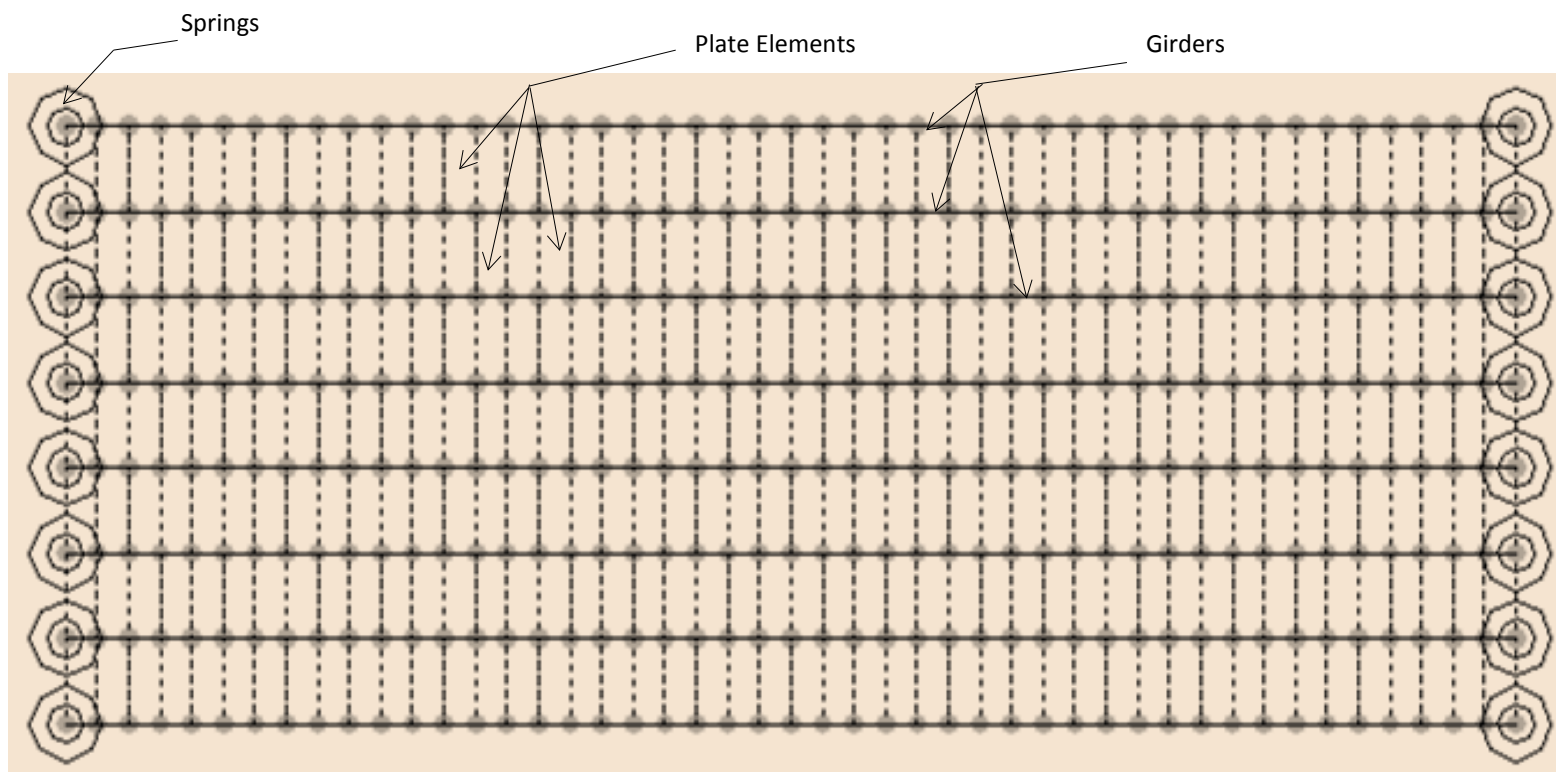


Figure B-78. Finite element model of Steel-Timber Bridge 10

Table B-20. Model calibration for Steel-Timber Bridge 10

Calibration Parameters	Bridge Components	Plan Value	Calibrated Value
Moment of Inertia, I (in ⁴)	Girders	1621	1667
Modulus of Elasticity, E (Ksi)	Deck	1600	1200
Rotational Stiffness, kr (Kips-in/rad)	Support Connections (springs)	0	59674
Statistical Results	Percent Error		10.45%
	Correlation Coefficients		0.92

Once model calibration was completed, the analytical model was loaded with 121 farm vehicles covering a wide range of axle spacings, weights, and gage widths. The analytical strain response was then used to compute analytical LLDFs for each simulation vehicle using Equation (1).

To interpret the results efficiently, the LLDFs of the girders were grouped together as either interior or exterior girder LLDFs. Statistical limits for the interior and exterior girder LLDFs were determined from cumulative distribution function (CDF) curves defined to be at the 95% confidence thresholds.

B.10.5 Results

The envelopes of LLDFs for Steel-Timber Bridge 10 are presented in Figure B-79 for both the field and analytical LLDFs for each girder. In addition to the envelopes, the AASHTO LLDFs and statistical control limits for each group of interior and exterior girders are also shown.

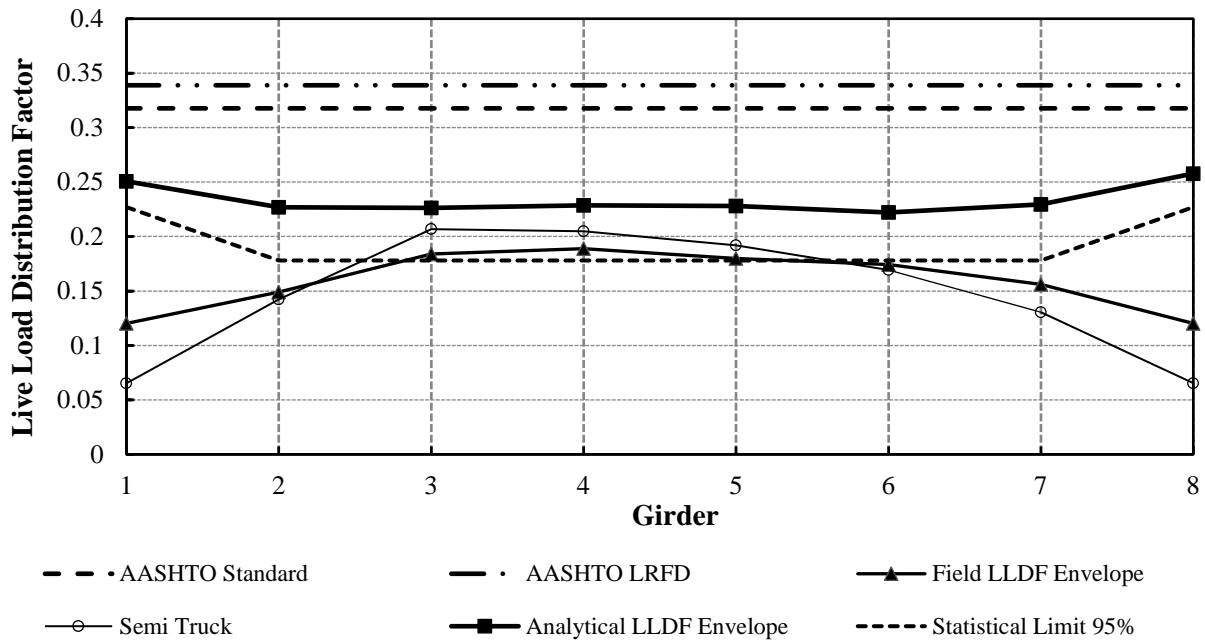


Figure B-79. LLDFs for Steel-Timber Bridge 10

It appears that the analytical LLDF envelope for all the girders is much smaller than those from the AASHTO standard and LRFD specifications. The peak value of the analytical exterior girder LLDFs was observed in G8, which has an LLDF of 0.26, while that of the interior girders was found in G2, G3, G4, G5, and G7, which have LLDFs of 0.23. The statistical limits for either the interior or exterior girder group also show smaller values than the AASHTO specifications. The field LLDF envelope represents the highest LLDF observed in each girder due to field testing using farm vehicles, whereas the semi-truck envelope represents the extreme LLDFs for field testing using a five-axle semi-truck. The field LLDF envelope has smaller values than that for the semi-truck for most of the girders.

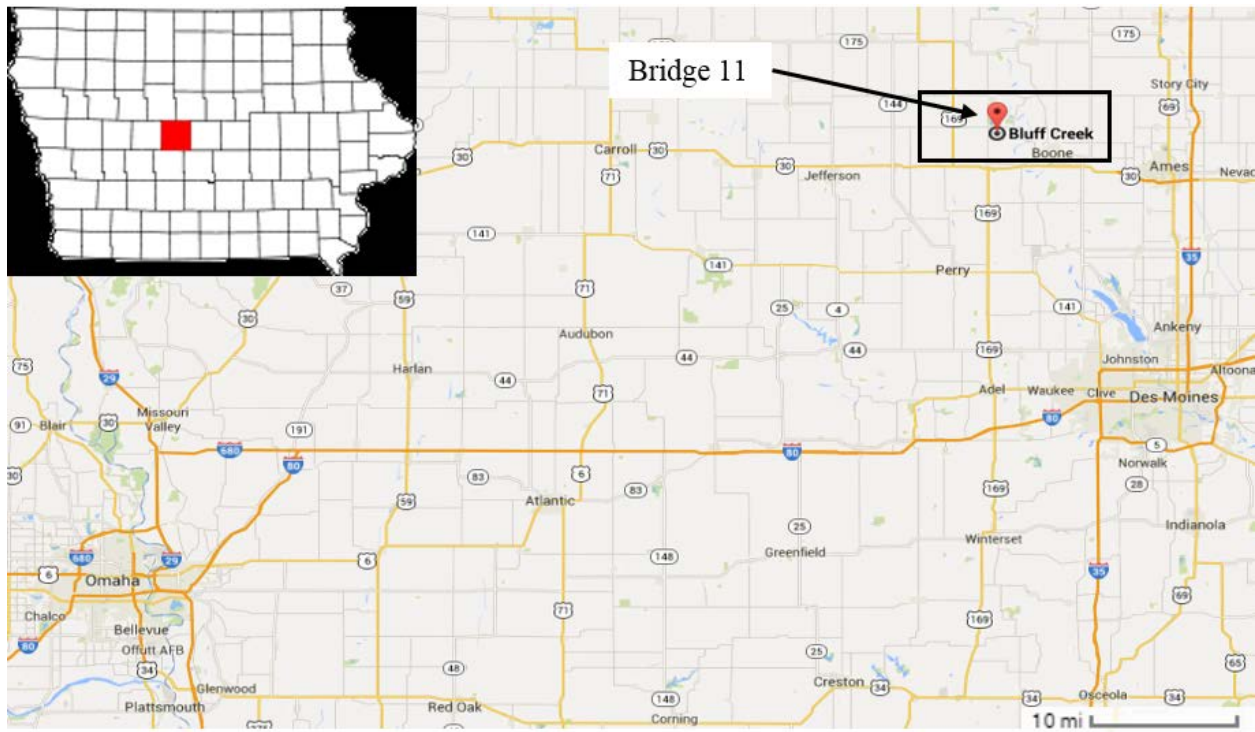
B.11 Steel-Timber Bridge 11

This mini test and evaluation report documents the results of field testing and subsequent analysis of a steel girder bridge with a timber deck (Steel-Timber Bridge 11) under multiple implements of husbandry. For completeness, this mini-report includes a description of the bridge, a description of the live load testing procedures followed, sample data, a description of analytical modeling, plots of analytical results, and a discussion of the overall behavior of the steel girder bridge under implements of husbandry.

B.11.1 Background

The steel-timber bridge described here is known in the National Bridge Inventory (NBI) database as Bridge 77790 and will be henceforth be referred to as Steel-Timber Bridge 11. The bridge is

on I Avenue between 170th Street and 200th Street, about 5 miles south of Fraser, in Boone County, Iowa. Figure B-80 shows the general location of the bridge.



Map: ©Google 2014

Figure B-80. Location overview of Steel-Timber Bridge 11

B.11.2 Bridge Description

Steel-Timber Bridge 11 is open to one-lane traffic and has three spans with overall dimensions of 73.5 ft long by 18.0 ft wide with zero degrees of skew. The deck is comprised of continuous timber decking with a thickness of 4 in. An elevation view and an end view of the bridge are shown in Figure B-81. The bridge consists of eight steel girders with spacing between adjacent girders of 1.2 ft. The girders are I cross-section and are approximately 14.3 in. by 6.9 in. Figure B-82 shows a typical cross-section and plan view of the bridge.



Figure B-81. Steel-Timber Bridge 11: South elevation view (left) and east end view (right)

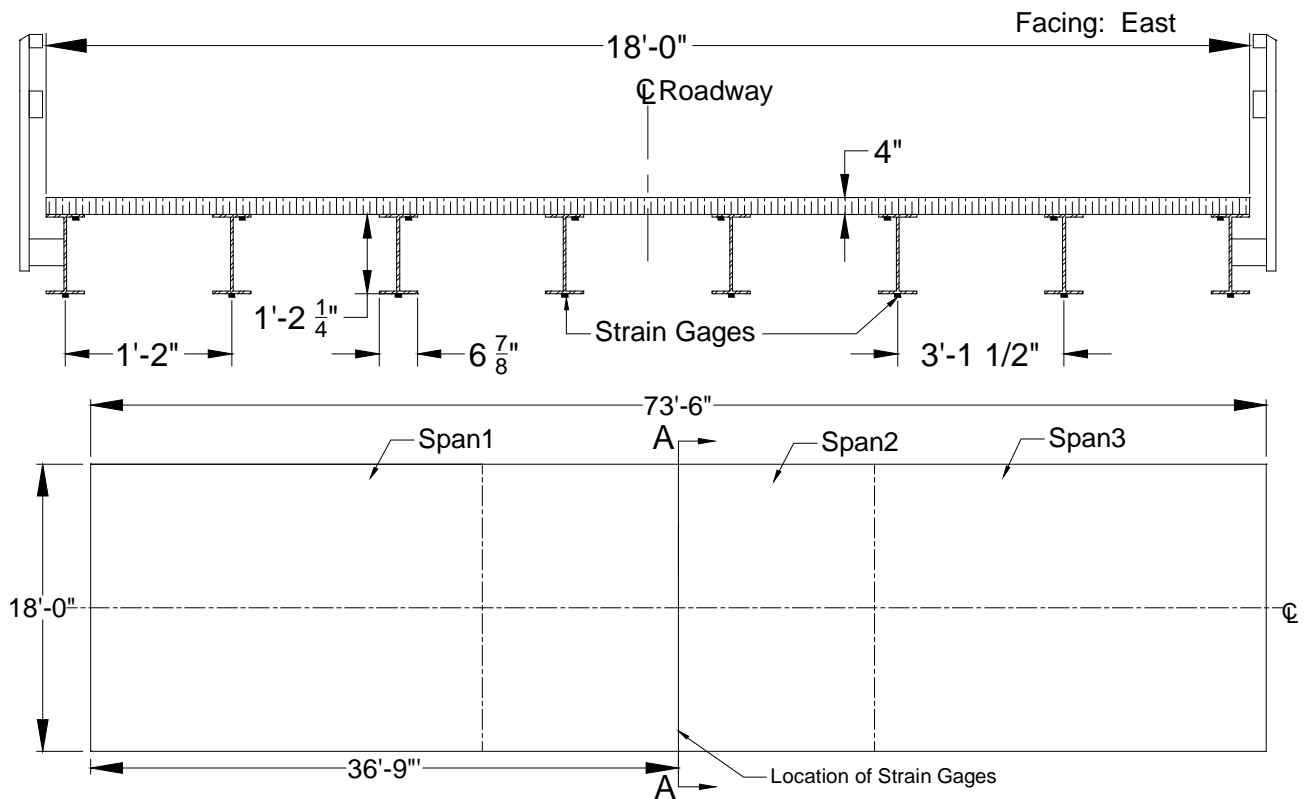


Figure B-82. Steel-Timber Bridge 11: Cross-section A-A (top) and plan (bottom)

B.11.3 Field Testing

Field testing of this bridge was conducted for two reasons. First, field testing was conducted to determine experimental live load distribution factors (LLDFs) for the individual bridge girders. Second, these field data were also used to calibrate analytical models, which were then used to conduct a detailed parametric study related to a wide variety of implements of husbandry. A

description of field tests, the procedures followed, and sample field results are detailed in the following sections.

Field Inspections

According to the most recent field inspection report, the Steel-Timber Bridge 11 timber deck is in fair condition with minor section loss. The steel girders are in average condition and show signs of rust. These inspection-based observations were corroborated by the Iowa State University field testing team.

Instrumentation Plan

Given that the primary goal of the testing plan was to measure the live load response of the primary load-carrying members, a network of multiple strain gages was used to measure the strain under the weight of the vehicles. The strain gages were attached to the bottom of the girders at mid-span as shown in Figure B-82. The strain sensors used to conduct this testing were installed with a 3 in. gage length, and data were collected at a rate of 20 Hz during static testing.

Test Load Paths

The vehicles utilized during field testing of this bridge consisted of four common farm vehicles and one typical highway truck. The vehicles included a terragator, a tractor with grain wagon, a tractor with one liquid manure applicator tank, a tractor with two liquid manure applicator tanks, and a typical five-axle semi-truck. The individual axle loads, total weights, and lengths of the five vehicles used for field testing are summarized in Table B-21. As shown in Figure B-83, the configurations of the farm vehicles were notably different from that of the conventional highway truck.

Table B-21. Axle weight and total length of each testing vehicle

Farm Vehicles	Weight (lbs)					Total	Total Length (ft-in.)
	Front Axle	Rear Axle	Grain Wagon	Tanks	Trailer		
Tractor w/ 1 tank	11,800	15,900	-	48,800	-	76,500	40'-8"
Tractor w/ 2 tanks	11,800	15,900	-	32,600	-	68,900	63'-7"
Terragator	11,060	32,400	-	-	-	43,460	25'-7"
Tractor Grain Wagon	18,840	18,660	15,660	-	-	53,160	35'-2"
Semi-Truck	10,760	33,856	-	-	33,084	77,700	52'-1"



Tractor w/ 1 tank



Tractor w/ 2 tanks



Terragator



Tractor Grain Wagon



Semi Truck

Figure B-83. Farm vehicles used for field testing

During testing, the vehicles were driven across the bridge from west to east. In general the centerlines of the bridge and vehicle were approximately aligned. Static load testing was completed with the vehicles traveling at approximately 3 mph such that the pseudo-static bridge response could be captured.

Sample Field Results

Representative plots from static load testing showing the strain experienced by one of the girders under all test vehicles is shown in Figure B-84. It was observed that the girders at the center of the bridge experienced the maximum strain magnitudes as the test vehicles crossed the bridge.

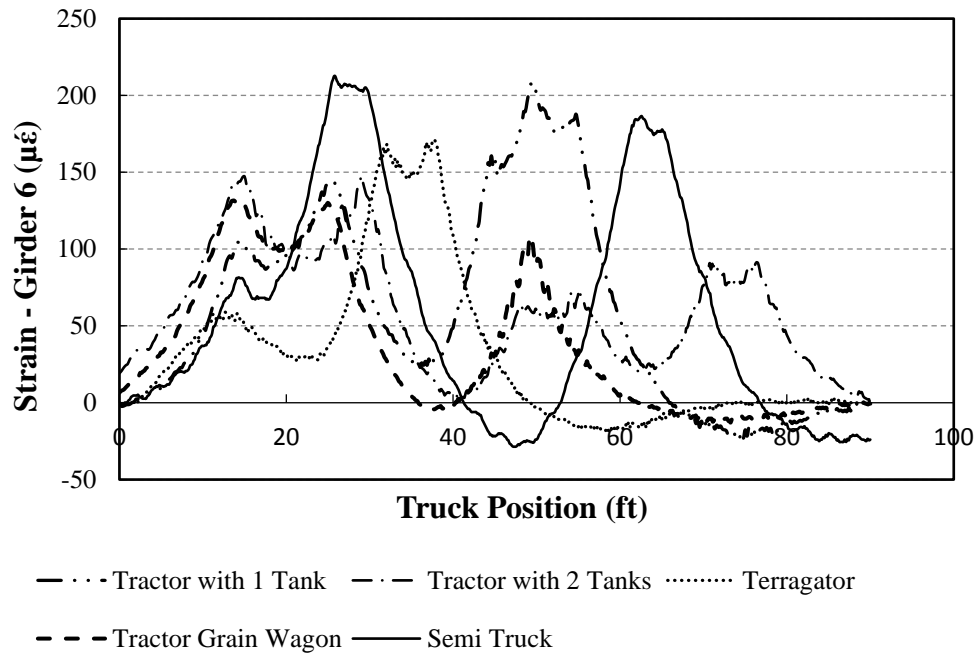


Figure B-84. Strain plot of a girder for all test vehicles for Steel-Timber Bridge 11

The semi-truck normally results in higher strains compared to other farm vehicles, and this tendency can be seen in Figure B-84. These recorded strains were employed to calculate the field LLDFs for each girder based upon the following equation.

$$LLDF^f = \frac{\epsilon^m \max_{i,t}}{\sum_{i=1}^n \epsilon^m \max_{i,t}} \quad (1)$$

Where $LLDF^f$ is the field live load distribution factor and ϵ^m are the measured maximum strains for individual girders over time, respectively.

B.11.4 Analytical Modeling

In lieu of field testing with a large number of vehicles, finite element analysis (FEA) simulations were used to estimate LLDFs for other vehicle configurations. As a result, analytical LLDFs were determined based upon FEA simulations of over 121 different farm vehicles on Bridge 11. The FEA model was developed as described subsequently, and specific bridge information is presented in the following sections.

Model Generation

The bridge was initially modeled with the geometric and material properties taken directly from available bridge plans and/or field inspections using the BDI (Bridge Diagnostics, Inc.) finite element software WinGEN. A modulus of elasticity of 1600 ksi and 29000 ksi was used for all timber and steel components in the model respectively. The FEA model consisted of beam elements for the girders, shell elements for the deck, and rotational springs that simulated rotational restraint at the abutments and piers. Figure B-85 shows a representative model of the bridge.

Model Calibration

To improve the model accuracy, a calibration process that identified the bridge properties that resulted in the lowest error was completed. Based upon similarities in the response and observed field condition, a single cross-section was considered for all the girders. Table B-22 summarizes the original and calibrated values for the various bridge components along with percent error and correlation coefficient values.

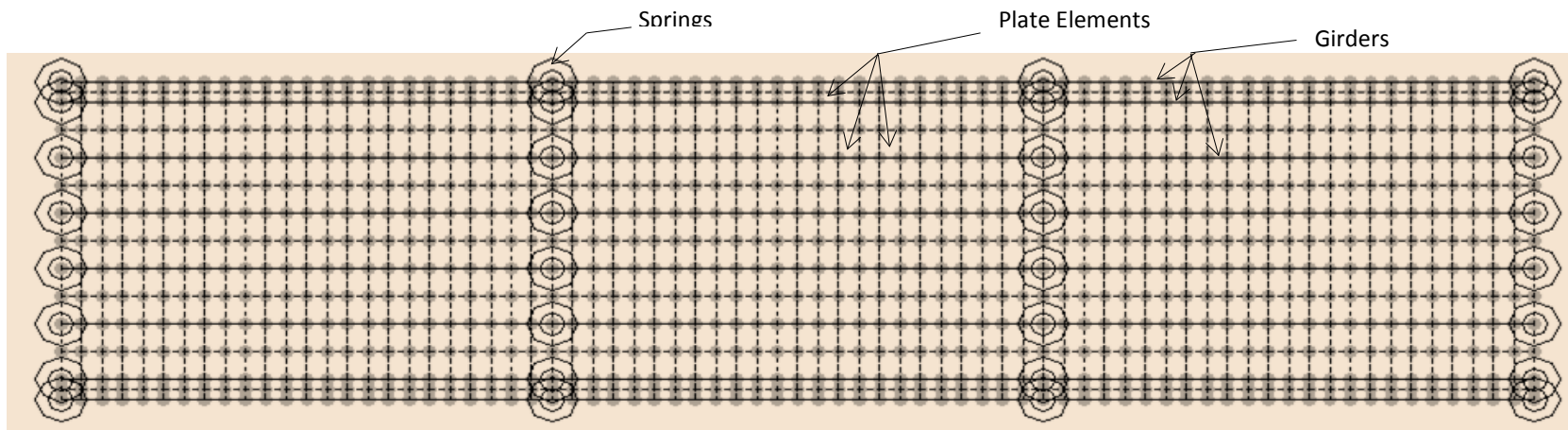


Figure B-85. Finite element model of Steel-Timber Bridge 11

Table B-22. Model calibration for Steel-Timber Bridge 11

Calibration Parameters	Bridge Components	Plan Value	Calibrated Value
Moment of Inertia, I (in ⁴)	Exterior Girders	418	315
Modulus of Elasticity, E (Ksi)	Deck	1600	1200
Rotational Stiffness, kr (Kips-in/rad)	Support Connections (springs)	0	86294
Statistical Results	Percent Error		14.7%
	Correlation Coefficients		0.88

Once model calibration was completed, the analytical model was loaded with 121 farm vehicles covering a wide range of axle spacings, weights, and gage widths. The analytical strain response was then used to compute analytical LLDFs for each simulation vehicle using Equation (1).

To interpret the results efficiently, the LLDFs of the girders were grouped together as either interior or exterior girder LLDFs. Statistical limits for the interior and exterior girder LLDFs were determined from cumulative distribution function (CDF) curves defined to be at the 95% confidence thresholds.

B.11.5 Results

The envelopes of LLDFs for Steel-Timber Bridge 11 are presented in Figure B-86 for both the field and analytical LLDFs for each girder. In addition to the envelopes, the AASHTO LLDFs and statistical control limits for each group of interior and exterior girders are also shown.

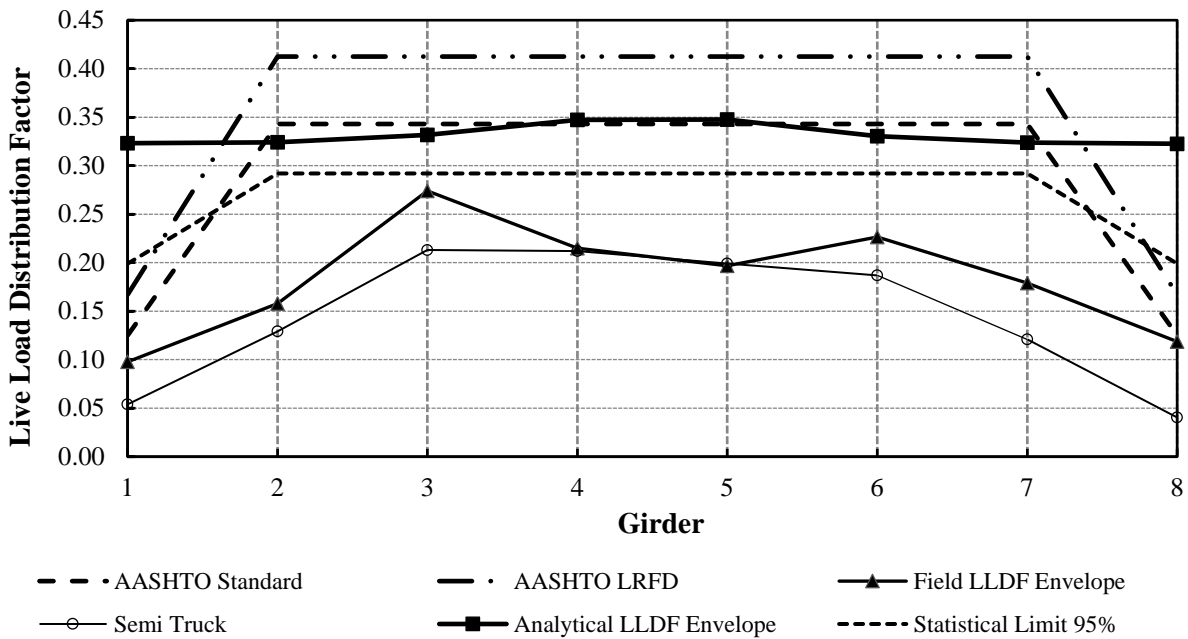


Figure B-86. LLDFs for Steel-Timber Bridge 11

It appears that the analytical LLDF envelope for all the girders is smaller than those from the AASHTO standard and LRFD specifications. The peak value of the analytical exterior girder LLDFs was observed in G8, which has an LLDF of 0.32, while that of the interior girders was found in G4 and G5, which have LLDFs of 0.34. The statistical limits for either the interior or exterior girder group also show smaller values than the AASHTO specifications. The field LLDF envelope represents the highest LLDF observed in each girder due to field testing using farm vehicles, whereas the semi-truck envelope represents the extreme LLDFs for field testing using a five-axle semi-truck. The field LLDF envelope has larger values than that for the semi-truck for most of the girders.

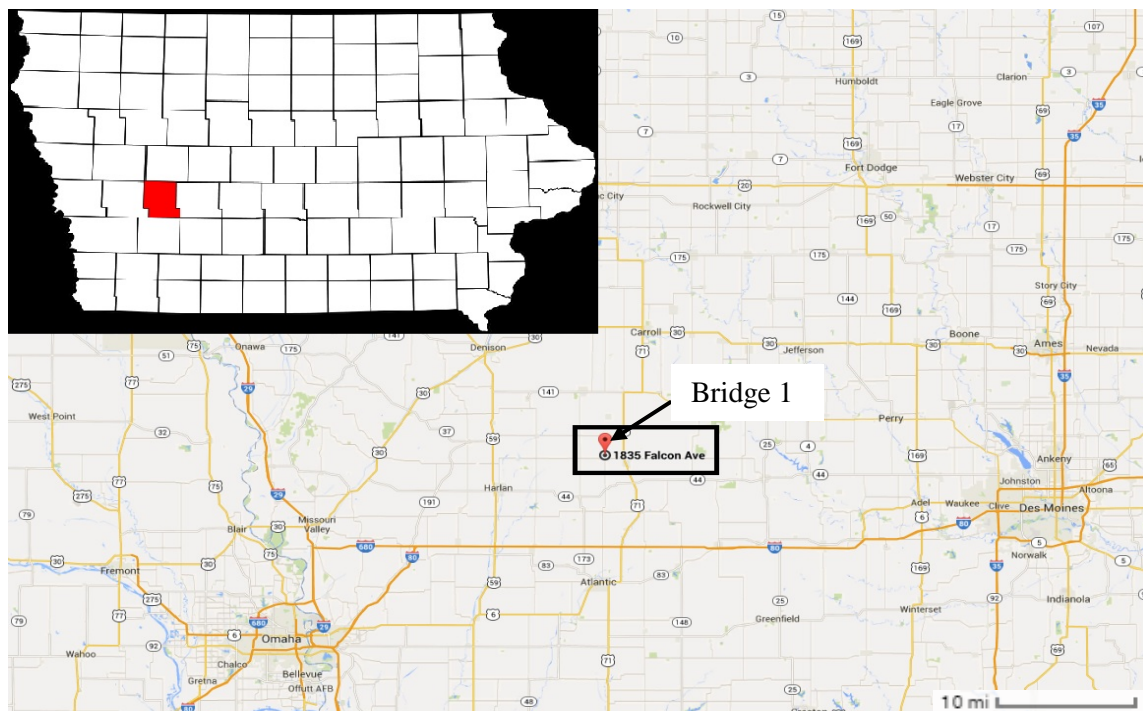
APPENDIX C. FIELD TESTED TIMBER-TIMBER BRIDGES

C.1 Timber-Timber Bridge 1

This mini test and evaluation report documents the results of field testing and subsequent analysis of a timber girder bridge with a timber deck (Timber-Timber Bridge 1) under multiple implements of husbandry. For completeness, this mini-report includes a description of the bridge, a description of the live load testing procedures followed, sample data, a description of analytical modeling, plots of analytical results, and a discussion of the overall behavior of the timber girder bridge under implements of husbandry.

C.1.1 Background

The timber-timber bridge described here is known in the National Bridge Inventory (NBI) database as Bridge 68790 and will be henceforth be referred to as Timber-Timber Bridge 1. The bridge is located about 20 miles east of Prairie Rose State Park, on Falcon Avenue, in Audubon County, Iowa. Figure C-1 shows the general location of the bridge.



Map: ©Google 2014

Figure C-1. Location overview of Timber-Timber Bridge 1

C.1.2 Bridge Description

Timber-Timber Bridge 1 is open to single-lane traffic and has two equal spans with overall dimensions of 30 ft long by 18 ft wide with zero degrees of skew. The deck is comprised of

continuous timber decking with a thickness of 3 in. An elevation view and an end view of the bridge are shown in Figure C-2. The bridge consists of 17 timber girders with variable spacing between adjacent girders (varying from 4.5 in to 18.5 in.) The girders have a rectangular cross-section measuring approximately 15.1 in. by 3.8 in. Figure C-3 shows a typical cross-section and plan view of the bridge.



Figure C-2. Timber-Timber Bridge 1: West elevation view (left) and north end view (right)

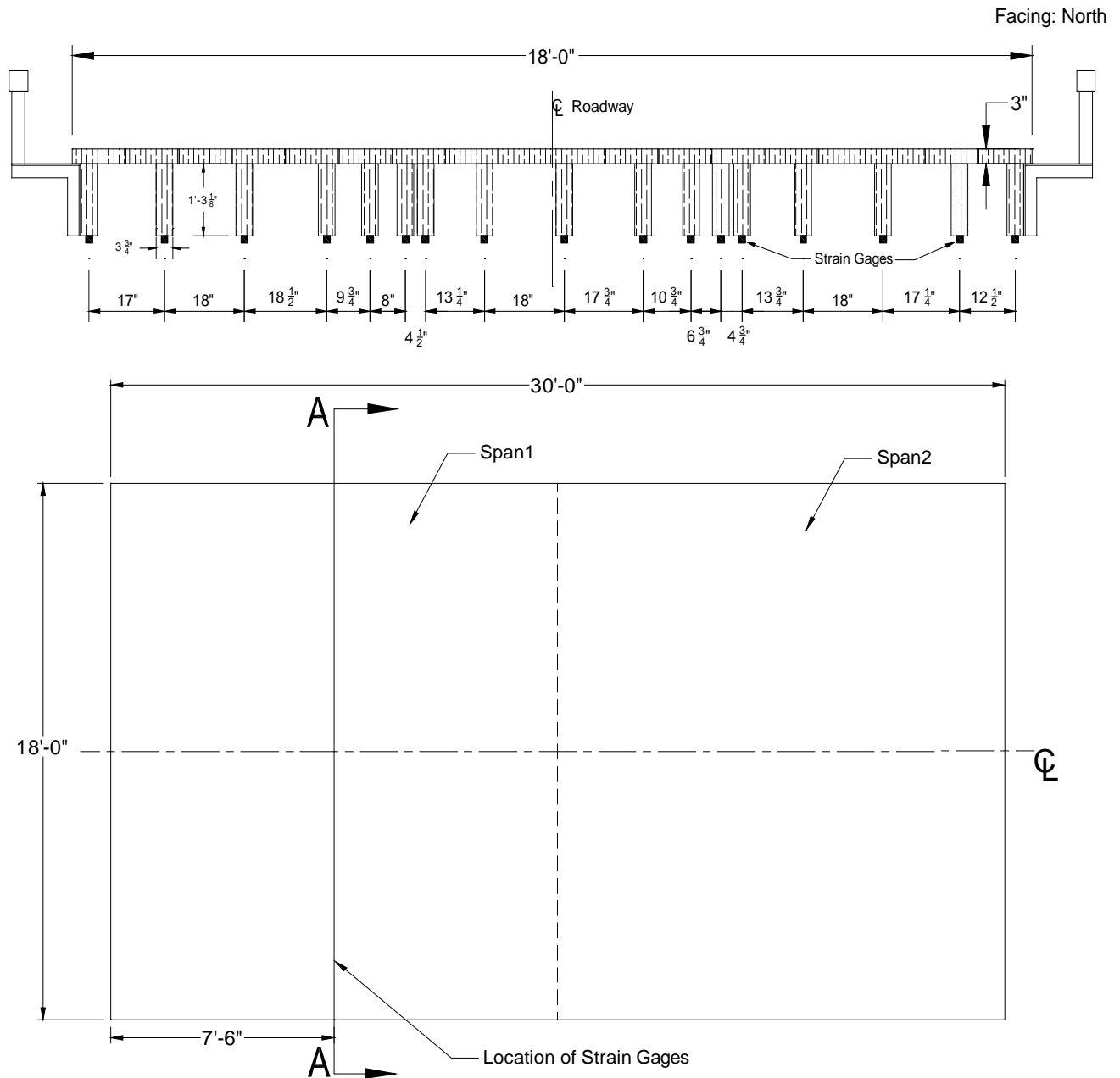


Figure C-3. Timber-Timber Bridge 1: Cross-section A-A (top) and plan (bottom)

C.1.3 Field Testing

Field testing of this bridge was conducted for two reasons. First, field testing was conducted to determine experimental live load distribution factors (LLDFs) and dynamic impact factors for the individual bridge girders. Second, these field data were also used to calibrate analytical models, which were then used to conduct a detailed parametric study related to a wide variety of implements of husbandry. A description of field tests, the procedures followed, and sample field results are detailed in the following sections.

Field Inspections

According to the most recent field inspection report, the Timber-Timber Bridge 1 timber girders are not in good condition and show obvious signs of normal wear, tear, and decay. The bridge piers are also not in a good condition, showing similar signs of deterioration. These inspection-based observations were corroborated by the Iowa State University field testing team, who observed cracking and deterioration in multiple timber girders. At the time of testing, the deck was considered to be in average condition.

Instrumentation Plan

Given that the primary goal of the testing plan was to measure the live load response of the primary load-carrying members, a network of multiple strain gages was used to measure the strain under the weight of the vehicles. The strain gages were attached to the bottom of the girders at mid-span of Span 1 as shown in Figure C-3. The strain sensors used to conduct this testing were installed with a 3 in. gage length, and data were collected at a rate of 20 Hz during static testing and at 20 Hz during dynamic testing.

Test Load Paths

The vehicles utilized during field testing of this bridge consisted of four common farm vehicles and one typical highway truck. The vehicles included a terragator, a grain cart, a honey wagon with one tank, a honey wagon with two tanks, and a typical five-axle semi-truck. The individual axle loads, total weights, and lengths of the five vehicles used for field testing are summarized in Table C-1. As shown in Figure C-4, the configurations of the farm vehicles were notably different from that of the conventional highway truck.

Table C-1. Axle weight and total length of each testing vehicle

Farm Vehicles	Weight (lbs)					Total	Total Length (ft-in.)
	Front Axle	Rear Axle	Grain Wagon	Honey Wagon	Trailer		
Tractor Honey Wagon (empty)	10,960	15,740	-	26,720	-	53,420	40'-4"
Tractor Honey Wagon (half full with water)	10,580	22,800	-	40,620	-	74,000	40'-4"
Terragator	23,380	17,840	-	-	-	41,220	19'-0"
Tractor Grain Wagon	24,480	19,700	11,980	-	-	56,160	31'-0"
Semi-Truck	10,760	33,856	-	-	33,084	77,700	52'-1"



Honey Wagon



Honey Wagon- two tanks



Terragator



Tractor Grain Wagon



Semi Truck

Figure C-4. Farm vehicles used for field testing

During testing, the vehicles were driven across the bridge from north to south. In general the centerlines of the bridge and vehicle were approximately aligned. Initial static load testing was completed with the vehicles traveling at approximately 3 mph such that the pseudo-static bridge response could be captured. Later, dynamic load testing was completed with the vehicles traveling at approximately 15 mph (maximum safe speed at the site).

Sample Field Results

Representative plots from static load testing showing the strain experienced by one of the girders under all test vehicles is shown in Figure C-5. It was observed that the girders at the center of the bridge experienced the maximum strain magnitudes as the test vehicles crossed the bridge.

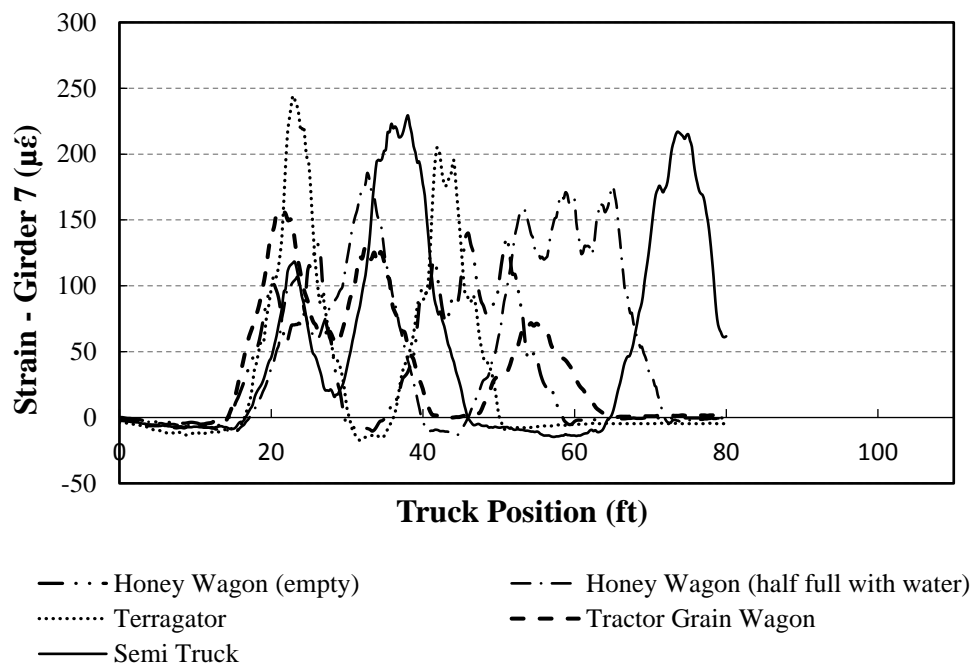


Figure C-5. Strain plot of a girder for all test vehicles for Timber-Timber Bridge 1

Although the semi-truck normally results in higher strains compared to other farm vehicles, the terragator occasionally yields somewhat greater strains than the truck. This tendency can be seen in Figure C-5. These recorded strains were employed to calculate the field LLDFs for each girder based upon the following equation.

$$LLDF^f = \frac{\epsilon^m \max_{i,t}}{\sum_{i=1}^n \epsilon^m \max_{i,t}} \quad (1)$$

Where $LLDF^f$ is the field live load distribution factor and ϵ^m are the measured maximum strains for individual girders over time, respectively.

A representative plot showing the comparison between static and dynamic strain for one of the girders under a test vehicle is shown in Figure C-6. It was generally observed that the girders experience more strain under dynamic loads than under static loading. The strain values from dynamic load tests were utilized to calculate the dynamic amplification factors (DAFs) for each girder.

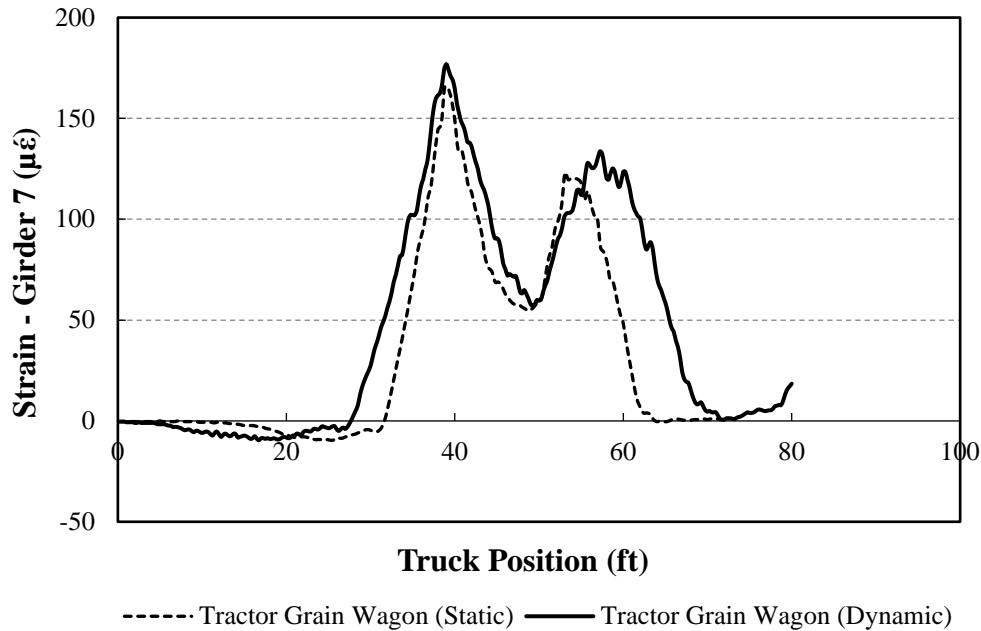


Figure C-6. Comparison between static and dynamic strain for Timber-Timber Bridge 1

C.1.4 Analytical Modeling

In lieu of field testing with a large number of vehicles, finite element analysis (FEA) simulations were used to estimate LLDFs for other vehicle configurations. As a result, analytical LLDFs were determined based upon FEA simulations of over 121 different farm vehicles on Timber-Timber Bridge 1. The FEA model was developed as described subsequently, and specific bridge information is presented in the following sections.

Model Generation

The bridge was initially modeled with the geometric and material properties taken directly from available bridge plans and/or field inspections using the BDI (Bridge Diagnostics, Inc.) finite element software WinGEN. A modulus of elasticity of 1600 ksi was used for all timber components in the model. The FEA model consisted of beam elements for the girders, shell elements for the deck, and rotational springs that simulated rotational restraint at the abutments and piers. Figure C-7 shows a representative model of the bridge.

Model Calibration

To improve the model accuracy, a calibration process that identified the bridge properties that resulted in the lowest error was completed. Based upon similarities in the response and observed field condition, it was assumed that the girders could be grouped into four groups, where within each group the girders had the same properties: (1) G2 and G16, (2) G6 and G7, (3) G11, and (4) G1, G3, G4, G5, G8, G9, G10, G13, G14, G15, and G17. Also note that a very low field and analytical strain was observed for G12, and the response at this location was not considered during model calibration. Table C-2 summarizes the original and calibrated values for the various bridge components along with percent error and correlation coefficient values. The moderately high percent error is most likely due to the highly variable material properties associated with timber components.

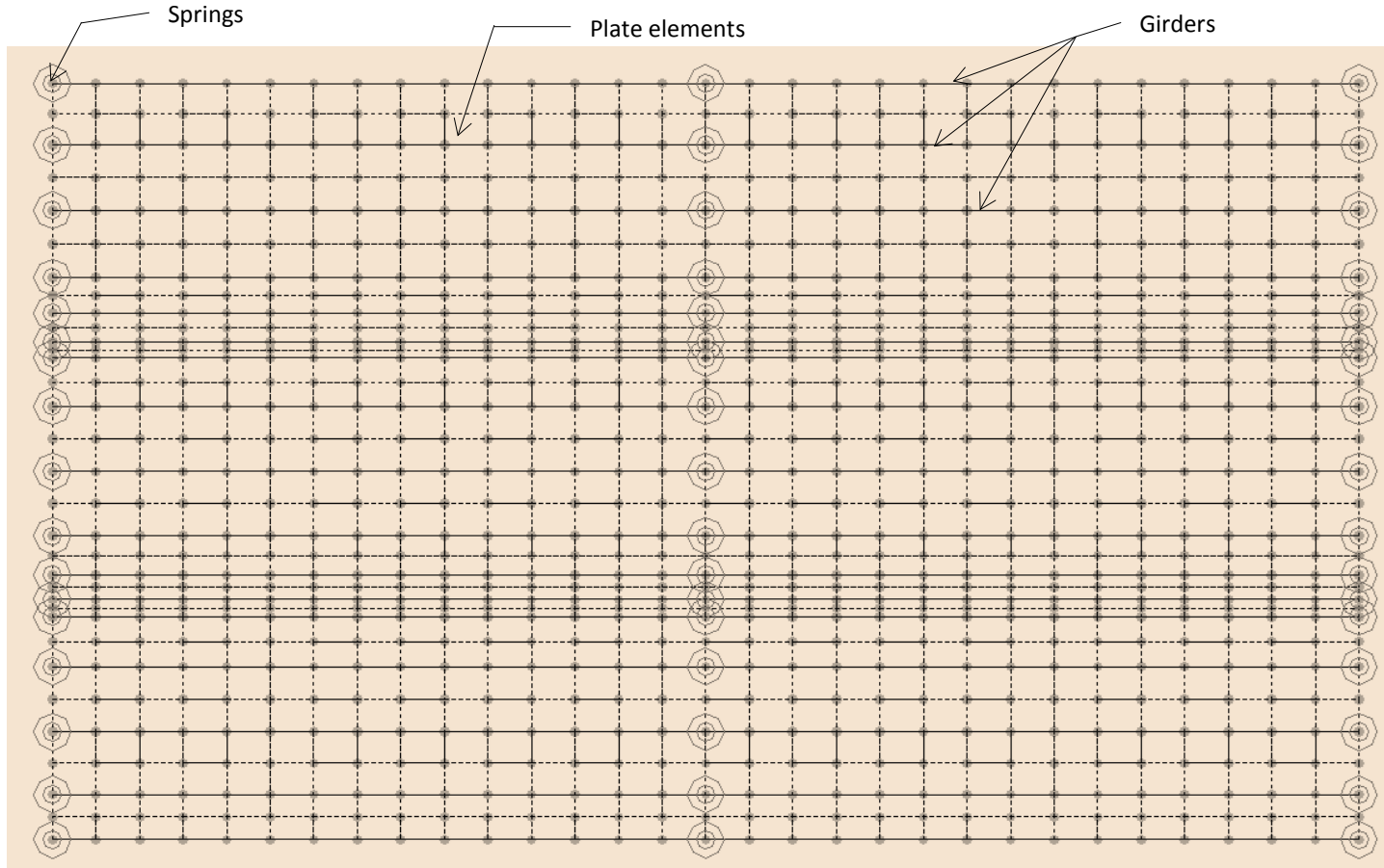


Figure C-7. Finite element model of Timber-Timber Bridge 1

Table C-2. Model calibration for Timber-Timber Bridge 1

Calibration Parameters	Bridge Components	Plan Value	Calibrated Value
Moment of Inertia, I (in ⁴)	Girder 2,16	1365	1207
	Girders 6,7		1184
	Girder 11		960.8
	Other Girders		1699
Modulus of Elasticity, E (Ksi)	Deck	1600	1201
Rotational Stiffness, kr (Kips-in/rad)	Support Connections (springs)	0	36288
Statistical Results	Percent Error		17.12%
	Correlation Coefficients		0.92

Once model calibration was completed, the analytical model was loaded with 121 farm vehicles covering a wide range of axle spacings, weights, and gage widths. The analytical strain response was then used to compute analytical LLDFs for each simulation vehicle using Equation (1).

To interpret the results efficiently, the LLDFs of the girders were grouped together as either interior or exterior girder LLDFs. Statistical limits for the interior and exterior girder LLDFs were determined from cumulative distribution function (CDF) curves defined to be at the 95% confidence thresholds.

C.1.5 Results

The envelopes of LLDFs for Timber-Timber Bridge 1 are presented in Figure C-8 for both the field and analytical LLDFs for each girder. In addition to the envelopes, the AASHTO LLDFs and statistical control limits for each group of interior and exterior girders are also shown.

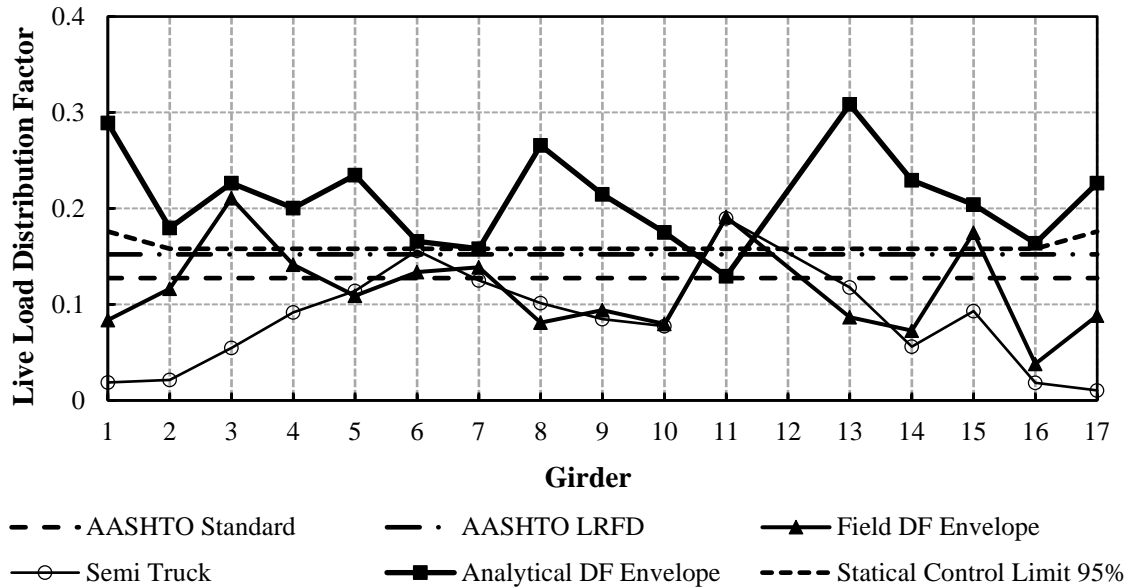


Figure C-8. LLDFs for Timber-Timber Bridge 1

It appears that the analytical LLDF envelope for most girders is larger than those from the AASHTO standard and LRFD specifications. The peak value of the analytical exterior girder LLDFs was observed in G1, which has an LLDF of 0.29, while that of the interior girders was found in G13, which has an LLDF of 0.31. The field LLDF envelope represents the highest LLDF observed in each girder due to field testing using farm vehicles, whereas the semi-truck envelope represents the extreme LLDFs for field testing using a five-axle semi-truck. The field LLDF envelope has larger values than that for the semi-truck for most of the girders, indicating for this bridge that farm vehicles result in higher values of LLDFs compared to those from the conventional highway vehicle. The statistical limits for either the interior or exterior girder group also show larger values than the AASHTO specifications.

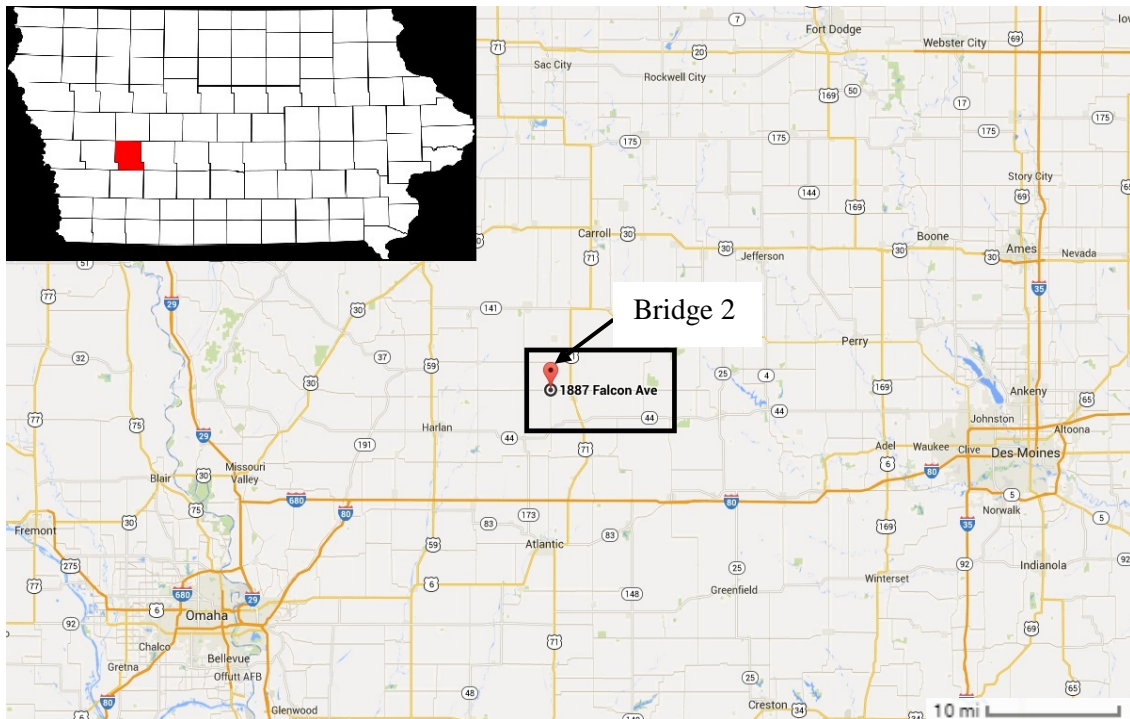
C.2 Timber-Timber Bridge 2

This mini test and evaluation report documents the results of field testing and subsequent analysis of a timber girder bridge with a timber deck (Timber-Timber Bridge 2) under multiple implements of husbandry. For completeness, this mini-report includes a description of the bridge, a description of the live load testing procedures followed, sample data, a description of analytical modeling, plots of analytical results, and a discussion of the overall behavior of the timber girder bridge under implements of husbandry.

C.2.1 Background

The timber-timber bridge described here is known in the National Bridge Inventory (NBI) database as Bridge 68800 and will be henceforth be referred to as Timber-Timber Bridge 2. The

bridge is located about 20 miles east of Prairie Rose State Park, on Falcon Avenue, in Audubon County, Iowa. Figure C-9 shows the general location of the bridge.



Map: ©Google 2014

Figure C-9. Location overview of Timber-Timber Bridge 2

C.2.2 Bridge Description

Timber-Timber Bridge 2 is open to two-lane traffic and has three spans with overall dimensions of 62 ft long by 20 ft wide with 25 degrees of skew. The deck is comprised of continuous timber decking with a thickness of 6 in. An elevation view and an end view of the bridge are shown in Figure C-10. The bridge consists of 27 timber girders with variable spacing between adjacent girders (varying from 6.6 in to 11.8 in.) The girders have a rectangular cross-section measuring approximately 16 in. by 4 in. Figure C-11 shows a typical cross-section and plan view of the bridge.



Figure C-10. Timber-Timber Bridge 2: West elevation view (left) and south end view (right)

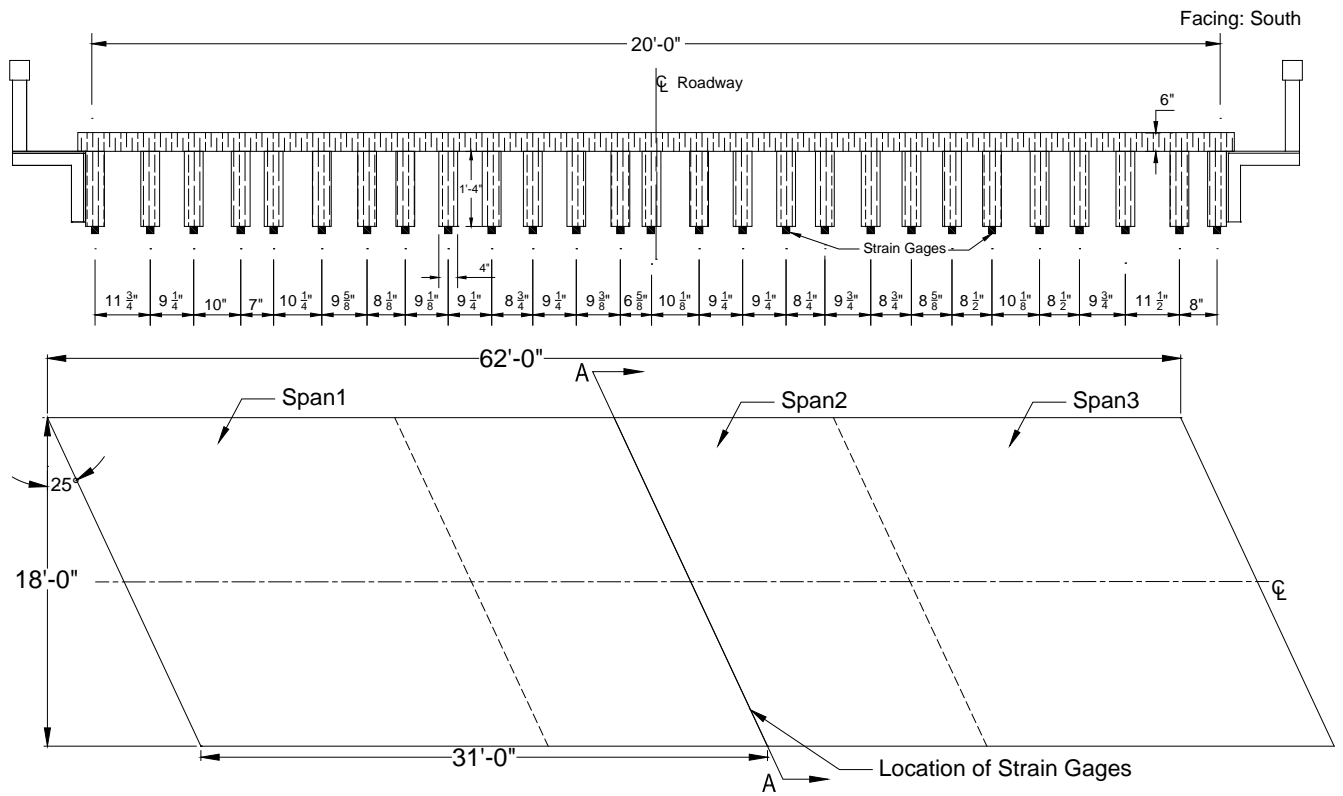


Figure C-11. Timber-Timber Bridge 2: Cross-section A-A (top) and plan (bottom)

C.2.3 Field Testing

Field testing of this bridge was conducted for two reasons. First, field testing was conducted to determine experimental live load distribution factors (LLDFs) and dynamic impact factors for the individual bridge girders. Second, these field data were also used to calibrate analytical

models, which were then used to conduct a detailed parametric study related to a wide variety of implements of husbandry. A description of field tests, the procedures followed, and sample field results are detailed in the following sections.

Field Inspections

According to the most recent field inspection report, the Timber-Timber Bridge 2 timber deck is in good condition with some minor problems. The timber girders are not in good condition and show obvious signs of normal wear, tear, and decay. The bridge piers are also not in a good condition, showing similar signs of deterioration. These inspection-based observations were corroborated by the Iowa State University field testing team, who observed cracking and deterioration in multiple timber girders.

Instrumentation Plan

Given that the primary goal of the testing plan was to measure the live load response of the primary load-carrying members, a network of multiple strain gages was used to measure the strain under the weight of the vehicles. The strain gages were attached to the bottom of the girders at mid-span of Span 2 as shown in Figure C-11. The strain sensors used to conduct this testing were installed with a 3 in. gage length, and data were collected at a rate of 20 Hz during static testing and at 20 Hz during dynamic testing.

Test Load Paths

The vehicles utilized during field testing of this bridge consisted of four common farm vehicles and one typical highway truck. The vehicles included a terragator, a grain cart, a honey wagon with one tank, a honey wagon with two tanks, and a typical five-axle semi-truck. The individual axle loads, total weights, and lengths of the five vehicles used for field testing are summarized in Table C-3. As shown in Figure C-12, the configurations of the farm vehicles were notably different from that of the conventional highway truck.

Table C-3. Axle weight and total length of each testing vehicle

Farm Vehicles	Weight (lbs)					Total	Total Length (ft-in.)
	Front Axle	Rear Axle	Grain Wagon	Honey Wagon	Trailer		
Tractor Honey Wagon (empty)	10,960	15,740	-	26,720	-	53,420	40'-4"
Tractor Honey Wagon (half full with water)	10,580	22,800	-	40,620	-	74,000	40'-4"
Terragator	23,380	17,840	-	-	-	41,220	19'-0"
Tractor Grain Wagon	24,480	19,700	11,980	-	-	56,160	31'-0"
Semi-Truck	10,760	33,856	-	-	33,084	77,700	52'-1"



Honey Wagon



Honey Wagon- two tanks



Terragator



Tractor Grain Wagon



Semi Truck

Figure C-12. Farm vehicles used for field testing

During testing, the vehicles were driven across the bridge from north to south. In general the centerlines of the bridge and vehicle were approximately aligned. Initial static load testing was completed with the vehicles traveling at approximately 3 mph such that the pseudo-static bridge response could be captured. Later, two sets of dynamic load testing was completed with the vehicles traveling at approximately 10 and 15 mph (maximum safe speed at the site) respectively.

Sample Field Results

Representative plots from static load testing showing the strain experienced by one of the girders under all test vehicles is shown in Figure C-13. It was observed that the girders at the center of the bridge experienced the maximum strain magnitudes as the test vehicles crossed the bridge.

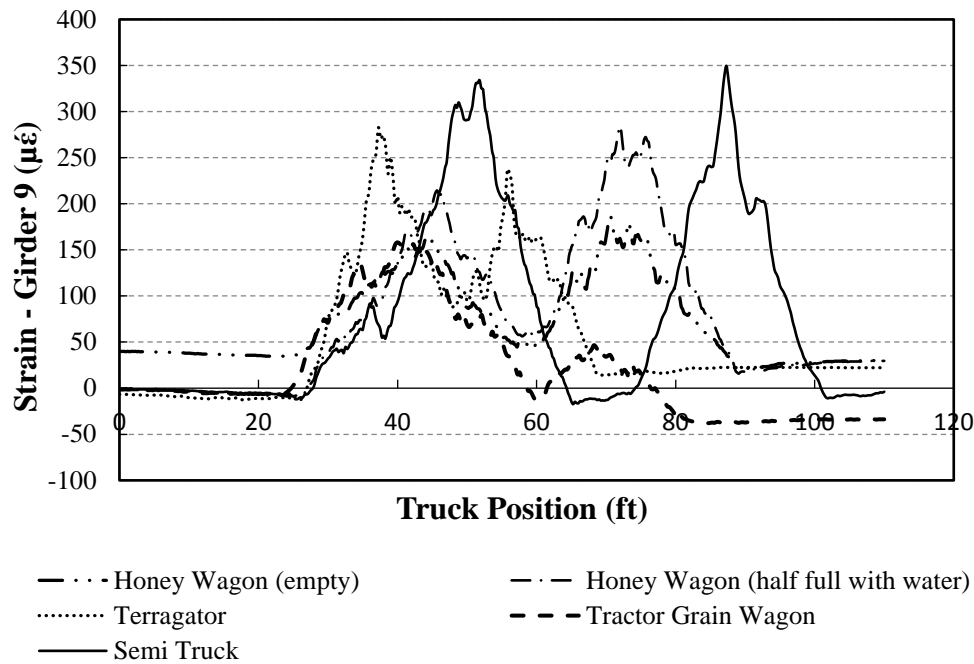


Figure C-13. Strain plot of a girder for all test vehicles for Timber-Timber Bridge 2

The semi-truck normally results in higher strains compared to other farm vehicles, and this tendency can be seen in Figure C-13. These recorded strains were employed to calculate the field LLDFs for each girder based upon the following equation.

$$LLDF^f = \frac{\epsilon^m \max i, t}{\sum_{i=1}^n \epsilon^m \max i, t} \quad (1)$$

Where $LLDF^f$ is the field live load distribution factor and ϵ^m are the measured maximum strains for individual girders over time, respectively.

A representative plot showing the comparison between static and dynamic strain for one of the girders under a test vehicle is shown in Figure C-14. It was generally observed that the girders experience more strain under dynamic loads than under static loading. The strain values from dynamic load tests were utilized to calculate the dynamic amplification factors (DAFs) for each girder.

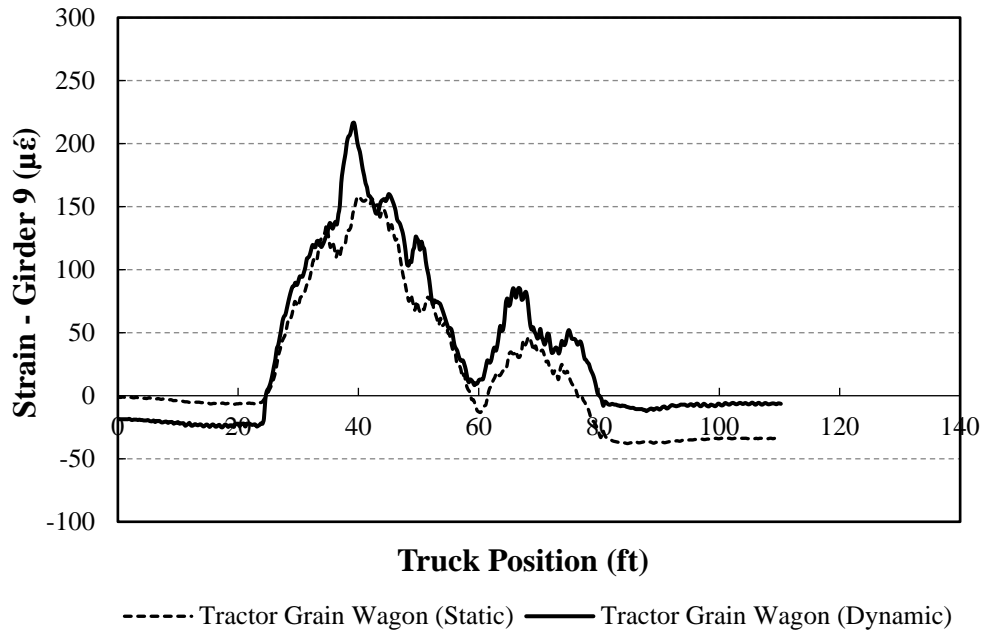


Figure C-14. Comparison between static and dynamic strain for Timber-Timber Bridge 2

C.2.4 Analytical Modeling

In lieu of field testing with a large number of vehicles, finite element analysis (FEA) simulations were used to estimate LLDFs for other vehicle configurations. As a result, analytical LLDFs were determined based upon FEA simulations of over 121 different farm vehicles on Timber-Timber Bridge 2. The FEA model was developed as described subsequently, and specific bridge information is presented in the following sections.

Model Generation

The bridge was initially modeled with the geometric and material properties taken directly from available bridge plans and/or field inspections using the BDI (Bridge Diagnostics, Inc.) finite element software WinGEN. A modulus of elasticity of 1600 ksi was used for all timber components in the model. The FEA model consisted of beam elements for the girders, shell elements for the deck, and rotational springs that simulated rotational restraint at the abutments and piers. Figure C-15 shows a representative model of the bridge.

Model Calibration

To improve the model accuracy, a calibration process that identified the bridge properties that resulted in the lowest error was completed. Based upon similarities in the response and observed field condition, a single cross-section was considered for all the girders. Table C-4 summarizes the original and calibrated values for the various bridge components along with percent error and correlation coefficient values. The moderately high percent error is most likely due to the highly variable material properties associated with timber components.

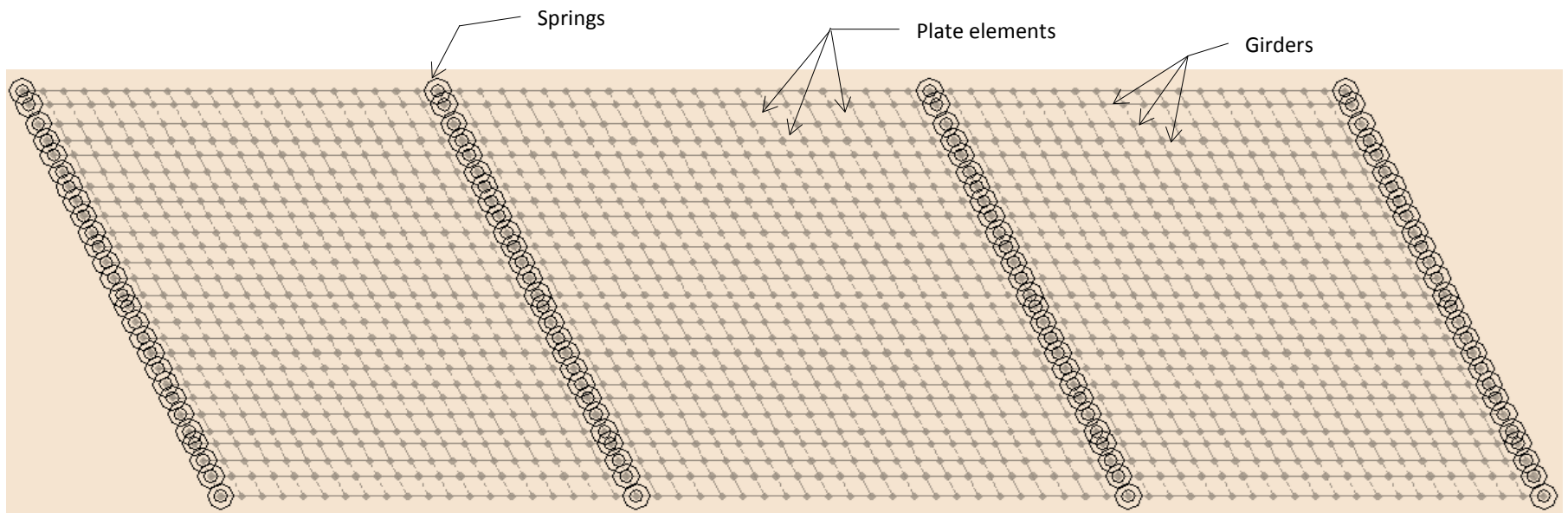


Figure C-15. Finite element model of Timber-Timber Bridge 2

Table C-4. Model calibration for Timber-Timber Bridge 2

Calibration Parameters	Bridge Components	Plan Value	Calibrated Value
Moment of Inertia, I (in ⁴)	All Girders	1365	1081
Modulus of Elasticity, E (Ksi)	Deck	1600	1200
Rotational Stiffness, kr (Kips-in/rad)	Support Connections (springs)	0	69036
Statistical Results	Percent Error		21.90%
	Correlation Coefficients		0.88

Once model calibration was completed, the analytical model was loaded with 121 farm vehicles covering a wide range of axle spacings, weights, and gage widths. The analytical strain response was then used to compute analytical LLDFs for each simulation vehicle using Equation (1).

To interpret the results efficiently, the LLDFs of the girders were grouped together as either interior or exterior girder LLDFs. Statistical limits for the interior and exterior girder LLDFs were determined from cumulative distribution function (CDF) curves defined to be at the 95% confidence thresholds.

C.2.5 Results

The envelopes of LLDFs for Timber-Timber Bridge 2 are presented in Figure C-16 for both the field and analytical LLDFs for each girder. In addition to the envelopes, the AASHTO LLDFs and statistical control limits for each group of interior and exterior girders are also shown.

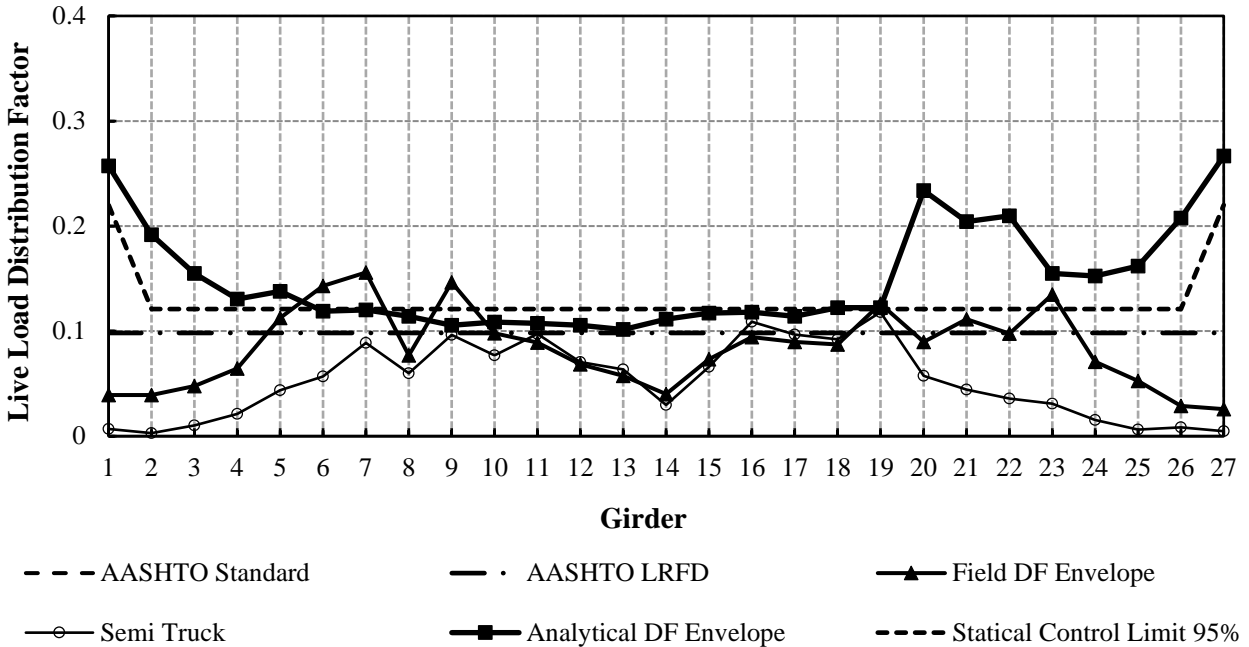


Figure C-16. LLDFs for Timber-Timber Bridge 2

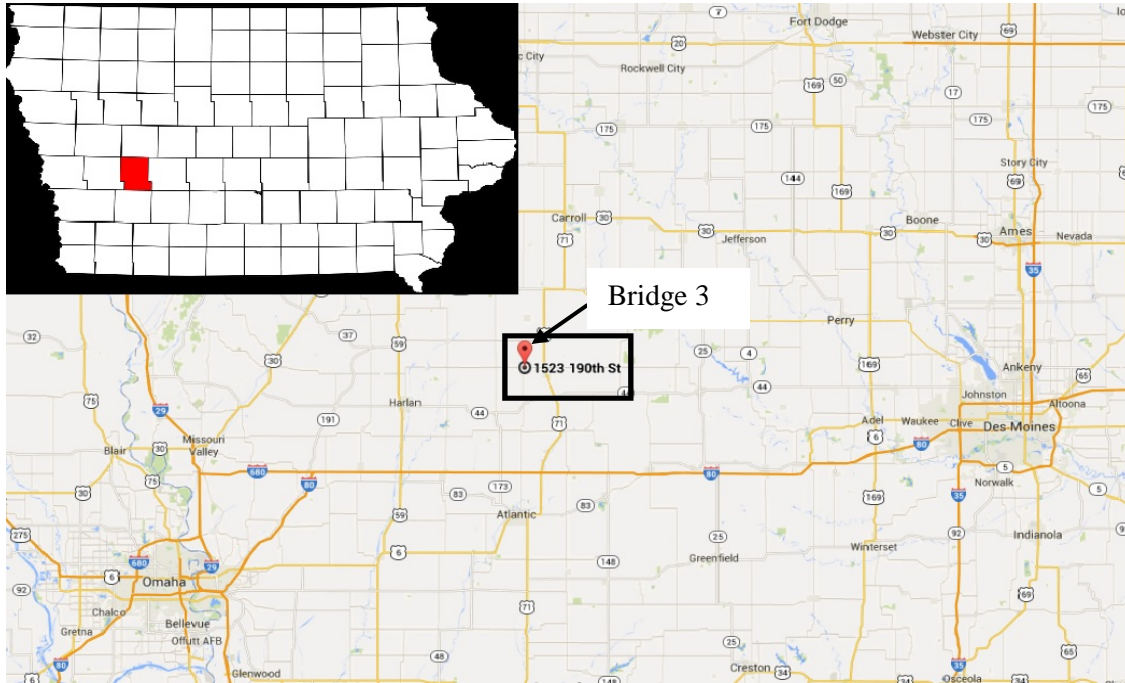
Because Timber-Timber Bridge 2 is a two-lane traffic bridge, it has the same value for LLDF as that in the AASHTO standard and LRFD specifications. It appears that the analytical LLDF envelope for all the girders is larger than those from the AASHTO values. The peak value of the analytical exterior girder LLDFs was observed in G27, which has an LLDF of 0.27, while that of the interior girders was found in G20, which has an LLDF of 0.23. The field LLDF envelope represents the highest LLDF observed in each girder due to field testing using farm vehicles, whereas the semi-truck envelope represents the extreme LLDFs for field testing using a five-axle semi-truck. The field LLDF envelope has larger values than that for the semi-truck for most of the girders, indicating for this bridge that farm vehicles result in higher values of LLDFs compared to those from the conventional highway vehicle. The statistical limits for either the interior or exterior girder group also show larger values than the AASHTO specifications.

C.3 Timber-Timber Bridge 3

This mini test and evaluation report documents the results of field testing and subsequent analysis of a timber girder bridge with a timber deck (Timber-Timber Bridge 3) under multiple implements of husbandry. For completeness, this mini-report includes a description of the bridge, a description of the live load testing procedures followed, sample data, a description of analytical modeling, plots of analytical results, and a discussion of the overall behavior of the timber girder bridge under implements of husbandry.

C.3.1 Background

The timber-timber bridge described here is known in the National Bridge Inventory (NBI) database as Bridge 68930 and will be henceforth be referred to as Timber-Timber Bridge 3. The bridge is located about 20 miles east of Prairie Rose State Park, on 190th Street, in Audubon County, Iowa. Figure C-17 shows the general location of the bridge.



Map: ©Google 2014

Figure C-17. Location overview of Timber-Timber Bridge 3

C.3.2 Bridge Description

Timber-Timber Bridge 3 is open to one-lane traffic and has two spans with overall dimensions of 61 ft long by 18 ft wide with 30 degrees of skew. The deck is comprised of continuous timber decking with a thickness of 3 in. An elevation view and an end view of the bridge are shown in Figure C-18. The bridge consists of 18 timber girders with variable spacing between adjacent girders (varying from 3.0 in to 12.0 in.) The girders have a rectangular cross-section measuring approximately 16 in. by 6 in. Figure C-19 shows a typical cross-section and plan view of the bridge.



Figure C-18. Timber-Timber Bridge 3: Elevation view (left) and east end view (right)

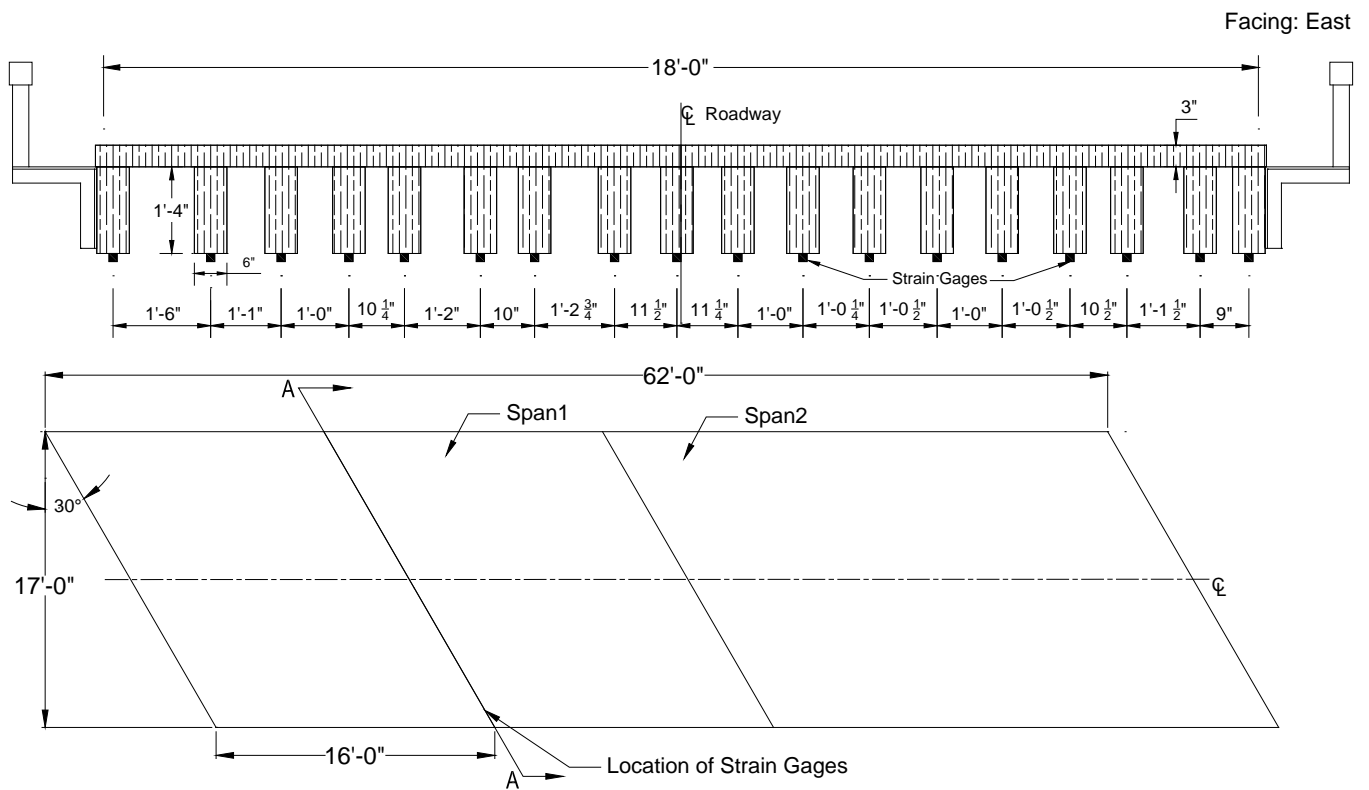


Figure C-19. Timber-Timber Bridge 3: Cross-section A-A (top) and plan (bottom)

C.3.3 Field Testing

Field testing of this bridge was conducted for two reasons. First, field testing was conducted to determine experimental live load distribution factors (LLDFs) and dynamic impact factors for the individual bridge girders. Second, these field data were also used to calibrate analytical models, which were then used to conduct a detailed parametric study related to a wide variety of

implements of husbandry. A description of field tests, the procedures followed, and sample field results are detailed in the following sections.

Field Inspections

According to the most recent field inspection report, the Timber-Timber Bridge 3 timber deck is in satisfactory condition with minor deterioration. The timber girders are not in good condition and show obvious signs of normal wear, tear, and decay. The bridge piers are also not in a good condition, showing similar signs of deterioration. These inspection-based observations were corroborated by the Iowa State University field testing team, who observed cracking and deterioration in multiple timber girders.

Instrumentation Plan

Given that the primary goal of the testing plan was to measure the live load response of the primary load-carrying members, a network of multiple strain gages was used to measure the strain under the weight of the vehicles. The strain gages were attached to the bottom of the girders at mid-span of Span 1 as shown in Figure C-19. The strain sensors used to conduct this testing were installed with a 3 in. gage length, and data were collected at a rate of 100 Hz during static testing and at 100 Hz during dynamic testing.

Test Load Paths

The vehicles utilized during field testing of this bridge consisted of four common farm vehicles and one typical highway truck. The vehicles included a terragator, a grain cart, a honey wagon with one tank, a honey wagon with two tanks, and a typical five-axle semi-truck. The individual axle loads, total weights, and lengths of the five vehicles used for field testing are summarized in Table C-5. As shown in Figure C-20, the configurations of the farm vehicles were notably different from that of the conventional highway truck.

Table C-5. Axle weight and total length of each testing vehicle

Farm Vehicles	Weight (lbs)					Total	Total Length (ft-in.)
	Front Axle	Rear Axle	Grain Wagon	Honey Wagon	Trailer		
Tractor Honey Wagon (empty)	10,960	15,740	-	26,720	-	53,420	40'-4"
Tractor Honey Wagon (half full with water)	10,580	22,800	-	40,620	-	74,000	40'-4"
Terragator	23,380	17,840	-	-	-	41,220	19'-0"
Tractor Grain Wagon	24,480	19,700	11,980	-	-	56,160	31'-0"
Semi-Truck	10,760	33,856	-	-	33,084	77,700	52'-1"



Honey Wagon



Honey Wagon- two tanks



Terragator



Tractor Grain Wagon



Semi Truck

Figure C-20. Farm vehicles used for field testing

During testing, the vehicles were driven across the bridge from west to east. In general the centerlines of the bridge and vehicle were approximately aligned. Initial static load testing was completed with the vehicles traveling at approximately 3 mph such that the pseudo-static bridge response could be captured. Later, two sets of dynamic load testing was completed with the vehicles traveling at approximately 10 and 15 mph (maximum safe speed at the site) respectively.

Sample Field Results

Representative plots from static load testing showing the strain experienced by one of the girders under all test vehicles is shown in Figure C-21. It was observed that the girders at the center of the bridge experienced the maximum strain magnitudes as the test vehicles crossed the bridge.

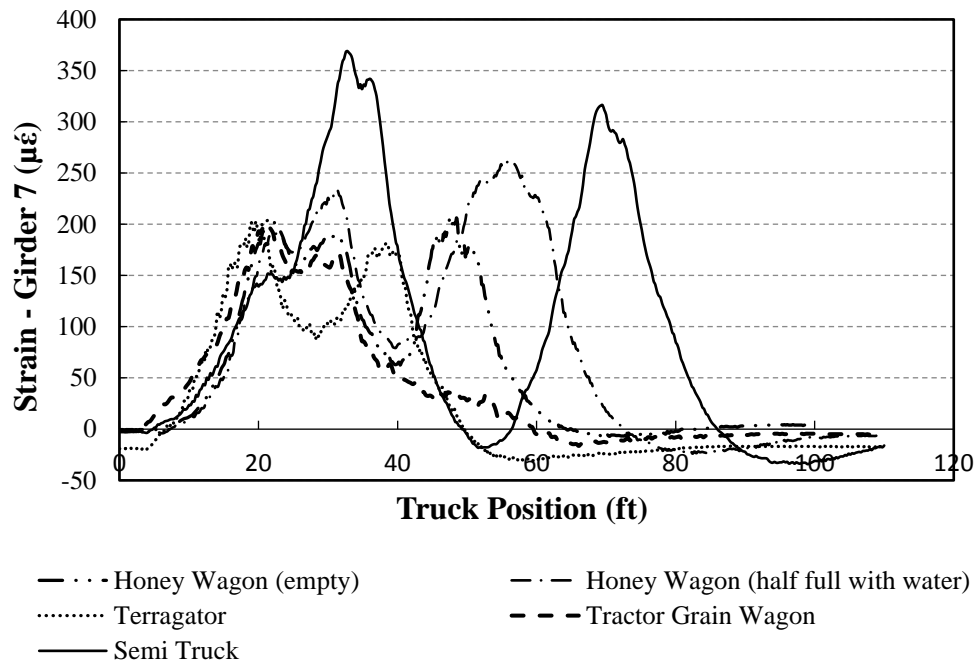


Figure C-21. Strain plot of a girder for all test vehicles for Timber-Timber Bridge 3

The semi-truck normally results in higher strains compared to other farm vehicles, and this tendency can be seen in Figure C-21. These recorded strains were employed to calculate the field LLDFs for each girder based upon the following equation.

$$LLDF^f = \frac{\epsilon^m \max i, t}{\sum_{i=1}^n \epsilon^m \max i, t} \quad (1)$$

Where $LLDF^f$ is the field live load distribution factor and ϵ^m are the measured maximum strains for individual girders over time, respectively.

A representative plot showing the comparison between static and dynamic strain for one of the girders under a test vehicle is shown in Figure C-22. It was generally observed that the girders experience more strain under dynamic loads than under static loading. The strain values from dynamic load tests were utilized to calculate the dynamic amplification factors (DAFs) for each girder.

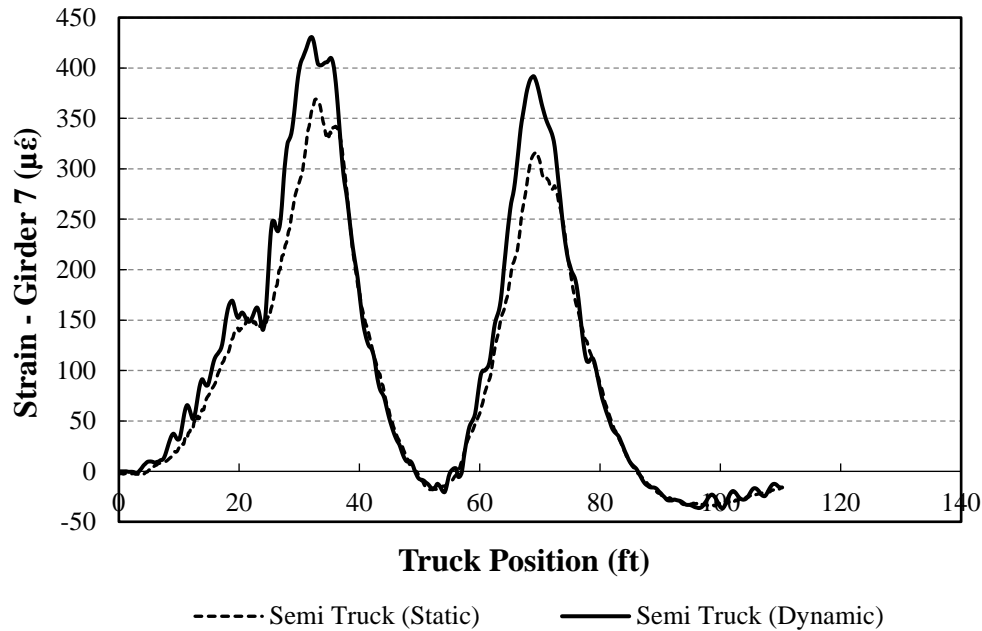


Figure C-22. Comparison between static and dynamic strain for Timber-Timber Bridge 3

C.3.4 Analytical Modeling

In lieu of field testing with a large number of vehicles, finite element analysis (FEA) simulations were used to estimate LLDFs for other vehicle configurations. As a result, analytical LLDFs were determined based upon FEA simulations of over 121 different farm vehicles on Timber-Timber Bridge 3. The FEA model was developed as described subsequently, and specific bridge information is presented in the following sections.

Model Generation

The bridge was initially modeled with the geometric and material properties taken directly from available bridge plans and/or field inspections using the BDI (Bridge Diagnostics, Inc.) finite element software WinGEN. A modulus of elasticity of 1600 ksi was used for all timber components in the model. The FEA model consisted of beam elements for the girders, shell elements for the deck, and rotational springs that simulated rotational restraint at the abutments and piers. Figure C-23 shows a representative model of the bridge.

Model Calibration

To improve the model accuracy, a calibration process that identified the bridge properties that resulted in the lowest error was completed. Based upon similarities in the response and observed field condition, a single cross-section was considered for all the girders. Table C-6 summarizes the original and calibrated values for the various bridge components along with percent error and correlation coefficient values. The moderately high percent error is most likely due to the highly variable material properties associated with timber components.

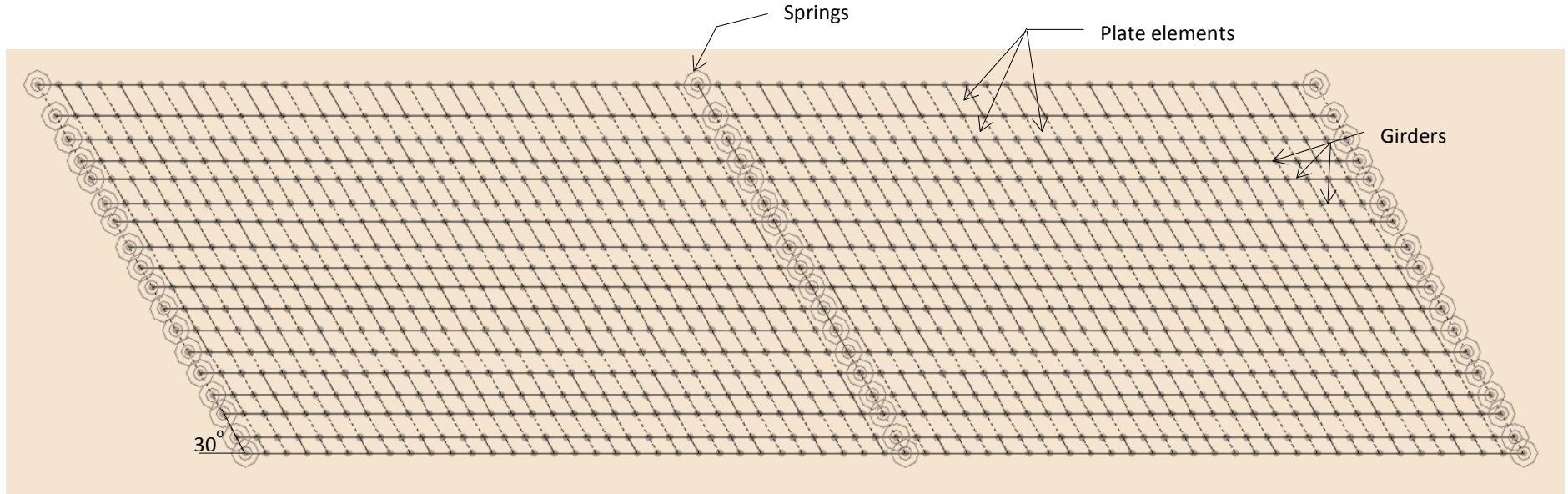


Figure C-23. Finite element model of Timber-Timber Bridge 3

Table C-6. Model calibration for Timber-Timber Bridge 3

Calibration Parameters	Bridge Components	Plan Value	Calibrated Value
Moment of Inertia, I (in ⁴)	All Girders	2048	1850
Modulus of Elasticity, E (Ksi)	Deck	1600	1200
Rotational Stiffness, kr (Kips-in/rad)	Support Connections (springs)	0	15931
Statistical Results	Percent Error		23.80%
	Correlation Coefficients		0.86

Once model calibration was completed, the analytical model was loaded with 121 farm vehicles covering a wide range of axle spacings, weights, and gage widths. The analytical strain response was then used to compute analytical LLDFs for each simulation vehicle using Equation (1).

To interpret the results efficiently, the LLDFs of the girders were grouped together as either interior or exterior girder LLDFs. Statistical limits for the interior and exterior girder LLDFs were determined from cumulative distribution function (CDF) curves defined to be at the 95% confidence thresholds.

C.3.5 Results

The envelopes of LLDFs for Timber-Timber Bridge 3 are presented in Figure C-24 for both the field and analytical LLDFs for each girder. In addition to the envelopes, the AASHTO LLDFs and statistical control limits for each group of interior and exterior girders are also shown.

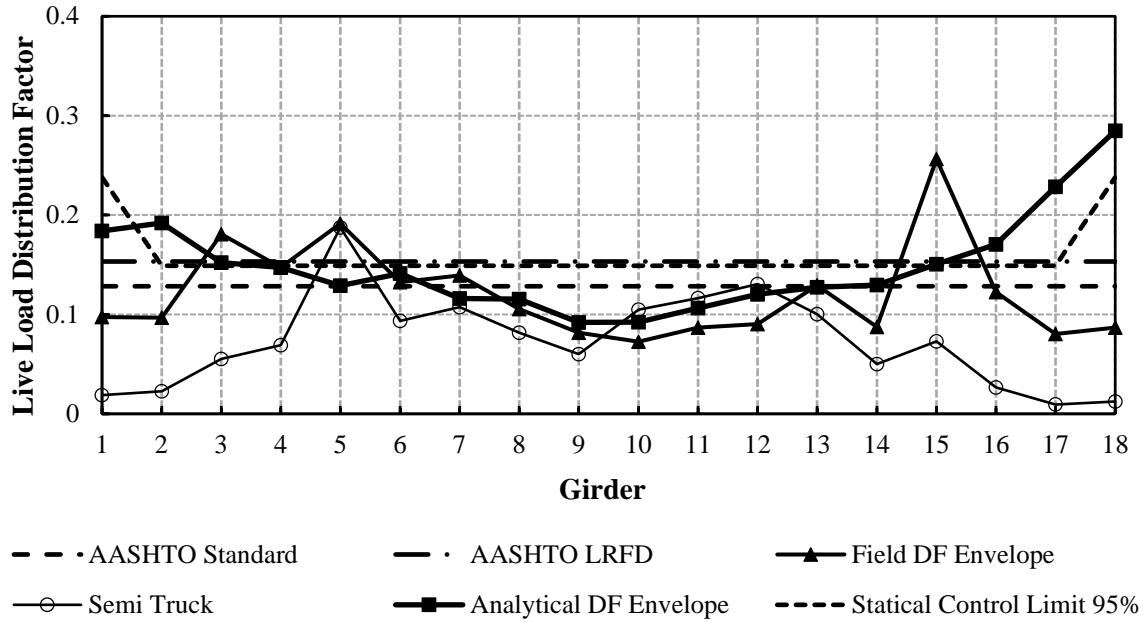


Figure C-24. LLDFs for Timber-Timber Bridge 3

It appears that the analytical LLDF envelope for most girders is larger than those from the AASHTO standard and LRFD specifications. The peak value of the analytical exterior girder LLDFs was observed in G18, which has an LLDF of 0.28, while that of the interior girders was found in G17, which has an LLDF of 0.23. The field LLDF envelope represents the highest LLDF observed in each girder due to field testing using farm vehicles, whereas the semi-truck envelope represents the extreme LLDFs for field testing using a five-axle semi-truck. The field LLDF envelope has larger values than that for the semi-truck for most of the girders, indicating for this bridge that farm vehicles result in higher values of LLDFs compared to those from the conventional highway vehicle. The statistical limits for either the interior or exterior girder group also show larger values than the AASHTO specifications.

APPENDIX D. FARM IMPLEMENT INVENTORY

This farm vehicle inventory includes 121 farm vehicles and implements that were used in this study. Through internet searches and manufacturer inquiries, information regarding axle weights and configurations was gathered for 121 farm vehicles and implements. These combinations encompassed most combinations seen on US secondary roadway bridges.

The table below summarizes the characteristics of the farm vehicle inventory. The table classifies each vehicle as grain cart or tanker or agricultural truck depending on the use. It also includes the number of axles, axle spacing, and weight of each axle and the spacing between consecutive axles. This information was used to model the vehicular input loads on the finite element models.

Table D-1. Farm vehicle inventory

		1	2	3	4	5	6	1	2	3	4	5	6	1	2	3	4	5
1	Grain Semi	Semi Trailer	4	6.1	6.1	6.1		17300	17460	16600	16720			4.0	4.0	4.0		
2	John Deere 8520 & Kinze 1050 ROW	Grain Cart	3	7.0	7.0	7.0		11525	11525	73381				9.9	23.9			
3	John Deere 8520 & Houle 3-axle Tank	Manure Tanker	5	7.0	7.0	7.0	7.0	11525	11525	26600	26600	26600		9.9	14.8	5.7	5.7	
4	John Deere 8520 & Houle 2-axle Tank	Manure Tanker	4	7.0	7.0	7.0		11525	11525	31290	31290			9.9	17.5	5.7		
5	New Holland TD5050 & Houle 3-axle Tank	Manure Tanker	5	6.6	6.6	7.0	7.0	8070	8070	26600	26600	26600		7.7	15.0	5.7	5.7	
6	New Holland TD5050 & Houle 2-axle Tank	Manure Tanker	4	6.6	6.6	7.0	7.0	8070	8070	31290	31290			7.7	18.0	5.7		
7	New Holland TD5050 & Kinze 1050 ROW	Grain Cart	3	6.6	6.6	7.0		8070	8070	73381				7.7	24.6			
8	New Holland T4040 & Houle 3-axle Tank		5	5.1	5.1	7.0	7.0	6724	6724	26600	26600	26600		7.2	15.0	5.7	5.7	
9	New Holland T4040 & Houle 2-axle Tank		4	5.1	5.1	7.0	7.0	6724	6724	31290	31290			7.2	18.0	5.7		
10	New Holland T4040 & Kinze 1050 Row		3	5.1	5.1	7.0		6724	6724	73381				7.2	24.6			
11	John Deere 8520 & Balzer 6350 Narrow	Manure Tanker	4	7.0	7.0	7.3	7.3	11525	11525	36183	36183			9.9	24.3	5.6		
12	New Holland TD5050 & Balzer 6350 Narrow	Manure Tanker	4	6.6	6.6	7.3	7.3	8070	8070	36183	36183			7.7	24.5	5.6		
13	New Holland T4040 & Balzer 6350 Narrow		4	5.1	5.1	7.3	7.3	6724	6724	36183	36183			7.2	24.5	5.6		
14	Terragator 8400	Agricultural Truck	2	7.0	7.5			9338	10758					16.8				
15	John Deere 8520 with Brent 1082 Grain Wagon		3	7.0	7.0	7.8		11525	11525	15660				9.9	23.9			
16	New Holland TD5050 with Grain Wagon	Agricultural Truck	3	6.6	6.6	7.8		8070	8070	15660				7.7	23.9			
17	New Holland T4040 with Grain Wagon		3	5.1	5.1	7.8		6724	6724	15660				7.2	23.9			
18	John Deere 8520 & Better-Bilt 3400	Manure Tanker	4	7.0	7.0	7.9	7.9	11525	11525	18421	18421			9.9	22.7	4.1		
19	New Holland TD5050 & Better-Bilt 3400	Manure Tanker	4	6.6	6.6	7.9	7.9	8070	8070	18421	18421			7.7	23.0	4.1		
20	New Holland T4040 & Better-Bilt 3400		4	5.1	5.1	7.9	7.9	6724	6724	18421	18421			7.2	23.0	4.1		
21	Terragator 7300	Agricultural Truck	2	0.0	8.0			9338	10758					22.8				
22	John Deere 8520 & Kinze 1050 SOF	Grain Cart	3	7.0	7.0	8.0		11525	11525	72101				9.9	23.9			
23	John Deere 8520 & Better-Bilt 4950	Manure Tanker	4	7.0	7.0	8.0	8.0	11525	11525	27252	27252			9.9	25.3	4.4		
24	New Holland TD5050 & Better-Bilt 4950	Manure Tanker	4	6.6	6.6	8.0	8.0	8070	8070	27252	27252			7.7	25.5	4.4		
25	New Holland TD5050 & Kinze 1050 SOF	Grain Cart	3	6.6	6.6	8.0		8070	8070	72101				7.7	24.6			
26	New Holland T4040 & Better-Bilt 4950		4	5.1	5.1	8.0	8.0	6724	6724	27252	27252			7.2	25.5	4.4		
27	Hew Holland T4040 & Kinze 1050 SOF		3	5.1	5.1	8.0		6724	6724	72101				7.2	24.6			
28	Terragator 2505	Agricultural Truck	3	0.0	8.0	8.0		11060	16200	16200				19.2	6.4			
29	Versatile 280 & Kinze 1050 ROW	Grain Cart	3	8.0	8.0	7.0		11800	15900	73381				10.7	24.0			

			1	2	3	4	5	6	1	2	3	4	5	6	1	2	3	4	5
30	Versatile 280 & Kinze 1050 SOF	Grain Cart	3	8.0	8.0	8.0			11800	15900	72101				10.7	24.0			
31	Versatile 280 & Better-Bilt 4950	Manure Tanker	4	8.0	8.0	8.0	8.0		11800	15900	27252	27252			10.7	25.5	4.4		
32	Versatile 280 & Better-Bilt 3400	Manure Tanker	4	8.0	8.0	7.9	7.9		11800	15900	18421	18421			10.7	23.0	4.1		
33	Versatile 280 & Balzer 6350 Narrow	Manure Tanker	4	8.0	8.0	7.3	7.3		11800	15900	36183	36183			10.7	24.5	5.6		
34	Versatile 280 & Houle 3-axle Tank	Manure Tanker	5	8.0	8.0	7.0	7.0	7.0	11800	15900	26600	26600	26600		10.7	15.0	5.7	5.7	
35	Versatile 280 & Houle 2-axle Tank	Manure Tanker	4	8.0	8.0	7.0	7.0		11800	15900	31290	31290			10.7	18.0	5.7		
36	Versatile 280 with Half Full Houle 7300 Tank	Agricultural Truck	5	8.0	8.3	8.0	8.0	8.0	11800	15900	16267	16267	16267		10.7	18.4	5.8	5.8	
37	John Deere 8520 & Better-Bilt 6600	Manure Tanker	5	7.0	7.0	8.4	8.4	8.4	11525	11525	24826	24826	24826		9.9	23.6	5.2	5.2	
38	Versatile 280 & Better-Bilt 6600	Manure Tanker	5	8.0	8.0	8.4	8.4	8.4	11800	15900	24826	24826	24826		10.7	24.0	5.2	5.2	
39	New Holland TD5050 & Better-Bilt 6600	Manure Tanker	5	6.6	6.6	8.4	8.4	8.4	8070	8070	24826	24826	24826		7.7	24.0	5.2	5.2	
40	New Holland T4040 & Better-Bilt 6600		5	5.1	5.1	8.4	8.4	8.4	6724	6724	24826	24826	24826		7.2	24.0	5.2	5.2	
41	Case 340B		3	8.5	8.5	8.5			31614	16160	16160				13.7	6.8			
42	John Deere 9200 & Kinze 1050 ROW	Grain Cart	3	8.7	8.7	7.0			18840	18660	73381				11.3	24.0			
43	John Deere 9200 & Kinze 1050 SOF	Grain Cart	3	8.7	8.7	8.0			18840	18660	72101				11.3	24.0			
44	John Deere 9200 & Better-Bilt 6600	Manure Tanker	5	8.7	8.7	8.4	8.4	8.4	18840	18660	24826	24826	24826		11.3	24.0	5.2	5.2	
45	John Deere 9200 & Better-Bilt 4950	Manure Tanker	4	8.7	8.7	8.0	8.0		18840	18660	27252	27252			11.3	25.5	4.4		
46	John Deere 9200 & Better-Bilt 3400	Manure Tanker	4	8.7	8.7	7.9	7.9		18840	18660	18421	18421			11.3	23.0	4.1		
47	John Deere 9200 & Balzer 6350 Narrow	Manure Tanker	4	8.7	8.7	7.3	7.3		18840	18660	36183	36183			11.3	24.5	5.6		
48	John Deere 9200 & Houle 3-axle Tank	Manure Tanker	5	8.7	8.7	7.0	7.0	7.0	18840	18660	26600	26600	26600		11.3	15.0	5.7	5.7	
49	John Deere 9200 & Houle 2-axle Tank	Manure Tanker	4	8.7	8.7	7.0	7.0		18840	18660	31290	31290			11.3	18.0	5.7		
50	John Deere 9200 with Brent 1082 Grain Wagon	Agricultural Truck	3	8.7	8.7	7.8			18840	18660	15660				11.3	23.9			
51	Case 380 & Better-Bilt 6600	Manure Tanker	5	8.7	8.7	8.4	8.4	8.4	20240	16060	24826	24826	24826		12.9	24.0	5.2	5.2	
52	Case 380 & Better-Bilt 4950	Manure Tanker	4	8.7	8.7	8.0	8.0		20240	16060	27252	27252			12.9	25.5	4.4		
53	Case 380 & Better-Bilt 3400	Manure Tanker	4	8.7	8.7	7.9	7.9		20240	16060	18421	18421			12.9	23.0	4.1		
54	Case 380 & Balzer 6350 Narrow	Manure Tanker	4	8.7	8.7	7.3	7.3		20240	16060	36183	36183			12.9	24.5	5.6		
55	Case 380 & Houle 3-axle Tank	Manure Tanker	5	8.7	8.7	7.0	7.0	7.0	20240	16060	26600	26600	26600		12.9	15.0	5.7	5.7	
56	Case 380 & Houle 2-axle Tank	Manure Tanker	4	8.7	8.7	7.0	7.0		20240	16060	31290	31290			12.9	18.0	5.7		
57	Case 380 & Kinze 1050 ROW	Grain Cart	3	8.7	8.7	7.0			20240	16060	73381				12.9	24.6			
58	Case 380 & Kinze 1050 SOF	Grain Cart	3	8.7	8.7	8.0			20240	16060	72101				12.9	24.6			
59	Case 380 with Brent 1082 Grain Wagon		3	8.7	8.7	7.8			20240	20240	15660				12.9	23.9			
60	John Deere 8520 with 2 Empty NUHN QT Quad Tanks	Agricultural Truck	6	7.0	7.0	9.5	9.5	9.5	11525	11525	7150	7150	9150	9150	9.9	21.0	6.3	17.2	6.3
61	John Deere 9200 with 2 Empty NUHN QT Quad Tanks	Agricultural Truck	6	8.7	8.7	9.5	9.5	9.5	18840	18660	7150	7150	9150	9150	11.3	21.0	6.3	17.2	6.3
62	New Holland TD5050 with 2 Empty NUHN QT Quad Tanks		6	6.6	6.6	9.5	9.5	9.5	8070	8070	7150	7150	9150	9150	7.7	18.0	6.3	17.2	6.3
63	New Holland T4040 with 2 Empty NUHN QT Quad Tanks		6	5.1	5.1	9.5	9.5	9.5	6724	6724	7150	7150	9150	9150	7.2	18.0	6.3	17.2	6.3
64	Case 380 with 2 Empty NUHN QT Quad Tanks	Agricultural Truck	5	8.7	8.7	9.5	9.5	9.5	20240	16060	7150	7150	9150	9150	12.9	21.0	6.3	17.2	6.3
65	John Deere 9620 & Kinze 1050 ROW	Grain Cart	3	9.7	9.7	7.0			20175	20175	73381				11.5	24.6			
66	John Deere 9620 & Kinze 1050 SOF	Grain Cart	3	9.7	9.7	8.0			20175	20175	72101				11.5	24.6			
67	John Deere 9620 & Better-Bilt 6600	Manure Tanker	5	9.7	9.7	8.4	8.4	8.4	20175	20175	24826	24826	24826		11.5	24.3	5.2	5.2	
68	John Deere 9620 & Better-Bilt 4950	Manure Tanker	4	9.7	9.7	8.0	8.0		20175	20175	27252	27252			11.5	26.0	4.4		
69	John Deere 9620 & Better-Bilt 3400	Manure Tanker	4	9.7	9.7	7.9	7.9		20175	20175	18421	18421			11.5	23.4	4.1		
70	John Deere 9620 & Balzer 6350 Narro	Manure Tanker	4	9.7	9.7	7.3	7.3		20175	20175	36183	36183			11.5	25.0	5.6		
71	John Deere 9620 & Houle 3-axle Tank	Manure Tanker	5	9.7	9.7	7.0	7.0	7.0	20175	20175	26600	26600	26600		11.5	15.5	5.7	5.7	
72	John Deere 9620 & Houle 2-axle Tank	Manure Tanker	4	9.7	9.7	7.0	7.0		20175	20175	31290	31290			11.5	18.2	5.7		
73	John Deere 9620 with Brent 1082 Grain Wagon	Agricultural Truck	3	9.7	9.7	7.8			20175	20175	15660				11.5	23.9			
74	John Deere 9620 with 2 Empty NUHN QT Quad Tanks	Agricultural Truck	6	9.7	9.7	9.5	9.5	9.5	20175	20175	7150	7150	9150	9150	11.5	21.0	6.3	17.2	6.3

			1	2	3	4	5	6	1	2	3	4	5	6	1	2	3	4	5
75	John Deere 9620 & Balzer 1250	Grain Cart	4	9.7	9.7	10.0	10.0		20175	20175	43512	43512			11.5	21.9	6.5		
76	John Deere 9620 & Balzer 1500	Grain Cart	5	9.7	9.7	10.0	10.0	10.0	20175	20175	34443	34443	34443		11.5	18.6	6.5	6.5	
77	John Deere 8520 & Balzer 1250	Grain Cart	4	7.0	7.0	10.0	10.0		11525	11525	43512	43512			9.9	21.2	6.5		
78	John Deere 8520 & Balzer 1500	Grain Cart	5	7.0	7.0	10.0	10.0	10.0	11525	11525	34443	34443	34443		9.9	17.9	6.5	6.5	
79	John Deere 9200 & Balzer 1250	Grain Cart	4	8.7	8.7	10.0	10.0		18840	18660	43512	43512			11.3	21.5	6.5		
80	John Deere 9200 & Balzer 1500	Grain Cart	5	8.7	8.7	10.0	10.0	10.0	18840	18660	34443	34443	34443		11.3	18.0	6.5	6.5	
81	Versatile 280 & Balzer 1250	Grain Cart	4	8.0	8.0	10.0	10.0		11800	15900	43512	43512			10.7	21.5	6.5		
82	Versatile 280 & Balzer 1500	Grain Cart	5	8.0	8.0	10.0	10.0	10.0	11800	15900	34443	34443	34443		10.7	18.0	6.5	6.5	
83	Case 380 & Balzer 1250	Grain Cart	4	8.7	8.7	10.0	10.0		20240	16060	43512	43512			12.9	21.9	6.5		
84	Case 380 & Balzer 1500	Grain Cart	5	8.7	8.7	10.0	10.0	10.0	20240	16060	34443	34443	34443		12.9	18.6	6.5	6.5	
85	New Holland TD5050 & Balzer 1250	Grain Cart	4	6.6	6.6	10.0	10.0		8070	8070	43512	43512			7.7	21.9	6.5		
86	New Holland TD5050 & Balzer 1500	Grain Cart	5	6.6	6.6	10.0	10.0	10.0	8070	8070	34443	34443	34443		7.7	18.6	6.5	6.5	
87	New Holland T4040 & Balzer 1250		4	5.1	5.1	10.0	10.0		6724	6724	43512	43512			7.2	21.9	6.5		
88	New Holland T4040 & Balzer 1500		5	5.1	5.1	10.0	10.0	10.0	6724	6724	34443	34443	34443		7.2	18.6	6.5	6.5	
89	Case 600 with 2 Empty NUHN QT Quad Tanks		6	10.0	10.0	9.5	9.5	9.5	23000	23000	7150	7150	9150	9150	12.8	18.0	6.3	17.2	6.3
90	Case 600 with Grain Wagon		3	10.0	10.0	7.8			23000	23000	15660				12.8	23.9			
91	Case 600 & Better-Bilt 6600		5	10.0	10.0	8.4	8.4	8.4	23000	23000	24826	24826	24826		12.8	24.0	5.2	5.2	
92	Case 600 & Better-Bilt 4950		4	10.0	10.0	8.0	8.0		23000	23000	27252	27252			12.8	25.5	4.4		
93	Case 600 & Better-Bilt 3400		4	10.0	10.0	7.9	7.9		23000	23000	18421	18421			12.8	23.0	4.1		
94	Case 600 & Balzer 6350 Narrow		4	10.0	10.0	7.3	7.3		23000	23000	36183	36183			12.8	24.5	5.6		
95	Case 600 & Houle 3-axle Tank		5	10.0	10.0	7.0	7.0	7.0	23000	23000	26600	26600	26600		12.8	15.0	5.7	5.7	
96	Case 600 & Houle 2-axle Tank		4	10.0	10.0	7.0	7.0		23000	23000	31290	31290			12.8	18.0	5.7		
97	Case 600 & Kinze 1050 Row		3	10.0	10.0	7.0			23000	23000	73381				12.8	24.6			
98	Case 600 & Kinze 1050 SOF		3	10.0	10.0	8.0			23000	23000	72101				12.8	24.6			
99	Case 600 & Balzer 1250		4	10.0	10.0	10.0	10.0		23000	23000	43512	43512			12.8	21.9	6.5		
100	Case 600 & Balzer 1500		5	10.0	10.0	10.0	10.0	10.0	23000	23000	34443	34443	34443		12.8	18.6	6.5	6.5	
101	Versatile 535 with 2 Empty NUHN QT Quad Tanks		6	10.0	10.0	9.5	9.5	9.5	22500	22500	7150	7150	9150	9150	12.8	18.0	6.3	17.2	6.3
102	Versatile 535 with Grain Wagon		3	10.0	10.0	7.8			22500	22500	15660				12.8	23.9			
103	Versatile 535 & Better-Bilt 6600		5	10.0	10.0	8.4	8.4	8.4	22500	22500	24826	24826	24826		12.8	24.0	5.2	5.2	
104	Versatile 535 & Better-Bilt 4950		4	10.0	10.0	8.0	8.0		22500	22500	27252	27252			12.8	25.5	4.4		
105	Versatile 535 & Better-Bilt 3400		4	10.0	10.0	7.9	7.9		22500	22500	18421	18421			12.8	23.0	4.1		
106	Versatile 535 & Balzer 6350 Narrow		4	10.0	10.0	7.3	7.3		22500	22500	36183	36183			12.8	24.5	5.6		
107	Versatile 535 & Houle 3-axle Tank		5	10.0	10.0	7.0	7.0	7.0	22500	22500	26600	26600	26600		12.8	15.0	5.7	5.7	
108	Versatile 535 & Houle 2-axle Tank		4	10.0	10.0	7.0	7.0		22500	22500	31290	31290			12.8	18.0	5.7		
109	Versatile 535 & Kinze 1050 Row		3	10.0	10.0	7.0			22500	22500	73381				12.8	24.6			
110	Versatile 535 & Kinze 1050 SOF		3	10.0	10.0	8.0			22500	22500	72101				12.8	24.6			
111	Versatile 535 & Balzer 1250		4	10.0	10.0	10.0	10.0		22500	22500	43512	43512			12.8	21.9	6.5		
112	Versatile 535 & Balzer 1500		5	10.0	10.0	10.0	10.0	10.0	22500	22500	34443	34443	34443		12.8	18.6	6.5	6.5	
113	John Deere 9620 & J&M 1075-22	Grain Cart	3	9.7	9.7	12.2			20175	20175	68700				11.5	19.5			
114	John Deere 8520 & J&M 1075-22	Grain Cart	3	7.0	7.0	12.2			11525	11525	68700				9.9	18.8			
115	John Deere 9200 & J&M 1075-22	Grain Cart	3	8.7	8.7	12.2			18840	18660	68700				11.3	19.0			
116	Versatile 280 & J&M 1075-22	Grain Cart	3	8.0	8.0	12.2			11800	15900	68700				10.7	19.0			
117	Case 380 & J&M 1075-22	Grain Cart	3	8.7	8.7	12.2			20240	16060	68700				12.9	19.5			
118	New Holland TD5050 & J&M 1075-22	Grain Cart	3	6.6	6.6	12.2			8070	8070	68700				7.7	19.5			
119	New Holland T4040 & J&M 1075-22		3	5.1	5.1	12.2			6724	6724	68700				7.2	19.5			

	1	2	3	4	5	6	1	2	3	4	5	6	1	2	3	4	5
120 Case 600 & J&M 1075-22	3	10.0	10.0	12.2			23000	23000	68700				12.8	19.5			
121 Versatile 535 & J&M 1075-22	3	10.0	10.0	12.2			22500	22500	68700				12.8	19.5			

APPENDIX E. BRIDGE INVENTORY

The bridge inventory consists of data for a total of 174 bridges supplied by the participating states (Iowa, Oklahoma, and Wisconsin). Of these bridges, 151 had sufficient data for the parametric study in Volume I for the three bridge types:

1. Steel girder bridges with concrete deck (Steel-Concrete): Table E-1
2. Steel girder bridges with timber deck (Steel-Timber): Table E-2
3. Timber girder bridges with timber deck (Timber-Timber): Table E-3

Each bridge is classified as one of the following:

- One-lane traffic bridges (bridge width < 20 ft)
- Multiple-lane traffic bridges (bridge width \geq 20 ft)
- Skewed bridges (skew angle > 0 degrees)

The bridge characteristics used to create the finite element models are summarized in the following tables based on the classification above. The bridge number in these tables correspond to the results presented in the reports.

Span and rating information for all 174 bridges used in Volume II are listed in the following tables.

Table E-1a. One-way traffic lane steel-concrete bridges

Bridge No.	Total Bridge Length (ft)	Number of Spans	Maximum Span Length (ft)	Girder Spacing (ft)	Number of Girders	Bridge Width (ft)	Deck Thickness (in.)	Skew (deg)
1	30.0	1	29.0	2.0	10	17.8	7.5	7°
2	28.0	1	26.0	2.3	9	17.1	7.5	0°
3	34.0	1	32.0	2.3	8	16.0	7.5	0°
4	42.0	1	40.0	2.4	9	19.5	7.5	0°
5	53.0	1	50.0	6.4	4	19.7	7.5	0°

Table E-1b. Multiple traffic lane steel-concrete bridges

Bridge No.	Total Bridge Length (ft)	Number of Spans	Maximum Span Length (ft)	Girder Spacing (ft)	Number of Girders	Bridge Width (ft)	Deck Thickness (in.)	Skew (deg)
1	32.0	1	30.0	1.7	14	24.5	7.8	0°
2	37.0	1	34.0	2.0	16	30.7	7.5	0°
3	40.0	1	39.0	2.0	15	31.0	7.5	0°
4	39.0	1	37.0	2.4	11	24.5	7.0	0°
5	43.0	1	41.0	3.0	9	24.1	7.5	0°
6	43.0	1	42.0	3.5	8	24.5	6.5	0°
7	39.0	1	32.0	3.6	7	22.0	7.5	0°
8	43.0	1	43.0	3.9	9	31.3	6.5	0°
9	43.0	1	43.0	4.4	7	28.2	7.5	0°
10	160.0	3	80.0	4.6	6	23.4	4.6	0°
11	68.5	2	34.3	5.4	6	31.5	6.0	0°
12	68.0	1	66.0	5.8	5	23.6	5.8	0°
13	104.0	2	52.0	7.3	5	34.0	6.0	0°
14	62.0	2	31.0	7.5	4	26.0	6.5	0°
15	227.0	2	112.0	9.3	5	40.0	8.5	0°
16	293.0	4	93.5	9.3	4	30.0	8.6	0°
17	266.0	4	85.5	9.3	4	30.0	8.2	0°
18	292.0	4	93.5	9.3	4	30.0	7.8	0°
19	232.0	3	132.0	9.5	5	32.0	8.3	0°
20	83.0	1	80.0	9.5	3	20.1	7.0	0°
21	57.0	1	55.0	9.5	3	20.0	7.0	0°
22	236.0	4	79.0	9.7	4	32.0	8.8	6°
23	240.0	4	66.0	9.7	4	29.8	8.5	1°
24	316.0	4	94.0	10.0	4	32.0	8.5	2°

Table E-1c. Skewed steel-concrete bridges

Bridge No.	Total Bridge Length (ft)	Number of Spans	Maximum Span Length (ft)	Girder Spacing (ft)	Number of Girders	Bridge Width (ft)	Deck Thickness (in.)	Skew (deg)
1	59.0	1	59.0	1.8	14	22.7	7.5	45°
2	35.0	1	32.0	2.3	10	21.0	6.5	25°
3	32.0	1	28.0	2.5	9	20.3	9.5	45°
4	31.0	1	30.0	3.5	8	24.7	10.5	30°
5	44.0	1	40.0	3.9	10	35.8	7.5	30°
6	99.0	3	61.0	4.6	6	23.5	4.6	45°
7	57.0	1	50.0	5.5	6	28.0	7.5	23°
8	191.6	3	72.0	6.5	5	28.0	6.0	45°
9	85.0	3	42.0	6.7	4	23.5	5.3	45°
10	55.0	1	55.0	7.2	4	24.0	6.5	55°
11	57.0	1	55.0	7.4	4	24.0	7.5	30°
12	284.0	4	81.0	7.7	4	24.0	6.8	41°
13	324.0	4	92.0	8.0	4	24.0	7.5	47°
14	266.0	4	74.0	9.0	4	28.0	8.5	32°
15	325.0	4	104.0	9.3	4	30.0	8.5	26°
16	240.0	4	66.0	9.7	4	29.9	8.6	20°

Table E-2a. One-way traffic lane steel-timber bridges

Bridge No.	Total Bridge Length (ft)	Number of Spans	Maximum Span Length (ft)	Girder Spacing (ft)	Number of Girders	Bridge Width (ft)	Deck Thickness (in.)	Skew (deg)
1	20.0	1	19.0	1.5	11	16.3	4.0	0°
2	60.0	1	59.0	1.9	10	17.5	4.0	0°
3	24.0	1	23.0	2.3	9	18.0	4.0	0°
4	24.0	1	23.0	2.3	9	18.9	4.0	0°
5	30.0	1	29.0	2.3	9	19.4	4.0	0°
6	61.0	1	60.0	2.3	9	18.0	4.0	0°
7	62.0	1	60.0	2.3	9	18.0	4.0	0°
8	34.0	1	33.0	2.3	9	19.0	4.0	0°
9	63.0	1	61.0	2.3	9	18.6	4.0	0°
10	24.0	1	23.0	2.4	9	19.0	4.0	0°
11	60.0	1	59.0	2.4	9	19.3	4.0	0°
12	76.0	3	38.0	2.4	9	19.7	4.0	0°
13	177.0	3	58.5	2.5	7	16.0	3.0	0°
14	60.0	1	59.0	2.5	8	17.3	3.5	0°
15	26.0	1	24.0	2.5	9	18.0	4.0	0°
16	24.0	1	23.0	2.5	9	19.4	4.0	0°
17	62.0	1	60.0	2.5	9	19.7	4.0	0°
18	46.2	1	46.2	2.5	8	18.0	3.0	0°
19	59.0	1	58.0	2.6	7	16.2	3.4	0°
20	61.0	1	60.0	2.6	7	16.4	6.0	0°
21	62.0	2	46.0	2.8	8	18.7	4.0	0°
22	24.5	1	24.5	3.1	8	18.0	3.0	0°
23	42.5	1	42.5	5.0	4	15.0	6.0	0°

Table E-2b. Multiple traffic lane steel-timber bridges

Bridge No.	Total Bridge Length (ft)	Number of Spans	Maximum Span Length (ft)	Girder Spacing (ft)	Number of Girders	Bridge Width (ft)	Deck Thickness (in.)	Skew (deg)
1	59.0	1	59.2	1.5	17	23.3	2.8	0°
2	39.4	2	19.7	1.7	15	22.5	3.0	0°
3	29.5	1	29.5	1.7	13	20.3	3.0	0°
4	34.0	1	33.0	1.8	14	24.0	3.0	0°
5	30.0	1	29.0	2.0	11	20.0	3.0	0°
6	41.0	1	39.0	2.2	9	20.3	4.0	0°
7	25.0	1	24.0	2.3	9	20.0	4.0	0°
8	61.0	1	59.0	2.4	9	20.0	4.0	0°
9	35.0	1	33.0	2.5	13	31.0	6.0	0°
10	34.0	1	32.0	2.5	11	23.9	4.0	0°
11	32.0	1	31.0	2.5	9	20.5	6.0	0°
12	28.0	1	26.0	2.5	9	20.0	4.0	0°
13	56.0	2	31.3	2.6	10	24.8	4.0	0°
14	38.0	1	38.0	2.7	9	22.2	4.0	0°
15	52.0	1	51.0	2.8	8	20.0	4.0	0°
16	34.2	1	32.0	2.8	11	29.2	4.0	0°
17	75.7	2	42.0	3.2	7	23.7	4.0	0°
18	66.0	2	42.0	3.2	7	21.0	3.0	0°
19	102.0	3	34.0	3.5	8	24.0	3.0	0°
20	40.5	2	20.3	4.4	7	26.4	6.0	0°
21	49.0	1	49.0	4.5	6	23.0	6.0	0°

Table E-2c. Skewed steel-timber bridges

Bridge No.	Total Bridge Length (ft)	Number of Spans	Maximum Span Length (ft)	Girder Spacing (ft)	Number of Girders	Bridge Width (ft)	Deck Thickness (in.)	Skew (deg)
1	23.0	1	21.0	2.3	9	18.0	4.0	20
2	28.0	1	27.0	2.3	9	20.0	4.0	15
3	50.0	1	49.0	2.3	9	18.7	3.8	36
4	42.3	1	41.0	2.4	11	24.8	4.0	45
5	39.0	1	37.3	2.4	9	19.4	4.0	28
6	24.0	1	22.0	2.5	9	19.0	4.0	15
7	42.0	1	40.0	2.5	9	19.4	4.0	23
8	24.0	1	23.0	2.5	8	20.0	4.0	30
9	24.0	1	23.0	2.7	7	16.3	4.0	15
10	39.0	1	38.0	2.8	7	20.5	3.0	45

Table E-3a. One-way traffic lane timber-timber bridges

Bridge No.	Total Bridge Length (ft)	Number of Spans	Maximum Span Length (ft)	Girder Spacing (ft)	Number of Girders	Bridge Width (ft)	Deck Thickness (in.)	Skew (deg)
1	66.0	3	22.0	0.8	23	17.8	2.8	0°
2	38.0	2	19.0	0.9	22	18.9	3.0	0°
3	66.0	3	23.0	1.0	20	18.1	3.0	0°
4	63.0	3	21.0	1.0	19	17.6	3.0	0°
5	70.0	3	23.0	1.0	19	17.8	3.0	0°
6	25.0	1	23.0	1.1	17	18.3	2.8	0°
7	57.0	3	23.0	1.2	16	18.0	3.0	0°
8	40.0	2	23.0	1.3	13	15.7	3.0	0°
9	21.0	1	19.0	1.3	13	15.7	3.0	0°
10	25.0	1	23.0	1.3	13	16.0	3.0	0°

Bridge No.	Total Bridge Length (ft)	Number of Spans	Maximum Span Length (ft)	Girder Spacing (ft)	Number of Girders	Bridge Width (ft)	Deck Thickness (in.)	Skew (deg)
11	24.0	1	23.0	1.3	14	17.4	3.0	0°
12	54.0	3	19.0	1.4	14	17.7	2.8	0°
13	24.0	1	23.0	1.4	14	17.7	3.0	0°
14	71.0	3	23.0	1.4	14	17.7	2.8	0°
15	62.0	3	23.0	1.4	14	17.8	2.8	0°
16	62.0	3	23.0	1.4	14	18.0	3.0	0°
17	62.0	3	23.0	1.4	14	18.0	3.0	0°
18	21.0	1	19.5	1.4	15	19.5	3.0	0°
19	130.0	3	58.0	1.4	12	15.8	3.0	0°
20	24.0	1	23.0	1.4	19	17.9	3.0	0°
21	70.0	3	23.0	1.4	21	18.0	2.8	0°
22	58.0	3	23.0	1.5	13	17.4	3.0	0°
23	24.0	1	23.0	1.5	13	17.8	3.0	0°
24	24.0	1	23.0	1.5	13	17.8	3.0	0°
25	54.0	3	23.0	1.5	13	17.8	3.0	0°
26	54.0	3	23.0	1.5	13	18.0	3.0	0°
27	46.7	3	16.0	1.6	13	19.0	4.0	0°
28	29.0	1	28.0	1.6	13	19.0	4.0	0°
29	24.0	1	23.0	1.8	10	16.5	2.8	0°
30	58.0	3	19.0	2.0	10	17.8	3.0	0°
31	91.7	4	23.5	2.1	9	16.7	2.8	0°
32	76.0	3	35.0	2.2	14	17.8	3.0	0°
33	73.9	3	26.0	2.2	8	15.2	4.5	0°

Table E-3b. Multiple traffic lane timber-timber bridges

Bridge No.	Total Bridge Length (ft)	Number of Spans	Maximum Span Length (ft)	Girder Spacing (ft)	Number of Girders	Bridge Width (ft)	Deck Thickness (in.)	Skew (deg)
1	26.0	1	24.0	0.8	28	23.9	3.0	0°
2	69.0	3	24.0	0.8	28	23.9	3.0	0°
3	71.0	3	23.0	0.9	23	20.0	3.0	0°
4	24.0	1	23.0	1.3	17	21.3	3.0	0°
5	54.0	3	23.0	1.4	18	23.8	3.0	0°
6	24.0	1	23.0	1.4	19	23.8	3.0	0°
7	55.0	3	23.0	1.5	16	22.2	3.0	0°
8	31.0	2	15.0	2.0	13	23.9	3.0	0°
9	125.0	7	21.0	2.1	12	21.9	3.4	0°

Table E-3c. Skewed timber-timber bridges

Bridge No.	Total Bridge Length (ft)	Number of Spans	Maximum Span Length (ft)	Girder Spacing (ft)	Number of Girders	Bridge Width (ft)	Deck Thickness (in.)	Skew (deg)
1	24.0	1	24.0	0.9	22	18.3	2.8	22
2	23.0	1	23.0	1.3	17	21.4	3.0	13
3	23.0	1	23.0	1.5	13	17.6	2.8	10
4	23.0	1	23.0	1.7	10	15.3	2.8	15
5	26.0	1	26.0	2.0	11	20.0	4.0	47
6	72.0	3	24.0	1.3	19	24.0	3.0	40
7	23.0	1	22.0	1.3	18	23.6	2.8	24
8	36.0	2	17.0	1.5	17	23.9	3.0	40
9	74.3	3	25.0	1.8	14	23.0	2.8	30
10	26.2	1	25.3	2.5	13	21.8	3.0	30

Table E-4. 174 Bridges used in Volume II

Bridge ID from Tables E-1a–E-3c							
FHWA Number	Bridge ID for Moment Ratios	Bridge ID for OR Ratios	Table	Bridge No.	Minimum Span Length (ft)	Number of Spans	HS20 Operating Rating (tons)
298820	Br1_1	Br1_1a	2a	1	19	1	4
60620		Br1_1b	3a	9	19	1	38.4
245005	Br1_2	Br1_2	3a	18	20	1	34.2
8910	Br1_3	Br1_3	N/A	N/A	20	1	28
122322	Br1_4	Br1_4	2c	1	21	1	91.7
123441	Br1_5	Br1_5a	2c	6	22	1	79.9
285860		Br1_5b	3c	7	22	1	46.6
245710	Br1_6	Br1_6	3a	20	23	1	10.4
123940	Br1_7	Br1_7a	2a	3	23	1	40.2
122301		Br1_7b	2a	4	23	1	71.6
121881		Br1_7c	2a	10	23	1	73.2
122261		Br1_7d	2a	16	23	1	66.5
122101		Br1_7e	2c	8	23	1	91.9
290440		Br1_7f	2c	9	23	1	52.3
290530		Br1_7g	3a	6	23	1	32.8
60640		Br1_7h	3a	10	23	1	29.9
121610		Br1_7i	3a	11	23	1	37.9
289830		Br1_7j	3b	4	23	1	48.1
160240		Br1_7k	3b	6	23	1	12
290111		Br1_7l	3a	13	23	1	33.9
288000		Br1_7m	3a	23	23	1	37.4
287150	Br1_7n	3a	24	23	1	47.5	
11478	Br1_7o	3a	29	23	1	N/A	
363200	Br1_8	Br1_8a	2b	7	24	1	58.5
122871		Br1_8b	2a	15	24	1	54.5
270391		Br1_8c	3b	1	24	1	0.68
290000		Br1_8d	3c	1	24	1	31.3
26692	Br1_9	Br1_9	3c	10	25	1	N/A
269710	Br1_10	Br1_10a	1a	2	26	1	0.25
125012		Br1_10b	2b	12	26	1	99
269420		Br1_10c	3c	5	26	1	0.72
122820	Br1_11	Br1_11	2c	2	27	1	41
93091	Br1_12	Br1_12	1c	3	28	1	34.9
22963		Br1_12a	3a	28	28	1	N/A
284231	Br1_13	Br1_13a	1a	1	29	1	40
361970		Br1_13b	2b	5	29	1	25.6

Bridge ID from Tables E-1a–E-3c							
FHWA Number	Bridge ID for Moment Ratios	Bridge ID for OR Ratios	Table	Bridge No.	Minimum Span Length (ft)	Number of Spans	HS20 Operating Rating (tons)
122131		Br1_13c	2a	5	29	1	68.3
94821	Br1_14	Br1_14a	1b	1	30	1	60.1
92971		Br1_14b	1c	4	30	1	84.6
246180	Br1_15	Br1_15	2b	11	31	1	18.9
269880		Br1_16a	1c	2	32	1	0.4
268750		Br1_16b	1a	3	32	1	31.4
123050	Br1_16	Br1_16c	1b	7	32	1	36.6
263921		Br1_16d	2b	10	32	1	38.3
93682		Br1_16e	2b	16	32	1	63.2
96361		Br1_17a	2b	4	33	1	32.2
121541	Br1_17	Br1_17b	2a	8	33	1	65.5
94511		Br1_17c	2b	9	33	1	39.8
263921	Br1_18	Br1_18a	1b	2	34	1	57.9
93682		Br1_18b	N/A	N/A	34	1	63.2
95031	Br1_19	Br1_19	1b	4	37	1	52.9
285961	Br1_20	Br1_20	2c	5	37	1	57.4
160440	Br1_21	Br1_21	2c	10	38	1	19.5
320641	Br1_22	Br1_22a	1b	3	39	1	32.3
122832		Br1_22b	2b	6	39	1	58.8
285291		Br1_23a	1a	4	40	1	49.9
268950	Br1_23	Br1_23b	1c	5	40	1	33.2
124451		Br1_23c	2c	7	40	1	48.3
284381	Br1_24	Br1_24	1b	5	41	1	75.4
96091	Br1_25	Br1_25	2c	4	41	1	37.9
94051	Br1_26	Br1_26	1b	6	42	1	42.8
p-32-903	Br1_27	Br1_27	2a	23	43	1	N/A
96490	Br1_28	Br1_28a	1b	8	43	1	31
355810		Br1_28b	1b	9	43	1	17
286481	Br1_29	Br1_29	2c	3	49	1	35.5
p-37-174		Br1_29a	2b	21	49	1	N/A
269630	Br1_30	Br1_30a	1c	7	50	1	20
262620		Br1_30b	1a	5	50	1	34.5
125521	Br1_31	Br1_31	2b	15	51	1	39.4
b-52-042		Br1_32	1c	10	55	1	N/A
302990	Br1_32	Br1_32a	1c	11	55	1	36
60660		Br1_32b	1b	21	55	1	32.2
286590	Br1_33	Br1_33	2a	19	58	1	29.8

**Bridge ID from
Tables E-1a–E-3c**

FHWA Number	Bridge ID for Moment Ratios	Bridge ID for OR Ratios	Table	Bridge No.	Minimum Span Length (ft)	Number of Spans	HS20 Operating Rating (tons)
289591		Br1_34a	1c	1	59	1	47.8
286570		Br1_34b	2a	2	59	1	34.8
285610	Br1_34	Br1_34c	2a	11	59	1	22.3
125761		Br1_34d	2b	8	59	1	48.8
284641		Br1_34e	2a	14	59	1	26.1
288151	Br1_35	Br1_35	2b	1	59	1	49
122241		Br1_36a	2a	6	60	1	59.6
122201	Br1_36	Br1_36b	2a	7	60	1	33.1
123071		Br1_36c	2a	17	60	1	36.9
179650		Br1_36d	2a	20	60	1	25.3
125861	Br1_37	Br1_37	2a	9	61	1	36
94431	Br1_38	Br1_38	1b	12	66	1	68.4
60560	Br1_39	Br1_39	1b	20	80	1	37.6
263390	Br2_1	Br2_1	3b	8	15	2	31.1
270151	Br2_2	Br2_2	3c	8	17	2	12.8
68970	Br2_3	Br2_3	3a	2	19	2	62.4
289870	Br2_4	Br2_4	3a	8	17	2	32.4
p-09-902	Br2_5	Br2_5	2b	20	20	2	N/A
b-37-046	Br2_6	Br2_6	1b	14	31	2	N/A
122561	Br2_7	Br2_7	2a	21	14	2	48.1
b-13-028	Br2_8	Br2_8	1b	11	34	2	N/A
b-13-075	Br2_9	Br2_9	1b	13	52	2	N/A
601605	Br2_10	Br2_10	1b	15	112	2	63
606515	Br2_11	Br2_11	N/A	N/A	118	2	70.2
13774	Br3_1	Br3_1	3a	27	15	3	N/A
286050	Br3_2	Br3_2	3a	12	18	3	32
161010		Br3_3a	3b	5	16	3	28.5
289980	Br3_3	Br3_3b	3a	25	16	3	37.3
289860		Br3_3c	3a	26	16	3	37.6
285360	Br3_4	Br3_4	3b	7	16	3	37.3
287490	Br3_5	Br3_5	3a	7	17	3	27.7
290520	Br3_6	Br3_6	3a	22	18	3	38.9
287380	Br3_7	Br3_7	3a	30	19	3	46.8
286580		Br3_8a	3a	15	20	3	35
287850	Br3_8	Br3_8b	3a	16	20	3	30.5
289900		Br3_8c	3a	17	20	3	28.9
285680		Br3_8d	3c	4	20	3	32.3

**Bridge ID from
Tables E-1a–E-3c**

FHWA Number	Bridge ID for Moment Ratios	Bridge ID for OR Ratios	Table	Bridge No.	Minimum Span Length (ft)	Number of Spans	HS20 Operating Rating (tons)
290351	Br3_9	Br3_9	3a	4	20	3	32.9
287920	Br3_10	Br3_10	3c	3	21	3	31.1
286141	Br3_11	Br3_11	3a	1	22	3	37.5
288201	Br3_12	Br3_12	3a	3	22	3	30.4
363596	Br3_13	Br3_13	3b	2	23	3	0.76
284750		Br3_14a	3a	5	23	3	32.6
286681	Br3_14	Br3_14b	3a	21	23	3	27.6
289991		Br3_14c	3b	3	23	3	32.4
284480		Br3_14d	3a	14	23	3	23.5
67180	Br3_15	Br3_15	3c	6	24	3	15.5
12324	Br3_16	Br3_16	3a	33	23	3	N/A
13474	Br3_17	Br3_17	3c	9	24	3	N/A
121931	Br3_18	Br3_18	2a	12	19	3	36.4
244880	Br3_19	Br3_19	3a	32	17	3	4
245360	Br3_20	Br3_20	1c	9	22	3	41.5
95621	Br3_21	Br3_21	1c	6	19	3	77.2
284890	Br3_22	Br3_22	3a	19	36	3	30.8
43340	Br3_23	Br3_23	N/A	N/A	46	3	0
93231	Br3_24	Br3_24	1b	10	39	3	64.8
246460	Br3_25	Br3_25	2a	13	59	3	21.7
b-05-048	Br3_26	Br3_26	1c	8	59	3	N/A
606750	Br3_27	Br3_27	1b	19	50	3	69.7
284690	Br4_1	Br4_1	3c	2	17	4	30.6
13489	Br4_2	Br4_2	3a	31	22	4	N/A
30620	Br4_3	Br4_3a	N/A	N/A	43	4	54.5
30610		Br4_3b	1b	22	43	4	59.2
32110	Br4_4	Br4_4a	1c	16	52	4	50
32120		Br4_4b	1b	23	52	4	49.7
21990	Br4_5	Br4_5	N/A	N/A	49	4	50
28170	Br4_6	Br4_6	N/A	N/A	53	4	31.7
18640	Br4_7	Br4_7	N/A	N/A	57	4	31.9
22400	Br4_8	Br4_8	1c	14	55	4	45
18330	Br4_9	Br4_9	N/A	N/A	57	4	37
23370	Br4_10	Br4_10	1b	17	48	4	42
45360	Br4_11	Br4_11	N/A	N/A	48	4	43.9
53660	Br4_12	Br4_12	1c	12	59	4	29.5
602050	Br4_13	Br4_13	N/A	N/A	52	4	63

Bridge ID from Tables E-1a–E-3c							
FHWA Number	Bridge ID for Moment Ratios	Bridge ID for OR Ratios	Table	Bridge No.	Minimum Span Length (ft)	Number of Spans	HS20 Operating Rating (tons)
602555	Br4_14	Br4_14a	N/A	N/A	50	4	53.7
600230		Br4_14b	1b	18	50	4	48.1
602025	Br4_15	Br4_15	N/A	N/A	50	4	62.7
22270	Br4_16	Br4_16	N/A	N/A	59	4	61.3
19270	Br4_17	Br4_17	1b	16	51	4	54.5
19250	Br4_18	Br4_18	N/A	N/A	51	4	66
605485	Br4_19	Br4_19	N/A	N/A	53	4	62.9
23000	Br4_20	Br4_20	N/A	N/A	59	4	45.5
605065	Br4_21	Br4_21	N/A	N/A	55	4	56.6
22950	Br4_22	Br4_22	1b	24	52	4	76.8
22190	Br4_23	Br4_23	1c	13	70	4	33.8
602435	Br4_24	Br4_24	1c	15	56	4	49.8
602455	Br4_25	Br4_25	N/A	N/A	56	4	60.6
28000	Br4_26	Br4_26	N/A	N/A	70	4	59.7
22990	Br4_27	Br4_27	N/A	N/A	54	4	50.8
600050	Br4_28	Br4_28	N/A	N/A	56	4	70.6
602465	Br4_29	Br4_29	N/A	N/A	59	4	44.8
605500	Br4_30	Br4_30	N/A	N/A	59	4	58
22980	Br4_31	Br4_31	N/A	N/A	60	4	59
600130	Br4_32	Br4_32	N/A	N/A	60	4	51.1
605515	Br4_33	Br4_33	N/A	N/A	63	4	56
603655	Br4_34	Br4_34	N/A	N/A	66	4	55.5
605085	Br4_35	Br4_35	N/A	N/A	66	4	62.5
22600	Br4_36	Br4_36	N/A	N/A	69	4	49.9
15225	Br4_37	Br4_37	N/A	N/A	68	4	66.4
605510	Br4_38	Br4_38	N/A	N/A	77	4	50.6
600770	Br4_39	Br4_39	N/A	N/A	100	4	80.5

APPENDIX F. SURVEY RESPONSES

Survey

Bridge Weight Limits for Implements of Husbandry Survey

State: _____

Name of DOT official completing the survey: _____

May we contact you regarding questions on this survey (Yes/No)? _____

Please provide contact information: _____

A. Questionnaire

1. What is your state's definition of an "implement of husbandry?"
2. Must implements of husbandry comply with bridge posting signs?
3. In addition to limits on bridge posting signs, what are the **gross** vehicle weight limits for implements of husbandry on **bridges**? If certain implements of husbandry are exempt from gross weight limits, please list them.
4. In addition to limits on bridge posting signs, what are the **single axle** weight limits for implements of husbandry on **bridges**? If certain implements of husbandry are exempt from single axle weight limits, please list them.
5. Is the weight of the tractor or other towing vehicle included in either of these weight limits (gross or single axle)?
6. Please provide the respective website addresses to the information listed above.

B. Current Information.

Listed below are the single axle and gross weight limits for a selected group of states. If your state is included in the table below, please check the information to ensure that it is consistent with the answers provided in the questionnaire above. The weight limits shown were determined for the three-axle vehicle in Figure F-1.

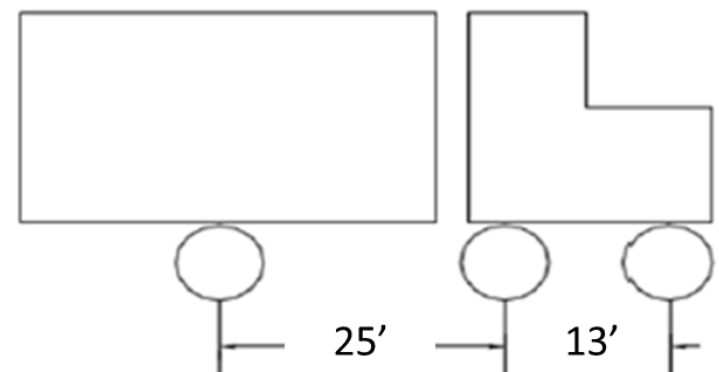


Figure F-1. Three-axle vehicle

Responses

Table F-1. Definition of implements of husbandry

State	Definition of Implement of Husbandry
Alabama	Farm equipment.
Alaska	Farm equipment.
Arizona	In the border area currently we allow the following: The vehicle or vehicle combination must be transporting perishable fresh fruits or vegetables in a sealed container and must meet the criteria as below: 1. The overall Gross Vehicle Weight cannot exceed 90,800 lbs. 2. The vehicle configuration must have at least five axles, and 3. The axle group weight configuration cannot exceed the maximum weight allowed in Arizona Administrative Code R17-6-411.
Arkansas	A vehicle used in the operation of a farm or ranch.
California	A vehicle which is used exclusively in the conduct of agricultural operations. An implement of husbandry does not include a vehicle if its existing design is primarily for the transportation of persons or property on a highway, unless specifically designated as such by some other provision of this code.
Colorado	No state definition.
Florida	Any vehicle designed and adapted exclusively for agricultural, horticultural, or livestock-raising operations or for lifting or carrying an implement of husbandry and in either case not subject to registration if used upon the highways.
Hawaii	Such terms as "farm equipment", "agricultural equipment", "vehicles transporting agricultural products and equipment", and "vehicles used in agricultural operations and activities."
Illinois	Every vehicle designed and adapted exclusively for agricultural, horticultural, or livestock raising operations, including farm wagons, wagon trailers or like vehicles used in connection therewith, or for lifting or carrying an implement of husbandry provided that no farm wagon, wagon trailer or like vehicle having a gross weight of more than 36,000 pounds, shall be included hereunder.
Iowa	Vehicle or special mobile equipment designed for agricultural purposes and used exclusively in an agricultural operation.
Kansas	Every vehicle designed or adapted and used exclusively for agricultural operations and only incidentally moved or operated upon the highways. Such term shall include, but not be limited to, a fertilizer spreader or nurse tank used exclusively for dispensing or spreading water, dust or liquid fertilizers or agricultural chemicals, as defined in K.S.A. 2-2202, and amendments thereto, regardless of ownership. For the purpose of this section or for the purpose of the act of which this section is a part, "implement of husbandry" shall not include: (a) A truck mounted with a fertilizer spreader used or manufactured principally to spread animal dung; (b) a mixer-feed truck owned and used by a feedlot, as defined by K.S.A. 47-1501, and amendments thereto, and specially designed and used exclusively for dispensing feed to livestock in such feedlot; or (c) a truck permanently mounted with a spreader used exclusively for dispensing or spreading water, dust or liquid fertilizers or agricultural chemicals, as defined in K.S.A. 2-2202, and amendments thereto, regardless of ownership.
Minnesota	Any vehicle designed or adapted exclusively for agricultural, horticultural or livestock operations, or for lifting and carrying an implement of husbandry. Any towed vehicle, which meets this definition, is also an implement of husbandry. This includes wagon trailers and implement trailers used in a farm operation.

State	Definition of Implement of Husbandry
Missouri	All self-propelled machinery operated at speeds of less than 30 mph, specifically designed for, or especially adapted to be capable of, incidental over-the-road and primary offroad usage and used exclusively for the application of commercial plant-food materials or agricultural chemicals, and not specifically designed or intended for transportation of such chemicals and materials.
Nebraska	Any sort of farm equipment, machinery, combines, trucks, etc.
Nevada	Information not provided.
New York	A vehicle designed or adapted exclusively for agricultural, horticultural or livestock raising operations or for lifting or carrying an implement of husbandry.
Ohio	No state definition.
Oklahoma	Every device, whether it is self-propelled, designed and adapted so as to be used exclusively for agricultural, horticultural or livestock-raising operations or for lifting or carrying an implement of husbandry and, in either case, not subject to registration if operated upon the highways. 1. Farm wagon type tank trailers of not over one thousand two hundred (1,200) gallons capacity, used during the liquid fertilizer season as field storage "nurse tanks" supplying the fertilizer to a field applicator and moved on highways only for bringing the fertilizer from a local source of supply to farms or field or from one farm or field to another, shall be considered implements of husbandry for purposes of this title. 2. Trailers or semitrailers owned by a person engaged in the business of farming and used exclusively for the purpose of transporting farm products to market or for the purpose of transporting to the farm material or things to be used thereon shall also be considered implements of husbandry for purposes of this title. Provided, no truck or semitrailer with an axle weight of twenty thousand (20,000) pounds or more, which is used to haul manure and operated on the public roads or highways of this state shall be considered an implement of husbandry for the purposes of this title. 3. Utility-type, all-terrain vehicles with a maximum curb weight of one thousand five hundred (1,500) pounds which are equipped with metal front or rear carrying racks when used for agricultural, horticultural or livestock-raising operations shall be considered implements of husbandry for purposes of this title.
Pennsylvania	Farm equipment that meets all of the following criteria: (1) Is equipped with pneumatic tires except if prohibited by religious beliefs. (2) Is infrequently operated or moved upon highways. (3) Is used in agriculture for any of the following purposes: (i) performance of agriculture production or harvesting activities for the farmer's agricultural operations; or (ii) transportation of agricultural products or agricultural supplies for the benefit of the farmer's agricultural operations. The term also includes earthmoving equipment and any other vehicle determined by the department to be an implement of husbandry.
South Dakota	No definition in statute.

State	Definition of Implement of Husbandry
Vermont	<p>Farm Tractor means a traveling power plant or a self-propelled device which functions as part of crop production, harvesting, feeding, or livestock management, or is used for drawing a farm trailer. Farm tractor also means a self-propelled vehicle designed to perform single-purpose functions, such as land preparation, crop protection, or harvesting. The term "farm tractor" shall not include a "motor truck" as defined in subdivision (20) of this section.</p> <p>Farm Trailer means a single vehicle or equipment, designed and adapted exclusively for tilling, planting, harvesting, management, or for carrying inputs or outputs from agricultural, horticultural, or livestock-raising operations, or farm equipment without motive power, designed to be drawn by a motor vehicle, a farm truck, or a farm tractor, and, in any case, not subject to registration if used upon the highway.</p> <p>Vermont also has some other definitions that address certain types of motor vehicles used exclusively on a farm or commercial operations that service farms.</p>
Virginia	<p>Unladen self-propelled equipment and tracked vehicles used in the mining and construction industry as set out in 46.2-1149, and 46.2-1149.7 which are conceptually very similar.</p>
Washington	<p>A farm implement includes any device that directly affects the production of agricultural products, including fertilizer and chemical applicator apparatus (complete with auxiliary equipment). For purposes of this section, the implement must be nondivisible, weigh less than sixty-five thousand pounds, and comply with the requirements of RCW 46.44.091. The implement must be less than twenty feet in width and not exceed sixteen feet in height. However, for purposes of this section, farm implements must not exceed fourteen feet in height in the counties of Whatcom, Skagit, Island, Snohomish, and King. If the implement is self-propelled, it must not exceed forty feet in length, or seventy feet overall length if being towed. The implement must move on pneumatic tires, or solid rubber tracks that will not damage public highways with parts that extend beyond the tracks. Implements exceeding any of these criteria must meet all requirements for special permits as referenced in other sections in this chapter and chapter 46.44 RCW.</p>
West Virginia	<p>Every vehicle which is designed for or adapted to agricultural purposes and used by the owner thereof primarily in the conduct of his or her agricultural operations, including, but not limited to, trucks used for spraying trees and plants: Provided, That the vehicle may not be let for hire at any time. (WV Code 17A-1-1 Definitions)</p>
Wisconsin	<p>A self-propelled or towed vehicle that is manufactured, designed, or reconstructed to be used and that is exclusively used in the conduct of agriculture operations.</p>

Table F-2. Gross weight limits and single-axle weight limits

State	Husbandry vehicle type	Tractor included in weight limit?	Gross Weight Limits (lbs) 3-axle vehicle (Figure 1)	Single-Axle Weight Limit (lbs) 3-axle vehicle (Figure 1)	Websites
Alabama	All	N	Exempt	Exempt	http://www.dot.state.al.us/maweb/doc/Title32Chapter9.pdf
Alaska	All	Y	Exempt	Exempt	http://www.touchngo.com/lglcntr/akstats/Statutes/Title19/Chapter10/Section065.htm
Arizona	All	Y	90,800	20,000	ADOT Motor Vehicle Division Office Memo T5621 dated May 11, 2010
Arkansas	Compacted seed cotton	Y	80,000	28,000	http://www.arkansashighways.com/act300/AR%20Motor%20Vehicle%202013%20Edition.pdf sec 27-35-202
	Animal feed and solid waste	Y	80,000	21,600	http://www.arkansashighways.com/act300/AR%20Motor%20Vehicle%202013%20Edition.pdf sec 27-35-203
California	All	Y	80,000	20,000	https://www.dmv.ca.gov/portal/dmv/detail/pubs/vctop/vc/vc
Colorado	All	Y	80,000 for interstate; 85,000 for non-interstate	20,000	https://www.codot.gov/business/permits/truckpermits/documents
Florida	All	Y	Federal bridge formula	22,000	http://www.fdotmaint.com/permit ; Weight Restrictions Chart
Hawaii	All	N	They must follow the same as other vehicles on the highways except at on-grade roadway crossings that the owners of the vehicles must construct and maintain structurally suitable pavement sections.	No difference from other vehicles	Information not provided

State	Husbandry vehicle type	Tractor included in weight limit?	Gross Weight Limits (lbs) 3-axle vehicle (Figure 1)	Single-Axle Weight Limit (lbs) 3-axle vehicle (Figure 1)	Websites
Illinois	Implements of husbandry, as defined in Chapter 1 of this Code, temporarily operated or towed in a combination upon a highway provided such combination does not consist of more than 3 vehicles or, in the case of hauling fresh, perishable fruits or vegetables from farm to the point of first processing, not more than 3 wagons being towed by an implement of husbandry	Y	66,000	Exempt	http://www.ilga.gov/legislation/ilcs/ilcs4.asp?DocName=062500050HCh%2E+15&ActID=1815&ChapterID=49&SeqStart=153100000&SeqEnd=158100000
Iowa	Wheeled grain carts, wheeled tank wagons, wheeled fence-line feeders	N	80,000	20,000	
	All others, excluding tracked and flotation vehicles	N	Exempt	Exempt	

State	Husbandry vehicle type	Tractor included in weight limit?	Gross Weight Limits (lbs) 3-axle vehicle (Figure 1)	Single-Axle Weight Limit (lbs) 3-axle vehicle (Figure 1)	Websites
Kansas	All	Y	Federal bridge formula	20,000	http://kslegislature.org/li/b2015_16/statute/008_000_0000_chapter/http://www.sos.ks.gov/pubs/kar/2009/3%20036_36-Department%20of%20Transportation,%202009%20KAR%20Vol%203.pdf
Minnesota	All	Y	30' betwn frnt & rear axles (3 axle=58,500, 4 axle=62,000, 5 axle=67,000) 50' betwn frnt & rear axles (3 axle=60,000, 4 axle=75,500, 5 axle=79,500) 60' betwn frnt & rear axles (3 axle=60,000, 4 axle=80,000, 5 axle=85,500)	9 tons for 9 ton roads, 10 tons for 10 ton roads	https://www.revisor.mn.gov/statutes/?id=169.824
Missouri	All	Y	80,000	20,000	http://www.modot.org/mcs/
Nebraska	Agricultural floater-spreader implement to carry/apply fertilizer, chemicals or related products	N	Exempt	Exempt	-
	All others	N	48,000	48,000	-
Nevada	Information not provided	Y	Information not provided	Information not provided	Information not provided
New York	All	Y	Same as other vehicles	22,400	www.nypermits.org
Ohio	All	Y	80,000	20,000	Information not provided

State	Husbandry vehicle type	Tractor included in weight limit?	Gross Weight Limits (lbs) 3-axle vehicle (Figure 1)	Single-Axle Weight Limit (lbs) 3-axle vehicle (Figure 1)	Websites
Oklahoma	All	Y	Information not provided	20,000	https://www.dps.state.ok.us/ohp/SFarm.pdf
Pennsylvania	All	Y	Legal Load	Legal Load	http://www.pacode.com/ http://www.dot3.state.pa.us/vehicle_code/index.shtml
South Dakota	All	Y	Federal bridge formula	20,000	http://law.lis.virginia.gov/vacode/title46.2/chapter10/section46.2-1149/ http://law.lis.virginia.gov/vacode/title46.2/chapter10/section46.2-1149.7/
Vermont**	Farm truck and farm trailer	Y	60,000	600 lbs/in tire width	http://legislature.vermont.gov/statutes/
Virginia	All	Y	Legal limits	Analyzed	http://law.lis.virginia.gov/vacode/title46.2/chapter10/section46.2-1149/ http://law.lis.virginia.gov/vacode/title46.2/chapter10/section46.2-1149.7/
Washington	All	Y	65,000	22,000 lbs max or 600 lbs/in for four-tire axles; 10,000 lbs max or 500 lbs/in for two-tire axles	http://apps.leg.wa.gov/WAC/default.aspx?cite=468-38-290 http://app.leg.wa.gov/RCW/default.aspx?cite=46.44.041 http://app.leg.wa.gov/RCW/default.aspx?cite=46.44.042
West Virginia	All	Y	Exempt	Exempt	http://www.legis.state.wv.us/WVcode/code.cfm?chap=17a&art=1 http://www.legis.state.wv.us/WVcode/Code.cfm?chap=17c&art=17#17 http://www.legis.state.wv.us/WVcode/ChapterEntire.cfm?chap=17c&art=17&ion=12#17#17
Wisconsin	Empty 2 vehicle combination transporting a potato harvester	Y	Exempt	Exempt	
	All Others	Y	15% over Federal Bridge Formula	15% over Federal Bridge Formula	

** Need not comply with bridge posting signs